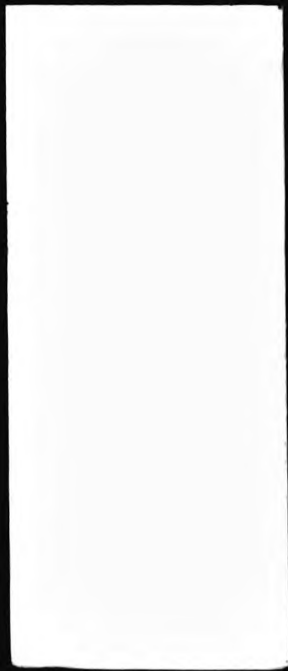


This PDF was created from the British Library's microfilm copy of the original thesis. As such the images are greyscale and no colour was captured.

Due to the scanning process, an area greater than the page area is recorded and extraneous details can be captured.

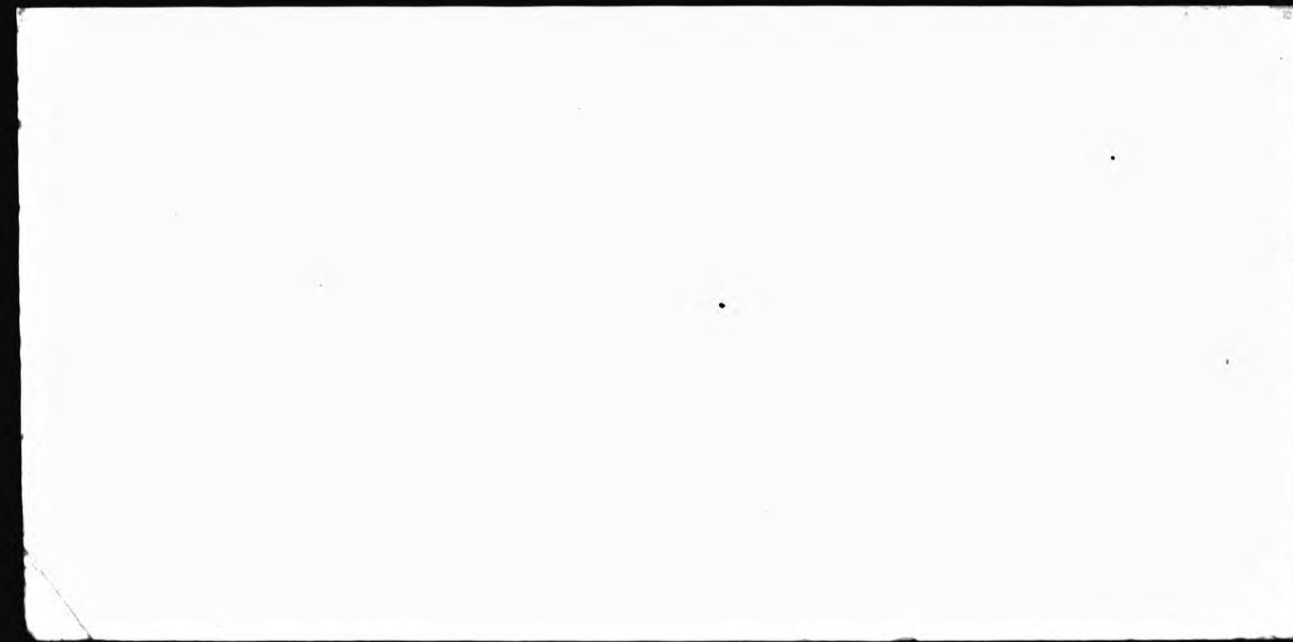
This is the best available copy



DX



179741



THE BRITISH LIBRARY
BRITISH THESIS SERVICE

TITLE AN INVESTIGATION INTO THE POLYETHYLENE
EXTRUDATES PRODUCED BY SIMULTANEOUS
ORIENTATION AND HIGH TEMPERATURE
QUENCHING.

AUTHOR Colin
BERRY

DEGREE Ph.D

**AWARDING
BODY** University of North London

DATE 1994

**THESIS
NUMBER** DX179741

THIS THESIS HAS BEEN MICROFILMED EXACTLY AS RECEIVED

The quality of this reproduction is dependent upon the quality of the original thesis submitted for microfilming. Every effort has been made to ensure the highest quality of reproduction. Some pages may have indistinct print, especially if the original papers were poorly produced or if awarding body sent an inferior copy. If pages are missing, please contact the awarding body which granted the degree.

Previously copyrighted materials (journals articles, published texts etc.) are not filmed.

This copy of the thesis has been supplied on condition that anyone who consults it is understood to recognise that its copyright rests with its author and that no information derived from it may be published without the author's prior written consent.

Reproduction of this thesis, other than as permitted under the United Kingdom Copyright Designs and Patents Act 1988, or under specific agreement with the copyright holder, is prohibited.

AN INVESTIGATION INTO THE POLYETHYLENE EXTRUDATES PRODUCED
BY SIMULTANEOUS ORIENTATION AND HIGH TEMPERATURE QUENCHING

by

COLIN BERRY

A THESIS SUBMITTED TO THE UNIVERSITY OF NORTH LONDON
FOR THE DEGREE OF DOCTOR OF PHILOSOPHY

London School of Polymer Technology
University of North London
Holloway Road
London N7

MARCH 1993

ABSTRACT

An apparatus was designed and constructed to allow a molten polymer extrudate under tension - or draw-down - to pass through a volume of liquid metal alloy in order that the extrudate would rapidly reach the temperature of the metal and be fully quenched on leaving the medium.

The temperature of the medium could be controlled to an accuracy of $\pm 0.5^{\circ}\text{C}$ and the molten extrudates could be subjected to a wide range of draw-downs whilst maintaining a continuous production of extrudate.

High density polyethylene (HDPE) extrudates were prepared from three dies - circular, strip and flat-film - at a range of liquid metal alloy temperatures ($111 - 123^{\circ}\text{C}$) and over a wide range of draw-downs.

The effect of processing on the HDPE extrudates was analysed by tensile testing, cyclic strain recovery, shrinkage testing, density measurements and annealing in air and liquid metal at 117°C . It was found that the level of draw-down and the temperature of the quenching medium had a profound effect upon the resultant properties of the extrudate.

Extrudates prepared using a low level of orientation and low bath temperature are similar to those quenched in air, i.e. having a pronounced yield point, whereas those prepared using a high level of orientation and a high bath temperature exhibited properties similar to those of amorphous samples, i.e. high modulus and low extension at break. However, if the extrudate remains in the bath longer than is necessary to quench it, this effect is reversed.

A possible mechanism was proposed to explain the relationship between the values of the processing parameters used, the morphology of the resultant HDPE extrudates and their properties.

ACKNOWLEDGEMENTS

Firstly, I should like to thank BXL Plastics Ltd. for initiating and financing the work presented in this thesis.

I should also like to thank my supervisor, Mr. David Dunning, for his support and encouragement throughout this period of research, and for his help and suggestions in the preparation of this thesis.

My thanks go to all of the staff of the London School of Polymer Technology for their help, but especially to Mr. Brian Durrant for his expert assistance in the preparation of the extrudates, to Mr. Dave Westney for his equally expert assistance in the tensile testing of said extrudates, and also to Mr. Percy Gayapersad for his general assistance and knowledgeable cricket conversations.

My thanks also go to Mr. Bob Hurley in the workshop for the construction of the apparatus used in the experiments, without which this work would not be possible.

Finally, my love and many thanks to my friend and companion, Ms. Breda Corish, for her support, financial and otherwise, throughout this period of research.

READER'S GUIDE TO SYMBOLS AND ABBREVIATIONS

A - the cross-sectional area of an extrudate.

A₀ - the cross-sectional area of a die.

a:b ratio - the ratio of the a dimension to the b dimension of an extrudate.

(a:b)/(a:b)₀ ratio - the a:b ratio of an extrudate divided by the a:b ratio of the die used in the experiment.

a dimension - the greatest dimension of the cross-section of an extrudate.

ADD - actual draw-down, the area of the die divided by the cross-sectional area of an extrudate.

ARD - air residence distance, the distance between the mouth of the die and the surface of the liquid metal during an experiment.

b dimension - the dimension of an extrudate perpendicular to the a dimension.

BT - bath temperature.

CSR - cyclic strain recovery.

DDR - draw-down ratio, the haul-off speed divided by the output rate.

D(O) - degree of orientation.

E - strain, or percentage elongation.

E_{br} - elongation at break.

HDPE - high density polyethylene.

"HE" - hard elastic, a form of polymer morphology.

HOS - haul-off speed.

k, k_1, k_2 - constants.

l_o - initial length of sample used in shrinkage recovery tests.

L_o - initial length of sample used in cyclic strain recovery tests.

l_r - final length of sample used in shrinkage recovery tests.

L_s - length of sample under strain in cyclic strain recovery tests.

L_u - length of sample 15 seconds after strain is removed in cyclic strain recovery tests.

O - orientation.

"O" - ordinary, or spherulitic, polymer morphology.

OR - output rate of polymer from the extruder.

PE - polyethylene.

PP - polypropylene.

PMMA - poly (methyl methacrylate).

PS - polystyrene.

PTFE - poly (tetrafluoroethylene).

PVA - poly (vinyl alcohol).

qt - quenching time for extrudate in liquid metal alloy.

R - recovery from a strain.

RD - residence distance, the distance that any point on the extrudate travels in the liquid metal alloy.

RRt - residual residence time, the difference between the residence time and the quenching time.

Rt - the time taken by any point on the extrudate to pass through the liquid metal alloy.

S - stress.

S_{br} - stress at break.

SHC - specific heat capacity.

SK - shish kebab, a form of polymer morphology.

S_y - yield stress.

S_{10%} - stress at 10% elongation.

SR - shrinkage recovery.

T_a - temperature of annealing.

t_a - time of annealing.

T_c - temperature of crystallisation.

TC - thermal conductivity.

T_m - temperature of melting.

t_R - relaxation time for a sample in cyclic strain recovery tests.

CONTENTS

TITLE

ABSTRACT

ACKNOWLEDGEMENT

READER'S GUIDE TO SYMBOLS AND ABBREVIATIONS

<u>CHAPTER 1</u>	<u>Introduction</u>	1
1.1	Crystalline structure of organic compounds	1
1.2	Polymer morphology	2
1.2.1	Lamellar single crystals	7
1.2.2	Crystallisation from an unstressed melt	10
1.2.2.1	Spherulitic morphology	10
1.2.2.2	Mechanism of spherulitic growth	14
1.2.3	Crystallisation from a stressed melt	17
1.2.4	Effect of degree of crystallinity on polymer properties	21
1.2.5	Effect of pressure on polymer crystallinity	22
1.3	Annealing of materials	24
1.3.1	Annealing of inorganic materials	24
1.3.2	Annealing of semi-crystalline polymers	24
1.3.3	Annealing of oriented polymer samples	29
1.4	"Hard Elastic" polymers	30
1.4.1	A detailed comparison of "Hard Elastic" and "Ordinary" forms of a semi-crystalline polymer	31
1.4.1.1	Tensile deformation	31
1.4.1.2	Strain recovery	33
1.4.2	"Hard Elastic" morphology	36
1.5	The use of liquid metal alloy as quenching medium for polymer melts	41
1.6	Quenching apparatus design	42
1.7	Objectives of current work	43

<u>CHAPTER 2</u>	<u>Factors involved in the design of apparatus</u>	44
2.1	Specification of quenching apparatus	44
2.2	Dimensions of bath	46
2.2.1	Internal height	47
2.2.2	Internal width	47
2.2.3	Internal breadth at top	47
2.2.4	Internal breadth at base	47
2.2.5	Wall section thickness	48
2.2.6	Cartridge heaters	48
2.2.7	Temperature controllers	48
2.2.8	Inclusion of tap	49
2.2.9	Material for bath	49
2.2.10	Construction of bath	50
2.3	Roller system	51
2.4	Haul-off equipment	52
2.5	Mobility of apparatus	53
<u>CHAPTER 3</u>	<u>Experimental work</u>	54
3.1	Materials used	54
3.1.1	Metal alloy coolant	54
3.1.2	Grade of polymer	55
3.2	Equipment used in experimental work	56
3.2.1	Extrusion of polymer samples	56
3.2.2	Tensile testing of samples	57
3.2.3	Cyclic strain recovery	58
3.2.4	Shrinkage testing	59
3.2.5	Measurement of degree of crystallinity	60
3.3	Preparation of samples	61
3.3.1	Measurement of output rate	61
3.3.2	Loading extrudate onto haul-off system	61

3.3.3	Inserting the loaded roller system into the bath	62
3.3.4	Variation of haul-off speed	62
3.3.5	Variation of quenching temperature	63
3.3.6	Variation of output rate	63
3.3.7	Level of liquid metal alloy in bath	63
3.3.8	Position of bottom roller on frame	64
3.3.9	Position of bath	64

CHAPTER 4	Results	65
4.1	Control experiment	66
4.2	Polymer extrudates quenched in liquid metal alloy (1)	68
4.2.1	Extrudates from a circular die (at constant output - 20 rpm)	68
4.2.2	Stress-strain curves for extrudates from a circular die	70
4.3	Polymer extrudates quenched in liquid metal alloy (2)	82
4.3.1	Extrudates from a circular die (at constant bath temperature - 117c)	82
4.3.2	Stress-strain curves for extrudates from a circular die	84
4.4	Polymer extrudates quenched in liquid metal alloy (3)	94
4.4.1	Extrudates from a strip die (at constant bath temperature - 122c)	94
4.4.2	Stress-strain curves for strip extrudates	96
4.5	Polymer extrudates quenched in liquid metal alloy (4)	104
4.5.1	Extrudates from a strip die	104
4.5.2	Stress-strain curves for extrudates	108
4.6	Polymer extrudates quenched in liquid metal alloy (5)	121
4.6.1	Extrudates from a film die	121
4.6.2	Stress-strain curves for extrudates	125

4.7	Shrinkage recovery of extrudates	136
4.7.1	Extrudates from a circular die	136
4.7.2	Extrudates from a strip die	138
4.7.3	Extrudates from a film die	140
4.8	Annealing of extrudates	142
4.8.1	Annealed in liquid metal alloy at 117°C	142
4.8.2	Annealed in air at 117°C	149
4.8.3	Annealing in air at room temperature	153
4.9	Density of extrudates	154
4.9.1	Extrudates from a circular die (1 - from section 4.3)	154
4.9.2	Extrudates from a circular die (1 - from section 4.2)	156
4.10	Cyclic strain recovery	158
4.10.1	Extrudates from a circular die (from section 4.2)	158
4.10.2	Extrudates from a circular die (from section 4.3)	159
<u>CHAPTER 5</u>	<u>Discussion</u>	163
5.1	Variables used in the preparation of extrudates	165
5.2	Dimensions of extrudates	171
5.2.1	Cross-sectional area of extrudates	171
5.2.2	Shape of extrudates	173
5.3	Effect of primary variables on the tensile properties	180
5.3.1	Quantitative comparison of physical data	181
5.3.1.1	Stress at 10% strain	181
5.3.1.2	Stress at break	183
5.3.1.3	Elongation at break	184
5.3.2	General shape of stress-strain curves	185
5.4	Orientation of extrudates	187

5.5	Annealing of extrudates	189
5.6	Density of extrudates	191
5.7	Cyclic strain recovery	192
5.8	Effect of residual residence time on tensile properties	193
<u>CHAPTER 6</u>	<u>Mechanism of formation of morphology / deformation mechanism of polymer samples</u>	197
6.1	Zero Orientation	201
6.2	Low - Medium Draw-Down	202
6.3	High Draw-Down	210
<u>CHAPTER 7</u>	<u>Conclusions</u>	218
<u>APPENDICES</u>		221
(i)	Calculation of Approximate Residence Time	221
(ii)	Calculation of Cross-sectional Area for Circular Extrudates	222
(iii)	Actual Draw-down vs. Draw-down Ratio	224
(iv)	Calculation of Approximate Quench Time	225
(v)	$(a:b)/(a:b)_0$ vs. Draw-down Ratio	226
(vi)	Calculation of Residual Residence Time	226
(vii)	Effect of residual residence time on Stress at 10% Strain	227
(viii)	Density vs. Orientation	227
(ix)	Orientation as a function of Residual Residence Time	228
(x)	Density as a function of Residual Residence Time	228
(xi)	Models of composites of Spherulitic and Shish-Kebab morphology	229

REFERENCES

CHAPTER 1 - INTRODUCTION

1.1 CRYSTALLINE STRUCTURE OF ORGANIC COMPOUNDS

When low molecular weight organic compounds are cooled from the molten state to the solid state the microscopic structure is 100% crystalline; the molecules are regularly aligned in three dimensions, held in place by secondary forces between adjacent molecules, such as Van der Waals forces and hydrogen bonding (where possible). There are several crystalline close-packing geometries available to organic compounds, depending upon the shape of the molecule, the temperature of crystallisation, and the ambient pressure of the crystallisation process.

Unbranched alkanes, such as $C_{100}H_{202}$ (Fig. 1.1), may be regarded as very low molecular weight polyethylene; the spatial arrangement of the molecules in the crystalline state should be the same for both compounds. The n-alkane is completely chain-extended in the crystal lattice;¹this is not the case for polyethylene, as will be fully explained (section 1.2.1).

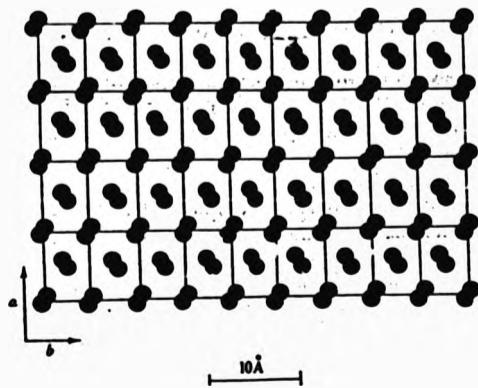


Fig. 1.1 - crystalline structure of $C_{100}H_{202}$ viewed along the length of the molecule¹.

1.2 POLYMER MORPHOLOGY

When a high molecular weight polymer is cooled below its melting point (T_m) the molecules attempt to form a close-packed crystalline structure in the same way as low molecular weight organic compounds. With the exception of lamellar single crystals prepared from dilute solution², which will be discussed later in this chapter, it is not possible to obtain totally crystalline polymer samples.³⁻¹⁰

There are several factors which prevent the formation of regular close-packing in high molecular weight polymers:

i) Steric Hindrance due to side-groups

Polymers that will crystallise to a reasonable extent (above 40% crystallinity) usually have side-groups which are small compared to the repeat unit, such as $-CH_3$ (Polypropylene, PP) or $-F$ (Polytetrafluoroethylene, PTFE), or no side-groups, such as $-H$ (Polyethylene, PE) or polyamides (nylons). Large side-groups, such as $-C_6H_5$ (Polystyrene, PS) or esters (Poly(methyl methacrylate), PMMA) reduce the crystalline content by increasing the distance between adjacent polymer chains, reducing the effect of the secondary forces which are responsible for crystal formation.

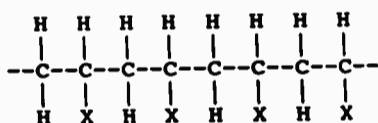
ii) Irregular arrangement of monomeric repeat units

This is seen in atactic homopolymers and random copolymers:

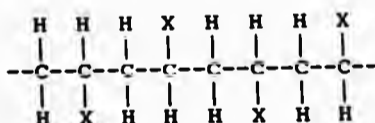
a) Tacticity of Homopolymers - the relative arrangement of the side-groups along a polymer chain in vinyl-type polymers also affects the ability of the polymer to crystallise. This arrangement is known as the tacticity of

the polymer; there are three possible conformations:

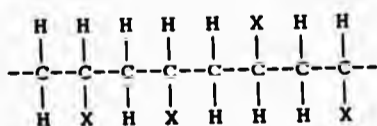
Isotactic - when all the side-groups (X) are in identical positions in terms of the stereochemistry of the molecule. The planar projection of an isotactic polymer may be represented as:



Syndiotactic - as above, but the side-groups alternate regularly:



Atactic - the side-groups are arranged randomly:



Usually, both the isotactic and syndiotactic forms of a polymer (such as PP) have the ability to crystallise, whereas the atactic form will not, because of the lack of stereoregularity. This is true of PS and PMMA also, but not of Poly(vinyl alcohol), PVA. PVA is able to crystallise in the atactic form, due to the small size of the side-group and the presence of inter- and intra-molecular hydrogen bonding.

The tacticity of a polymer is usually determined by the polymerisation process used in its manufacture; free-radical polymerisation leads to the atactic form through



random chain-growth in which the monomeric repeat unit bearing the free-radical may rotate about the C-C bond, whereas ionic polymerisation using a catalyst, such as those pioneered by Ziegler and Natta⁵, is stereospecific - that is the charged polymer chain and the monomeric repeat unit must always be in the same relative positions in order to react - leads to the formation of a stereoregular polymer tacticity.

b) Local order in co-polymers - when more than one monomer is involved in a polymerisation reaction, the result is a co-polymer. There are three main types of co-polymer:

Block Co-polymer - this is when each of the co-monomers (A, B) form alternating blocks - a few hundred monomeric repeat units forming small regions of homopolymer - to make a

AAAAAAAAAA-BBBBBBBB-AAAAAAAAA-BBBBBBBBBBBB-AAAAAA

polymer whose physical properties are a weighted average of those of the component polymers, but some tensile properties may be improved by the chemical bonding between otherwise immiscible polymer phases.

Graft Co-polymer - this is similar to a block co-polymer, except that monomer A forms a continuous "backbone" and monomer B forms the side-chains.

AA
 B B B B B
 B B B B B
 B B B B B
 B B B B B

Random Co-polymers - these are formed when there is no control over the addition of monomeric repeat units to the

polymer chain - neither is preferred in chemical terms, so the addition of the next unit is completely random. This gives rise to a structure of the type:

AAABAABBBABBABABABAAAABBBBAAAABBBBBBABABABABBBAAAABBA

Similarly to an atactic homopolymer, this form of copolymer is generally unable to crystallise because no two sections of polymer chain are alike to a sufficient degree.

In all three cases, A and B may be styrene and butadiene respectively. Block and graft copolymers are thermoplastics which may crystallise to a certain extent if the individual blocks are of a sufficient size; random copolymers are elastomers - e.g. styrene-butadiene rubber, SBR, which are useful only when cross-linked.

iii) Steric hindrance due to branching of polymer chains

Similarly to (i), side-chains of varying length, formed by random chain-transfer of the active site during free-radical polymerisation, cause reduction of the crystalline content by interfering with the regular spacing of the adjacent polymer chains.

iv) Cross-linking of polymer chains

This is the introduction of primary forces - chemical bonding - between adjacent polymer chains which greatly reduces the mobility of the polymer chains relative to each other. Polymers which have a low level of cross-links are elastomers, which may be stretched to a very high strain (>1000%) and yet show very high strain recovery. Elastomers, such as vulcanised natural rubber, may crystallise only when strained. This is known as strain-

induced crystallisation. As the level of cross-links increases, the maximum strain decreases as does the capacity for crystallisation. Highly cross-linked polymers are completely amorphous.


v) High viscosity and chain-entanglement in the melt

When a polymer has small side-groups, a low branching density, a stereoregular sequence of monomeric repeat units and no cross-links, it is possible to form large areas of highly-ordered polymer chains, up to 90% crystallinity, but it is impossible to make a wholly crystalline polymer by cooling the melt due to two factors:

i) the melt viscosity is very high - the mobility of the polymer chains in the melt is very low due to substantial interaction between the polymer chains and the length of the chains themselves. As a result, the energy required to free each polymer molecule so that it may be incorporated completely into a crystalline region is very great.

ii) in an unstressed melt, the polymer chains exist in a relaxed, randomly coiled, state; it follows that there are a great number of entanglements between polymer chains. As in (i) above, this prevents the polymer chains being fully incorporated into a crystalline region.

Compare this with the preparation of polymer samples from dilute solution (Section 1.2.1); the viscosity of the dilute solution is much lower than that of the melt. As a result, it is possible overcome the intermolecular forces and to disentangle the polymer molecules completely and, as a result, to free entire polymer chains in order to incorporate them completely into crystalline regions.



As a result, all polymer samples prepared by cooling from the melt are either amorphous (no ordered regions) or semi-crystalline (up to 90% crystallinity). When describing semi-crystalline polymers, it is usual to refer to the morphology of the polymer, which is the arrangement of crystalline and amorphous phases within the microstructure. The morphology may vary greatly according to the polymer, the grade of polymer used and the processing history (temperature of crystallisation, melt stresses, whether annealed, etc.) of the sample. This chapter describes the effect of processing on the morphology of a semi-crystalline polymer.

1.2.1 LAMELLAR SINGLE CRYSTALS

If a very dilute solution of a semi-crystalline polymer in a suitable solvent (e.g. 0.1% HDPE in toluene) is maintained at a constant temperature below the T_m for a period of several days, then a gelatinous precipitate is obtained.

After drying, examination by X-ray diffraction shows this to be an almost one hundred percent crystalline form of the polymer. It consists of a mat of similar structures called lamellar single crystals.^{2,11-13} These are shaped like flat plates, whose size is of the order of 5 x 5 x 0.1 μm (fig. 1.2).

It has been demonstrated that the lamellar thickness, L , is proportional to the temperature of crystallisation, T_c .^{14,15} For example: when $T_c = 90^\circ\text{C}$, $L = 100\text{nm}$; when $T_c = 130^\circ\text{C}$, $L = 355\text{nm}$ for HDPE.

Further studies of polymer single crystals led to the discovery that the polymer chains are aligned normal to the

plane of the lamella. As the length of a polymer chain (~500nm) is much greater than that of the lamellar thickness (~20nm in air-quenched PE), it was inferred that the chains must fold several times so that they are completely incorporated into the crystalline structure (fig. 1.3).¹⁶⁻¹⁹



Fig. 1.2 - Lamellar single crystals.²⁰

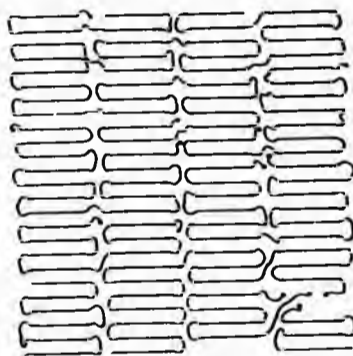


Fig. 1.3 - Chain-folding in single crystals.²

More recently, it was found that, for relatively low molecular weight Poly (ethylene oxide) samples, the lamellar thickness was an integral fraction of the chain length,²¹ i.e. a polymer chain forms an integral number of folds of equal length and the ends of the polymer chains are always on the surface of an ideal single crystal. When a single crystal is annealed (section 1.4.2) at a temperature above the original T_c , the lamellar thickness is observed to increase.²²

Since the discovery of single crystals, the information gained from their examination has been used in the study of melt-crystallised morphologies. Single crystals are assumed to form by the same mechanism as the micro-crystalline areas in a semi-crystalline polymer (section 1.2.2) but it must be remembered that the processing histories are

different in two important respects: the viscosity of the crystallisation medium and the crystallisation time.

A dilute polymer solution may be considered as the melt of a polymer which has a high proportion of very low molecular weight chains, especially if the solvent is an alkane, and consequently has a very low viscosity compared to that of a polymer melt.

A semi-crystalline polymer sample is formed by rapidly cooling a polymer melt, whereas a lamellar single crystal is prepared from dilute solution over a relatively long period of time - many hours rather than a few seconds for an air-cooled polymer. The difference in polymer morphology effected by crystallisation from a dilute solution is twofold:

i) a polymer molecule will not come into contact with a crystalline polymer surface at the instant it is formed, as is the case in a melt. As this is the rate-determining step, it means that the rate of crystallisation from dilute solution is slow, compared to that in a cooling melt.

ii) once a polymer molecule has been adsorbed onto the surface of a crystal, the low viscosity of the dilute polymer solution allows the entire polymer molecule to be incorporated into the lamellar crystal. There are no chain entanglements to prevent this happening, unlike in the polymer melt.

The effect of time is similar in both cases, in that increasing time increases the degree of crystallinity in the polymer sample - the percentage crystallinity in the

case of the cooled polymer melt and the percentage of polymer which has crystallised out of solution in the case of the single crystals. However, the rate of change of degree of crystallinity is markedly different in the two cases:

a) the rate of formation of crystalline material is proportional to the concentration of polymer in the solution.² As long as the amount of polymer in solution is large compared to that crystallising out of solution, then the rate of crystallisation remains constant.


b) the effect of annealing a solid polymer sample is to increase the degree of crystallinity by 5-10 % at the most, unless high temperature and pressure annealing²³ is used, as some of the polymer molecules may be tied in the amorphous region by having both ends incorporated into different lamellae.

Therefore it is likely that there are enough similarities between the structure of a polymer single crystal and that of the crystalline units in a semi-crystalline polymer to use the former as a model for the behaviour of the latter.

1.2.2 CRYSTALLISATION FROM AN UNSTRESSED MELT

1.2.2.1 SPHERULITIC MORPHOLOGY

When a melt of a semi-crystalline polymer - such as high density polyethylene (HDPE) or isotactic polypropylene (iPP) - is allowed to cool in an unstressed state, the mechanism of polymer crystallisation is three-dimensional spherulitic growth.²⁴⁻²⁷



Spherulites are the largest structural unit in a semi-crystalline polymer morphology. A spherulite is a three-dimensional region of mixed crystalline and amorphous polymer material; if a spherulite is allowed to grow unimpeded its shape is spherical. In polymer melts, however, it is usual for the spherulites to impinge upon each other; as a result, the shape of a spherulite is more commonly polyhedral. The diameter of a spherulite is in the range from 5 μ m to 100 μ m, depending upon the nucleation density of the sample - the smaller the number of nuclei, the greater the final size of the spherulite. The rate of formation and growth of spherulites may be monitored simply by viewing a melt (of a semi-crystalline polymer) cooling through crossed polarisers in an optical microscope - the boundaries between spherulites are visible (Fig. 1.4).

The micro-structure of a spherulite is more complex than that of crystalline areas randomly dispersed in a matrix of amorphous material. The crystalline areas grow outwards in all directions from the nucleus at the centre of the spherulite; these are called fibrils as they are very much longer than they are wide and have the appearance of being fibrous (Figs. 1.5 & 1.6). However, the structure is not fibrous in the truest sense, but is comprised of a series of chain-folded lamellar plates.

The polymer chains are arranged in much the same way as in lamellar single crystals, the lamellae being arranged such that the major axis of the polymer molecule is perpendicular to the major axis of the fibril. The only continuity between adjacent lamellae is that from the tie molecules, molecules which are included in two or more adjacent lamellae.²⁸⁻⁹

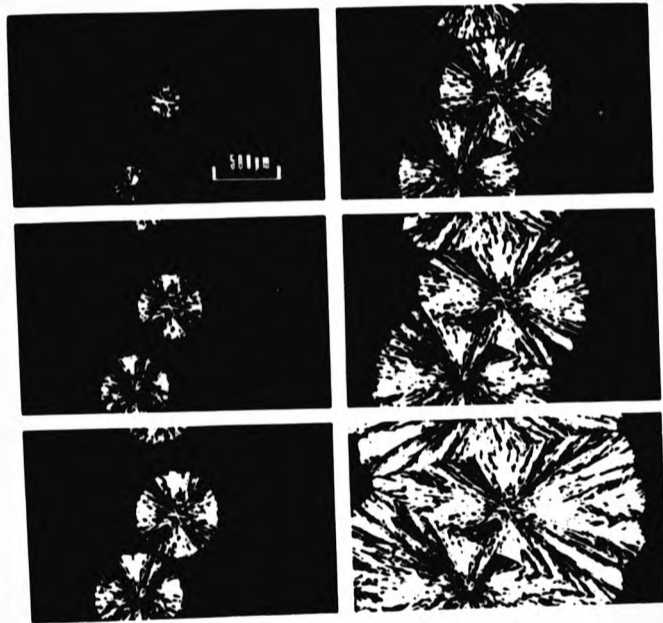


Fig. 1.4 - Spherulites forming from the melt - viewed through crossed polarisers.³

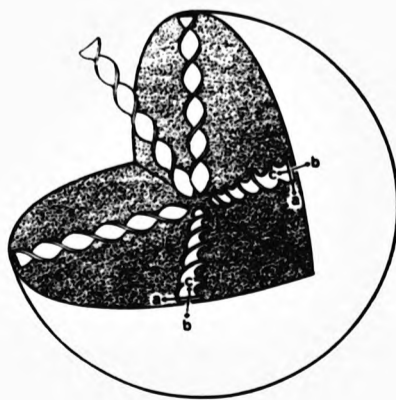


Fig. 1.5 - Fibrils in a PP spherulite.⁴

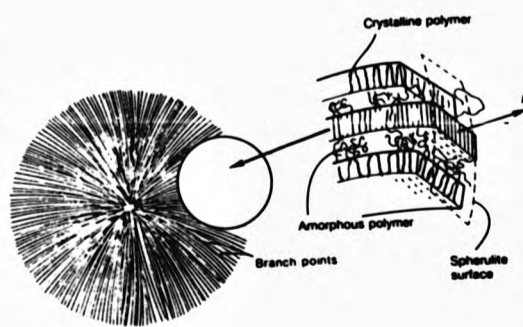


Fig. 1.6 - Schematic diagram of a spherulite.⁴


Hence the fibrils are not truly fibrous in nature, compared with polymer samples prepared from a rapidly agitated dilute solution, which have a chain-extended crystalline structure (section 1.2.3).³⁰⁻³⁷

The twisted-ribbon shape of the fibrils is due to screw-dislocation between adjacent lamellae - the planes of the lamellae are not parallel but instead the plane of the new lamella is rotated by a small angle with respect to the last lamella.³

Lamellae in a melt-cooled polymer morphology are not as perfect as the lamellar single crystals which are used as the theoretical model for lamellar behaviour. The surface of a lamella may have cracks or polymer chains protruding, having been prevented from becoming further incorporated in the lamella by physical constraints:

- i) the high melt viscosity may prevent a polymer chain from being fully incorporated into a lamella by restricting its mobility;
- ii) if both ends of a polymer chain are incorporated into different lamellae, it is almost impossible that the entire molecule may be incorporated into crystalline regions, so there must be a certain amount of amorphous material formed, especially if the two chain-ends are in different fibrils.

The new lamellar layer will form wherever the free energy is lowest, which is unlikely to be exactly the same conformation as the previous layer, especially if that is not a perfectly smooth surface. Similarly, small-angle branching of the fibrils (Fig. 1.5) is caused by a lamella forming at an angle to the side of the fibril, perhaps in a crack in the surface.



When a thin section of a spherulite is placed between crossed polarisers and viewed through an optical microscope, a Maltese Cross effect may be observed (Fig. 1.4), which is a characteristic of an isotropic semi-crystalline polymer. The Maltese Cross occurs when the principal optical directions are parallel to those of the microscope. When the sample is rotated, the Maltese Cross remains stationary. This shows that each radial unit - or fibril - has the same extinction directions, i.e. the polymer chains are not all aligned in the same direction but parallel or perpendicular to a radius.

1.2.2.2 MECHANISM OF SPHERULITIC GROWTH

Spherulitic growth is a two-stage process:²⁴⁻²⁷

a) Primary Nucleation

The formation of a crystalline surface, onto which other polymer chains may adsorb is known as nucleation. There are two possible mechanisms:

i) Homogeneous Nucleation - when sections of two or more polymer chains come into proximity in the melt, secondary forces bind the chains to make a nucleus.

ii) Heterogeneous Nucleation - when polymer chains adsorb onto a foreign surface, such as the mould wall or a dust particle in the melt, a nucleus is formed.

There is a third theory which proposes that small areas of crystallinity exist in polymer melts, even at temperatures significantly above the T_m , which act as nuclei when the melt is cooled. However, this should not apply to normal bulk cooling following extrusion or injection moulding, as high melt temperatures and high shear stresses are employed in these processes, which

reduce the probability of any ordered areas remaining in the melt.

In the majority of crystallisations, the nucleation is heterogeneous, although theoretical models use homogeneous nucleation as the basis for assumptions because it is easier to describe mathematically.

The rate of formation of nuclei is proportional to the supercooling of the polymer melt; the greater the difference between the T_m and the crystallisation temperature, T_c , the greater the number of nuclei formed per unit volume of polymer melt. The rapid increase in melt viscosity, a result of a high degree of supercooling, "freezes" bundles of polymer chains into nuclei; at lower levels of supercooling, only highly aligned bundles of chains would act as nuclei. Increasing the temperature increases the molecular motion of polymer chains which means that polymer bundles which are not highly aligned would tend to dissociate, that is they would no longer act as nuclei.

Under conditions for normal spherulitic growth, the greater the number of nuclei present per unit volume the greater the modulus of the quenched polymer; as there are more nuclei per unit volume, there are more spherulites per unit volume, so the average spherulite size is smaller. This increases the modulus of the polymer as the weak points, such as voids, are more evenly distributed throughout the material.

b) Secondary Nucleation

Once a nucleus has formed, crystallisation may take place. The nucleus may be considered a smooth crystalline

surface; crystallisation now proceeds by the addition of chain segments to the surface of the nucleus. As in the case of single crystal formation (Section 1.2.1)², lamellae produced at a constant value of supercooling have a characteristic thickness which is known as the chain-fold length. The initial stage in secondary nucleation is for sufficient chain segments to be adsorbed onto the surface of the nucleus to make the chain-fold length appropriate to the T_c used. Once this row has been deposited, the following rows are deposited rapidly, using the first row as a guideline. This continues until there is no room to deposit another row in this layer - as the same process is taking place at many sites on the nucleus - then one layer of polymer segments is complete and the process is repeated for the next layer of segments. As the individual lamellae grow outwards, each cuboid in shape but forming fibrils which are shaped like twisted ribbons (Fig. 1.5), interstices develop between them which contain polymer chains which are prevented from entering lamellar regions, i.e. amorphous material.

The optimum range of temperatures for effective crystallisation from an unstressed melt is:⁵

$T_{c \text{ max}}$ - 10°C below the melting point. Above this the segmental movement is too great - i.e. the formation of ordered regions is reversible because the polymer chains have too much energy - so a highly-crystalline morphology may not result from cooling at such high temperatures.

$T_{c \text{ min}}$ - 30°C above the glass transition temperature; below this temperature, the polymer chains do not have sufficient mobility to fold into lamellae efficiently.

1.2.3 CRYSTALLISATION FROM A STRESSED MELT

When a polymer melt is stressed, as it is when extruded or injection moulded, the melt becomes oriented in the direction of that stress; the degree of orientation is related to the magnitude of the stress. At zero stress, the polymer chains are coiled randomly to maximise the entropy of the melt; at an infinitely high stress, the polymer chains are uncoiled and parallel, with the major axis of the chain in the direction of the stress. Therefore the true picture of polymer melts such as those found in industry and research is somewhere between these two extremes, that of polymer chains beginning to uncoil, not parallel with each other but exhibiting a preference towards the direction of the stress.

However it is simpler, when carrying out an empirical study of such systems, to regard all oriented polymer melts as having parallel chains, varying only in the magnitude of the orientation. This may be regarded as the reduction of entropy in the polymer due to external forces - i.e. the draw-down imposed when the molten polymer extrudate is hauled off under tension. The magnitude of orientation of a polymer sample may be measured by heating the sample to just above its melting point and measuring the entropy-driven change in dimensions (Section 3.2.4).

When a stressed polymer melt is quenched, the degree of orientation retained in the quenched sample is dependent upon the time taken to quench the polymer; the longer the quenching time, the lower the orientation in the quenched sample, as entropy causes stress relaxation in the polymer melt. However, it may be assumed that melt stresses are retained in the solid polymer in industrial processes in

which the melt is rapidly quenched.

Uniaxial orientation is the orientation of the polymer chains in the melt in a single direction. When an oriented melt is quenched, the properties of the polymer, both physical and mechanical, become anisotropic. That is to say that the magnitude of the properties of the polymer varies according to the direction in which it is measured; the tensile properties of a polymer, such as the modulus, the yield strength and the break strength, are increased in the direction of the imposed stress but decreased in the transverse direction. The impact strength of a polymer is reduced by uniaxial orientation, as it is determined by the strength along the weakest axis. In order to improve both tensile properties and the impact strength, biaxial orientation is needed - orientation in two directions.

When an uniaxially stressed melt is quenched, the mechanism of crystallisation depends on the magnitude of the stress:

i) "Low Stress" - at low stresses, the mechanism of crystallisation is "deformed" spherulitic - the spherulites are formed by the same process as described in section 1.2.2, with the exception that there are small quantities of chain-extended crystalline structures present (see (ii) below) - due to areas of high local orientation in the melt - which impose constraints upon the freedom of the growth of the spherulites and the fibrils within. As a result, the spherulites are now ellipsoid and the fibrils, whilst still being radial, are no longer equivalent throughout the sample. The lamellae show a tendency to align in the direction of the stress (see also diagrams in chapter 6).

ii) "High Stress" - at high stresses, the dominant mechanism of crystallisation is the formation of SK structures,³⁰⁻⁵³ rather than spherulites. As a result, the resultant polymer morphology changes completely. The high orientation of the polymer chains increases the probability of homogeneous nucleation (section 1.2.2.2) - through a mechanism analogous to strain-induced crystallisation in vulcanised rubbers - to such an extent that a chain-extended polymer backbone is formed, which can act as a multi-sited nucleus for secondary nucleation. The lamellae formed at these sites grow perpendicular to the chain-extended backbone, the direction of the polymer chains being the same as that of the external stress.⁵⁴⁻⁶⁴

In an ideal system, where the polymer chains all have the same length and the temperature is constant throughout, the shape of the structure would be that of the chain-extended backbones having identical single lamellae at regular spacings; in practice, the lamellae are not identical.

This polymer morphology is called a "shish kebab" (SK) structure; the chain-extended backbone is the skewer and the lamellae are the pieces of meat. Fig. 1.7 shows the "SK" structures as formed from a rapidly stirred dilute solution of polyethylene.

When "SK" structures are formed from an oriented polymer melt,⁵⁴ the range of chain lengths present and local fluctuations in the melt temperature will cause the "SK" structures to become yet more complex; there may be several layers of lamellae of diminishing lamellar thickness. As a result, these structures will not resemble Fig. 1.7a as much as a series of bipyramids connected by a chain-extended backbone.

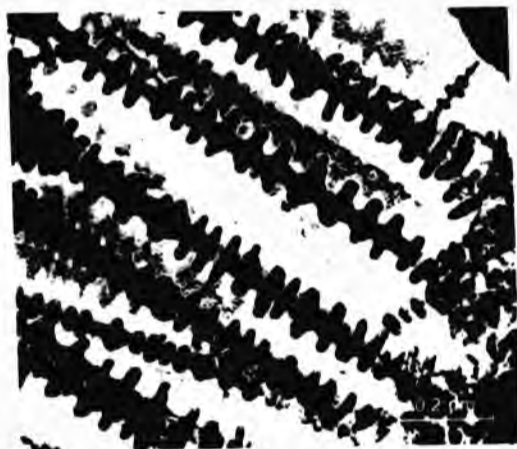


Fig. 1.7 - "shish kebab" structure of PE: a) electron micrograph¹⁴; b) Schematic diagram¹⁵.

If this structure is compared with the lamellar single crystals (Fig. 1.2) which result from an unoriented dilute solution², it demonstrates very clearly the effect of orientation of the polymer chains on the mechanism of crystallisation for a semi-crystalline polymer. It is reasonable to assume that a similar change of morphology will take place in melt crystallisation if the degree of orientation is sufficiently great.⁵⁵

The cases of "low" and "high" orientation described above are examples of the extremes found for a semi-crystalline polymer. However, the change between the two morphologies is probably continuous, with the occurrence of the SK structures increasing with increasing orientation of the polymer samples until the entire morphology is that of "SK" structures within an amorphous matrix. These intermediate cases, where spherulites, SK structures and regions of amorphous material co-exist are not well-documented as the properties of these materials are of lesser interest.

1.2.4 EFFECT OF DEGREE OF CRYSTALLINITY ON POLYMER PROPERTIES

The degree of crystallinity of a polymer is the percentage crystallinity present; it determines the modulus, tensile strength and density of that polymer - the greater the crystalline content, the larger the modulus and tensile strength of the polymer, as the crystalline regions of a polymer are more resistant to deformation, due to the inter- and intra-molecular forces which are present in crystalline regions of a semi-crystalline polymer but are not present in the amorphous areas.

The density of the polymer also increases with crystalline content, because of the close-packing in the lamellae which is not present in the amorphous regions. Hence the crystalline content of a polymer may be measured very accurately by density measurements, as the densities of wholly crystalline² and wholly amorphous (melt) forms of the polymer are known. Fig. 1.8 shows that the tensile strength of PE increases linearly with density which, in turn, is a measure of the degree of crystallinity.

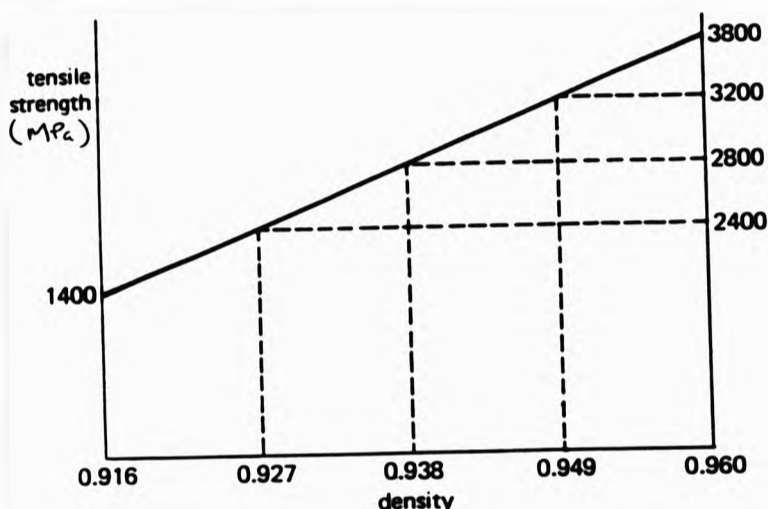


Fig. 1.8 - Effect of crystallinity on tensile strength of PE (Note that crystallinity increases with density).²

1.2.5 THE EFFECT OF PRESSURE ON POLYMER CRYSTALLINITY

The effect of ambient pressure on the physical transitions of materials - such as melting point, boiling point, changes in crystalline conformation and (in polymers) glass transition temperature - is dependent upon the sign of dV , the volume change effected by the phase change. For example, when the phase changes from to solid to liquid - fusion or melting - the effect of increasing the ambient pressure is to increase the melting point of the material if dV is positive, that is if the material expands on melting. The majority of organic and inorganic materials exhibit this behaviour. One important exception to this rule is water, H_2O , where dV is negative; the solid phase is less dense than the liquid phase, due to the hydrogen bonding between molecules preventing close-packing.

As a result, the effect of increasing the ambient pressure on the transition H_2O (s to l) - the melting point - occurs is to decrease the temperature at which it takes

place. However, the effect of increasing the ambient pressure on the transition H_2O (l to g) - the boiling point - is to increase the temperature at which it occurs. This is the same for all materials, as the gaseous phase of a material always has a greater volume than the liquid phase.

For semi-crystalline polymers, the phase change (s to l) always has a positive value of dV , as the melt is less closely-packed than the solid phase, irrespective of the degree of crystallinity of the polymer sample. If the ambient pressure is raised, the effect is to raise the temperature at which the (s to l) phase change takes place, or T_m . If the increase in pressure is sufficient, the T_m may be raised by as much as $100^\circ C$.

The effect of raising the melting point of the polymer under high pressure can be used in two ways when processing a polymer:

i) the melt may be quenched while under very high pressure (above 3 kbar for PE); this allows the formation of much greater lamellar thicknesses (up to 500nm compared with ~20nm for normal PE). This means that there are fewer folds per polymer chain. This process is called anabarcic crystallisation.³

ii) a polymer sample prepared by quenching in air at room temperature may be subsequently annealed (section 1.4) at the pressures and temperatures described in (i) above. It is possible to increase the lamellar thickness of PE to ~200nm by this method. This is known as superannealing. If the same temperature and pressure is used for anabarcic crystallisation and for superannealing of polymer samples, the lamellar thickness is always greater for the crystallised sample.²³

The use of high pressure allows the formation of a hexagonal crystal lattice which can accommodate the formation of lamellae having very few chain-folds which is not possible at low pressure. This conformation is metastable and reverts to the usual orthorhombic configuration at atmospheric pressure, but the increased lamellar thickness is retained in the stable form.⁶⁵⁻⁶⁷

1.3 ANNEALING OF MATERIALS

1.3.1 ANNEALING OF INORGANIC MATERIALS

Annealing is a technique which has been used for a long time in both the glass and the metal industries.³ It is the process of heating a shaped (metal) or blown (glass) sample to a temperature which is high enough to allow greatly increased atomic (metal) or molecular (glass) motion, yet not so high that the original shape of the sample is affected. This increased motion of the atoms/molecules permits reordering of microscopic structure of the material; this removes weak spots such as weld lines and, as a result, increases the modulus of the material.

The overall effect of annealing is the same for metals - which are completely crystalline owing to the small size and regular shape of the atoms - and for glass, which may be regarded as an inorganic amorphous polymer.

1.3.2 ANNEALING OF SEMI-CRYSTALLINE POLYMERS

As for inorganic materials, the technique of annealing polymeric materials is the treatment of moulded or extruded polymers using (increased) temperature, T_a , over a period of time, t_a .⁶⁷⁻⁶⁹ The effect of this treatment is to increase the tensile modulus of a semi-crystalline polymer (Fig. 1.9).

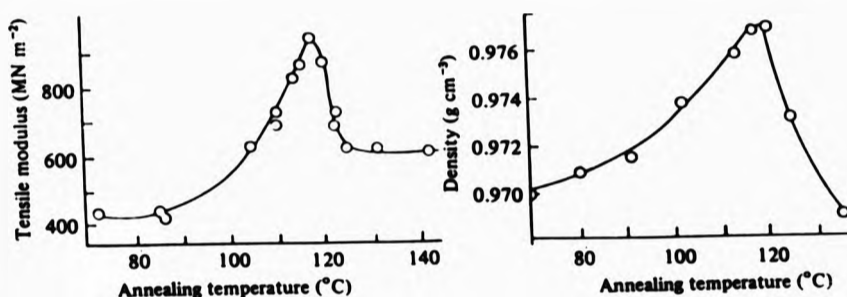


Fig. 1.9 - The effect of annealing temperature on a semi-crystalline polymer: i) Tensile Modulus; ii) Density.⁷⁶

The major difference between the two types of annealing is that the annealing of semi-crystalline polymers increases the strength by changing the morphology of the polymer, i.e. by increasing the degree of crystallinity of the polymer. This may be effected by one of two mechanisms, depending on T_a , which give rise to two distinct morphological forms:

i) "Low Temperature" annealing

When the T_a is less than or equal to the T_c , there will be enhanced molecular movement in the amorphous regions. As a result, there may be a slight increase in the degree of crystallinity, due to addition of chain segments to existing lamellae. The lamellar thickness, which is defined by the T_c , is unchanged. The result of this type of annealing is to increase the degree of crystallinity slightly and, therefore, increase the tensile properties of the polymer. The magnitude of this increase is dependent upon both T_a and the duration of the annealing.

ii) "High Temperature" annealing

When T_a is greater than T_c and more than 10°C below the

T_m , the morphology undergoes a significant change. It has been shown that a lamellar single crystal has a characteristic fold length which is dependent on the T_c and the molecular weight of the polymer²². It is reasonable to expect that the effect of annealing a melt-crystallised polymer sample within this range of temperatures is analogous to annealing a lamellar single crystal where the lamellar thickness increases with increasing T_a .

Lamellar thickening results from the migration of chain-ends through the crystal and proceeds by longitudinal diffusion of chain segments within the crystal lattice,²³ which is made possible by the initial decrease in density when a polymer sample is heated above its T_c (Fig. 1.10). Polymer molecules from the amorphous region must enter the crystal lattice to fill the holes left by such movement; if this does not happen, the increase of free energy in the system would prevent the original migration of the chain-ends, as this would create new surfaces within the lamella.

It has been shown that, for low molecular weight Poly (ethylene oxide), PEO, the lamellar thickness, L (nm), is given by the formula:¹⁶

$$L = P \times l_m \times (1 + n)^{-1} \quad (1)$$

where P is the number of monomer units in the chain

and l_m is the length of each monomer unit (nm)

and n is the number of folds per polymer molecule.

Therefore it is obvious, from equation (1), that for a polymer chain of a given length, there are a limited number of lamellar thicknesses available, the values of which may be predetermined. For example, if the chain length of a polymer molecule is 10,000 nm, then some of the available values for the fold length are:

Number of Folds	Fold Length
1	5,000nm
9	1,000nm
19	500nm
29	333nm
39	250nm
49	200nm
99	100nm

When a semi-crystalline polymer sample is annealed at a T_a above its T_c , the lamellar thickness increases by decreasing the number of folds present, one at a time.¹⁴

The degree of crystallinity is increased by the addition of polymer chains from the amorphous regions to existing lamellae; the increase in crystallinity will be greater than in i) above due to the greater mobility of the polymer chains at the higher temperature. The relationship between the density of the polymer sample and the duration of annealing is more complex.³

Initially, the density decreases with time and reaches a minimum at about 10 minutes (Fig. 1.10); thereafter the density increases with time. This is due to the internal rearrangement of the lamellae by which the chain-fold distance is increased: the separation of adjacent chains in the lamellae must be increased in order to weaken the effect of the secondary forces before the chain segments may diffuse through the lamellae to increase the chain-fold length. Because the lamellae are temporarily "swollen", the density of the polymer is decreased during that time; as the lamellae re-form with the new chain-fold length, the intermolecular distance is reduced and the density increases. After all the lamellae have re-formed, the

density continues to increase with time as material is added to the lamellae from the amorphous regions.

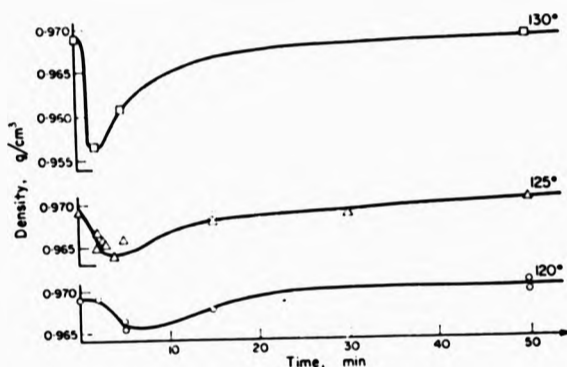


Fig. 1.10 - Effect of annealing time on density.⁶

When the T_a is less than 10°C below the T_m , however, the effect of annealing is reversed. The degree of crystallinity drops sharply with increasing T_a (Fig. 1.9). This is because the increased mobility of the polymer segments is now sufficient to remove polymer material from the lamellae into the amorphous regions. It is possible that the chain-fold length continues to increase with increasing T_a , but the amount of crystalline material decreases.

As a result, there is an optimum value of T_a at about 10°C below T_m which gives a maximum value of the density and, therefore, the degree of crystallinity and the tensile properties, such as the tensile strength, the modulus and the yield stress of the polymer. There is also a minimum annealing time, after which the density is higher than the initial sample; after this point, the degree of crystallinity of the polymer increases with time of annealing. Hence, the effect of annealing an unoriented polymer sample is simply to increase the degree of

crystallinity of the polymer which will lead to an increase of a few percent in the modulus or tensile properties, depending on the T_a and the period of annealing.

1.3.3 ANNEALING ORIENTED POLYMER SAMPLES

The effect of annealing on an oriented polymer sample may follow one of two mechanisms, depending upon the initial morphology of the sample as processed:

a) "Low Orientation"

Prepared from a "Low Stress" melt (Section 1.3[i]) - the initial morphology is "deformed spherulitic". The tensile properties of the sample are dependent upon both the degree of orientation and the degree of crystallinity: increasing the degree of orientation increases the tensile properties of the sample in the direction of orientation; increasing the degree of crystallinity of a polymer increases the tensile properties in all directions. Annealing a polymer sample which has a "low" degree of orientation (low O) increases the degree of crystallinity; it may also cause some relaxation of the imposed stress in the polymer, the magnitude of which depends upon T_a and t_a , leading to a small reduction in the degree of orientation of the polymer. Even annealing at high T_a and t_a causes only a small reduction in the length of the sample in the direction of orientation compared to that caused by heating to 5°C above the melting point of the polymer, i.e. shrinkage testing (Section 3.2.4).

The overall effect of annealing a low O sample is similar to that of annealing an unoriented sample; the deformation mechanism is the same for annealed and unannealed samples and the tensile properties are a

combination of the effects of orientation and crystallinity. The maximum modulus possible is greater than that for the annealed unoriented polymer and is approximately double that of the "ordinary" form.

b) "High Orientation"

Prepared from a "High Stress" melt (Section 1.3(ii)) - the initial morphology of the sample is a composite of "Shish-Kebab" structures in an amorphous matrix (this is discussed fully in chapter. 6). The effect of annealing this morphology at temperatures above its T_c is to produce a new form of the polymer, whose tensile characteristics differ in every respect from those of polymer samples which have the spherulitic morphology.⁷¹⁻⁷⁴

As a result, it must be supposed that semi-crystalline polymers produced under these conditions undergo tensile deformations by a completely different mechanism and, therefore, must have a different morphology to the spherulitic morphology described previously (Section 1.2.2.1).

This type of polymer morphology is called "Hard Elastic" and its structure and deformation mechanism is fully described in section 1.4.

1.4 "HARD ELASTIC" POLYMERS

When a highly oriented polymer sample is treated by annealing at a temperature 10-20°C below the melting point of the polymer, the resulting form of the polymer is "Hard Elastic" ("HE").^{37, 75-106}

This form of a polymer is called "HE" due to the increased tensile properties ("Hard") and the increased recovery from a 100% strain ("Elastic"). In theory, it is

possible to prepare the "HE" form of any semi-crystalline polymer which can exhibit the "shish-kebab" structure. The differences between "HE" and "Ordinary" forms of a semi-crystalline polymer are discussed more fully in the following sections.

Some polymers which have been prepared in the "HE" form are: Polyethylene,⁹⁹⁻¹⁰¹ polypropylene,^{75-76, 81-82, 87, 90} Polyoxymethylene and co-polymers,^{37, 75, 81-82} Poly (3-methylbutene),^{76, 82} poly (4-methylpentene),⁸¹ Poly (Ethylene Sulphide),⁸² and Poly (isobutylene oxide)⁸⁶.

1.4.1 A DETAILED COMPARISON OF "HARD ELASTIC" AND "ORDINARY" FORMS OF A SEMI-CRYSTALLINE POLYMER

1.4.1.1 TENSILE DEFORMATION

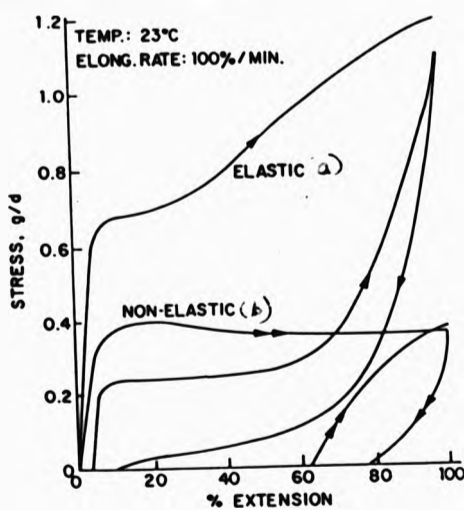



Fig. 1.11 - Stress - % extension curves for: a) "HE" type; b) "O" type samples⁷²

When a semi-crystalline polymer is processed under "O" conditions, the morphology of the sample is spherulitic, as described in section 1.2.2.1; under a tensile stress, deformation is plastic:

- a) $E = 0 - 5\%$: at first, the stress, S , increases approximately linearly with strain; $dS/dE = c$, where c is a constant. If the stress is removed during this stage of the deformation, the strain is almost completely reversible.
- b) $E = 5 - 10\%$: the rate of increase of stress with strain falls off (d^2S/dE^2 is negative) until a maximum value of stress is reached ($dS/dE = 0$ at $E = 10\%$). This is called the Yield Point. If the stress is removed during this stage, there is still a high degree of strain recovery (about 80%).
- c) $E = 10\%$ to about 20%: at this point, a "neck" starts to develop - part of the test piece becomes narrower as polymer chains there begin to align in the direction of the strain; the polymer structure is disrupted irreversibly - areas of sub-lamellar order are pulled out of adjacent lamellae to form new regions of highly-oriented crystalline order. As the cross-section of the sample is no longer constant the disruption of the polymer structure is concentrated at the narrowest point, which is where the effect of the load is greatest. As a result, the engineering stress required to produce further deformation decreases over the range $E = 11 - 20\%$ (Fig. 1.11b).
- d) $E = 20\%$ to about 500%: S is approximately constant for a large increase in E . As a result, this stage in the deformation of a semi-crystalline polymer sample is called cold-drawing. Usually, the entire polymer sample is converted from the initial spherulitic morphology to the oriented sub-lamellar structure during this stage. The strain recovery is very low during this stage, typically 30 - 40% recovery from a 50% strain.
- e) $E > 500\%$: after the cold-drawing is complete, the stress




begins to increase linearly with strain until fracture. This stage consists of further deformation of the new, sub-lamellar, structure. Much of this deformation is reversible, due to the highly-oriented nature of the new structure. It is common for the strain at break to be greater than 1000%. The shape of the stress-strain curve for an "O" polymer sample is that shown in Fig. 1.11b.

By comparison, the tensile deformation of a "HE" polymer form is similar to that of the "O" form only in the initial 10% strain. During this stage, the stress increases with increasing strain; however, no neck is formed at any stage in the deformation, so there is no yield point on the stress-strain curve. The stress continues to increase with increasing strain but the rate of change of stress with strain decreases. The sample fractures in the range 100 - 300% strain.

1.4.1.2 STRAIN RECOVERY

The mechanism for very high strain recovery in polymers - such as is found in vulcanised rubbers - is entropy-driven; entropy dictates that a molecule must have the greatest freedom of movement possible. When an amorphous polymer is stretched, the freedom of the polymer molecules is restricted by the orientation imposed. The entropy-driven recovery is not limited to the removal of the imposed stress; stress-relaxation takes place during the stretching of the sample by chain movement - chains which have been oriented to a certain extent re-assume the random coiled structure of maximum entropy. If this takes place whilst the sample is still stretched, the recovery when the stress is released will be low, because the entropy of the



system is high. In order to get high strain recovery, the polymer chains must be prevented from relaxing in the stretched sample. This requires that there must be connections between polymer chains, or tie points, which must not be severed during stretching. The chains should move relative to each other whilst retaining the original network structure. Then, when the sample is released, the low entropy of the system will cause the sample to return to its original shape. For rubbers, which have the best recovery characteristics, the tie points are provided by cross-linking - chemical bonding - between polymer chains.

If the "O" form of a polymer is stretched to less than 10% strain then released, the recovery will be high because the polymer structure has only been distorted but not destroyed. That is to say that the amorphous areas of the polymer are deformed by stretching the sample but the lamellae act as tie points, allowing a high recovery.

Once the yield point has been reached, however, this is not the case. At the yield point, the formation of the neck signals the beginning of the destruction of the polymer structure; after this, there is no possible mechanism for a high recovery. Spherulites are ruptured, lamellae are broken up due to the high localised stresses; polymer molecules and sub-lamellar crystalline aggregations are moved large distances - several chain-lengths in some cases - through the sample; chain segments may leave one crystalline structure, pass through amorphous material and join a new crystalline structure; material originally in the amorphous phase may join crystalline structures and vice versa.

If an "O" sample is stressed to 50% extension, then the

imposed stress is removed, there will be substantial damage to the structure of the sample. However, there will be amorphous areas which are somewhat oriented under the applied stress; as a result the sample will exhibit a recovery of 30-40% when the stress is removed.

When a "HE" polymer is strained, its deformation is completely different to that of an "O" semi-crystalline polymer or of a typical rubber.¹⁰⁷⁻¹²⁰ In fact, it most closely resembles the deformation of a toughened amorphous polymer, such as HIPS, which is modified brittle fracture. The tensile deformation of both of these forms follows this pattern:

- i) at low strains, voids are formed - the maximum void size is proportional to the strain, as is the total volume of the voids.
- ii) When the maximum void size is at a critical value, the appearance of the test sample changes abruptly, from translucent grey to opaque white.
- iii) As the strain increases, the voids continue to form and grow - at any strain there is a continuous range of void sizes, from the smallest measurable to the largest possible due to the magnitude of the strain.
- iv) The sample fractures. Strain at break may be less than 200%.

The strain recovery for the "HE" form is very high (60-95%) because the lamellae act as tie points for the chains in the amorphous areas. The full mechanism for the tensile deformation and the strain recovery for a "HE" polymer is given in the next section.

1.4.2. "HARD ELASTIC" MORPHOLOGY

"Hard Elastic" polymers are produced by the two-stage high-temperature annealing of highly-oriented polymer samples. After the initial process, which allows the polymer melt to crystallise when highly oriented, their morphology may be described as "shish-kebab"/amorphous composite (section 1.5). During the high-temperature (to within 10°C of the M.Pt.) annealing of the polymer sample, the lamellar thickness is increased, as is the overall degree of crystallinity of the polymer. Any tie molecules between adjacent lamellar regions of the "SK" structures, which are originally in the amorphous matrix, become incorporated further into the lamellar regions as the degree of crystallinity increases. This bridges the two adjacent lamellar areas (Fig. 1.13); small amounts of chain-extended crystallinisation may account for the traces of crystallinity whose axis is in the direction transverse to the axis of orientation observed in "true" HE polymers.³⁰ These taut tie molecules bridging adjacent lamellar regions from different "SK" structures creates a two-dimensional network of lamellar material.⁵¹⁻⁵³

At the same time, there is a secondary effect of the annealing process; as the lamellar rearrangements are taking place, the backbone of the "shish-kebab" structure "dissolves" in the amorphous phase. The high temperature of the annealing process allows the extended polymer chains to mobilise and then relax through an entropy-driven mechanism; although every one of the molecules that comprised the chain-extended backbone still remains a mutual tie-point for the two lamellae, they are no longer oriented. As a result of this contraction of the backbones,

the lamellar regions may become aligned in the solid polymer with their normals in the direction of the applied stress.

The combination of the two effects described above gives the characteristic "HE" polymer morphology: alternating sheets of crystalline and amorphous polymer aligned with the plane normals in the direction of orientation. This has been shown by electron microscopy (Fig. 1.12) The size of the amorphous and lamellar regions dimensions depend upon the processing history of the material.

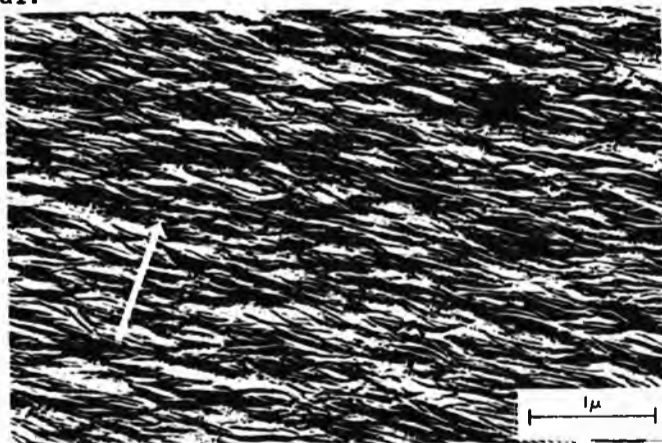


Fig. 1.12 - electron micrograph of "HE" morphology.⁷⁶

When an "HE" polymer sample is deformed along its major axis of orientation, the direction of stress, it is like deforming a sandwich; the weaker layer deforms preferentially. Therefore the amorphous layer, which is intrinsically weaker due to the lack of physical interaction between the polymer molecules, is deformed as the lamellar planes, fully intact, are pulled apart. A number of models have been proposed for the deformation mechanism of "HE" polymers,⁹⁹⁻¹⁰¹ one of which is the leaf-spring model (Fig. 1.13).

At a certain stage - above 20% strain - the chain-extended backbone is reformed (Fig. 1.13), along with smaller "fibrils", aggregates of polymer chains aligned by the applied deformation stress, which undergo strain crystallisation.

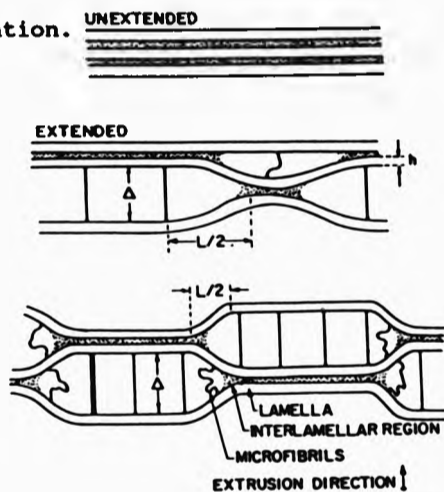


Fig. 1.13 - Leaf spring model of the deformation mechanism of an "HE" polymer sample.⁷⁵

Whilst the amorphous region is being deformed in this manner, the lamellae are not deformed at all - if they were deformed at low strains, the "HE" form of the polymer would not exhibit high strain recovery - so the cross-section of the sample remains constant throughout the initial stage of the deformation. As a result, the polymer sample undergoes a volume change during tensile deformation, due to the formation of voids throughout the amorphous regions of the sample. Void formation results from the construction of new internal surfaces in the polymer, which are generated by the combined effect of the high mobility of the polymer chains in the amorphous phase and the complete lack of mobility of the polymer chains in the lamellar planes.

When such a polymer sample is stressed, the polymer chains in the amorphous region are aligned to form fibrils

(Fig. 1.13); as the chains are pulled out of their original position, there is no material free to take its place, as the lamellae do not deform. As a result, holes - or voids - form in the amorphous region. The stress is spread evenly across the sample, due to the regular spacing of the fibrils, resulting in a large number of small voids instead of one large void.

When the deforming stress is removed, the high strain recovery observed is due to an energy-driven mechanism, due to the instability of the voids. When the stress is removed, the total free energy of the system is reduced and the total internal surface energy must decrease as a result. Hence the pore size decreases, but smaller voids remain, due to the retention of short fibrils in the relaxed sample.

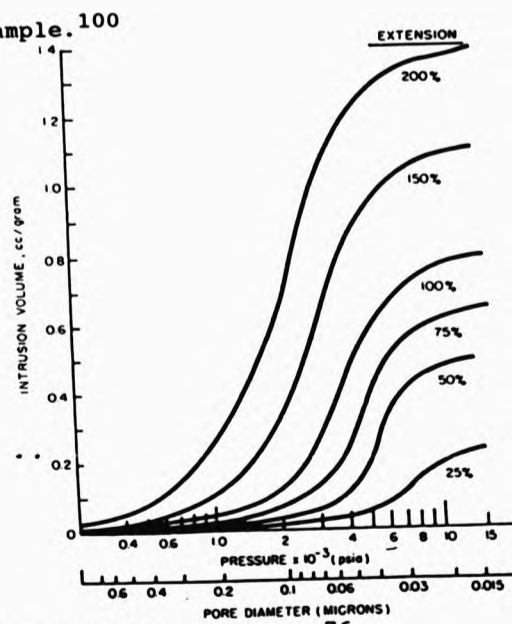


Fig. 1.14 - Porosimetry Testing⁷⁶

The size of the voids formed at a given strain varies greatly, but the maximum void size and the total volume of voids are directly proportional to the applied strain. Both

of these parameters and the distribution of voids in a strained "HE" sample may be demonstrated by mercury porosimetry (Fig. 1.14)⁷⁶. This is a technique which measures the volume of mercury absorbed by a porous polymer sample under a range of pressures. As mercury does not wet polymer surfaces, pressure must be applied to force the mercury into the voids. At low pressures, only the larger pores are filled; as the pressure is increased, progressively smaller pores are filled.

When the chain-extended backbone is fully reformed, i.e. strain crystallised, then further deformation of the sample proceeds by pulling polymer chains out of the lamellae, which requires more energy than deforming the amorphous phase. This results in the polymer chain-extended backbone growing in length as the sample is strained further. While this is happening, the maximum void size increases, as does the total volume of voids. The fibrils are thinner than the chain-extended backbone and, as a result, may break under this force. Consequently, the voids will interconnect, leading eventually to macroscopic fracture of the sample.

Conversely, in the deformation of "O" polymer samples, the lamellae are not aligned in the first place, so that amorphous material may move between lamellae when the sample is strained allowing the sample to narrow - voids cannot form when polymer material is freely mobile, as the material will flow in such a way as to prevent the formation of new surfaces, as this requires energy. Also, this mobility allows the polymer chains to crystallise in chain-extended position; this increase in strength of the amorphous region, coupled with the smaller lamellae of the "O" form of the polymer, explains how lamellae may be


deformed in the one case, but not in the other.

The two deformation mechanisms described above are models of the theoretical extremes of semi-crystalline polymer morphology, non-oriented and completely oriented. These extreme cases are the only ones which have been documented as the intermediary cases have not been deemed of interest so far. Depending upon the processing conditions, the morphology and deformation characteristics of a semi-crystalline polymer is likely to be a composite of these two extremes.

1.5 THE USE OF LIQUID METAL ALLOY AS QUENCHING MEDIUM FOR POLYMER MELTS.

It has been shown that, when a low melting point metal alloy is used as quenching medium for polymer melts, the crystalline content of HDPE increases when both the draw-down rate of the extruded polymer melt (a measure of the tension in the polymer melt and an indicator of the orientation in the quenched fibre) and the ambient quenching temperature are increased¹²¹. It was also noted that, when all other parameters were kept constant, the modulus and tensile strength of HDPE increased: a) with increasing draw-down ratio; b) with increasing ambient quenching temperature.

In that experiment, the low melting point metal alloy quenching medium was a quaternary eutectic of lead, tin, bismuth, indium and cadmium, which melts at 47°C. It was chosen due to its low melting point and high heat capacity in order to quench highly-strained polymer melts rapidly, freezing in the resulting orientation. As the quenching temperature approached the melting point of the polymer, it was observed that the samples produced had mechanical



properties higher than expected, e.g. the tensile modulus was approximately double that of HDPE quenched in air. It was found that these samples bore a close resemblance to samples of PP described in section 1.4, from which observation it was deduced that this may be a method of preparing "HE" HDPE alternative to the air quenching and annealing method already described. The advantage of this method is that it is an one-step process which might be suitable for the continuous production of "Hard Elastic" HDPE on a commercial level.

1.6 QUENCHING APPARATUS DESIGN

The work described in section 1.5 was carried out by hauling off under an external stress a polymer melt which has been extruded vertically upwards through a volume of the molten metal alloy contained within a temperature-controlled cylinder affixed directly onto the die. This method is not satisfactory for exact temperature control, as the die temperature may be in the range 160° - 200° C - normal for the processing of HDPE - but the bath temperature must be below 130° C in order to freeze the polymer melt; yet there is only a thin rubber insulator to prevent direct contact between the two. As a result, it was decided that the best way to overcome this problem was to extrude the polymer vertically downward into a bath, which was capable of being adjusted so that the die and molten metal alloy were in close proximity, but not in contact. The exact specifications for this apparatus are set out in section 2.1. Additionally, it was thought that it might be a more feasible engineering project to have the bath beneath the die, if there was to be a commercial

development of the process.

1.7 OBJECTIVES OF CURRENT WORK

The objectives of the current work are:


- i) The specification, design and production of an apparatus to produce HDPE extrudates which are quenched under tension by a liquid metal alloy coolant.
- ii) The production of HDPE extrudates as described in i) above under varying processing conditions; the main variables are the draw-down ratio and the quenching temperature. The effect of secondary factors, such as residence time in the liquid metal bath and annealing in liquid metal and air, are also studied.
- iii) The characterisation of the HDPE extrudates produced according to ii) above. The methods used are:
 - a) Tensile testing, which determines the yield stress (or the stress at 10% elongation, if there is no yield point), the stress at break, the elongation at break, the modulus and the recovery from a cyclic 50% strain.
 - b) Shrinkage recovery, which is a measure of the orientation of the polymer molecules in each solid polymer sample.
 - c) Density measurements, using a density column, which measures the density and, therefore, the degree of crystallinity of each polymer sample.
- iv) The establishment of a relationship between the processing conditions and the resulting morphology and deformation mechanism of each HDPE extrudate prepared by this method.

CHAPTER 2 - FACTORS INVOLVED IN THE DESIGN OF APPARATUS

2.1 SPECIFICATION OF QUENCHING APPARATUS

The brief for the initial stage of this course of work is to design and construct an apparatus which is capable of fulfilling the general requirements set down in Chapter One. The more detailed requirements are as follows:

- i) a bath which can hold a volume of liquid metal alloy - the size of which is determined in Section 2.2 - through which the polymer extrudate may pass in the processing stage. The bath must have the means to heat the metal alloy from room temperature - at which it is solid - to the required temperature, above 96°C , the melting point of the metal alloy coolant, and below 130°C , the melting point of the polymer. The bath must also be capable of keeping the temperature constant at the required level, to an accuracy of $\pm 0.25^{\circ}\text{C}$, as earlier work has shown that the tensile modulus of an HDPE fibre varies greatly with temperature at these temperatures.
- ii) a means must be devised by which the polymer extrudate may enter the liquid quenching medium, pass through a calculable distance of it, then exit it, as a continuous process.
- iii) a means must be devised to enable the polymer extrudate to pass through the liquid coolant under a constant tension, i.e. at a constant output rate, haul-off speed and residence time - in both media, air and liquid metal - which may be altered as required and measured exactly.
- iv) the apparatus must be capable of performing equally



well with fibres 1-2mm in diameter or films 0.2mm thick.

v) A number of dies (3) must be prepared which allow the polymer melt to be extruded vertically downwards; the direction of the haul-off is vertically downwards as the extrudates pass around a two-roller system (Section 2.3).

It is important that the direction of extrusion is the same as the direction of haul-off in order to eliminate the shear stresses which would otherwise act upon the melt as it is quenched. This ensures that the only forces acting upon the melt are in the direction of the stress and that the melt is unhindered when exiting the die.

This preparation involves:

a) the modification of an existing circular die by blocking off the original aperture and drilling a new one in the side. The circular die is located into the extruder by means of a screw thread; when the die is being screwed into the extruder, the die aperture is rotated also. Therefore, great care must be taken in order to ensure that the die is positioned so that the melt is extruded vertically downwards (for the reasons stated above) before starting an experiment.

b) the design and manufacture of adapters (2) to accommodate existing dies (flat film and strip) such that they may extrude vertically downwards. The size of the largest of the three dies (flat film) is a primary consideration when the quenching apparatus is being designed, as it dictates the minimum width of the apparatus.

2.2 DIMENSIONS OF BATH

- b) internal breadth at top
- e) section thickness
- c) internal width
- a) internal height
- f) 5/8" channels for cartridge heaters
- g) 3/8" channels for oil cooling
- h) probe for temperature control
- d) internal breadth at base

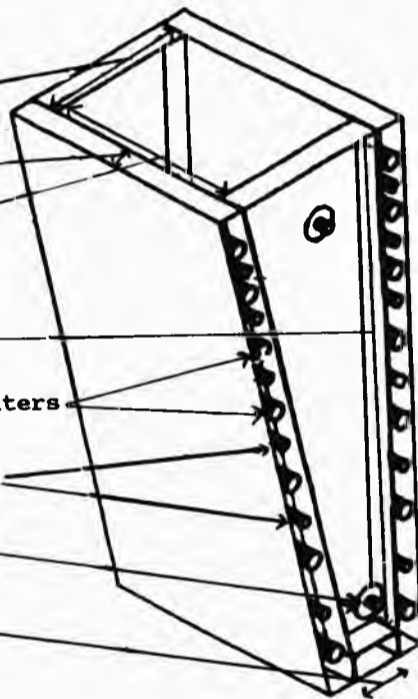


Fig. 2.1-shows the bath after assembly; the sections may be seen individually also.

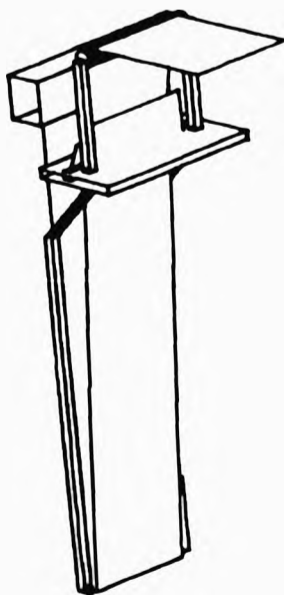



Fig. 2.2 - shows the polymer film extruded through a flat-film die and hauled off around two rollers.



The bath dimensions were designed to suit the following requirements (fig. 2.1):

2.2.1 INTERNAL HEIGHT

The internal height (Fig. 2.1a) is 500mm. This dimension defines the maximum residence distance, approximately double the depth; in earlier work, the maximum residence distance was approximately 250mm, so a maximum residence distance of 1m was chosen as greater than sufficient. Also, the maximum clearance between the film die and the trolley (at its lowest position) is 550mm, which is a limiting value for the external height - the base section thickness is 25.6mm, so the maximum internal height possible is 524.4mm. It also defines the volume capacity of the vessel, given that the other dimensions are the minimum required.

2.2.2 INTERNAL WIDTH


The internal width (Fig. 2.1c) is 185.6mm (7 1/4"). This was chosen to enable the location of an existing 10cm flat film die, whose external width is 183mm, close to the surface of the coolant when the bath is not completely full, minimising air-cooling of the extrudate.

2.2.3 INTERNAL BREADTH AT TOP

The internal breadth of the bath at the top (Fig. 2.1b) is 153.6mm (6"). This allows sufficient clearance for the location of the roller system next to the film die when the apparatus is in use.

2.2.4 INTERNAL BREADTH AT BASE

The internal breadth at the base (Fig. 2.1d) is 51.2mm (2"). The reason for this was to reduce the capacity of the bath without affecting the criteria (i) - (iii) above. The



internal breadth at the base may not be less than this because the roller system could not otherwise locate into the bath effectively.

2.2.5 WALL SECTION THICKNESS


The thickness (Fig.2.1e) of all wall sections is 25.6mm (1"). Apart from providing the strength to hold the coolant - see Section 2.2.8 - this is to accommodate the channels for the heaters described in chapter 2.2.6.

2.2.6 CARTRIDGE HEATERS

A series of channels (16mm, 5/8" diameter, Fig. 2.1f) has been drilled out of the walls of the bath in order to accommodate fourteen cartridge heaters (seven in each of the two 185.6mm, 7 1/4" wide walls). This provides a maximum of 4.2 KW of power to the bath. The spacing of the channels is arranged according to an arithmetic progression - the distance between the channels decreases regularly from the base of the bath to the top, to compensate for its increasing cross-section. A second series of channels (9.6mm, 3/8" diameter, Fig. 2.1g) has been drilled out in case oil-cooling is required for more accurate temperature control. These, smaller, channels are positioned equidistantly from the adjacent cartridge heater channels.

2.2.7 TEMPERATURE CONTROLLERS

The heating cartridges are divided into four zones - top left, top right, bottom left and bottom right - each of which is powered by one of four temperature controllers. There are four probes located in two sides of the bath (Fig. 2.1h); these probes monitor the temperature at fixed points inside the bath and relay the information back to



the temperature controller for that zone, which then alters its output accordingly. An electric thermometer with a 50cm probe is used to check the temperature profile through the bath, to ensure that there are no hot or cold spots within the bath.

2.2.8 INCLUSION OF TAP


A simple tap was built onto the bath, near the bottom of one of the side walls, to facilitate the removal of the liquid metal alloy after each experiment. This was due to the fact that the alloy does not change in volume when a change in temperature occurs. If the alloy is allowed to remain in the bath, the reduction in temperature of the apparatus causes the alloy to solidify at 96°C ; however the mild steel walls continue to contract below this temperature due to the coefficient of thermal expansion of the material. The result is a large shear stress exerted upon the bolts which hold the bath together; the bolts may shear off completely.

2.2.9 MATERIAL FOR BATH

The material chosen for the construction of the bath was mild steel plate; this is due to two factors being taken into consideration:

a) the metal alloy coolant contains lead, tin and bismuth: metals such as copper and aluminium will dissolve slowly in the molten alloy; steel is inert towards it.

b) the density of the metal alloy is very high ($9.6\text{g}/\text{cm}^3$), so the material must be strong enough to withstand the pressure generated by the weight of liquid in the bath; when full, the bath holds 75 Kg of the liquid metal alloy.



One inch thick mild steel plate was sufficiently strong to withstand this pressure.

2.2.10 CONSTRUCTION OF BATH

The five sections which comprise the bath - front wall, back wall, two side walls and the base (Fig. 2.1) - are joined together by means of a number of bolts which pass through channels in the front and back walls and locate exactly into threads drilled out of the edges of the side walls.

A sealant was used to make the bath more watertight - the liquid metal alloy has a very low viscosity at the temperatures used in these experiments which, combined with the very high density and large amounts used, lead to a certain amount of leakage from the vessel. This, however, could be kept to a minimum by re-applying the sealant to the joins occasionally. Nevertheless, the bath is placed on a large tray to collect any leakage.

2.3 ROLLER SYSTEM

The frame is made from mild steel - again to provide strength and chemical inertness against the molten metal alloy - and the rollers are made from PTFE (diagrams 2.2 & 2.3). The design of the system is such that it may be located into - or removed from - the bath at any time, even when an 100mm flat film die is located into the bath, hence the dog-leg shape. The second main consideration for the design is that the polymer extrudate should travel vertically downwards, so that there are no bending stresses acting on it. This dictates that the edge of the bottom roller must be directly beneath the die slit, that is 29mm from the wall of the bath. The gap in the horizontal plate is to allow the extrudate to exit the bath; there are no design considerations other than the dimensions of the extrudate after draw-down. The upper roller is simply to facilitate haul-off of the polymer.

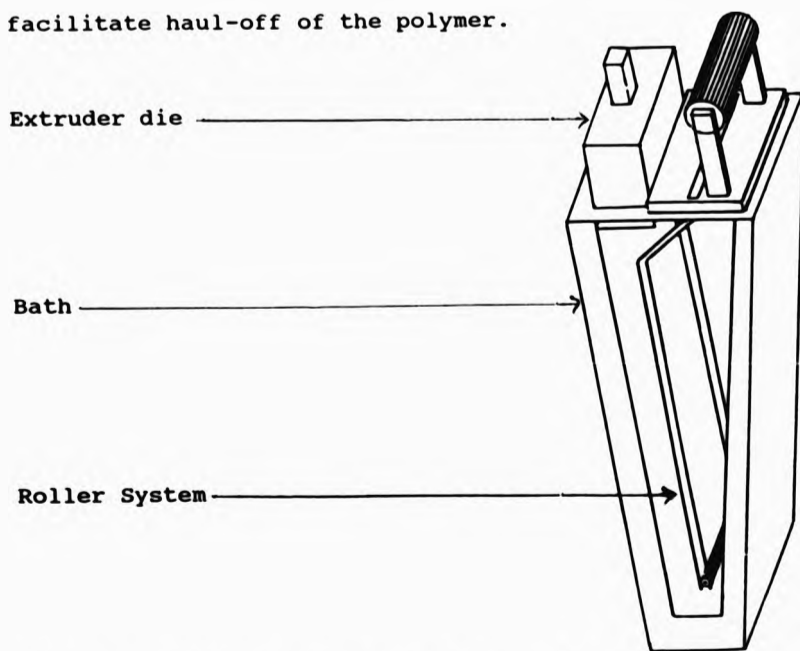
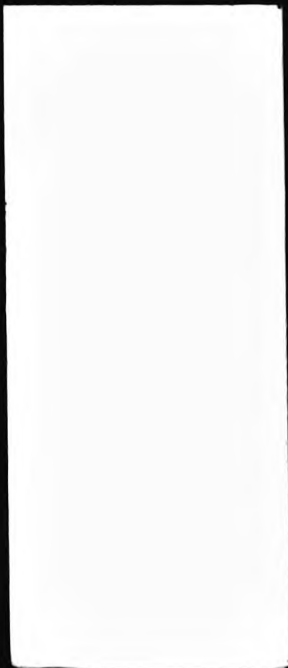


Fig. 2.3 - the roller system locates into the bath



2.4 HAUL-OFF EQUIPMENT

This comprises a pair of rubber-covered rollers on a frame - situated on a wooden base for stability - the lower of which is driven by a motor connected to it by a belt. The gap between the rollers may be varied by means of a screw on either support frame. This is essential for constant tension haul-off.

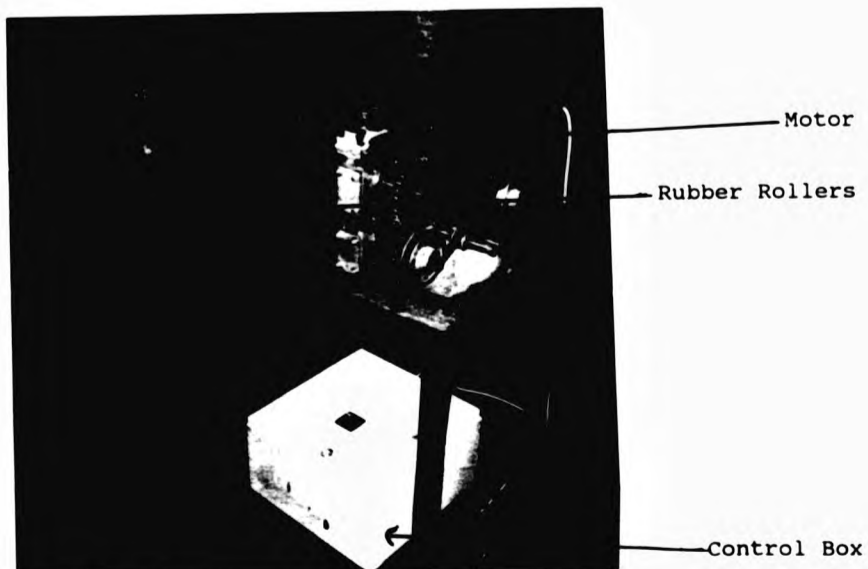


Fig. 2.4 - Haul-off apparatus

2.5 MOBILITY OF APPARATUS

The bath and the heat controllers are contained upon a "DANDYLIFT 400" trolley so that it may easily be located under whichever die is being used. The trolley has four wheels, two of which may be locked in place, and a moving table which may be raised hydraulically by means of a foot pedal. The table may also be lowered slowly by means of a lever, to ensure safe handling of the liquid metal alloy.

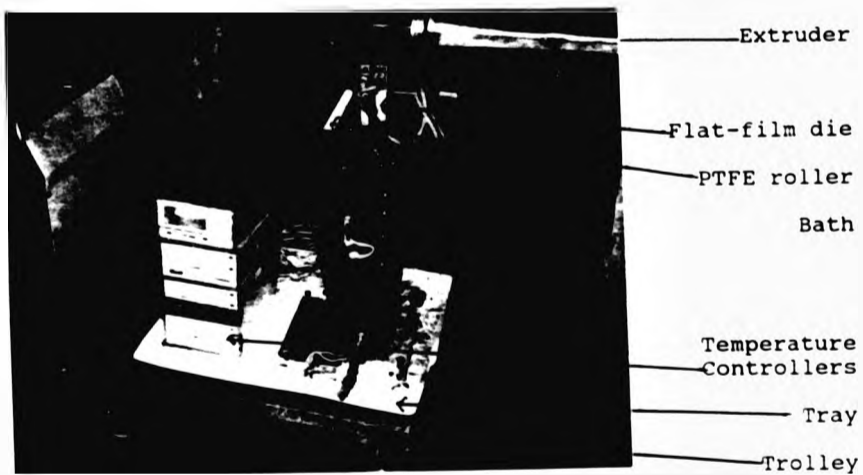


Fig. 2.5a - Full apparatus ready to be raised into position

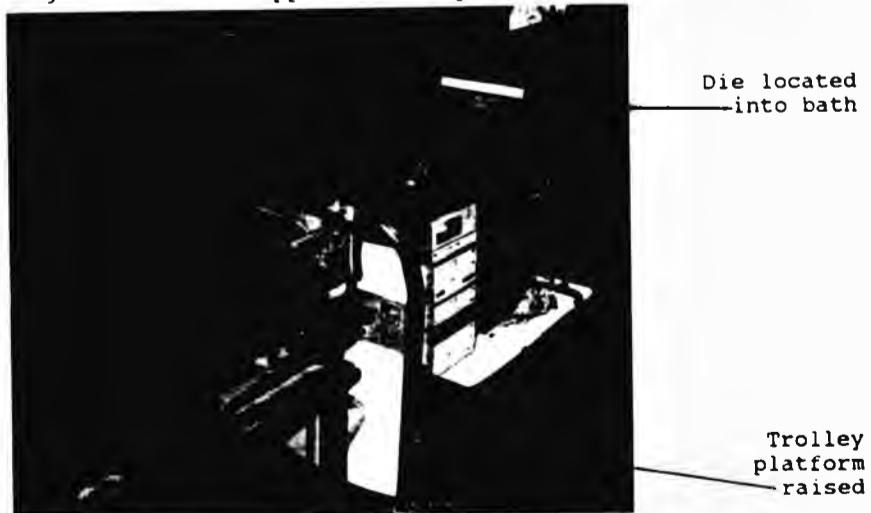


Fig. 2.5b - Full apparatus located into flat-film die

CHAPTER 3 - EXPERIMENTAL WORK

3.1 MATERIALS USED

3.1.1 METAL ALLOY COOLANT

The metal alloy used to quench the molten polymer extrudates was a ternary eutectic of lead (32%), tin (16%) and bismuth (52%) which melts at 96°C. The reasons for using this alloy over that described in section 1.5 were:

- a) the temperature range required for this work was 105°C-130°C; the metal alloy is molten throughout this range.
- b) the cost of this alloy is one quarter of that of the quaternary eutectic alloy used in previous work,¹²¹ due to the absence of cadmium and indium which are much more expensive than the other constituent elements;
- c) cadmium is a highly toxic element; using an alloy which is similar to that used previously but which does not contain cadmium greatly reduces the risk involved. Although the alloy still contains lead, which can cause brain damage if ingested, it is much safer to use.

3.1.2 GRADE OF POLYMER

Two grades of HDPE are used in the course of this work:

a) In all experiments which use the circular die, the grade of HDPE used is Hoechst's Hostalen GF 4750 - a grade designed specifically for producing highly oriented monofilaments:

Density at 23°C = 0.948 g/cm³

M.F.I. 190/2.16 = 0.4 g/10 min

Yield Stress . = 23 MPa

Tensile Modulus = 900 MPa

b) In all other experiments - i.e. those which use the strip or flat film dies, the grade of HDPE used is Hoechst's Hostalen GF 7750 M - a grade designed specifically for preparing highly oriented films:

Density at 23°C = 0.957 g/cm³

M.F.I. 190/2.16 = 0.5 g/10 min

Yield Stress = 28 MPa

Tensile Modulus = 1200 MPa

3.2 EQUIPMENT USED IN EXPERIMENTAL WORK

3.2.1 EXTRUSION OF POLYMER SAMPLES

In all experiments the HDPE was extruded through a Brabender Single-Screw Extruder (lab. size, 19mm barrel diameter) fitted with:

a) a custom-made 1.6mm diameter circular die which allowed the polymer to be extruded vertically downwards. The four zone temperatures used with this die were:

Zone 1: Feed Zone	- 160°C
Zone 2: Compression	- 160°C
Zone 3: Metering	- 170°C
Zone 4: Die	- 180°C

which gave the extrudate a melt temperature of 173°C, as measured by a needle pyrometer. Experiments 1, 2, and 3 used this apparatus.

b) a 13 x 3 mm strip die, encased in a specially designed dapter. The temperature of the extruder zones were as for (b) above. The five temperature zones used were:

Zone 1: Feed Zone	- 160°C
Zone 2: Compression	- 160°C
Zone 3: Metering	- 170°C
Zone 4: Adapter	- 180°C
Zone 5: Die	- 180°C

The extra extrusion zone is needed because the distance between the metering zone and the mouth of the die is increased by the presence of the adapter. The melt temperature was again 173°C. Experiments 4 and 5 used this apparatus.

c) a 100 x 0.5 mm flat film die, encased in a specially designed adapter which allowed the die to extrude vertically downwards. The melt temperature was again 173°C. Experiment 6 used this apparatus.

3.2.2 TENSILE TESTING OF SAMPLES

The HDPE samples were analysed by tensile testing using an Instron 1026 Tensometer. In all tests, the settings on the tensometer were:

- i) Jaw separation - 50mm. This defines the length of the sample to be tested.
- ii) Crosshead speed - 100mm/min. This is the speed of separation of the jaws.
- iii) Chart speed - 200mm/min. In one minute, a strain of 200% is represented by 200mm of chart paper; therefore an elongation of 1% is represented by 1mm on the chart.

The principal means of characterising the samples were:

- a) the stress-strain curve over the initial 20% strain;
- b) the yield stress - or point of inflexion on the stress-strain curve;
- c) the stress at break;
- d) the elongation at break.

All testing was carried out at room temperature, -25°C.

3.2.3 CYCLIC STRAIN RECOVERY

A sample is placed between the jaws of the tensometer and stretched at a constant speed to a given strain (50%); then the jaws are returned to the original position at the same speed. As soon as the jaws are at the starting position, the jaws begin to separate again. This cycle may be repeated as many times as is required, measuring the recovery each time. The percentage recovery is given by:

$$R = (L_S - L_U) / (L_S - L_O) \times 100 \% \quad (1)$$

where L_O is the original length of the sample;
and L_S is the length of the strained sample, i.e. $3L_O/2$;
and L_U is the length of the strained sample after it has been allowed to relax for approx. $15s^*$.

As $(L_S - L_O) = L_O / 2$ for a 50% strain, Equation (1) simplifies to:

$$R = 2(L_S - L_U) / L_O \times 100 \% \quad (2)$$

*The exact time of recovery depends on the value of R; for each sample the recovery time (i.e. the period during which the test piece is not under tension) is given by the sum of two parts. All samples have 15 seconds relaxation time as the jaws of the tensometer are closing (the return half of the cycle); when the jaws begin to separate again, the extra period of relaxation depends upon the degree of relaxation. For example, a sample with $R = 100\%$ would have 0s extra, as the sample would be in tension as soon as the jaws start to separate and a sample with $R = 0\%$ would have 30s as the sample would never be in tension.

$$t_R = 15 + \{(1 - R) \times 15\} \quad (3)$$

3.2.4 SHRINKAGE TESTING

The uniaxial orientation in a polymer sample - prepared using any of the dies described in section 3.2.1 - may be quantified simply by this method:

The length of a polymer sample (fibre, strip or uniaxial film) is measured in the direction of orientation (l_0). The sample is then placed on a metal tray which contains a thin film of silicon oil, which prevents the polymer sample from sticking to the tray. The tray is placed in an oven which is thermostatically controlled at $5^{\circ}\pm 2^{\circ}\text{C}$ above the T_m of the polymer for 15 minutes; the new length of the sample is now measured in the same direction as before (l_r). A convenient means of comparing the degree of orientation, $D(O)$, of the polymer samples prepared in this work is given by:

$$D(O) = \text{Log} (l_0/l_r) \quad (4)$$

This method is based upon the entropy-driven change in the conformation of the polymer molecules once the polymer sample has become molten. As the polymer molecules change from the highly linear anisotropic form to the randomly-coiled isotropic form the macroscopic effect on the polymer sample is that there is a change in the dimensions of the sample, i.e. the sample shrinks along its length and expands along its width and breadth. Hence, the greater the reduction in length, the greater the orientation in the original sample. The ratio l_0/l_r is one way of quantifying the magnitude of the orientation; the logarithm of that ratio is more convenient, as all the values obtained in this work were in the range 0 - 2.

3.2.5 MEASUREMENT OF DEGREE OF CRYSTALLINITY

The degree of crystallinity of a polymer sample may be measured using a density column; this is a column of liquid - a mixture of two liquids in fact - wherein the density of the liquid varies linearly with the position in the column. At the top of the column, the density is that of the less dense of the two component liquids; at the bottom, the density is that of the more dense. Small hollow glass beads of known density are used to calibrate the density column: the beads are dropped into the column and allowed to come to rest; the position of each bead is plotted on a graph against its density. The best straight line fit is calculated and drawn on the graph as the calibration curve.

When a polymer sample of unknown density is to be measured, it is placed in the density column and allowed to come to rest. When at rest, the position of the sample in the column is recorded and translated into density by using the calibration curve.

It is possible to measure the density of a polymer very accurately if the density column is carefully constructed. In order to measure a density accurately to four decimal places, the approximate density of the samples must be known to three decimal places. Hence if the polymer (as supplied by the manufacturer) has a density of 0.948g/cm^3 , then it is possible to construct a density column which varies from 0.945g/cm^3 to 0.965g/cm^3 over a column length of 1 m. This gives a resolution of 0.0002g/cm^3 per cm on the density column, so a change of 0.0001g/cm^3 is easily discernible.

3.3 PREPARATION OF SAMPLES

The preparation of HDPE samples for testing was carried out in the following manner:

3.3.1 MEASUREMENT OF OUTPUT RATE

The output rate of extruded HDPE was measured for a particular screw speed, which was monitored on the speed gauge on the extruder and verified using a tachometer; the temperature settings were kept constant and the same grades of HDPE were used throughout each experiment. Under these conditions, the melt pressure in the extruder barrel and the melt temperature at the die were constant. The melt pressure was monitored by a pressure gauge attached to the extruder; the melt temperature was checked occasionally using a digital thermometer with a needle probe, the tip of which was inserted into the die whilst extrusion was taking place. The output rate was measured by collecting the output for one minute - the weight of polymer collected was the output in g/min. Having measured the output, the screw speed was kept constant throughout the experiment.

3.3.2 LOADING EXTRUDATE ONTO HAUL-OFF SYSTEM

When a sufficient length of polymer melt had been extruded (approx. 250mm), the end of the extrudate was passed around the bottom roller of the roller system (Fig. 2.2) -which was resting laterally on top of the cooling bath (Fig.2.1) - through the slit in the steel plate in the roller system and over the second roller to the nip rolls which were moving at a speed sufficient to take up any slack on the extrudate.

3.3.3 INSERTING THE LOADED ROLLER SYSTEM INTO THE BATH

Having first ascertained that the bath was at the required temperature at various positions - on the surface at the point of entry of the extrudate and near the roller and at points in between - using the digital thermometer with the 50cm probe, the roller system was inserted into the bath. In order to ensure that the bottom roller was vertically below the die:

- a) the bath was located directly beneath the die.
- b) it was ensured that the lower half of the roller system (bottom roller and dog-leg frame) was parallel with the back wall - defined as the vertical wall of constant width (Fig.2.1).

The bath was capable of being raised or lowered by a foot-operated hydraulic pump on the trolley which held the bath - so that the distance that the polymer melt travelled through air before entering the quenching medium could be varied, to ensure that the extrudate was still molten on entering the liquid metal bath. If the polymer extrudate is not molten when entering the liquid metal bath then the experiment is invalid, as the polymer will have been quenched in air, not liquid metal alloy.

3.3.4 VARIATION OF HAUL-OFF SPEED

The haul-off speed is varied by means of a potentiometer connected to the power supply to the motor. The speed of rotation of the nip rolls is measured using a tachometer. In all experimental work using the circular die, haul-off speeds of 40, 60, 80, 100, 120 and 140rpm (the maximum possible) are used for each bath temperature and each

output rate. In the other experiments, a variety of haul-off speeds are used and the draw-down ratio calculated and the degree of orientation measured (section 3.2.4).

3.3.5 VARIATION OF QUENCHING TEMPERATURE

The temperature of the quenching medium was set by three dials adjusting the temperature on each of the three temperature controllers; changing the temperature profile (it was not necessarily constant throughout because of different rates of heat loss from different sections of the bath due to the shape of the bath) was performed by changing the settings on one or more of the controllers. The bath temperature was monitored constantly - before every sample was taken - using a digital thermometer and probe. Bath temperatures used in these experiments were integral in the range 111^o-125^oc.

3.3.6 VARIATION OF OUTPUT RATE

The change in output rate was determined by the screw-speed, all other extruder settings being constant. This was set before an experiment and never altered during it.

3.3.7 LEVEL OF LIQUID METAL ALLOY IN BATH

The depth of the liquid metal alloy governed two factors in the production of fibres described in section 3.3:

a) in conjunction with the position of the bottom roller on the frame (chapter 3.3.8), the level of the liquid metal alloy defined the residence distance for the fibre passing through the bath. The residence distance, in conjunction with the screw speed (i.e. the output rate) and the haul-off speed, defined the residence time for the extrudate (Appendix 1).

b) in conjunction with the position of the bath, i.e. the distance of the top edge of the bath relative to the die (section 3.3.9), the level of the liquid metal alloy in the bath defined the residence distance in air - the distance between the die and the surface of the quenching medium. In all experiments, the height of the liquid metal alloy was constant.

3.3.8 POSITION OF BOTTOM ROLLER ON FRAME

The bottom roller, which was located into the bath during experiments, was capable of being positioned at any point on the lower half of the support frame (Fig. 2.2). In conjunction with the level of the liquid alloy in the bath (section 3.3.7a) this determined the residence distance, etc. of the extrudate. In all experiments, the position was constant.

3.3.9 POSITION OF BATH

The position of the bath relative to the die was varied by means of a foot-operated hydraulic pump. In conjunction with the level of the liquid metal coolant (section 3.3.7b), this determined the residence distance in air of the extrudate. In all experiments thus far, its position was constant.

CHAPTER 4 - RESULTS

In this chapter, the following abbreviations are used:

BT - the bath temperature, i.e. the temperature of the liquid metal alloy used to quench the extrudates.

OR - the output rate, in revolutions per minute. The output, in grams per minute, is approximately proportional to the OR during any single experiment.

HOS - the haul-off speed, in revolutions per minute, is the speed of rotation of the rubber rollers used to haul-off the extrudates after passing through the liquid metal bath. The actual speed (in m/s) at which the quenched extrudate moves is proportional to the HOS.

DDR - the draw-down ratio is defined - for the purposes of this work- as the ratio of the HOS to the OR. The actual draw-down (ADD) is the ratio of the haul-off speed (in m/s) to the output speed (in m/s). It was not used in the construction of these experiments because it is difficult to calculate the ADD precisely.

a:b RATIO - this is the ratio of the long (a) and short (b) dimensions of the extrudates, which are orthogonal. For the strip and flat-film dies, each extrudate's cross-section is rectangular, so the a and b dimensions are width and breadth. For extrudates from the circular die, the a and b values should be equal, as diameters of a circle. However, many of these extrudates have a squashed circular cross-section; in these cases, the a dimension is parallel to the flat side and the b dimension perpendicular to it. In the following tables of dimensions, the a value is given first.

4.1 - CONTROL EXPERIMENT

TABLE 4.1.1 - DIMENSIONS, AREAS & A:B RATIOS OF EXTRUDATES
(OR = 6 RPM)

HAUL-OFF SPEED	DIMENSIONS (mm)	AREA (mm**2)	A:B RATIO
40rpm	0.67 0.66	0.35	1.02
60rpm	0.57 0.56	0.25	1.02
80rpm	0.49 0.47	0.19	1.03
100rpm	0.45 0.45	0.16	1.01
120rpm	0.40 0.39	0.13	1.02
140rpm	0.37 0.36	0.10	1.03

TABLE 4.1.2 - STRESS-STRAIN CURVES FOR CONTROL EXPERIMENT
STRESS (MPa)

Strain	HAUL-OFF SPEED					
	40rpm	60rpm	80rpm	100rpm	120rpm	140rpm
0%	0.00	0.00	0.00	0.00	0.00	0.00
2%	10.46	12.42	12.66	13.22	13.76	13.96
4%	18.16	19.23	19.80	20.65	22.08	22.55
6%	21.38	21.90	23.07	23.44	24.81	25.66
8%	22.51	22.73	23.25	24.12	25.24	26.38
10%	23.03	22.87	23.30	24.31	25.28	26.43
12%	23.09	22.79	23.27	24.28	25.28	26.53
14%	22.92	22.69	23.24	24.15	25.21	26.53
16%	22.61	22.49	23.18	24.12	25.21	26.53
18%	22.31	22.20	23.13	24.13	25.29	26.53
20%	21.85	22.00	23.04	24.10	25.40	26.58
Yield S	22.97	22.89	23.38	24.33	25.69	27.54
Break S	41.85	46.32	51.93	56.41	63.60	70.75
E(Br)	1244%	1156%	1063%	972%	962%	925%

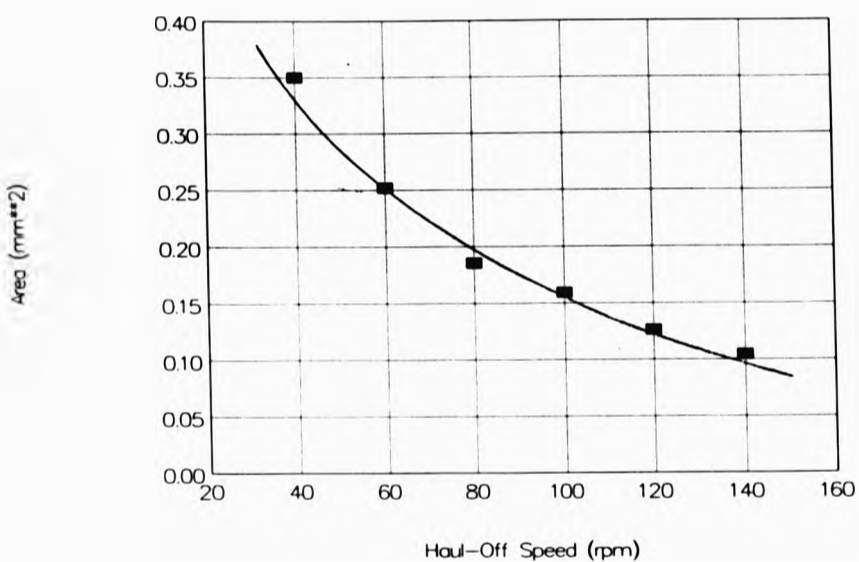


Fig. 4.1.1 - Area vs. HOS for the control experiment.

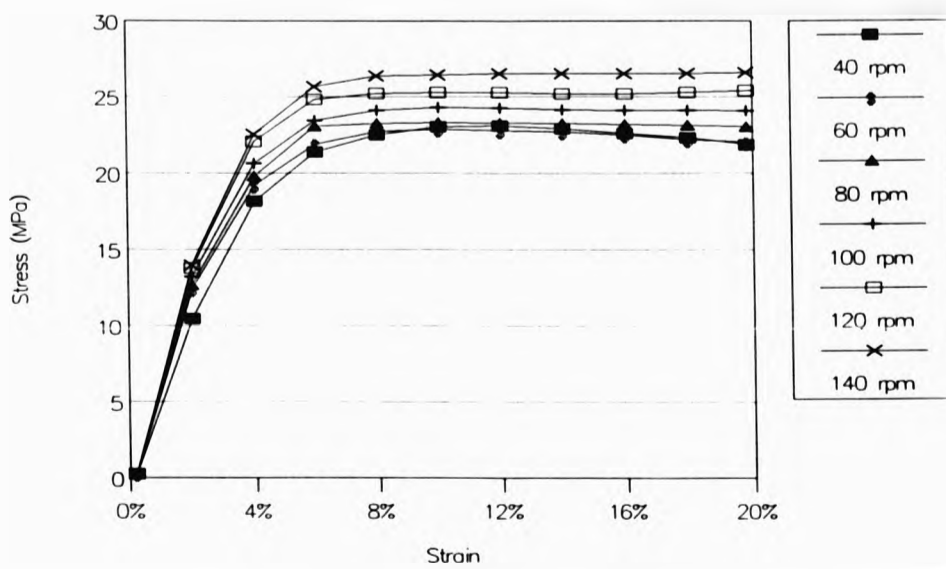


Fig. 4.1.2 - Stress VS. Strain for the Control Experiment.

4.2 - POLYMER EXTRUDATES QUENCHED IN LIQUID METAL ALLOY (1)

**4.2.1 - EXTRUDATES FROM A CIRCULAR DIE
(AT CONSTANT OUTPUT - 9 rpm)**

TABLE 4.2.1.1 - AVERAGE DIMENSIONS OF EXTRUDATES (mm)

HOS	BATH TEMPERATURE			
	111c	113c	115c	117c
40rpm	0.82	0.79	0.79	0.82
	0.79	0.76	0.71	0.72
60rpm	0.70	0.67	0.66	0.71
	0.64	0.62	0.60	0.57
80rpm	0.61	0.59	0.57	0.64
	0.56	0.54	0.48	0.46
100rpm	0.55	0.54	0.53	0.60
	0.50	0.50	0.43	0.40
120rpm	0.48	0.49	0.52	0.57
	0.43	0.43	0.39	0.36
140rpm	0.45	0.45	0.52	0.56
	0.40	0.39	0.34	0.36

TABLE 4.2.1.2 - AVERAGE AREA OF EXTRUDATES (mm²)

HOS	BATH TEMPERATURE			
	111c	113c	115c	117c
40rpm	0.52	0.49	0.46	0.49
60rpm	0.37	0.34	0.33	0.34
80rpm	0.28	0.26	0.23	0.25
100rpm	0.22	0.22	0.19	0.20
120rpm	0.17	0.17	0.17	0.17
140rpm	0.15	0.14	0.15	0.17

TABLE 4.2.1.3 - AVERAGE A:B RATIO OF EXTRUDATES

HOS	BATH TEMPERATURE			
	111c	113c	115c	117c
40rpm	1.046	1.048	1.113	1.142
60rpm	1.104	1.067	1.110	1.230
80rpm	1.097	1.094	1.192	1.401
100rpm	1.102	1.094	1.249	1.515
120rpm	1.136	1.135	1.340	1.581
140rpm	1.126	1.144	1.527	1.556

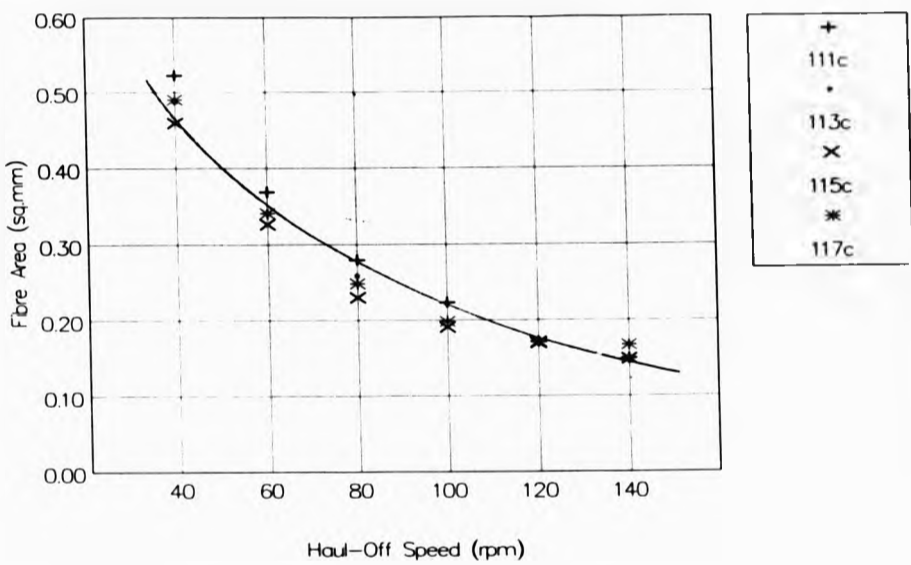


Fig. 4.2.1.2 - Area vs. HOS (experiment 2)

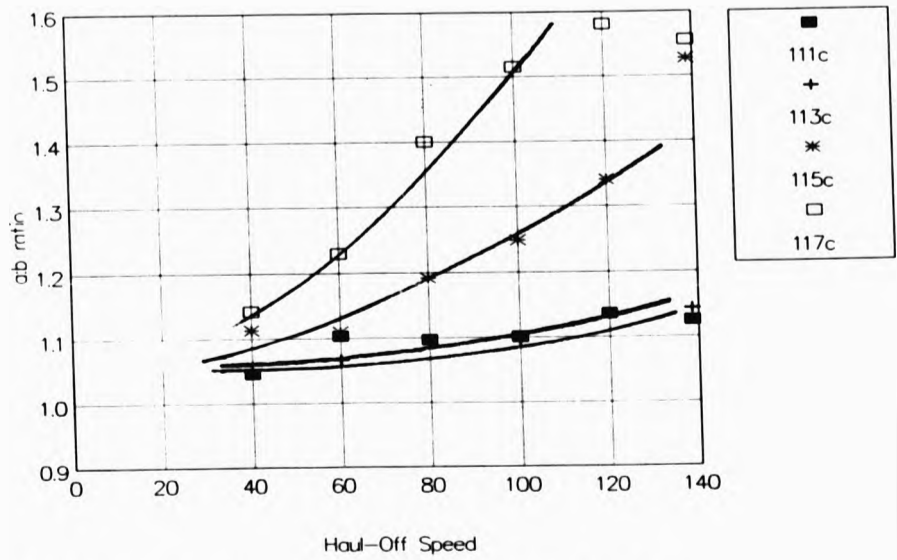


Fig. 4.2.1.3 - A:B ratio vs. HOS (experiment 2)

4.2.2 - STRESS-STRAIN CURVES FOR EXTRUDATES FROM A CIRCULAR DIE

**TABLE 4.2.2.1 - EXTRUDATES QUENCHED AT 111^o.
STRESS (MPa)**

Strain	HAUL-OFF SPEED					
	40rpm	60rpm	80rpm	100rpm	120rpm	140rpm
0%	0.00	0.00	0.00	0.00	0.00	0.00
2%	12.57	13.32	14.43	14.51	18.25	18.72
4%	18.71	19.55	21.61	23.72	27.74	31.30
6%	21.52	22.66	24.48	27.89	33.34	36.75
8%	22.85	23.94	25.84	29.86	37.07	41.86
10%	23.30	24.56	26.52	31.31	40.17	45.89
12%	23.47	24.86	26.98	32.35	42.73	49.19
14%	23.39	24.99	27.20	33.11	43.78	51.15
16%	23.12	24.91	27.38	33.47	43.90	51.42
18%	22.64	24.78	27.16	33.37	43.55	51.21
20%	22.09	24.61	26.88	33.09	43.32	51.35

**TABLE 4.2.2.2 - EXTRUDATES QUENCHED AT 113^o.
STRESS (MPa)**

Strain	HAUL-OFF SPEED					
	40rpm	60rpm	80rpm	100rpm	120rpm	140rpm
0%	0.00	0.00	0.00	0.00	0.00	0.00
2%	10.92	12.92	13.87	15.97	16.44	18.26
4%	18.94	21.58	24.15	25.55	27.56	31.08
6%	22.47	25.48	28.67	30.58	34.30	39.09
8%	24.20	27.40	31.26	33.57	38.71	44.96
10%	24.88	28.35	32.80	35.66	42.16	49.79
12%	25.12	28.89	33.96	37.34	45.14	53.79
14%	25.25	29.18	34.74	38.28	46.65	55.78
16%	25.19	29.36	35.05	38.42	46.89	55.91
18%	25.02	29.21	34.66	38.15	46.54	55.85
20%	24.82	28.91	34.31	37.93	46.42	56.34

**TABLE 4.2.2.3 - EXTRUDATES QUENCHED AT 115^o.
STRESS (MPa)**

Strain	HAUL-OFF SPEED					
	40rpm	60rpm	80rpm	100rpm	120rpm	140rpm
0%	0.00	0.00	0.00	0.00	0.00	0.00
2%	16.00	18.97	19.68	20.52	27.35	24.20
4%	22.19	26.59	29.41	32.78	43.60	42.53
6%	25.13	30.19	34.93	40.66	56.09	56.00
8%	26.69	33.47	38.58	47.01	66.32	66.23
10%	27.32	34.63	41.53	51.99	74.92	75.11
12%	27.67	35.47	43.49	56.72	81.38	83.19
14%	27.85	35.97	44.70	59.40	87.23	88.45
16%	27.95	36.03	44.83	60.56	89.06	90.40
18%	27.85	35.73	44.70	61.40	89.88	92.39
20%	27.56	35.51	44.91	62.14	90.77	93.26

**TABLE 4.2.2.4 - EXTRUDATES QUENCHED AT 117^o.
STRESS (MPa)**

Strain	HAUL-OFF SPEED					
	40rpm	60rpm	80rpm	100rpm	120rpm	140rpm
0%	0.00	0.00	0.00	0.00	0.00	0.00
2%	14.45	14.94	16.36	19.92	23.44	25.32
4%	21.61	24.41	28.06	34.06	41.32	45.18
6%	24.73	28.47	34.59	42.53	54.50	59.81
8%	25.91	30.37	38.74	50.63	64.90	71.10
10%	26.30	31.40	42.09	56.29	73.76	81.41
12%	26.49	32.29	44.87	61.49	81.52	89.54
14%	26.59	32.96	47.00	64.77	86.84	94.61
16%	26.61	33.40	48.14	66.28	88.82	96.45
18%	26.47	33.55	48.70	67.04	89.76	
20%	26.28	33.61	49.26	67.79	90.45	

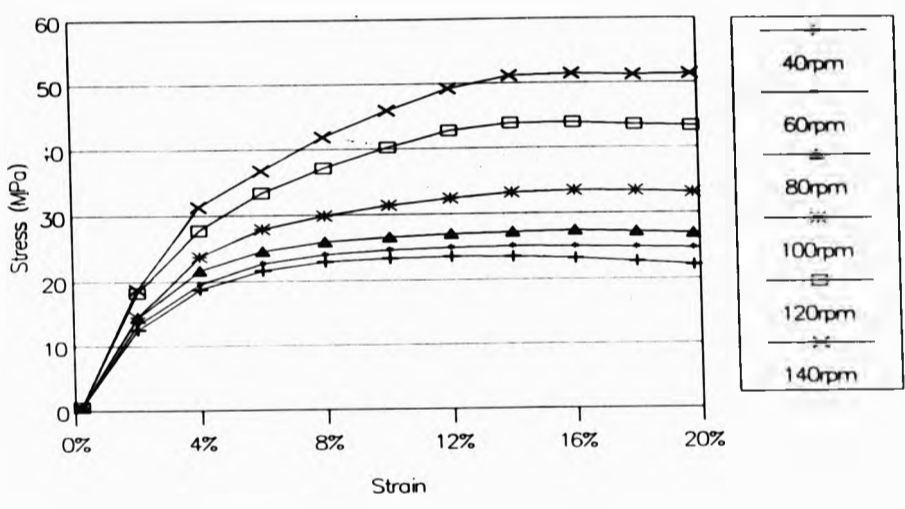


Fig.4.2.2.1 - Stress vs. Strain; BT = 111°C (experiment 2)

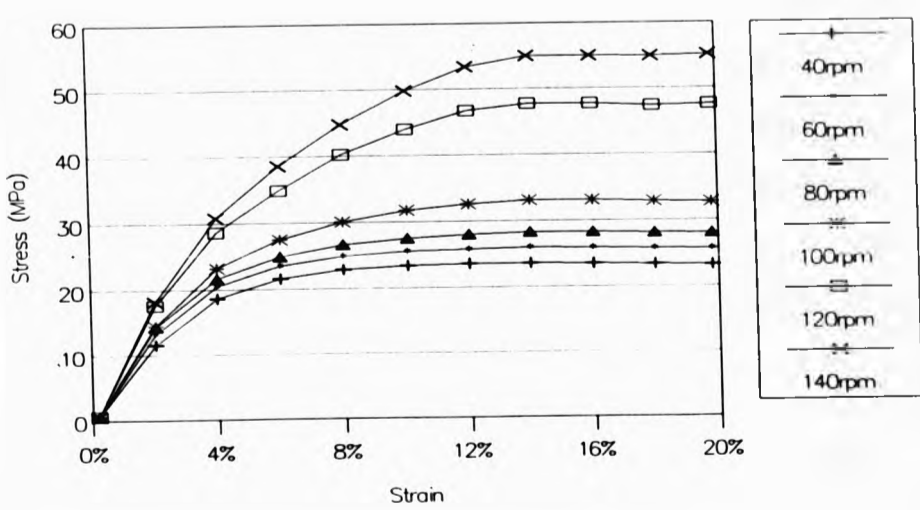


Fig. 4.2.2.2 - Stress vs. Strain; BT = 113°C (experiment 2)

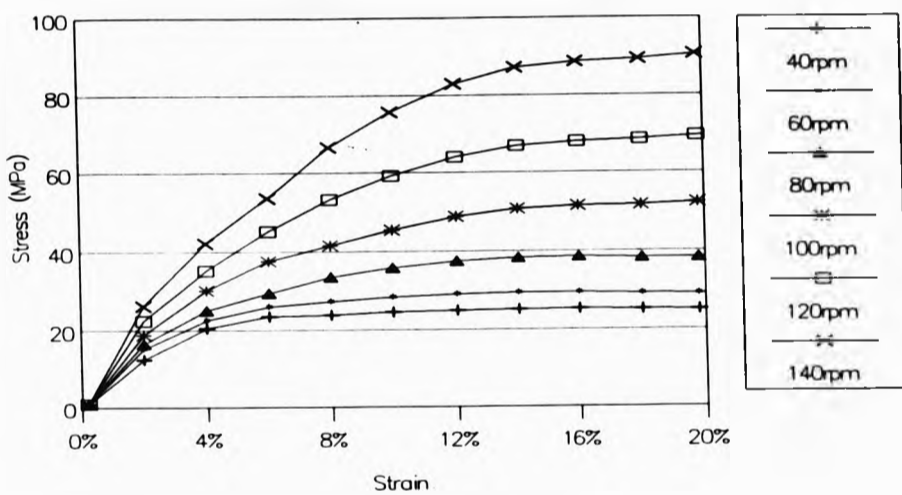


Fig.4.2.2.3 -Stress vs. Strain; BT = 115°C (experiment 2)

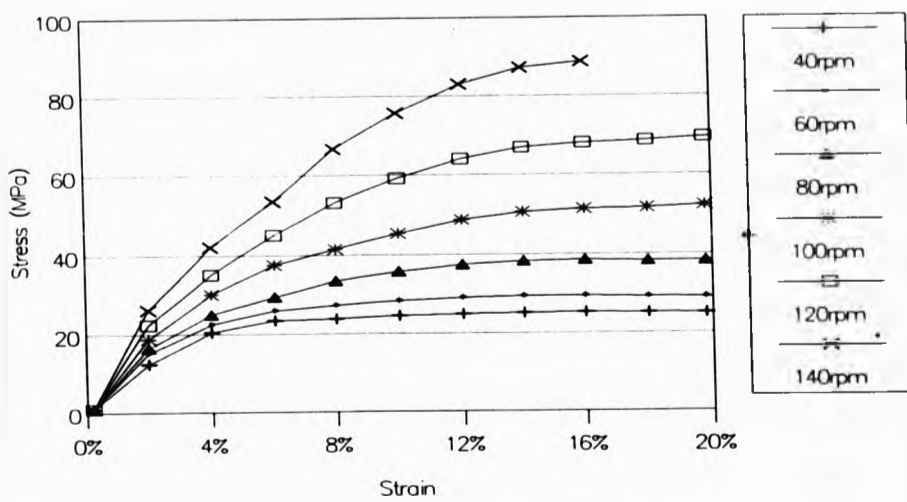


Fig. 4.2.2.4 - Stress vs. Strain; BT = 117°C (experiment 2)

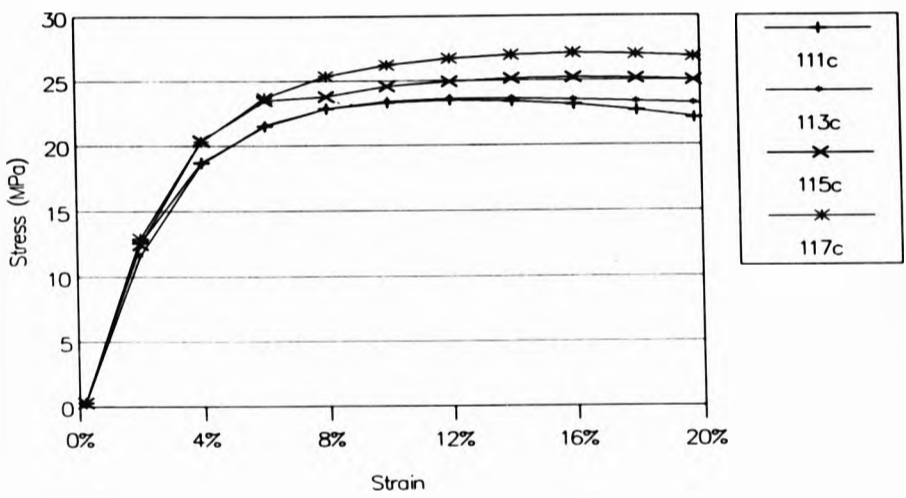
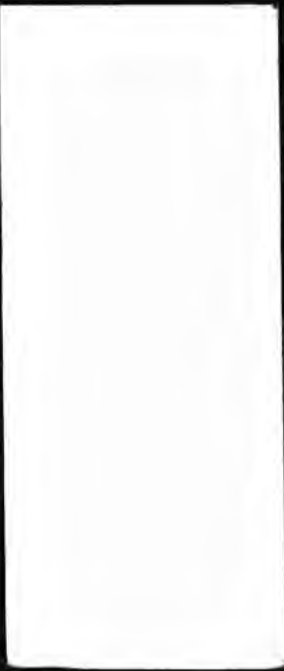


Fig. 4.2.2.5 - Stress vs. Strain; HOS = 40rpm (experiment 2)

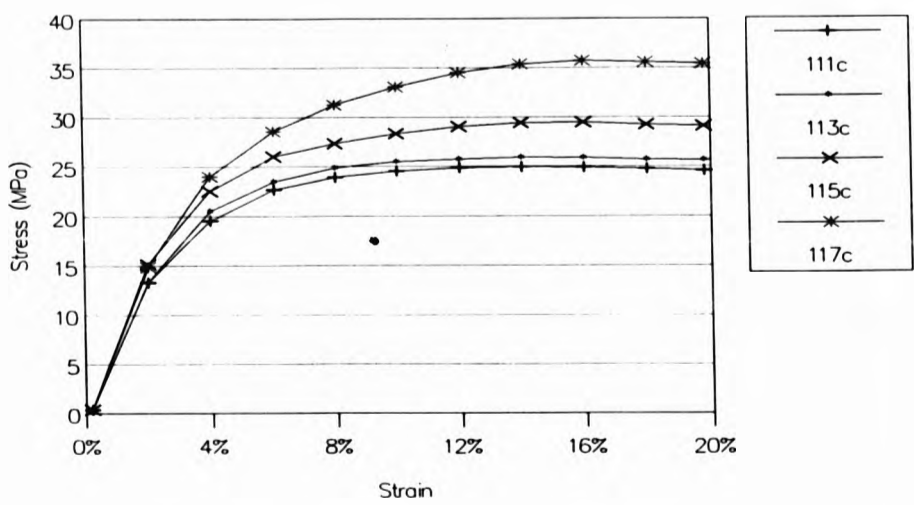


Fig. 4.2.2.6 - Stress vs. Strain; HOS = 60rpm (experiment 2)

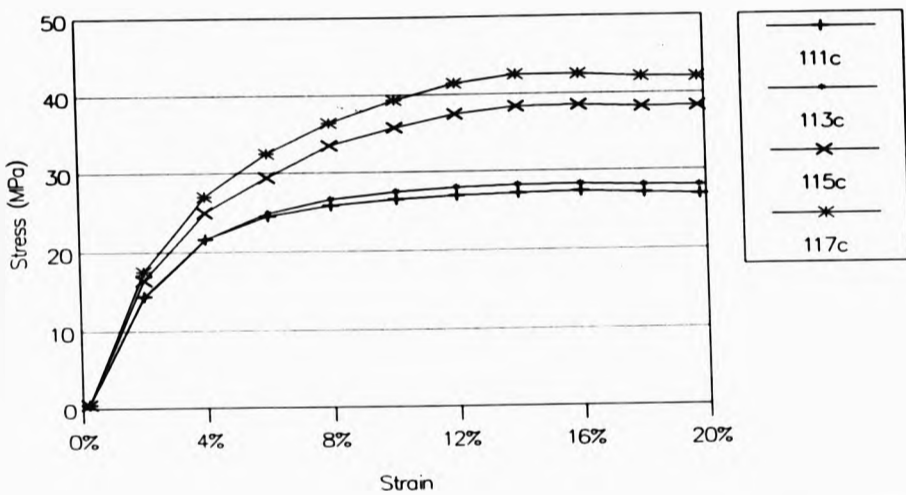


Fig. 4.2.2.7 - Stress vs. Strain; HOS = 80rpm (experiment 2)

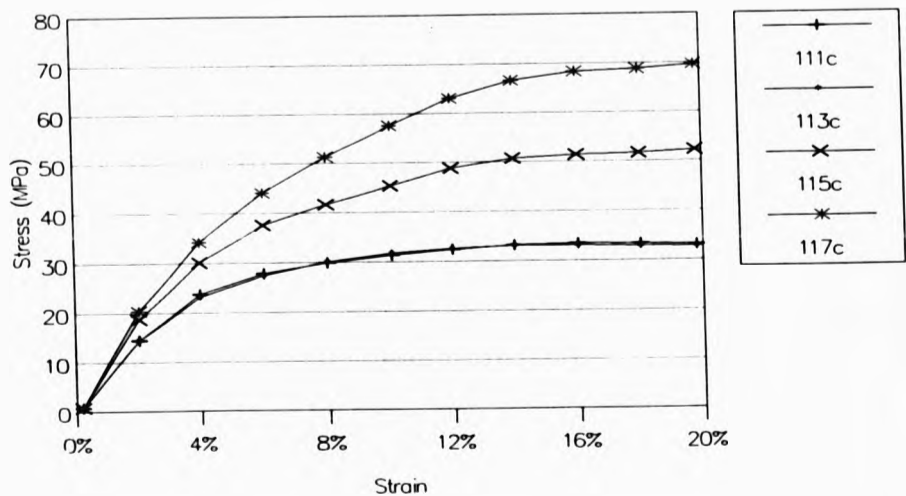


Fig. 4.2.2.8 - Stress vs. Strain; HOS = 100rpm (experiment 2)

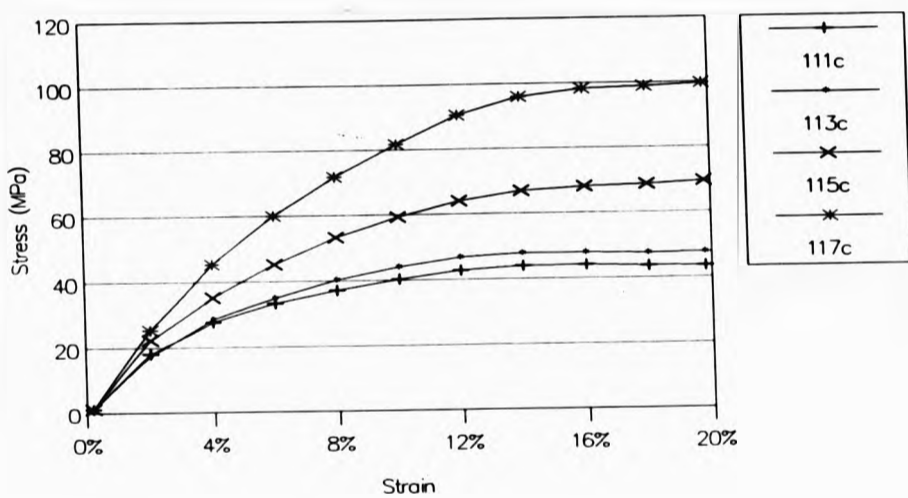


Fig. 4.2.2.9 - Stress vs. Strain; HOS = 120rpm (experiment 2)

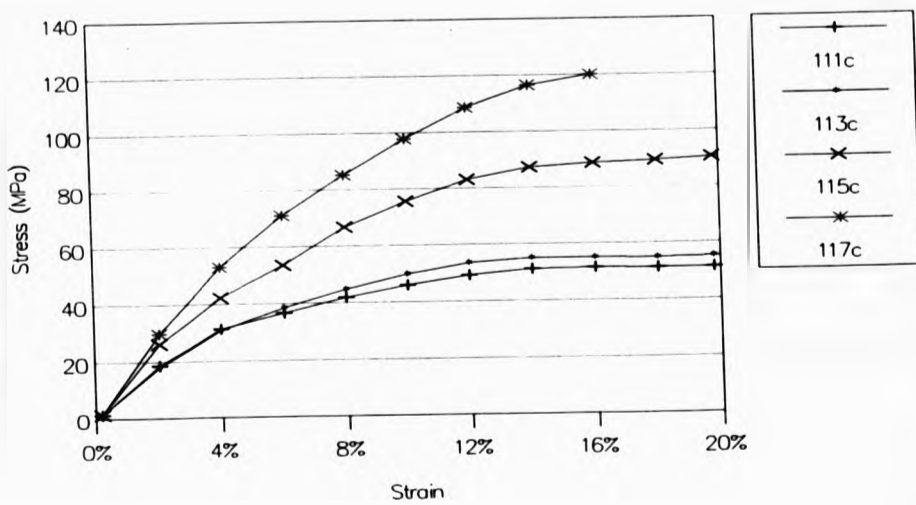


Fig. 4.2.2.10 - Stress vs. Strain; HOS = 140rpm (experiment 2)

TABLE 4.2.3 - YIELD STRESS OF EXTRUDATES
STRESS (MPa)

BT	HAUL-OFF SPEED					
	40rpm	60rpm	80rpm	100rpm	120rpm	140rpm
111c	23.52	25.14	27.48	33.71	44.23	51.62
113c	23.60	25.89	28.25	33.01	47.82	63.51
115c	25.23	29.45	38.50	51.57	68.40	89.39
117c	27.14	35.76	42.65	64.89	88.78	---

TABLE 4.2.4 - S10% OF EXTRUDATES
STRESS (MPa)

BT	HAUL-OFF SPEED					
	40rpm	60rpm	80rpm	100rpm	120rpm	140rpm
111c	23.30	24.56	26.52	31.31	40.17	45.89
113c	23.38	25.50	27.48	31.67	43.92	49.76
115c	24.56	28.34	35.76	45.38	59.20	75.68
117c	26.20	33.11	39.35	57.65	81.68	97.80

TABLE 4.2.5 - BREAK STRESS OF EXTRUDATES
STRESS (MPa)

BT	HAUL-OFF SPEED					
	40rpm	60rpm	80rpm	100rpm	120rpm	140rpm
113c	52.05	61.25	69.41	81.00	101.24	106.59
115c	45.57	55.07	66.10	78.93	94.17	111.99
117c	46.09	55.55	66.22	77.91	103.87	119.93

TABLE 4.2.6 - ELONGATION AT BREAK OF EXTRUDATES

BT	HAUL-OFF SPEED					
	40rpm	60rpm	80rpm	100rpm	120rpm	140rpm
113c	1098%	791%	601%	485%	388%	280%
115c	836%	781%	497%	430%	271%	208%
117c	640%	255%	217%	98%	64%	46%

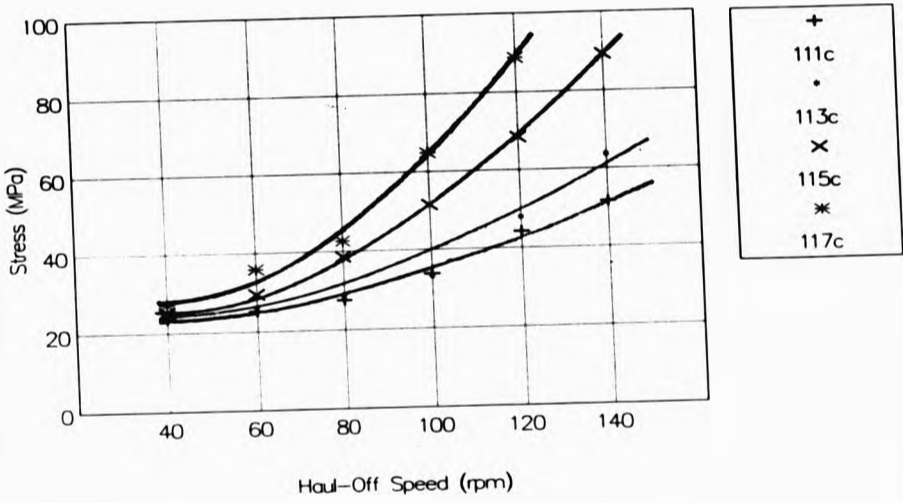


Fig. 4.2.3a - Yield Stress vs. HOS. (experiment 2)

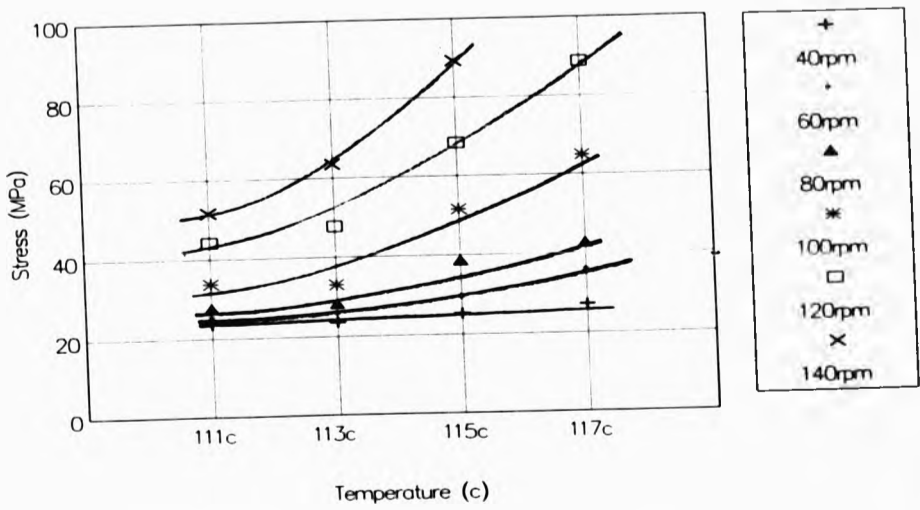


Fig. 4.2.3b - Yield Stress vs. BT (experiment 2)

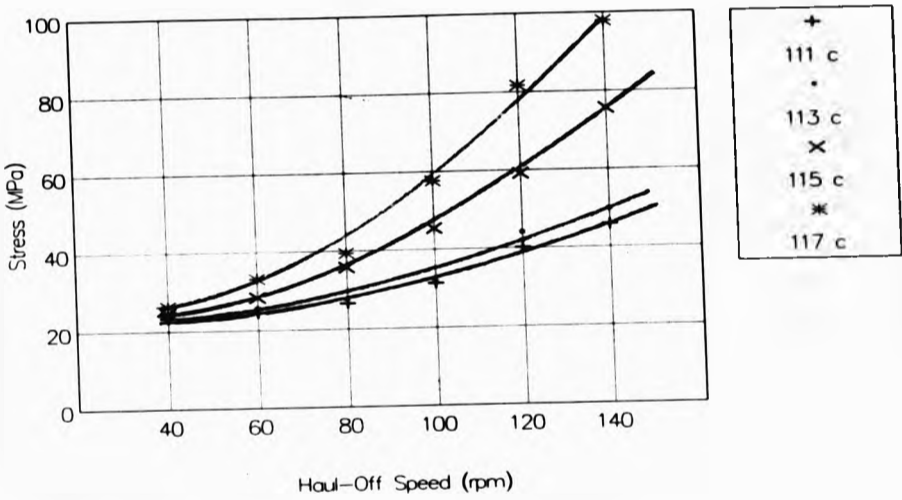


Fig. 4.2.4a - Stress at 10% Strain vs. HOS (experiment 2)

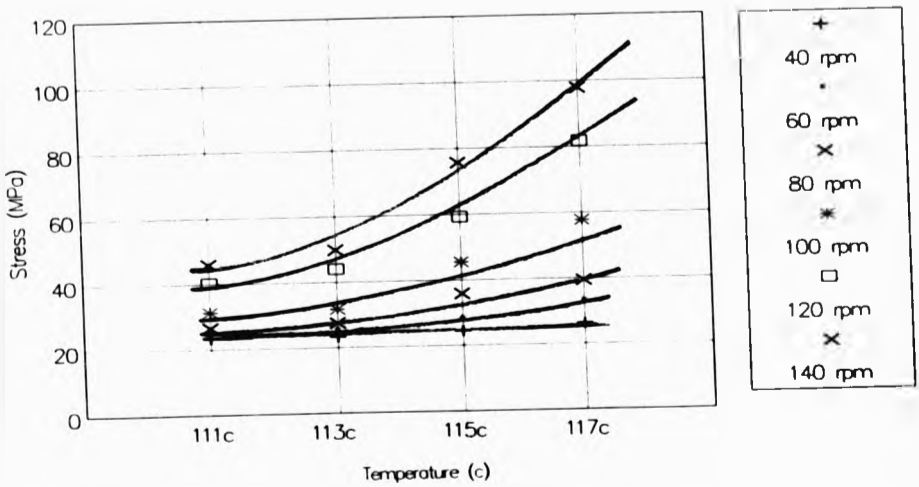


Fig. 4.2.4b - Stress at 10% Strain vs. BT (experiment 2)

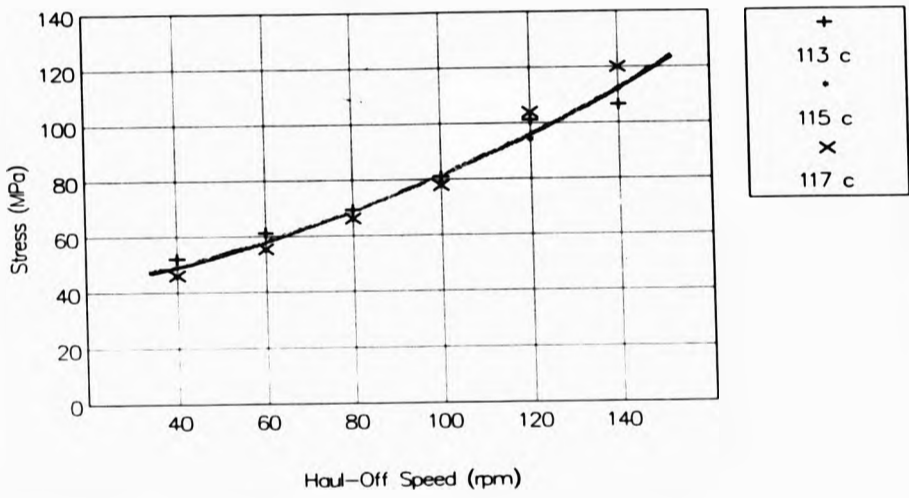


Fig. 4.2.5a - Break Stress vs. HOS. (experiment 2)

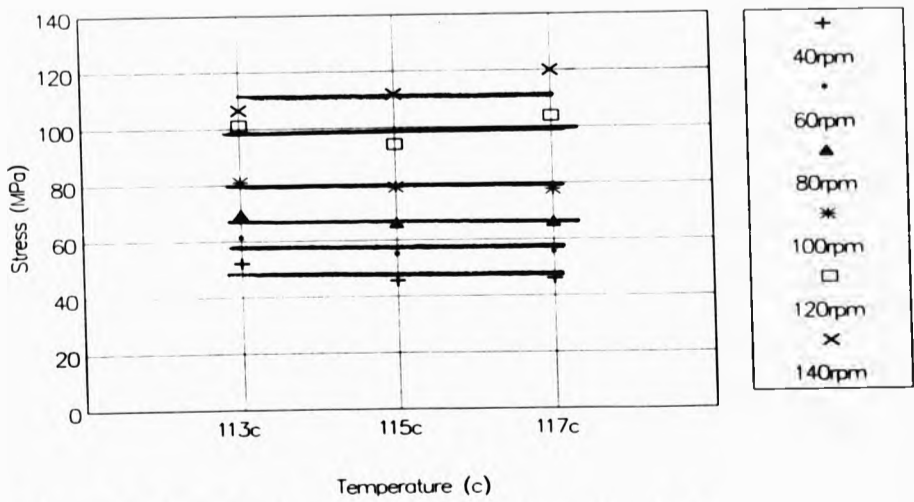


Fig. 4.2.5b - Break Stress vs. BT (experiment 2)

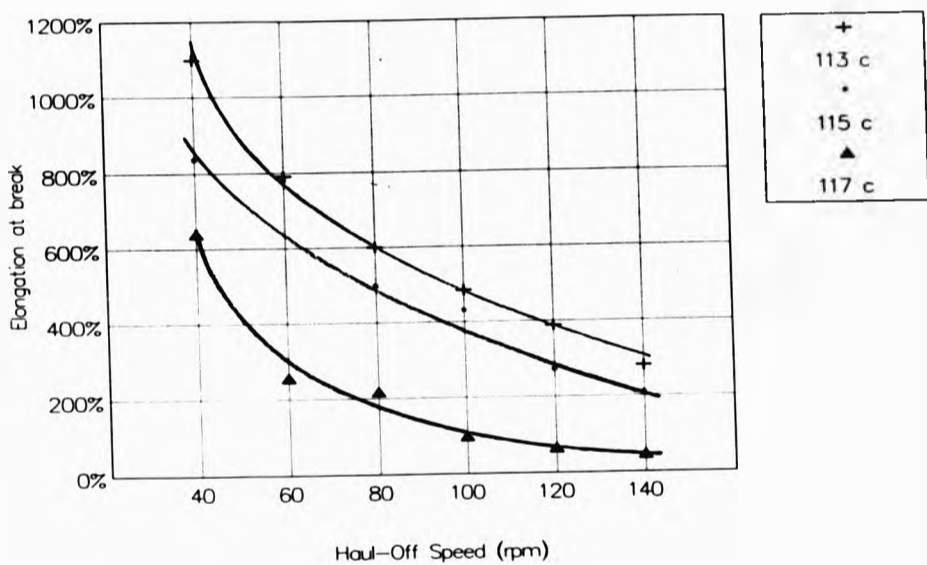


Fig. 4.2.6a - Elongation at Break vs. HOS. (experiment 2)

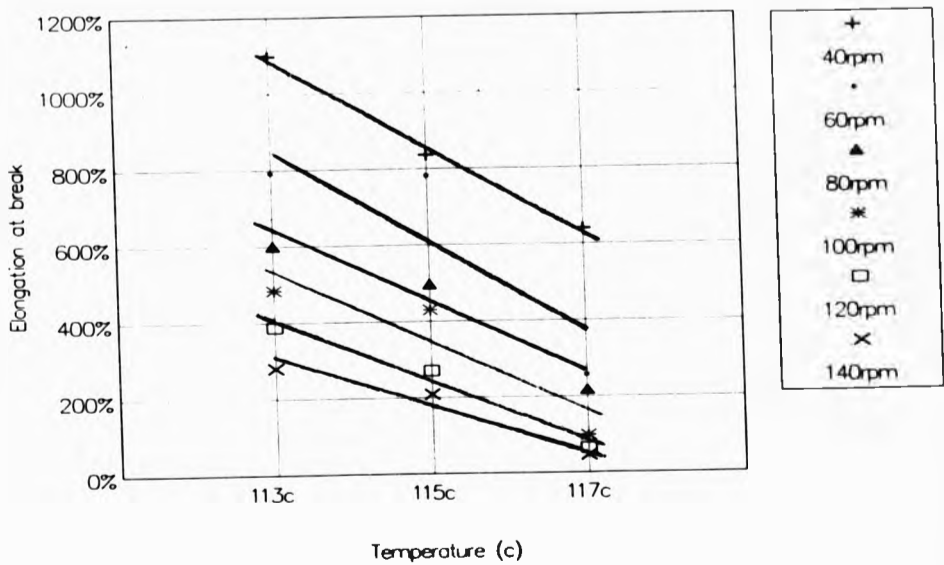


Fig. 4.2.6b - Elongation at Break vs. BT (experiment 2)

4.3 - POLYMER EXTRUDATES QUENCHED IN LIQUID METAL ALLOY (2)

4.3.1 - EXTRUDATES FROM A CIRCULAR DIE (AT CONSTANT BATH TEMPERATURE - 117C)

TABLE 4.3.1.1 - AVERAGE DIMENSIONS OF EXTRUDATES (mm)

DDR	OUTPUT RATE			
	5rpm	10rpm	20rpm	28rpm
x2	0.87	0.87	0.93	0.96
	0.85	0.84	0.78	0.80
x3	0.71	0.72	0.76	0.81
	0.71	0.68	0.65	0.63
x4	0.63	0.62	0.64	0.74
	0.63	0.55	0.54	0.52
x5	0.54	0.56	0.67	0.72
	0.53	0.49	0.46	0.43
x6	0.52	0.52	0.60	
	0.51	0.45	0.39	

TABLE 4.3.1.2 - AVERAGE AREA OF EXTRUDATES (mm²)

DDR	OUTPUT RATE			
	5rpm	10rpm	20rpm	28rpm
2x	0.58	0.59	0.61	0.63
3x	0.40	0.39	0.41	0.41
4x	0.31	0.28	0.29	0.29
5x	0.22	0.23	0.25	0.25
6x	0.21	0.20	0.19	

TABLE 4.3.1.3 - AVERAGE A:B RATIO OF EXTRUDATES

DDR	OUTPUT RATE			
	5rpm	10rpm	20rpm	28rpm
x2	1.02	1.03	1.19	1.21
x3	1.01	1.05	1.17	1.29
x4	1.01	1.12	1.19	1.43
x5	1.01	1.13	1.46	1.68
x6	1.02	1.17	1.56	

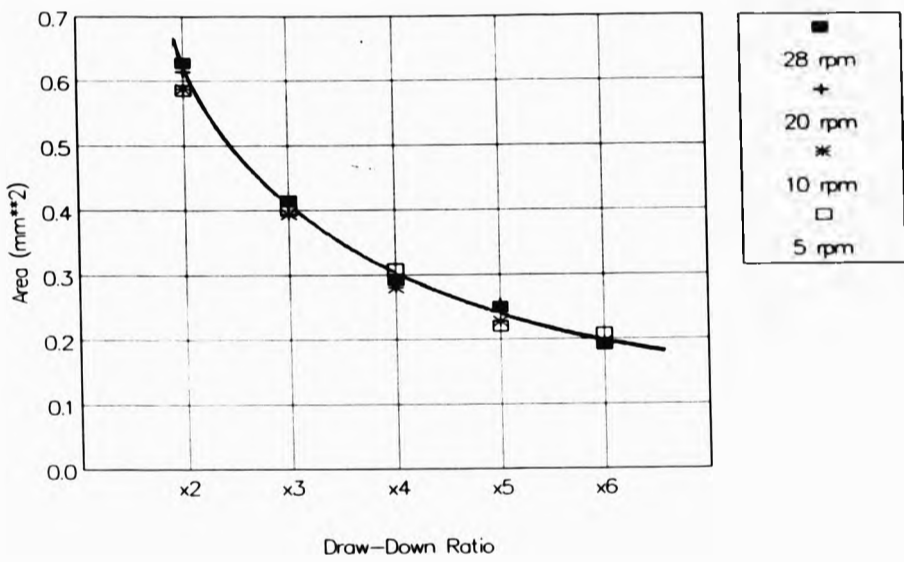


Fig. 4.3.1.2 - Area vs. DDR (experiment 3)

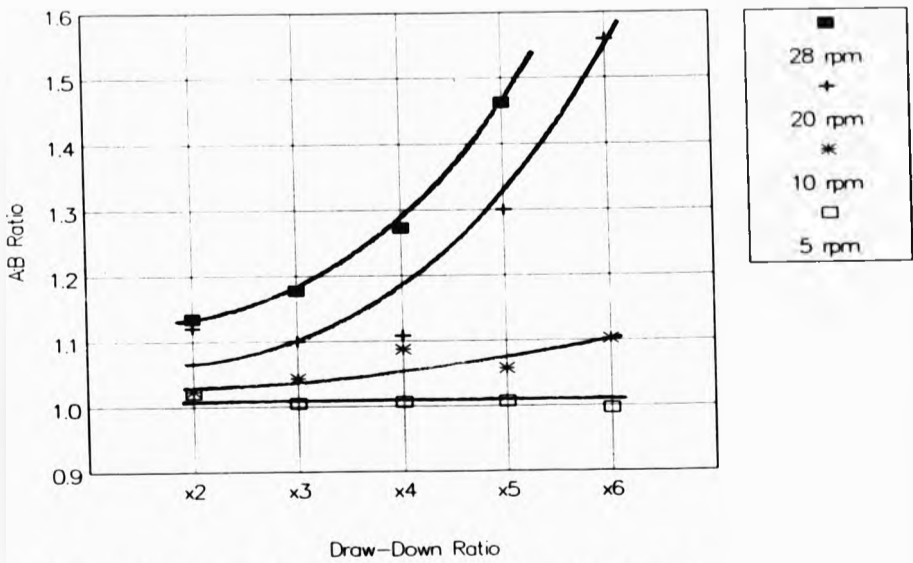


Fig. 4.3.1.3 - A:B ratio vs. DDR (experiment 3)

4.3.2 - STRESS-STRAIN CURVES FOR EXTRUDATES FROM A CIRCULAR DIE

**TABLE 4.3.2.1 - OUTPUT = 5 RPM
STRESS (MPa)**

STRAIN	DRAW-DOWN RATIO				
	x2	x3	x4	x5	x6
0%	0.00	0.00	0.00	0.00	0.00
2%	14.11	14.90	16.95	20.36	19.59
4%	18.36	19.24	20.23	23.08	22.87
6%	20.03	20.70	21.57	24.42	23.72
8%	20.80	21.36	22.07	25.11	24.29
10%	21.06	21.72	22.32	25.56	24.66
12%	21.09	21.76	22.39	25.73	24.66
14%	20.95	21.61	22.39	25.38	24.66
16%	20.75	21.36	22.33	25.29	24.37
18%	20.45	21.16	22.26	24.93	24.27
20%	19.72	20.77	21.94	24.84	23.89

**TABLE 4.3.2.2 - OUTPUT = 10 RPM.
STRESS (MPa)**

STRAIN	DRAW-DOWN RATIO				
	x2	x3	x4	x5	x6
0%	0.00	0.00	0.00	0.00	0.00
2%	15.63	18.67	20.64	23.33	24.99
4%	19.66	22.43	26.02	29.13	31.55
6%	21.46	24.24	28.64	32.37	35.95
8%	22.28	24.90	30.27	34.83	38.71
10%	22.52	25.66	31.12	35.61	40.16
12%	22.65	25.86	31.40	36.05	40.58
14%	22.66	25.85	31.46	35.88	40.58
16%	22.52	25.66	31.17	35.62	40.67
18%	22.35	25.55	30.88	35.62	40.67
20%	22.11	25.30	30.67	35.70	40.77

**TABLE 4.3.2.3 - OUTPUT = 20 rpm
STRESS (MPa)**

STRAIN	DRAW-DOWN RATIO				
	x2	x3	x4	x5	x6
0%	0.00	0.00	0.00	0.00	0.00
2%	16.42	18.95	22.37	27.50	33.52
4%	21.30	23.59	26.63	37.18	45.38
6%	23.55	25.40	28.49	43.42	53.87
8%	24.69	26.44	29.59	48.62	61.05
10%	25.38	27.03	30.42	53.19	67.05
12%	25.70	27.62	30.69	55.63	69.27
14%	26.03	28.01	30.76	57.13	69.93
16%	26.12	28.11	30.49	57.92	70.97
18%	26.12	28.11	30.28	58.86	72.14
20%	25.99	28.11	30.28	59.81	72.79

**TABLE 4.3.2.4 - OUTPUT = 28 rpm
STRESS (MPa)**

STRAIN	DRAW-DOWN RATIO			
	x2	x3	x4	x5
0%	0.00	0.00	0.00	0.00
2%	15.06	17.37	20.08	24.37
4%	20.26	23.09	28.07	38.64
6%	22.76	25.81	32.71	49.00
8%	23.92	27.22	35.81	57.44
10%	24.77	28.21	38.84	65.36
12%	25.17	29.01	41.57	72.49
14%	25.61	29.76	43.56	77.60
16%	25.96	30.51	45.83	79.78
18%	26.11	30.98	46.70	
20%	26.24	31.30	47.32	

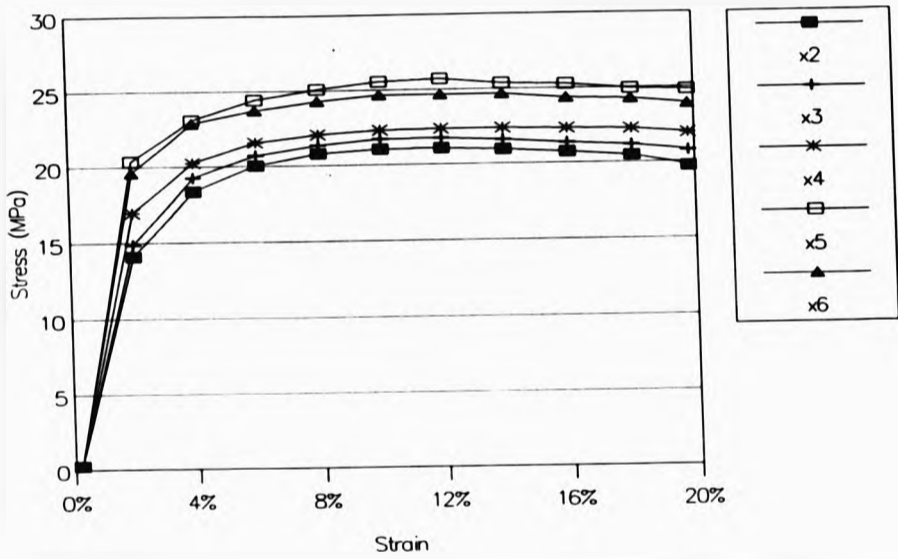


Fig. 4.3.2.1 - Stress vs. Strain; OR = 5 rpm (experiment 3)

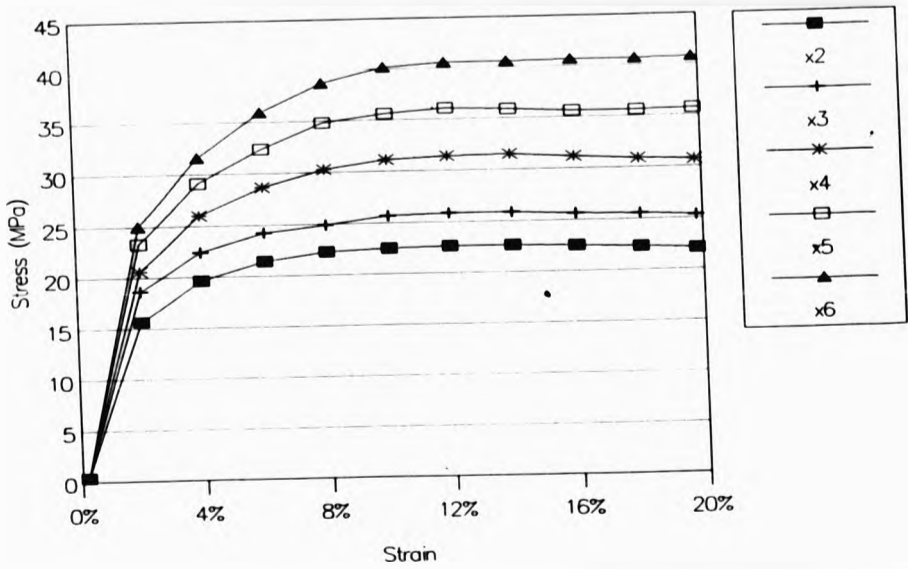


Fig. 4.3.2.2 - Stress vs. Strain; OR = 10 rpm (experiment 3)

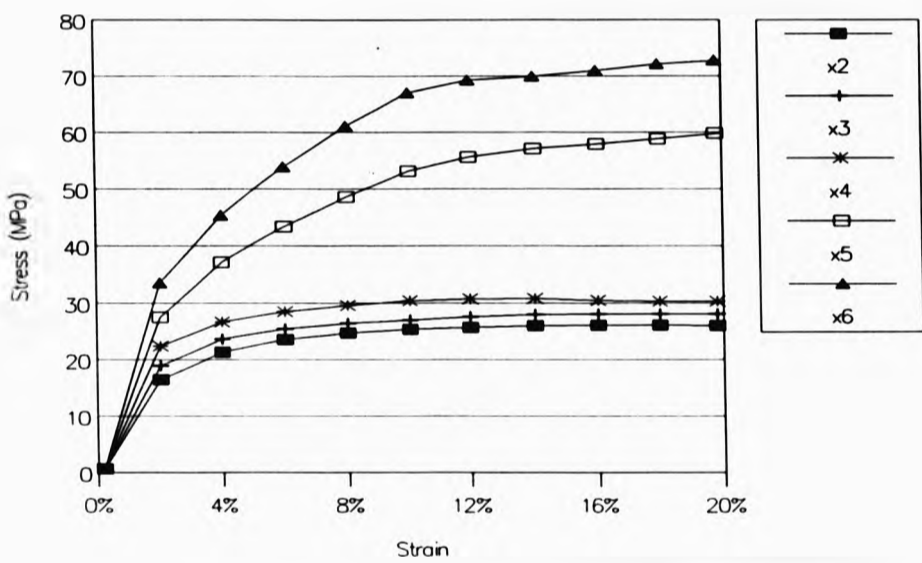


Fig. 4.3.2.3 - Stress vs. Strain; OR = 20 rpm (experiment 3)

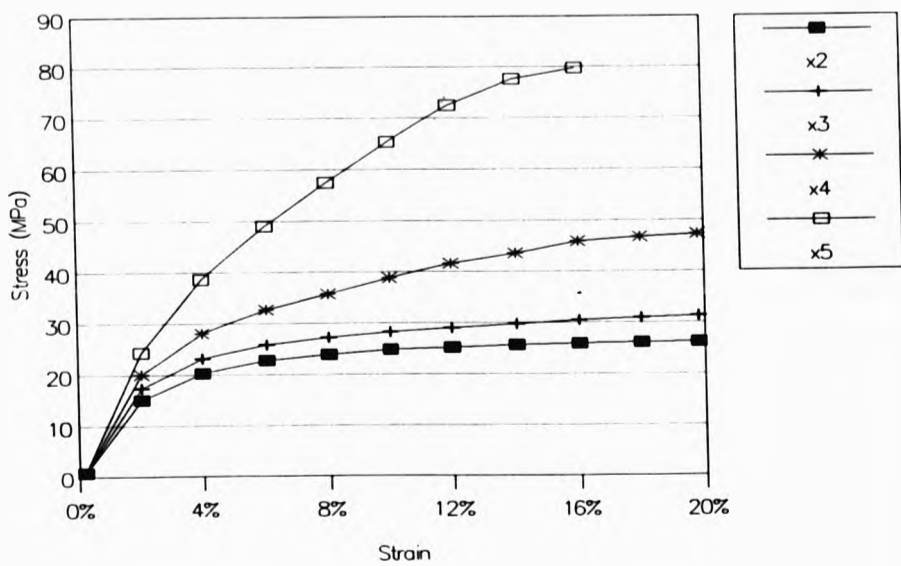


Fig. 4.3.2.4 - Stress vs. Strain; OR = 28 rpm (experiment 3)

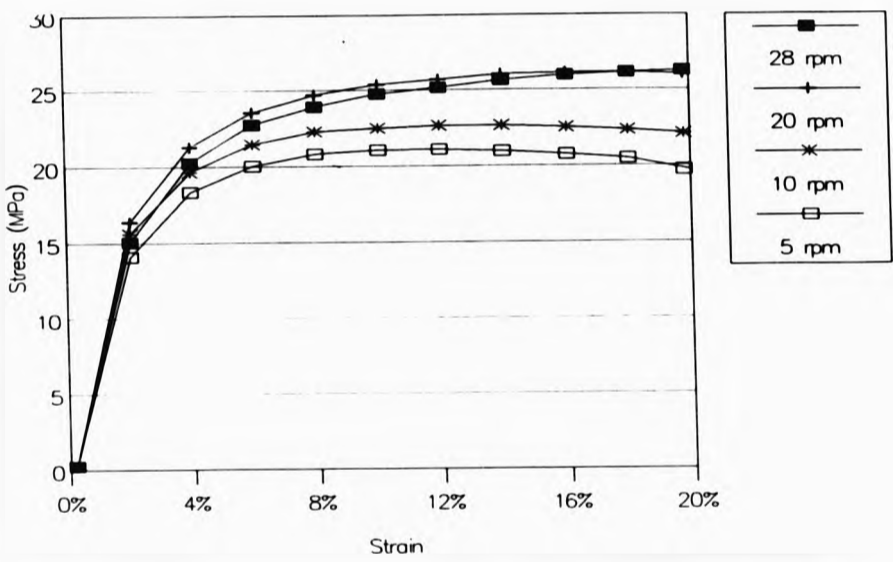


Fig. 4.3.2.5 - Stress vs. Strain; DDR = x2 (experiment 3)

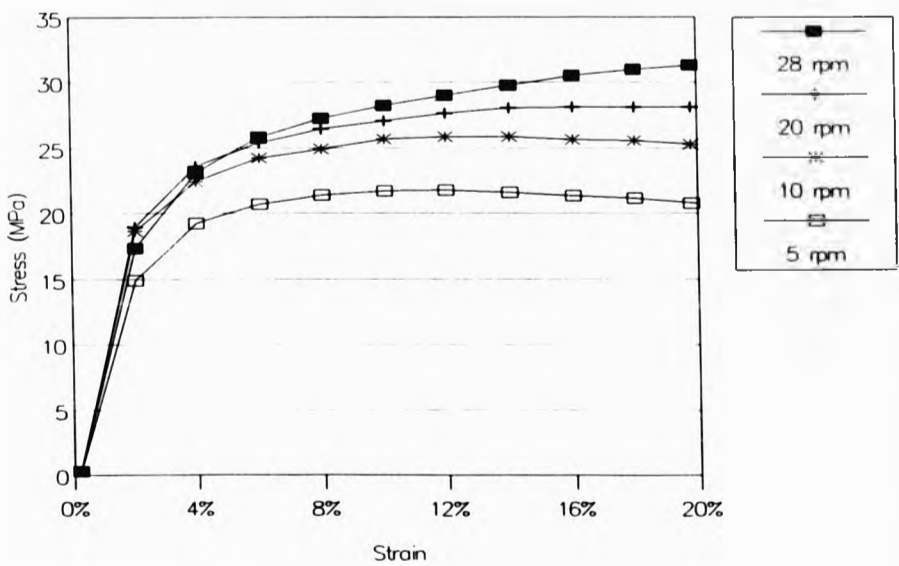


Fig. 4.3.2.6 - Stress vs. Strain; DDR = x3 (experiment 3)

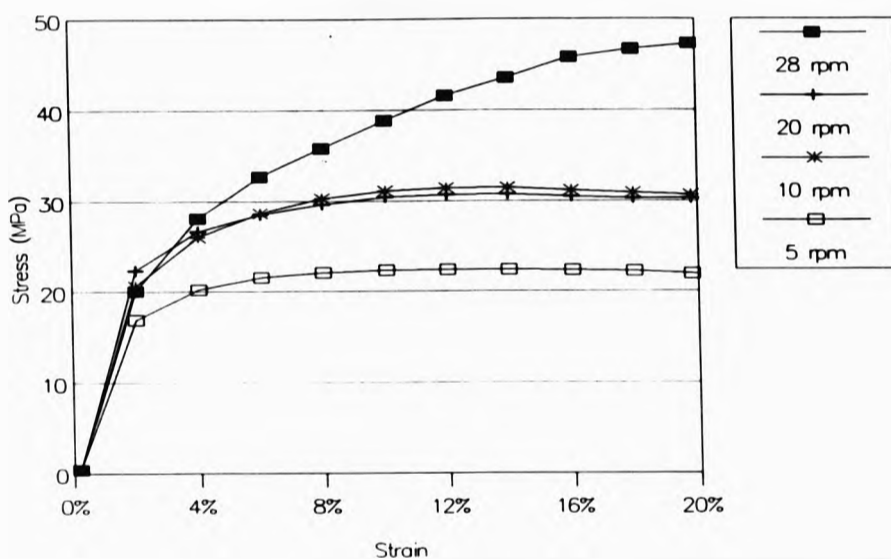


Fig. 4.3.2.7 - Stress vs. Strain; DDR = x4 (experiment 3)

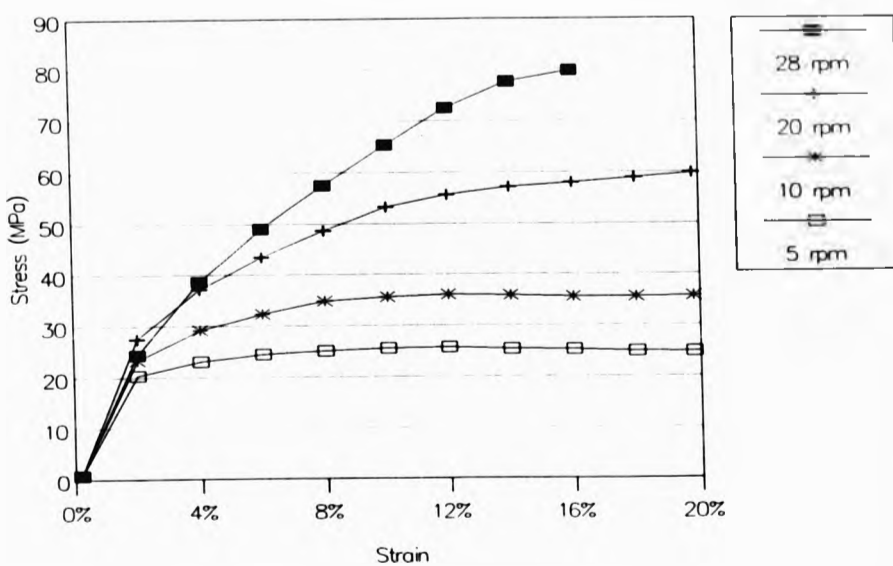


Fig. 4.3.2.8 - Stress vs. Strain; DDR = x5 (experiment 3)

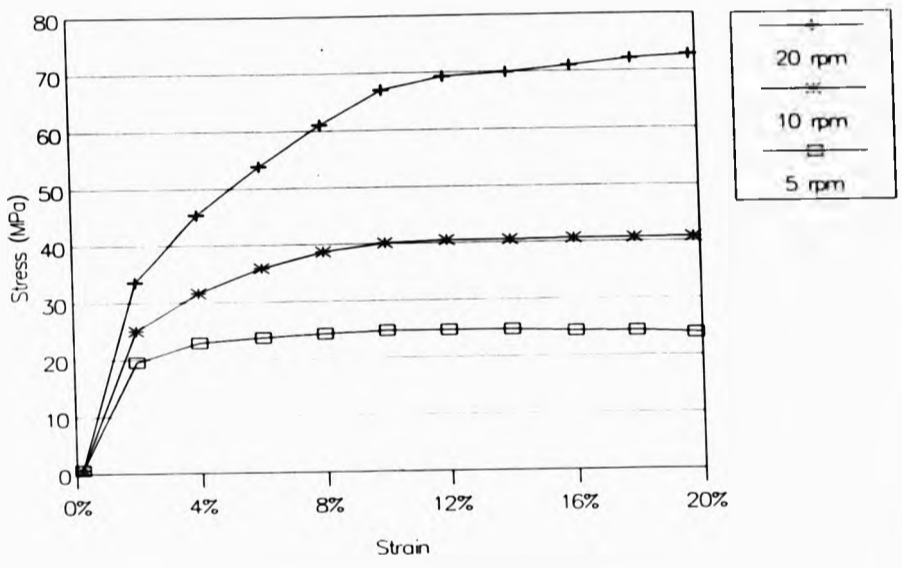


Fig. 4.3.2.9 - Stress vs. Strain; DDR = x6 (experiment 3)

**TABLE 4.3.3 - STRESS AT 10% STRAIN
STRESS (MPa)**

DDR	OUTPUT RATE			
	5rpm	10rpm	20rpm	28rpm
2x	21.06	22.52	25.38	24.77
3x	21.72	25.66	27.03	28.21
4x	22.32	31.12	30.42	38.84
5x	25.56	35.61	53.19	65.36
6x	24.66	40.16	67.05	

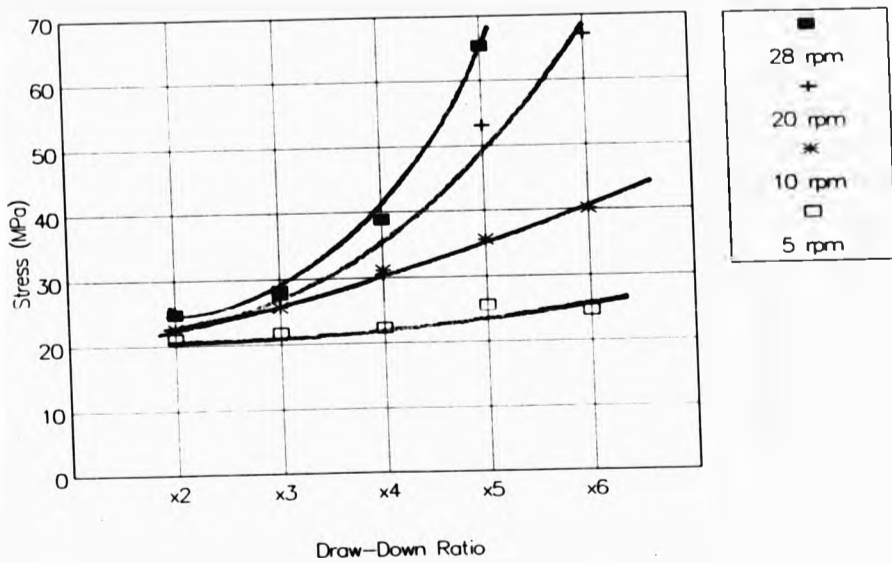


Fig. 4.3.3 - Stress at 10% Strain vs. DDR (experiment 3)

TABLE 4.3.4 - STRESS AT BREAK
STRESS (MPa)

DDR	OUTPUT RATE			
	5rpm	10rpm	20rpm	28rpm
2x	38.63	42.09	30.57	29.93
3x	44.85	43.33	35.08	37.64
4x	50.88	51.70	41.22	52.06
5x	57.23	59.88	62.08	80.60
6x	59.44	72.34	75.14	

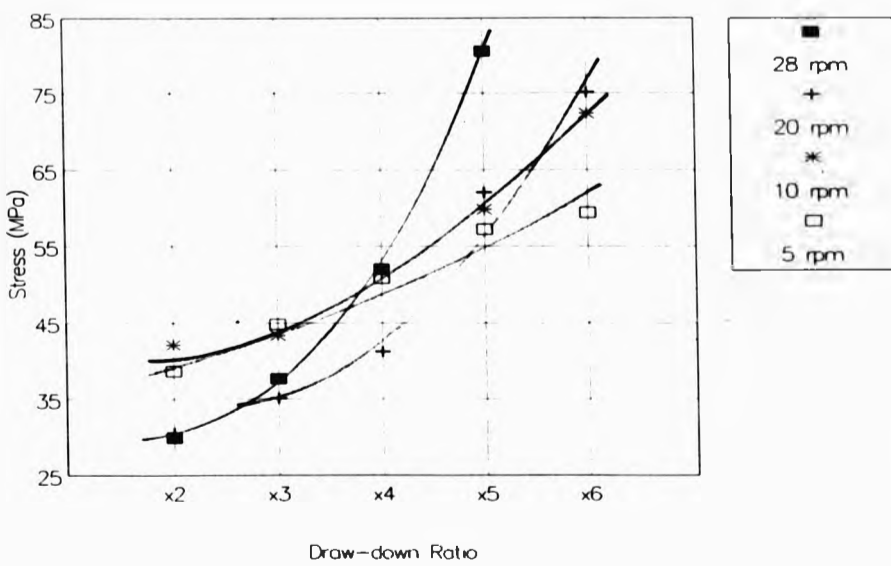


Fig. 4.3.4 - Stress at Break vs. DDR (experiment 3)

TABLE 4.3.5 - ELONGATION AT BREAK

DDR	OUTPUT RATE			
	5rpm	10rpm	20rpm	28rpm
2x	1180%	1059%	287%	217%
3x	1102%	644%	294%	151%
4x	1008%	429%	313%	72%
5x	786%	354%	46%	19%
6x	768%	289%	41%	

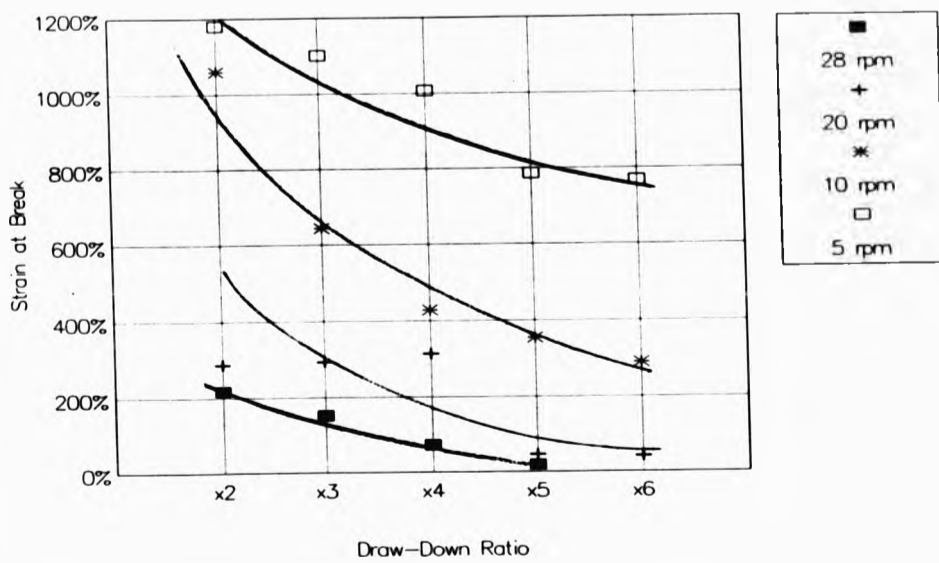


Fig. 4.3.5 - Elongation at Break vs. DDR (experiment 3)

4.4 - POLYMER EXTRUDATES QUENCHED IN LIQUID METAL ALLOY (3)

4.4.1 - EXTRUDATES FROM A STRIP DIE (AT CONSTANT BATH TEMPERATURE - 122c)

TABLE 4.4.1.1 - AVERAGE DIMENSIONS OF EXTRUDATES (mm)

DDR	OUTPUT RATE			
	5rpm	10rpm	20rpm	40rpm
x2.0	1.70 0.40	1.70 0.39	1.73 0.40	2.05 0.34
x2.5	1.60 0.33	1.62 0.34	1.60 0.35	1.83 0.31
x3.0	1.44 0.32	1.47 0.31	1.49 0.31	1.63 0.28
x3.5	1.34 0.28	1.37 0.29	1.41 0.30	1.45 0.28

TABLE 4.4.1.2 - AVERAGE AREAS OF EXTRUDATES (mm²)

DDR	OUTPUT RATE			
	5rpm	10rpm	20rpm	40rpm
x2.0	0.68	0.66	0.69	0.70
x2.5	0.53	0.55	0.56	0.57
x3.0	0.46	0.46	0.46	0.46
x3.5	0.38	0.40	0.42	0.41

TABLE 4.4.1.3 - AVERAGE A:B RATIOS OF EXTRUDATES

DDR	OUTPUT RATE			
	5rpm	10rpm	20rpm	40rpm
x2.0	4.25	4.36	4.32	6.03
x2.5	4.85	4.76	4.57	5.90
x3.0	4.50	4.74	4.81	5.82
x3.5	4.79	4.72	4.70	5.18

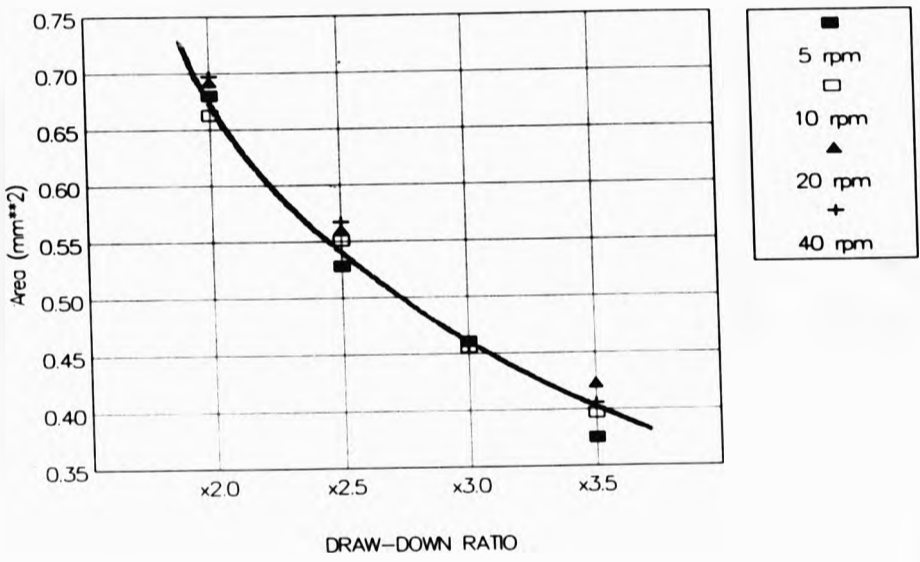


Fig. 4.4.1.2 - Area vs. DDR (experiment 4)

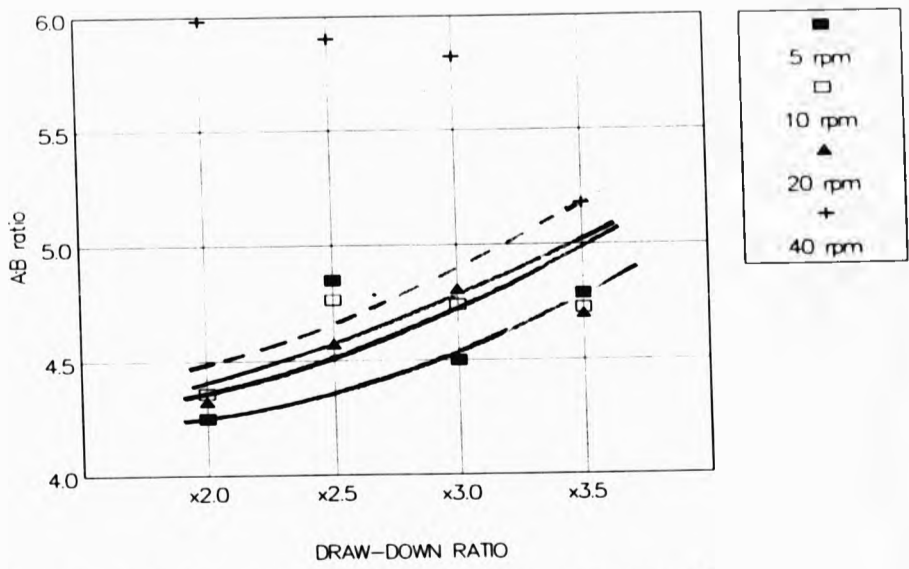


Fig. 4.4.1.3 - A:B ratio vs. DDR (experiment 4)

4.4.2 - STRESS-STRAIN CURVES FOR STRIP EXTRUDATES

**TABLE 4.4.2.1 - OUTPUT = 40rpm
STRESS (MPa)**

STRAIN	DRAW-DOWN RATIO			
	x2	x2.5	x3	x3.5
0%	0.00	0.00	0.00	0.00
2%	21.63	19.30	20.64	22.78
4%	31.01	30.07	29.67	32.06
6%	36.50	36.70	33.86	37.23
8%	39.88	40.98	36.61	41.40
10%	42.99	44.67	38.65	44.86
12%	46.18	47.97	41.71	48.74
14%	49.34	50.76	44.85	53.45
16%	52.38	53.08	47.77	57.18
18%	54.65	54.75	50.30	60.53
20%	56.19	55.81	52.36	63.15

**TABLE 4.4.2.2 - OUTPUT = 20rpm
STRESS (MPa)**

STRAIN	DRAW-DOWN RATIO			
	x2	x2.5	x3	x3.5
0%	0.00	0.00	0.00	0.00
2%	15.27	17.40	17.90	19.13
4%	22.05	23.57	25.46	27.49
6%	25.50	26.91	29.36	32.79
8%	27.39	28.75	31.70	35.88
10%	28.24	29.81	33.42	38.30
12%	28.98	30.63	34.75	40.52
14%	29.44	31.23	35.80	42.65
16%	29.77	31.55	36.28	43.99
18%	29.85	31.55	36.36	44.33
20%	29.77	31.41	36.36	44.57

**TABLE 4.4.2.3 - OUTPUT = 10rpm
STRESS (MPa)**

STRAIN	DRAW-DOWN RATIO			
	x2	x2.5	x3	x3.5
0%	0.00	0.00	0.00	0.00
2%	14.10	14.62	16.12	17.52
4%	20.08	21.66	22.54	24.25
6%	23.07	25.13	25.44	27.78
8%	24.12	26.51	26.60	29.75
10%	24.40	27.15	27.20	30.71
12%	24.49	27.35	27.42	31.58
14%	24.45	27.46	27.63	32.04
16%	24.36	27.42	27.63	32.13
18%	24.21	27.29	27.42	31.99
20%	23.97	27.09	27.12	31.86

**TABLE 4.4.2.4 - OUTPUT = 5rpm
STRESS (MPa)**

STRAIN	DRAW-DOWN RATIO			
	x2	x2.5	x3	x3.5
0%	0.00	0.00	0.00	0.00
2%	14.56	14.90	16.58	17.21
4%	21.20	21.51	22.50	23.61
6%	23.83	24.38	25.16	26.14
8%	24.80	25.69	26.05	26.59
10%	25.04	26.06	26.24	26.59
12%	24.88	26.19	26.28	26.42
14%	24.41	26.10	26.12	26.31
16%	23.55	25.79	25.82	26.03
18%	23.06	25.52	25.48	25.70
20%	22.65	25.15	25.18	25.54

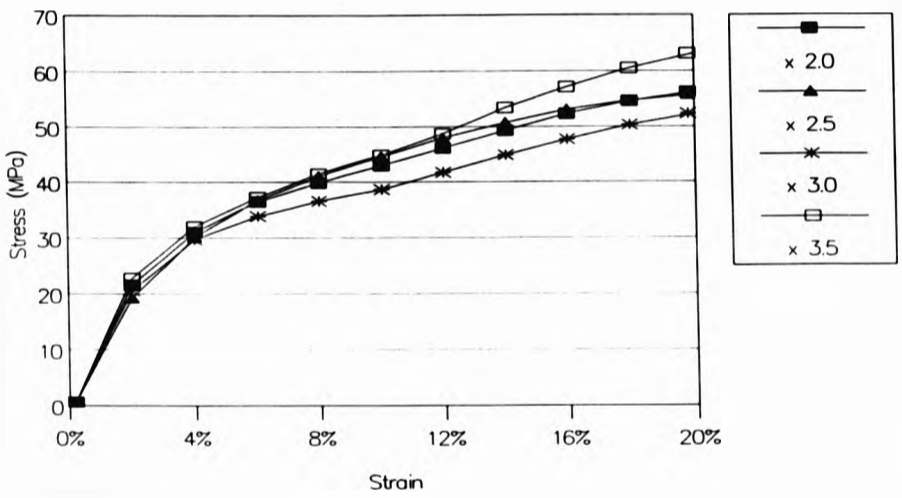


Fig. 4.4.2.1 - Stress vs. Strain; OR = 40 rpm (experiment 4)

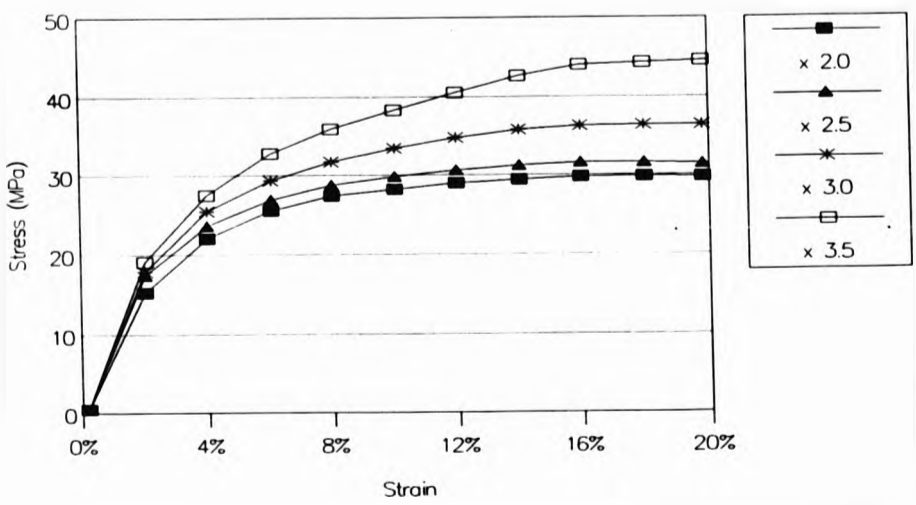


Fig. 4.4.2.2 - Stress vs. Strain; OR = 20 rpm (experiment 4)

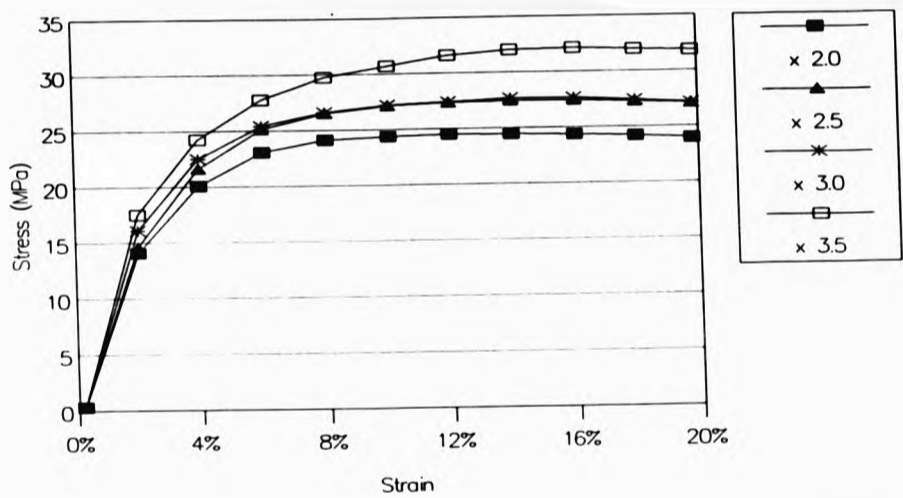


Fig. 4.4.2.3 - Stress vs. Strain; OR = 10 rpm (experiment 4)

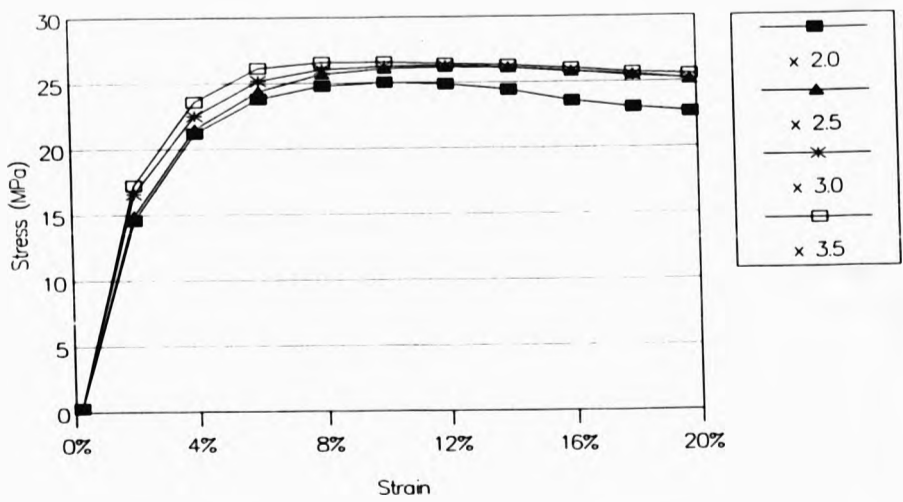


Fig. 4.4.2.4 - Stress vs. Strain; OR = 5 rpm (experiment 4)

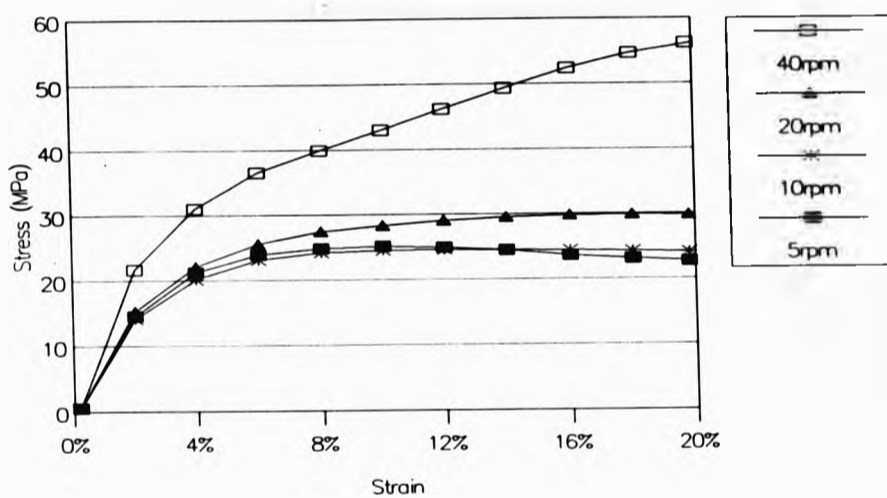


Fig. 4.4.2.5 - Stress vs. Strain; DDR = x 2 (experiment 4)

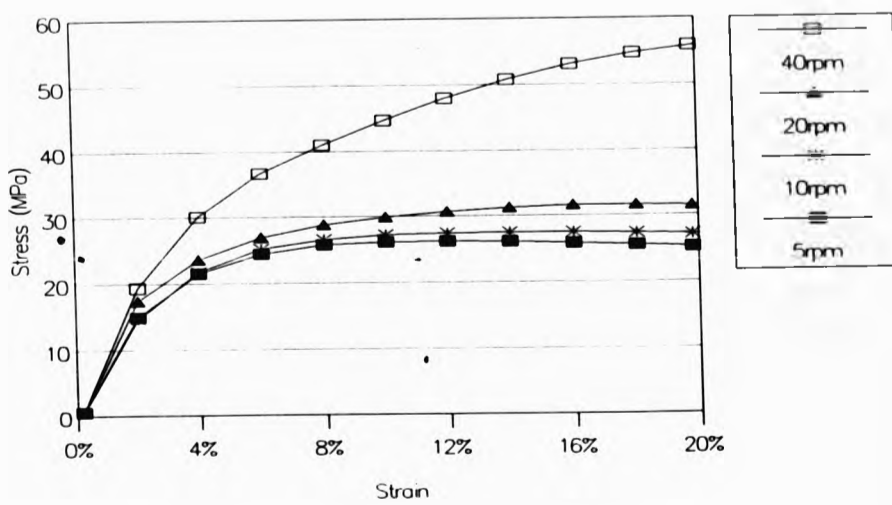


Fig. 4.4.2.6 - Stress vs. Strain; DDR = x 2.5 (experiment 4)

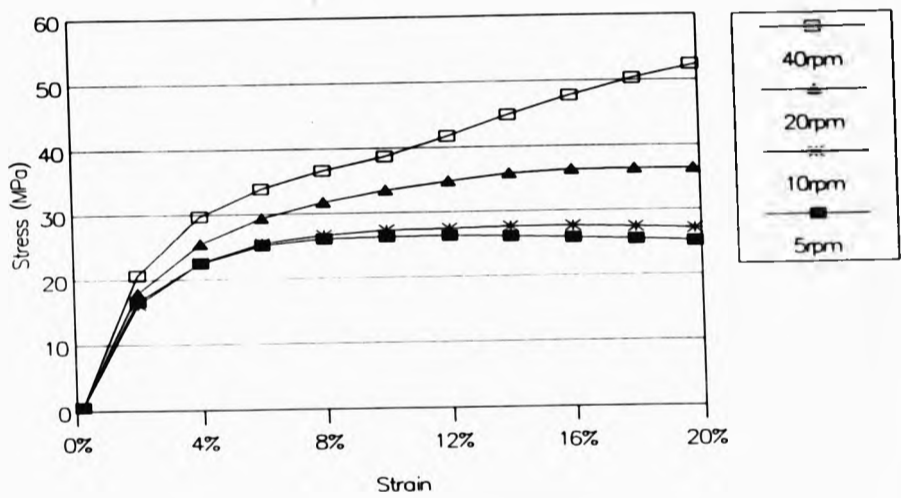


Fig. 4.4.2.7 - Stress vs. Strain; DDR = x 3 (experiment 4)

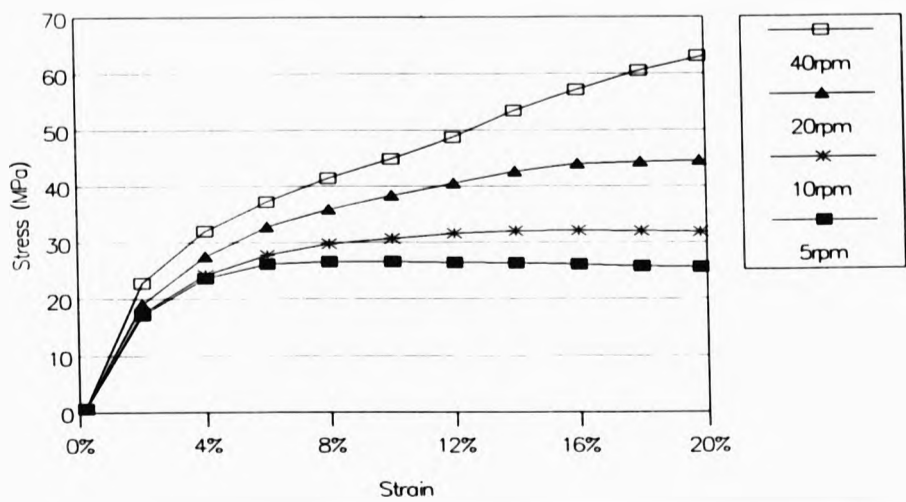


Fig. 4.4.2.8 - Stress vs. Strain; DDR = x 3.5 (experiment 4)

**TABLE 4.4.3 - STRESS AT 10% STRAIN
STRESS (MPa)**

OR	DRAW-DOWN RATIO			
	x2	x2.5	x3	x3.5
40rpm	42.99	44.67	38.65	44.86
20rpm	28.24	29.81	33.42	38.30
10rpm	24.40	27.15	27.20	30.71
5rpm	25.04	26.06	26.24	26.59

**TABLE 4.4.4 - STRESS AT BREAK
STRESS (MPa)**

OR	DRAW-DOWN RATIO			
	x2	x2.5	x3	x3.5
40rpm	57.9	63.5	58.2	65.3
20rpm	39.7	45.0	50.8	60.1
10rpm	38.8	42.6	44.5	52.2
5rpm	39.7	41.8	42.5	49.0

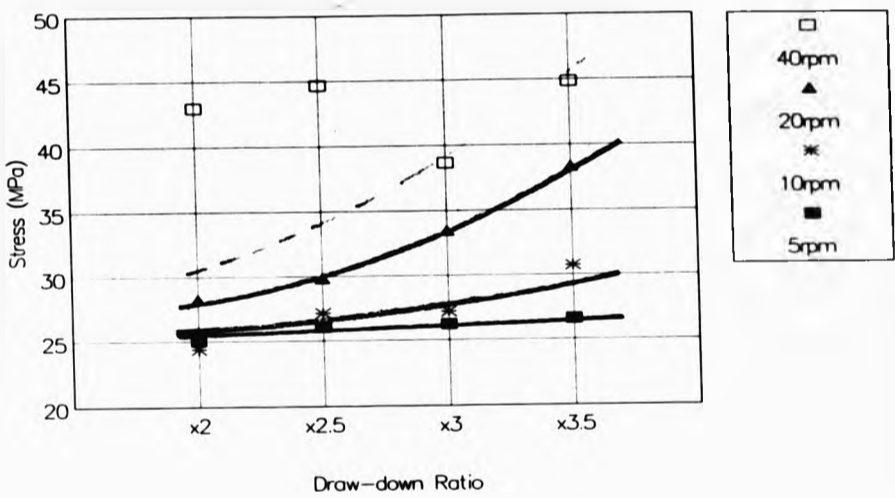


Fig. 4.4.3 - Stress at 10% strain vs. DDR (experiment 4)

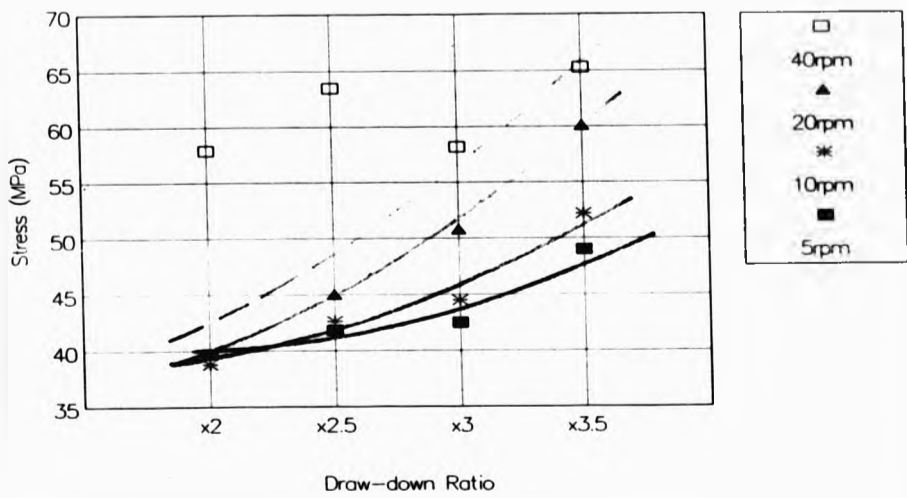


Fig. 4.4.4 - Stress at Break vs. DDR (experiment 4)

4.5 - POLYMER EXTRUDATES QUENCHED IN LIQUID METAL ALLOY (4)

4.5.1 - EXTRUDATES FROM A STRIP DIE

TABLE 4.5.1.1 - AVERAGE DIMENSIONS OF EXTRUDATES (mm)

DDR	OR=20rpm			OR=12rpm	OR=5rpm
	BT=118c	BT=120c	BT=122c	BT=122c	BT=123c
2.0	1.79 0.44				
2.5	1.50 0.37	1.42 0.34			
3.0	1.32 0.32	1.33 0.32			
3.5		1.22 0.29	1.28 0.28		
4.0		1.20 0.28	1.21 0.26	1.11 0.26	
4.5		1.12 0.27	1.24 0.25		
5.0		0.99 0.23	1.36 0.26	1.10 0.24	
5.5			1.24 0.25		
6.0				0.94 0.21	1.10 0.24
7.0				0.90 0.20	
8.0				0.90 0.19	0.95 0.20
10.0					0.83 0.18
12.0					0.78 0.16
14.0					0.74 0.14
16.0					0.73 0.13
18.0					0.68 0.12
20.0					0.64 0.12

TABLE 4.5.1.2 - AVERAGE AREAS OF EXTRUDATES (mm²)

DDR	OR=20rpm			OR=12rpm	OR=5rpm
	BT=118c	BT=120c	BT=122c	BT=122c	BT=123c
2.0	0.79				
2.5	0.55	0.49			
3.0	0.42	0.43			
3.5		0.35	0.35		
4.0		0.33	0.32	0.29	
4.5		0.30	0.31		
5.0		0.23	0.35	0.27	
5.5			0.30		
6.0				0.20	0.26
7.0				0.18	
8.0				0.17	0.19
10.0					0.15
12.0					0.12
14.0					0.10
16.0					0.09
18.0					0.08
20.0					0.08
22.0					0.07

TABLE 4.5.1.3 - AVERAGE A:B RATIOS

ddr	OR=20rpm			OR=12rpm	OR=5rpm
	BT=118c	BT=120c	BT=122c	BT=122c	BT=123c
2.0	4.07				
2.5	4.11	4.14			
3.0	4.12	4.12			
3.5		4.17	4.59		
4.0		4.37	4.58	4.23	
4.5		4.15	4.92		
5.0		4.22	5.29	4.51	
5.5			5.04		
6.0				4.48	4.58
7.0				4.54	
8.0				4.78	4.75
10.0					4.61
12.0					4.88
14.0					5.29
16.0					5.62
18.0					5.67
20.0					5.33

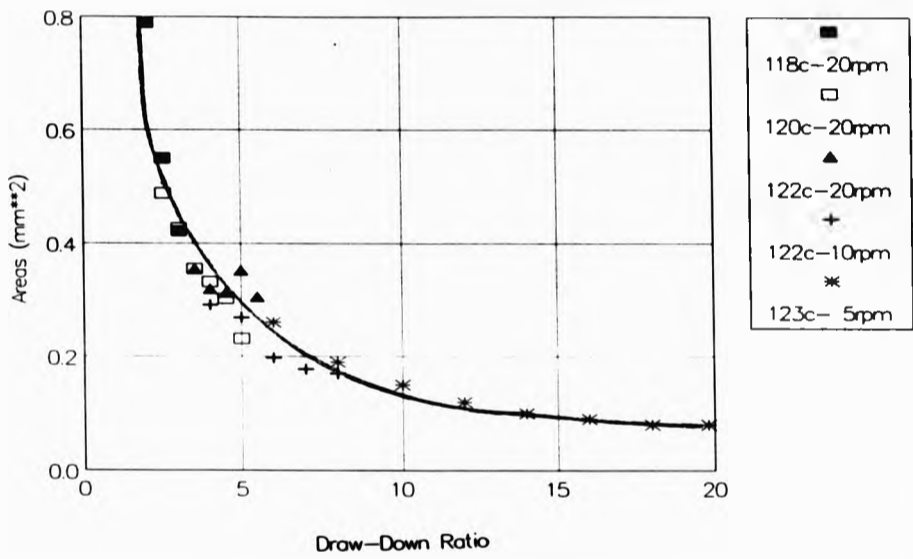


Fig. 4.5.1.2 - Area vs. DDR (experiment 5)

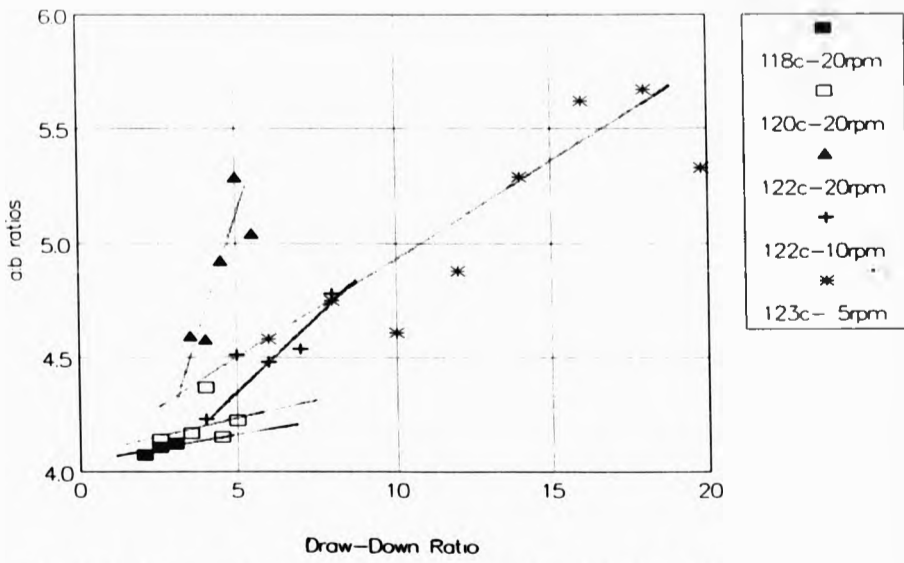


Fig. 4.5.1.3 - A:B ratio vs. DDR. (experiment 5)

4.5.2 - STRESS-STRAIN CURVES FOR EXTRUDATES

**TABLE 4.5.2.1 - OUTPUT = 20 rpm; QUENCHING TEMP. = 118°C
STRESS (MPa)**

Strain	HAUL-OFF SPEED		
	40 RPM	50 RPM	60 RPM
0%	0.0	0.0	0.0
2%	12.8	13.4	11.3
4%	19.0	19.9	21.5
6%	21.9	23.3	24.7
8%	23.3	24.8	26.3
10%	23.8	25.4	27.0
12%	24.0	25.7	27.3
14%	24.1	25.9	27.5
16%	24.0	25.9	27.5
18%	23.9	25.8	27.4
20%	23.8	25.6	27.2

**TABLE 4.5.2.2 - OUTPUT = 20 rpm; QUENCHING TEMP. = 120°C
STRESS (MPa)**

Strain	HAUL-OFF SPEED					
	50rpm	60rpm	70rpm	80rpm	90rpm	100rpm
0%	0.0	0.0	0.0	0.0	0.0	0.0
2%	14.4	16.3	17.1	17.8	17.3	17.3
4%	21.9	23.1	24.4	25.6	25.2	26.8
6%	25.2	26.3	27.9	29.6	29.4	31.4
8%	26.7	27.9	29.9	31.6	31.8	34.7
10%	27.4	28.8	31.1	33.1	33.8	37.1
12%	27.9	29.5	31.8	34.3	35.1	39.1
14%	28.1	29.9	32.4	35.2	36.3	40.4
16%	28.1	30.1	32.7	35.8	36.9	41.0
18%	28.0	30.0	32.7	36.0	37.1	41.4
20%	27.8	29.9	32.7	36.0	37.4	41.9

TABLE 4.5.2.3 - OUTPUT = 20 rpm; QUENCHING TEMP. = 122°C
STRESS (MPa)

Strain	HAUL-OFF SPEED				
	70rpm	80rpm	90rpm	100rpm	110rpm
0%	0.0	0.0	0.0	0.0	0.0
2%	19.6	20.1	24.5	25.3	25.2
4%	31.2	32.1	38.5	39.1	40.8
6%	38.1	38.6	47.0	48.4	49.6
8%	42.2	42.8	53.1	54.7	56.3
10%	45.7	46.5	58.7	60.4	62.9
12%	49.0	49.8	63.3	65.9	69.4
14%	52.0	52.9	67.9	70.8	75.7
16%	54.3	55.3	71.3	74.7	81.4
18%	55.7	56.8	73.6	76.6	85.6
20%	56.2	57.3	75.5	77.5	87.8

TABLE 4.5.2.4 - OUTPUT = 10 rpm; QUENCHING TEMP. = 122°C
STRESS (MPa)

Strain	HAUL-OFF SPEED				
	50rpm	60rpm	70rpm	80rpm	90rpm
0%	0.0	0.0	0.0	0.0	0.0
2%	16.9	21.2	22.2	24.6	28.0
4%	26.0	32.2	34.3	36.6	44.0
6%	30.4	38.5	42.3	43.7	53.8
8%	33.3	42.9	47.7	49.2	61.2
10%	35.2	45.8	51.9	53.9	68.0
12%	36.6	48.7	55.2	57.3	73.6
14%	37.2	51.0	57.3	59.4	77.7
16%	37.3	51.8	58.1	60.3	78.9
18%	37.3	52.3	58.8	61.2	80.1
20%	37.3	52.9	59.7	61.9	81.6

TABLE 4.5.2.5a - OUTPUT = 5 rpm; QUENCHING TEMP. = 123°C
STRESS (MPa)

Strain	HAUL-OFF SPEED			
	30 RPM	40 RPM	50 RPM	60 RPM
0%	0.0	0.0	0.0	0.0
2%	18.6	25.2	26.6	27.1
4%	26.7	38.1	37.4	41.6
6%	30.6	45.7	44.7	51.4
8%	33.2	51.0	49.9	58.0
10%	34.9	54.8	53.4	64.3
12%	35.6	57.9	56.1	68.3
14%	36.1	59.3	56.9	70.4
16%	36.1	59.6	57.5	71.5
18%	36.0	60.2	58.5	73.0
20%	35.6	61.0	59.3	74.6

TABLE 4.5.2.5b - OUTPUT = 5 rpm; QUENCHING TEMP. = 123°C
STRESS (MPa)

Strain	HAUL-OFF SPEED			
	70 RPM	80 RPM	90 RPM	100 RPM
0%	0.0	0.0	0.0	0.0
2%	34.0	36.8	38.8	38.1
4%	51.2	60.3	64.0	64.2
6%	63.5	77.8	81.6	82.1
8%	74.0	92.1	97.2	98.1
10%	82.6	106.3	112.5	113.9
12%	90.6	118.4	126.1	129.0
14%	95.1	127.1	134.5	137.2
16%	98.2	131.8	137.9	143.0
18%	101.1	135.3	141.3	147.2
20%	104.1	137.8	145.9	151.4

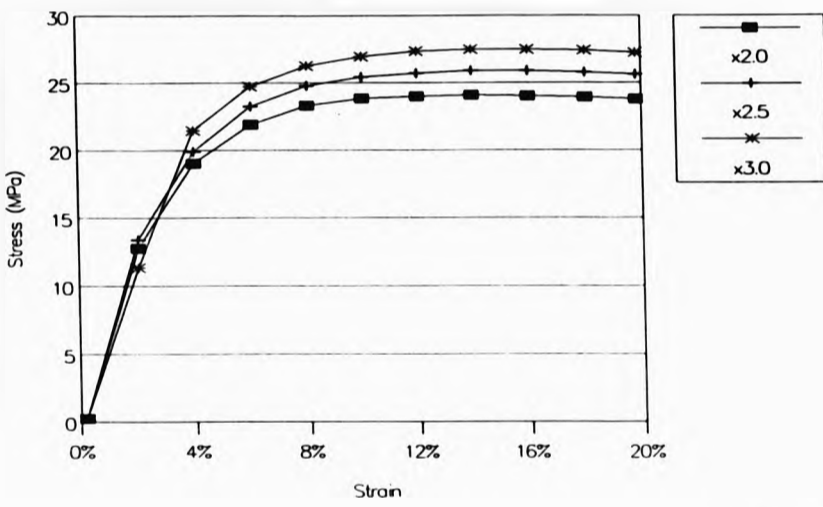


Fig. 4.5.2.1 - Stress vs. Strain; OR = 20 rpm, BT = 118°C (experiment 5)

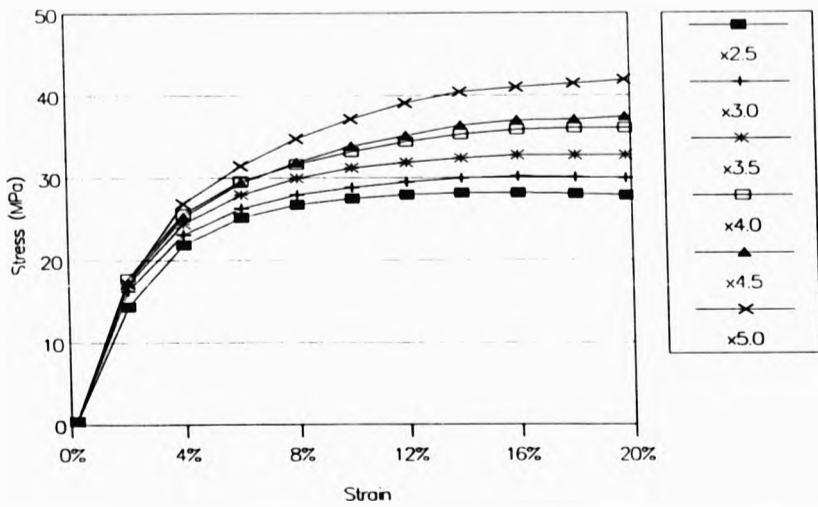


Fig. 4.5.2.2 - Stress vs. Strain; OR = 20 rpm, BT = 120°C (experiment 5)

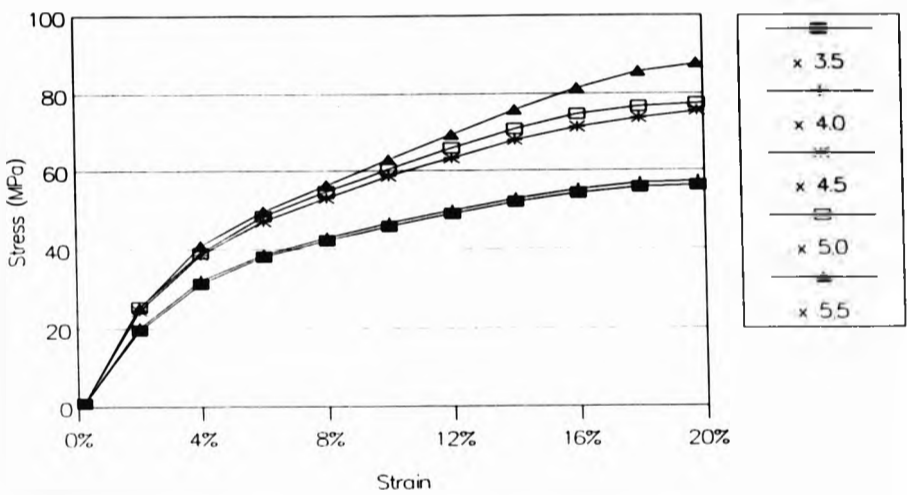


Fig. 4.5.2.3 - Stress vs. Strain; OR = 20 rpm, BT = 122°C (experiment 5)

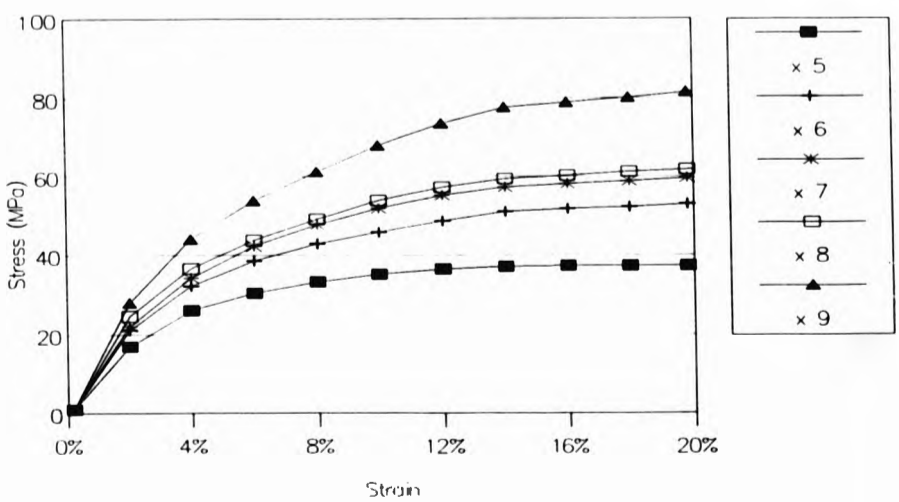


Fig. 4.5.2.4 - Stress vs. Strain; OR = 10 rpm, BT = 122°C (experiment 5)

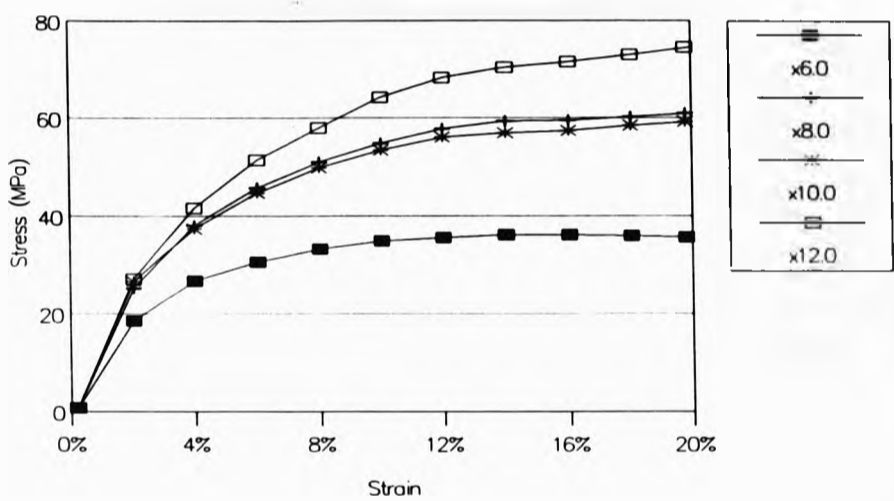


Fig. 4.5.2.5a - Stress vs. Strain; OR = 5 rpm; BT = 123°C (experiment 5)

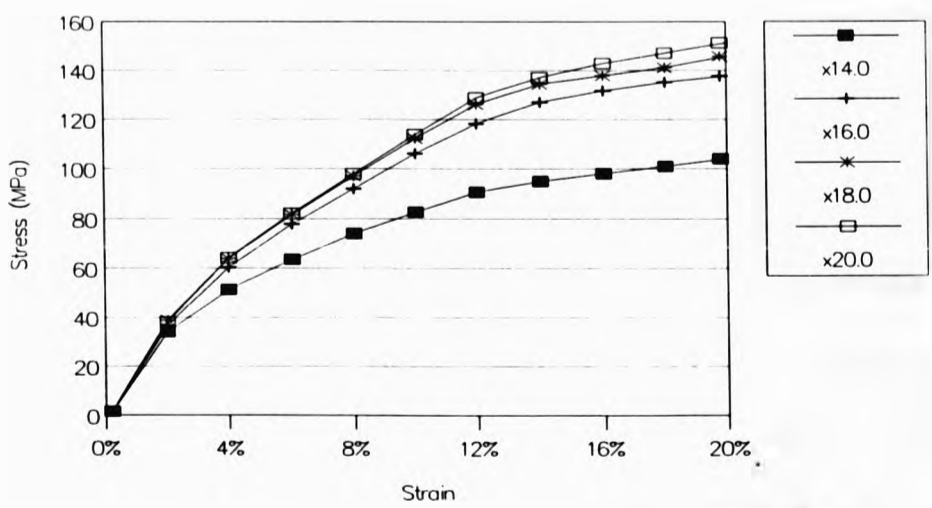


Fig. 4.5.2.5b - Stress vs. Strain; OR = 5 rpm; BT = 123°C (experiment 5)

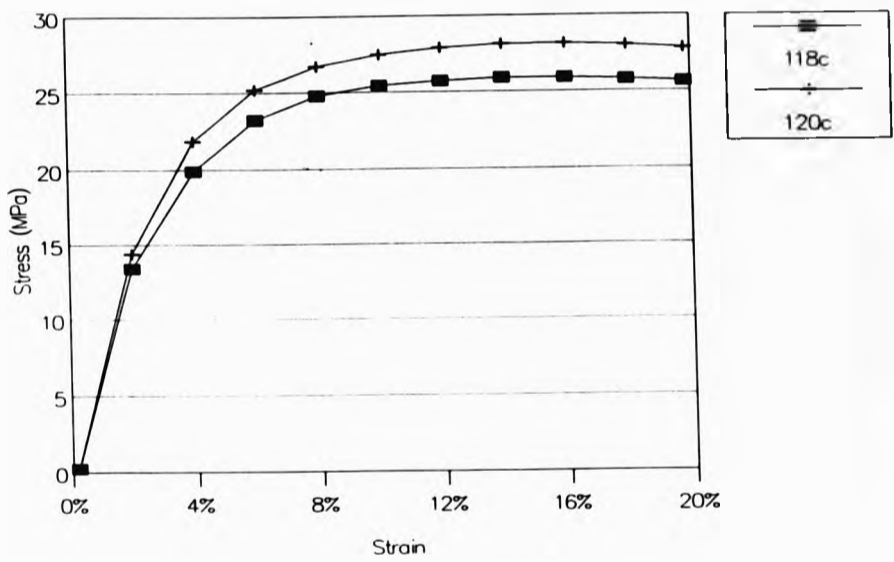


Fig. 4.5.2.6 - Stress vs. Strain; DDR = x2.5 (experiment 5)

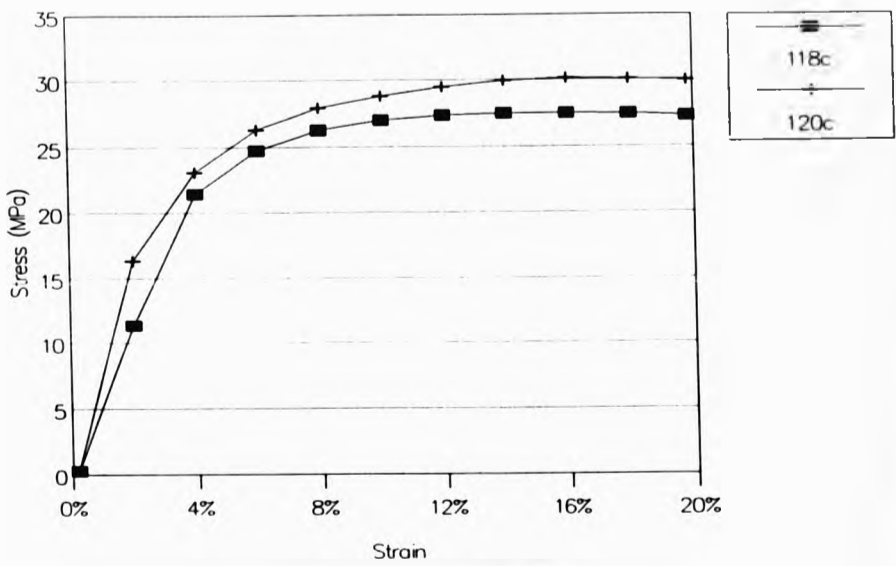


Fig. 4.5.2.7 - Stress vs. Strain; DDR = x3.0 (experiment 5)

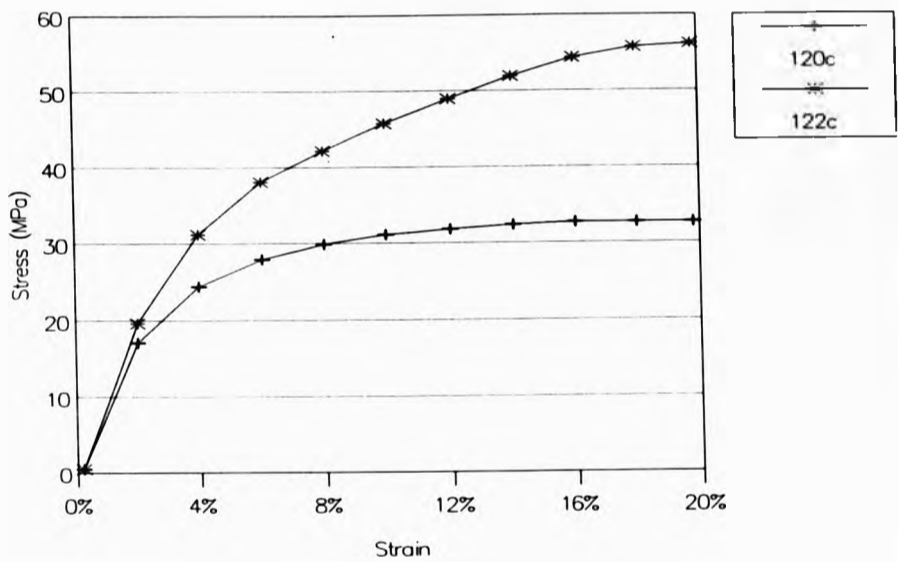


Fig. 4.5.2.8 - Stress vs. Strain; DDR = x3.5 (experiment 5)

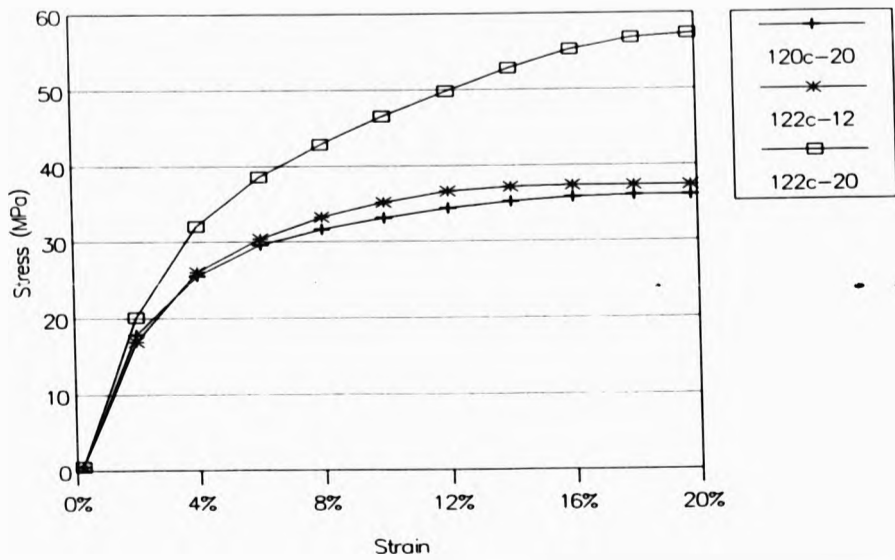


Fig. 4.5.2.9 - Stress vs. Strain; DDR = x4.0 (experiment 5)

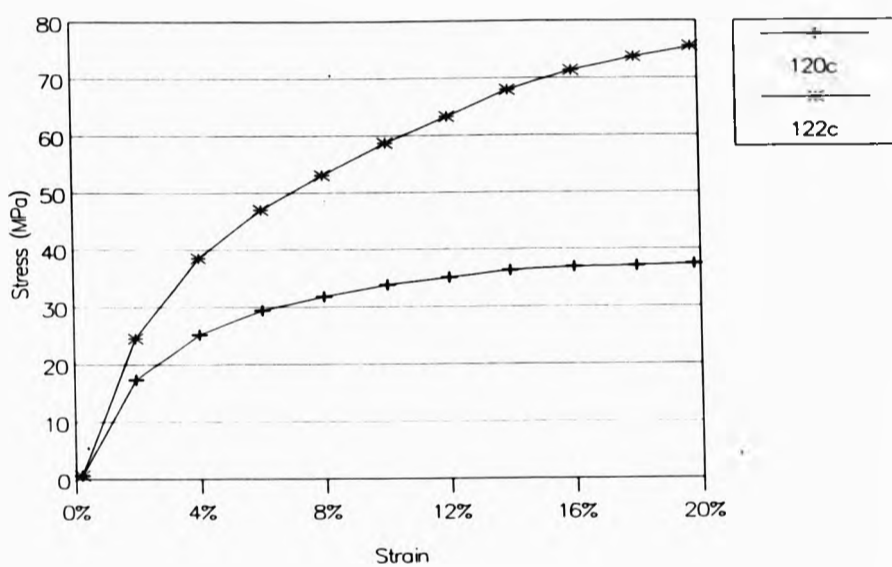


Fig. 4.5.2.10 - Stress vs. Strain; DDR = x4.5 (experiment 5)

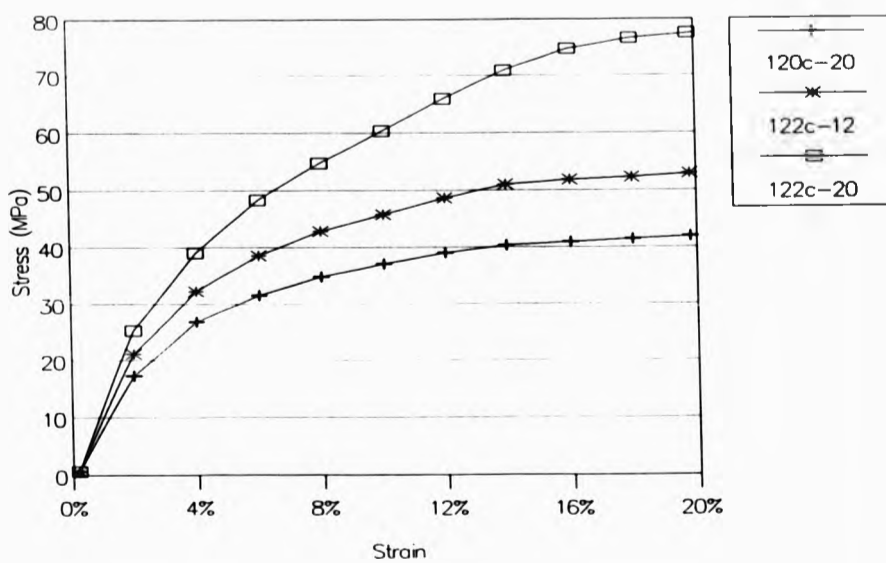


Fig. 4.5.2.11 - Stress vs. Strain; DDR = x5.0 (experiment 5)

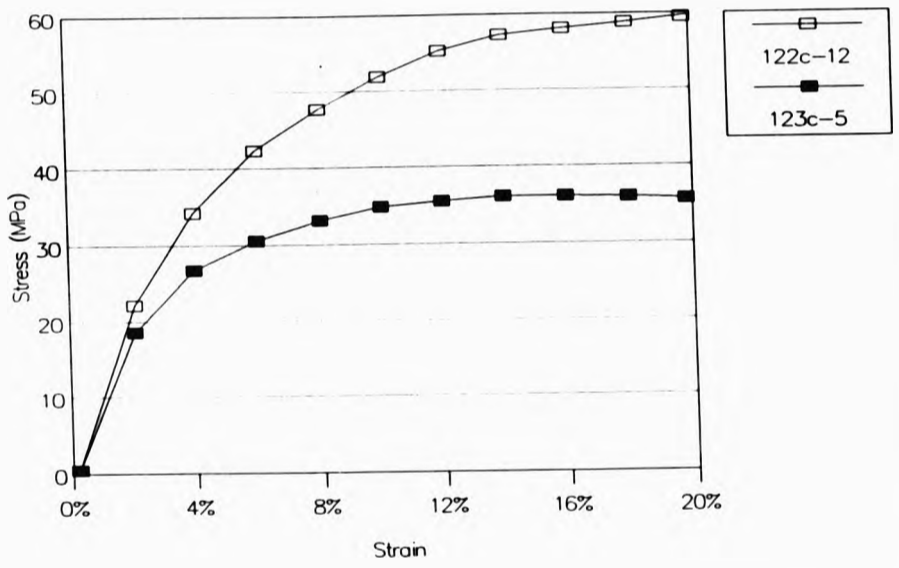


Fig. 4.5.2.12 - Stress vs. Strain; DDR = x6 (experiment 5)

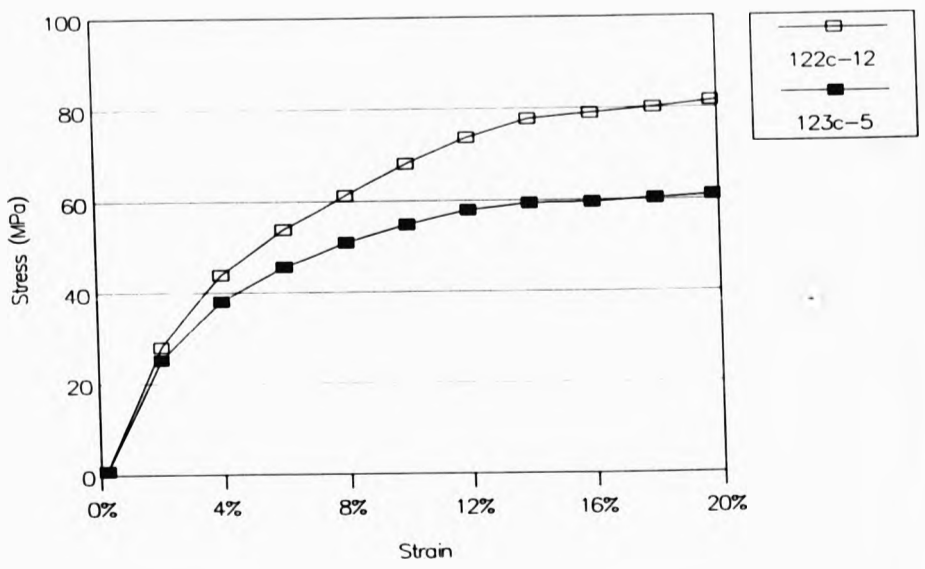


Fig. 4.5.2.13 - Stress vs. Strain; DDR = x8 (experiment 5)

TABLE 4.5.3 - STRESS AT 10% STRAIN (MPa)
(OR = 20rpm UNLESS DENOTED OTHERWISE)

DDR	BATH TEMPERATURE				
	118c	120c	122c	122c*	123c**
2.0	23.8				
2.5	25.4	27.4			
3.0	27.0	28.8			
3.5		31.1	45.7		
4.0		33.1	46.5	35.2	
4.5		33.8	58.7		
5.0		37.1	60.4	45.8	
5.5			62.9		
6.0				51.9	34.9
7.0				53.9	
8.0				68.0	54.8
10.0					53.4
12.0					64.3
14.0					82.6
16.0					106.3
18.0					112.5
20.0					113.9

* OR = 12 rpm
 ** OR = 5 rpm

**TABLE 4.5.4 - STRESS AT BREAK (MPa)
(OR = 20rpm UNLESS DENOTED OTHERWISE)**

DDR	BATH TEMPERATURE				
	118c	120c	122c	122c*	123c**
2.0	30.8				
2.5	38.9	42.6			
3.0	41.8	48.9			
3.5		52.1	56.4		
4.0		55.2	78.8	60.7	
4.5		60.3	67.7		
5.0		70.2	81.7	75.7	
5.5			100.6		
6.0				88.0	62.8
7.0				92.0	
8.0				103.2	95.9
10.0					101.3
12.0					117.9
14.0					143.4
16.0					157.4
18.0					167.6
20.0					180.7

* OR = 12 rpm
** OR = 5 rpm

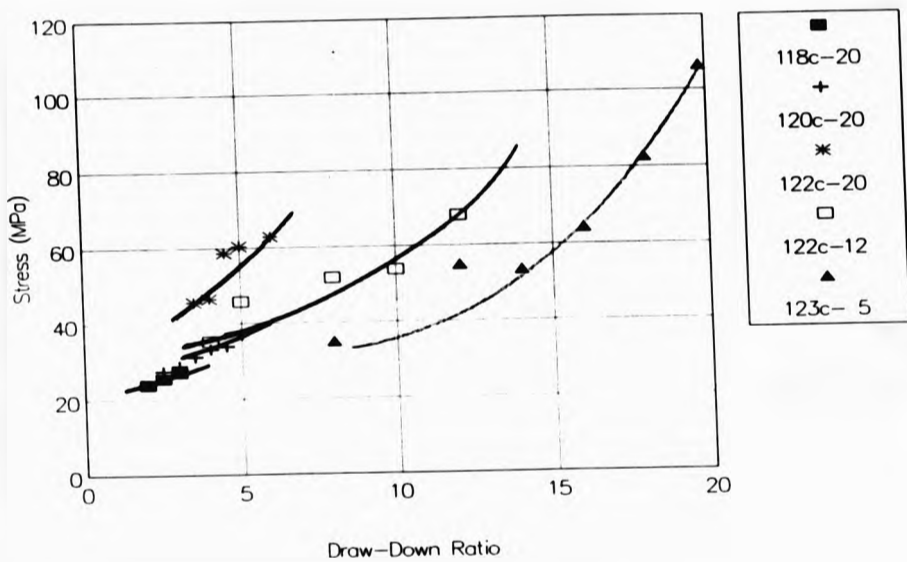


Fig. 4.5.3 - Stress at 10% Strain vs. DDR (experiment 5)

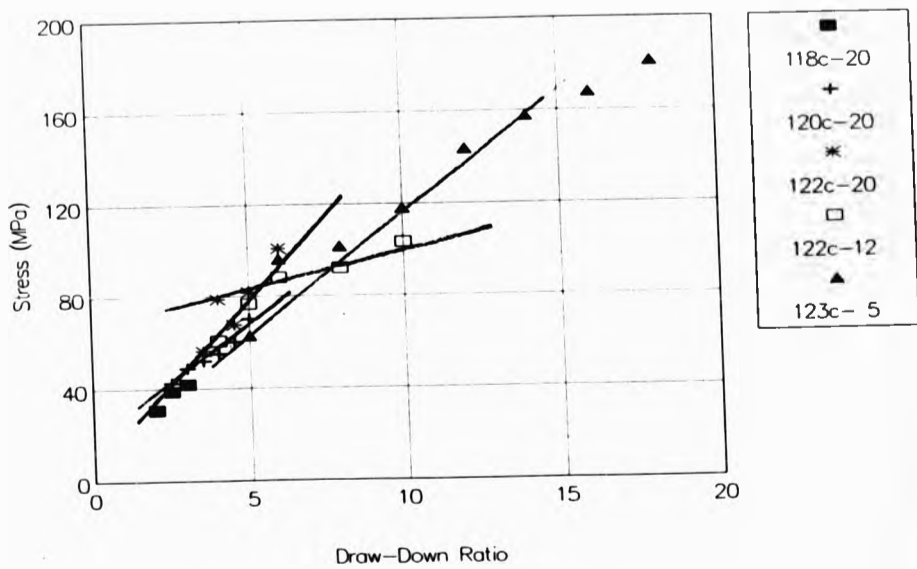


Fig. 4.5.4 - Stress at Break vs. DDR (experiment 5)

4.6 - POLYMER EXTRUDATES QUENCHED IN LIQUID METAL ALLOY (5)

4.6.1 - EXTRUDATES FROM A FILM DIE

TABLE 4.6.1.1 - AVERAGE DIMENSIONS OF EXTRUDATES (mm)

HOS	OR = 20rpm			OR = 12rpm	
	BT = 117c	BT = 118c	BT = 119c	BT = 122c	BT = 123c
15rpm	19.12 0.10				
20rpm	16.78 0.09				
25rpm	15.18 0.08				
30rpm		13.64 0.08			
35rpm		13.36 0.07			
40rpm		13.26 0.07	11.56 0.06		
45rpm		11.08 0.06	10.96 0.05		17.02 0.04
50rpm			10.64 0.06		
55rpm		11.80 0.06	10.30 0.05	14.78 0.04	15.80 0.04
60rpm			9.78 0.05	13.58 0.04	13.66 0.04
65rpm			9.54 0.05		
70rpm			9.02 0.05	13.04 0.04	13.14 0.04
75rpm			7.96 0.04	12.14 0.05	
80rpm			8.60 0.04		12.00 0.03
85rpm			9.10 0.04		
90rpm					12.70 0.03
100rpm					11.18 0.02

TABLE 4.6.1.2 - AVERAGE AREAS OF EXTRUDATES (mm²)

HOS	OR = 20rpm			OR = 12rpm	
	BT = 117c	BT = 118c	BT = 119c	BT = 122c	BT = 123c
15rpm	2.00				
20rpm	1.52				
25rpm	1.20				
30rpm		1.06			
35rpm		0.89			
40rpm		0.95	0.70		
45rpm		0.62	0.59		0.72
50rpm			0.55		
55rpm		0.72	0.50	0.65	0.58
60rpm			0.50	0.58	0.49
65rpm			0.49		
70rpm			0.41	0.56	0.49
75rpm			0.31	0.55	
80rpm			0.36		0.41
85rpm			0.35		
90rpm					0.38
100rpm					0.26

TABLE 4.6.1.3 - AVERAGE A:B RATIOS

HOS	OR = 20rpm			OR = 12rpm	
	BT = 117c	BT = 118c	BT = 119c	BT = 122c	BT = 123c
15rpm	184.91				
20rpm	186.44				
25rpm	192.15				
30rpm		177.14			
35rpm		201.20			
40rpm		186.24	192.67		
45rpm		200.72	202.96		399.53
50rpm			186.67		
55rpm			190.74	335.91	431.69
60rpm			191.02	317.29	381.56
65rpm			187.06		
70rpm			197.81	303.26	351.34
75rpm			200.00	268.58	
80rpm			207.23		350.88
85rpm			242.02		
90rpm					420.53
100rpm					473.73

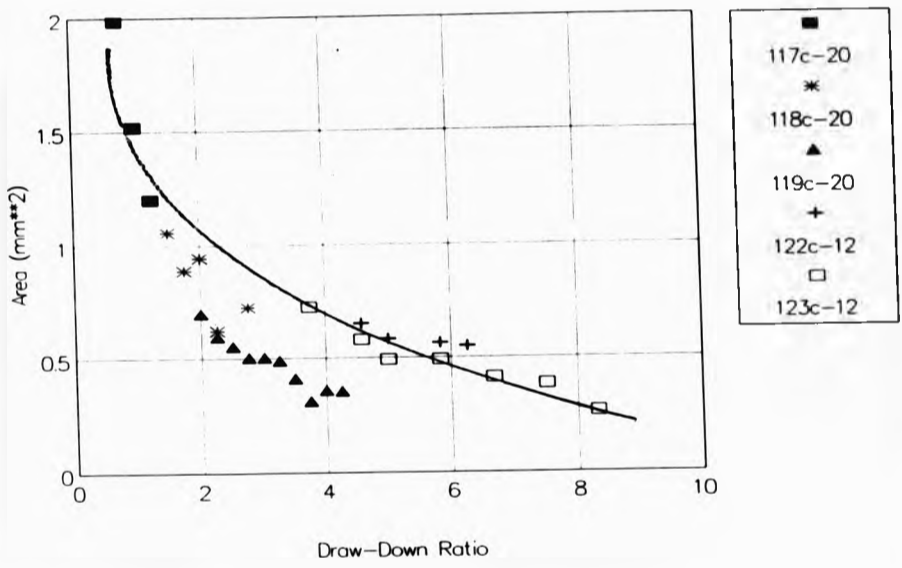


Fig. 4.6.1.2 - Area vs. DDR (experiment 6)

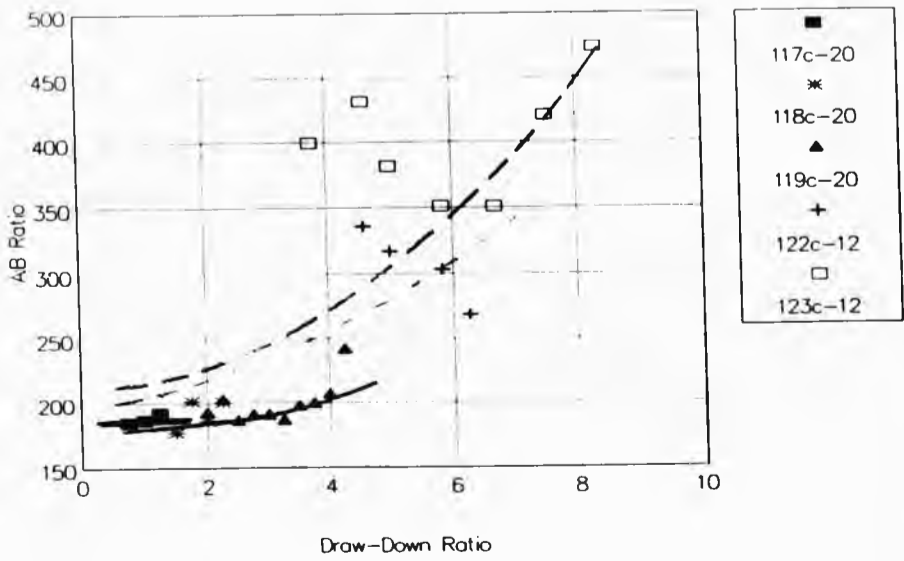


Fig. 4.6.1.3 - A:B ratio vs. DDR (experiment 6)

4.6.2 - STRESS-STRAIN CURVES FOR EXTRUDATES

TABLE 4.6.2.1 - OUTPUT = 20 rpm; BT = 117^oC
STRESS (MPa)

Strain	HAUL-OFF SPEED		
	15rpm	20rpm	25rpm
0%	0.00	0.00	0.00
2%	15.27	15.86	17.65
4%	21.71	21.83	24.31
6%	24.21	23.92	26.23
8%	25.03	24.42	26.62
10%	25.26	24.39	26.54
12%	25.17	24.20	26.41
14%	24.96	23.97	26.13
16%	24.67	23.73	25.93
18%	24.36	23.52	25.76
20%	24.06	23.35	25.61

TABLE 4.6.2.2 - OUTPUT = 20 rpm; BT = 118^oC
STRESS (MPa)

Strain	HAUL-OFF SPEED				
	30rpm	35rpm	40rpm	45rpm	55rpm
0%	0.00	0.00	0.00	0.00	0.00
2%	17.41	18.94	18.35	23.27	22.40
4%	24.50	25.89	25.45	30.71	29.76
6%	26.33	27.84	27.70	31.76	30.78
8%	26.49	28.08	27.98	31.55	30.69
10%	26.20	27.95	27.85	31.24	30.37
12%	25.85	27.80	27.73	30.92	30.05
14%	25.58	27.63	27.58	30.81	29.77
16%	26.18	27.50	27.42	30.65	29.58
18%	26.01	27.29	27.27	30.54	29.51
20%	25.86	27.16	27.12	30.45	29.43

TABLE 4.6.2.3a - OUTPUT = 20 rpm; BT = 119°C
STRESS (MPa)

Strain	HAUL-OFF SPEED			
	40rpm	45rpm	50rpm	55rpm
0%	0.00	0.00	0.00	0.00
2%	20.40	21.16	20.92	21.18
4%	29.02	28.66	30.20	29.89
6%	30.92	31.28	33.32	33.22
8%	31.00	32.23	34.46	34.74
10%	30.78	32.69	34.86	35.58
12%	30.51	32.90	35.02	35.95
14%	30.09	32.85	34.87	35.89
16%	29.91	32.64	34.55	35.48
18%	29.73	32.31	34.24	35.24
20%	29.56	32.11	33.71	35.05

TABLE 4.6.2.3b - OUTPUT = 20 rpm; BT = 119°C
STRESS (MPa)

Strain	HAUL-OFF SPEED			
	60rpm	70rpm	80rpm	90rpm
0%	0.00	0.00	0.00	0.00
2%	22.70	27.36	28.24	27.98
4%	32.17	35.73	39.60	41.62
6%	36.27	40.64	45.79	49.18
8%	37.95	43.27	50.02	53.89
10%	39.73	45.04	52.58	56.88
12%	40.21	45.81	53.73	58.22
14%	40.15	45.97	54.14	58.73
16%	39.83	45.96	54.30	59.28
18%	39.59	46.05	54.69	59.79
20%	39.44	46.13	55.14	60.50

TABLE 4.6.2.4 - OUTPUT = 12 rpm; BT = 122^oC
STRESS (MPa)

Strain	HAUL-OFF SPEED			
	55rpm	60rpm	70rpm	75rpm
0%	0.00	0.00	0.00	0.00
2%	33.28	35.68	33.13	32.30
4%	47.33	49.30	47.55	46.61
6%	54.08	56.16	55.21	54.45
8%	59.06	62.02	61.23	59.92
10%	62.76	66.09	65.50	64.80
12%	64.07	67.48	67.37	67.22
14%	64.38	67.93	67.89	67.71
16%	65.19	68.90	68.63	68.72
18%	66.09	69.76	69.60	69.75
20%	66.96	70.76	70.55	70.65

TABLE 4.6.2.5a - OUTPUT = 12 rpm; BT = 123^oC
STRESS (MPa)

Strain	HAUL-OFF SPEED			
	45rpm	55rpm	60rpm	70rpm
0%	0.00	0.00	0.00	0.00
2%	31.02	37.17	42.81	40.84
4%	42.83	51.99	58.52	56.81
6%	48.69	59.24	67.22	65.22
8%	52.63	64.37	74.02	72.35
10%	54.56	67.02	78.87	77.17
12%	54.62	67.20	79.99	78.88
14%	54.48	67.28	80.18	79.16
16%	54.48	67.36	80.77	80.03
18%	54.45	67.58	81.35	80.82
20%	54.42	67.70	81.89	81.51

TABLE 4.6.2.5b - OUTPUT = 12 rpm; BT = 123^oc
STRESS (MPa)

Strain	HAUL-OFF SPEED			
	80rpm	90rpm	100rpm	110rpm
0%	0.00	0.00	0.00	0.00
2%	44.83	48.75	55.89	65.61
4%	61.94	67.47	80.00	96.22
6%	71.93	78.05	94.68	115.85
8%	80.02	86.88	106.50	131.77
10%	85.76	92.11	114.61	143.53
12%	87.16	93.59	117.23	148.87
14%	87.82	93.96	118.59	153.62
16%	88.81	94.55	119.97	157.33
18%	89.76	95.24	121.35	159.89
20%	85.00	95.93	122.67	162.35

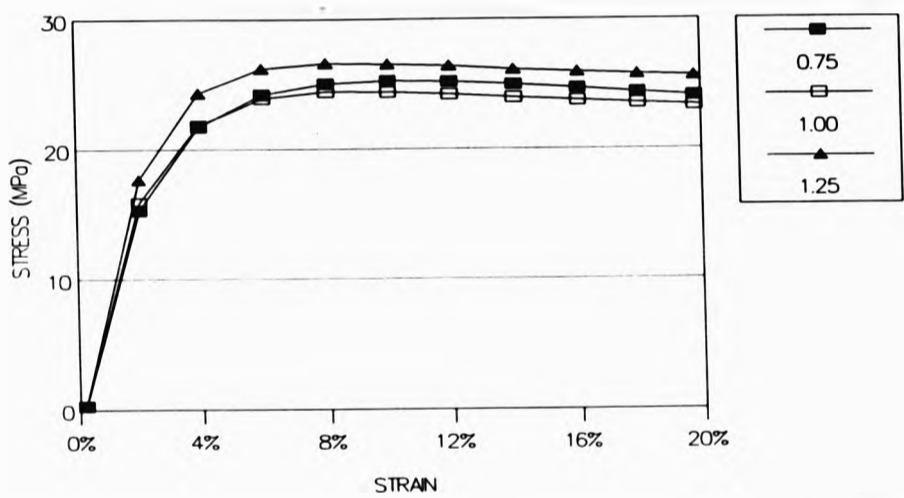


Fig. 4.6.2.1 - Stress vs. Strain (for values of DDR);
BT = 117°C, OR = 20 rpm (experiment 6)

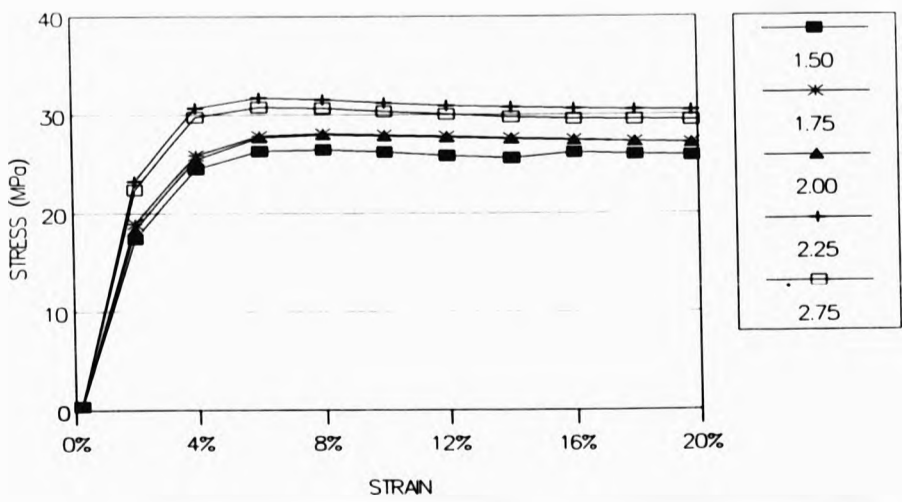


Fig. 4.6.2.2 - Stress vs. Strain (for values of DDR);
BT = 118°C, OR = 20rpm (experiment 6)

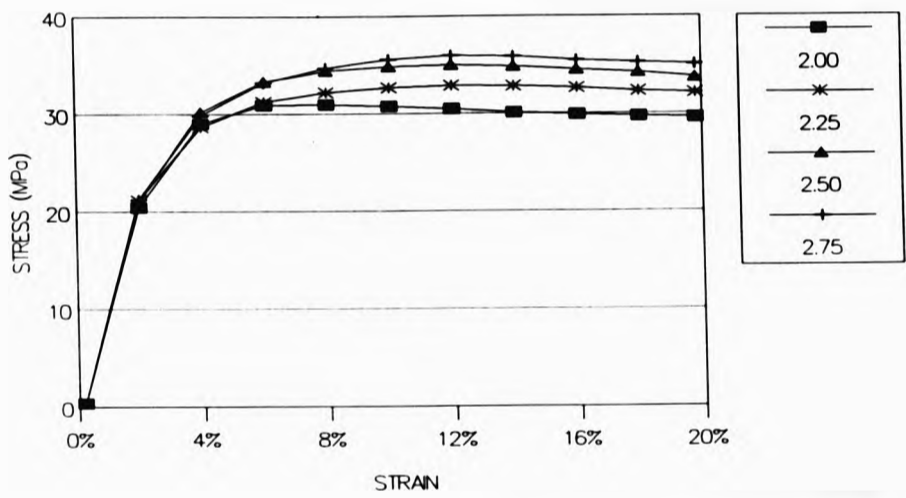


Fig. 4.6.2.3a - Stress vs. Strain (for values of DDR);
BT = 119°C, OR = 20rpm (experiment 6)

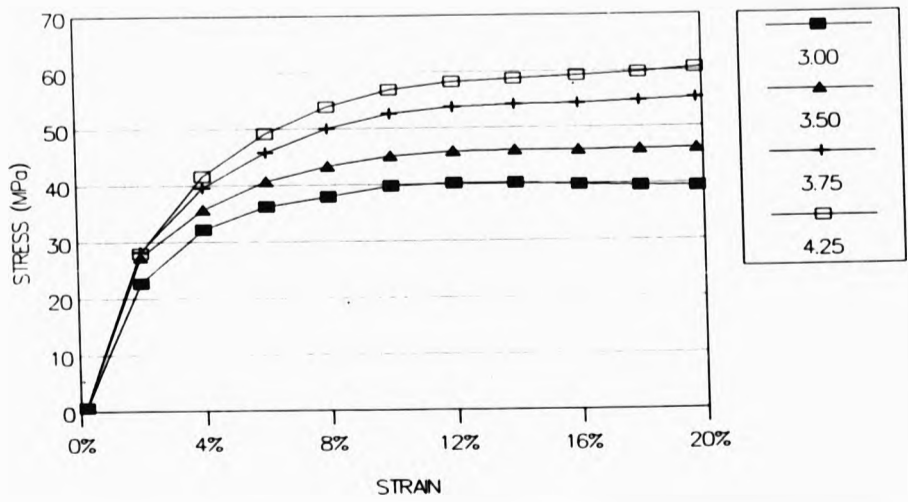


Fig. 4.6.2.3b - Stress vs. Strain (for values of DDR);
BT = 119°C, OR = 20 rpm (experiment 6)

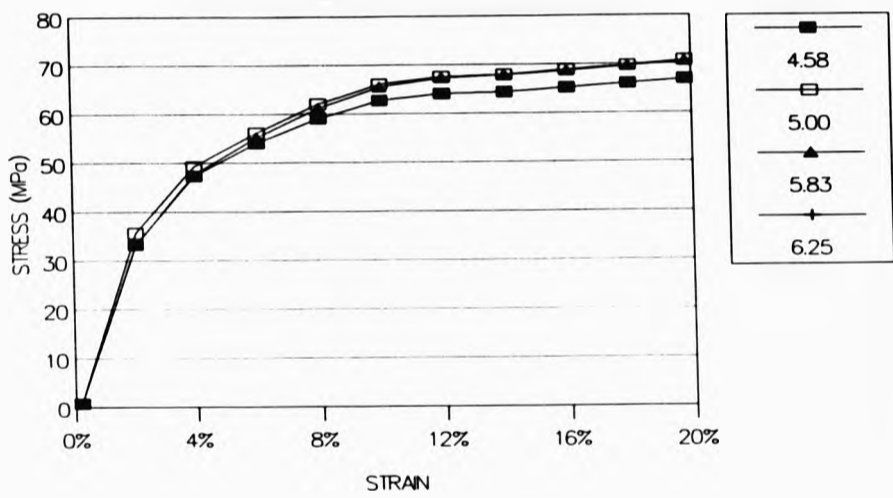


Fig. 4.6.2.4 - Stress vs. Strain (for values of DDR);
BT = 122°C, OR = 12rpm (experiment 6)

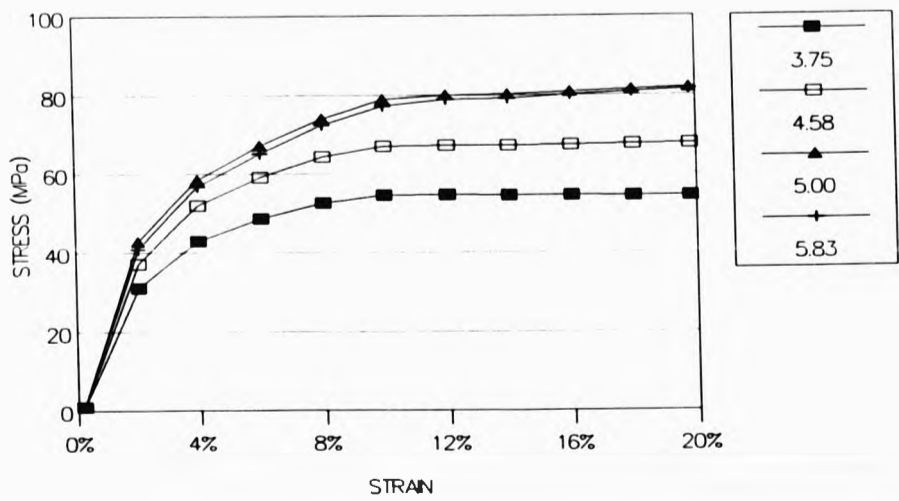


Fig. 4.6.2.5a - Stress vs. Strain (for values of DDR);
BT = 123°C, OR = 12rpm (experiment 6)

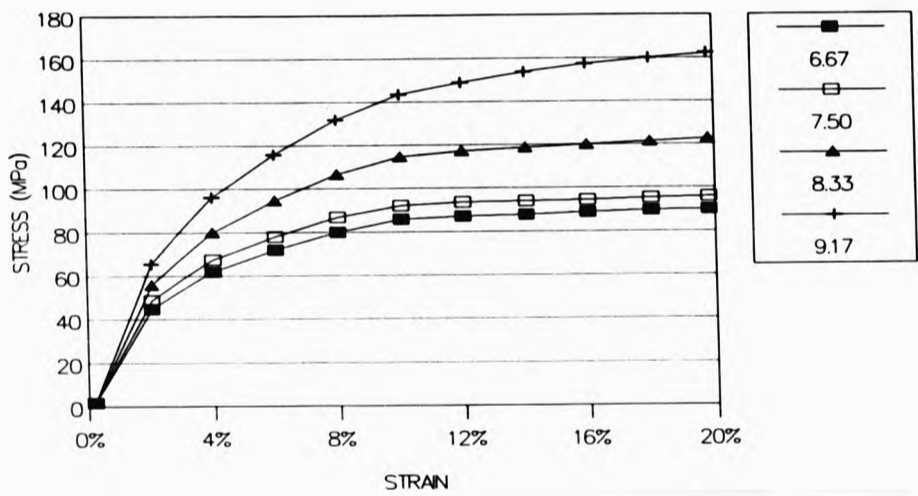


Fig. 4.6.2.5b - Stress vs. Strain (for values of DDR);
BT = 123°C, OR = 12rpm (experiment 6)

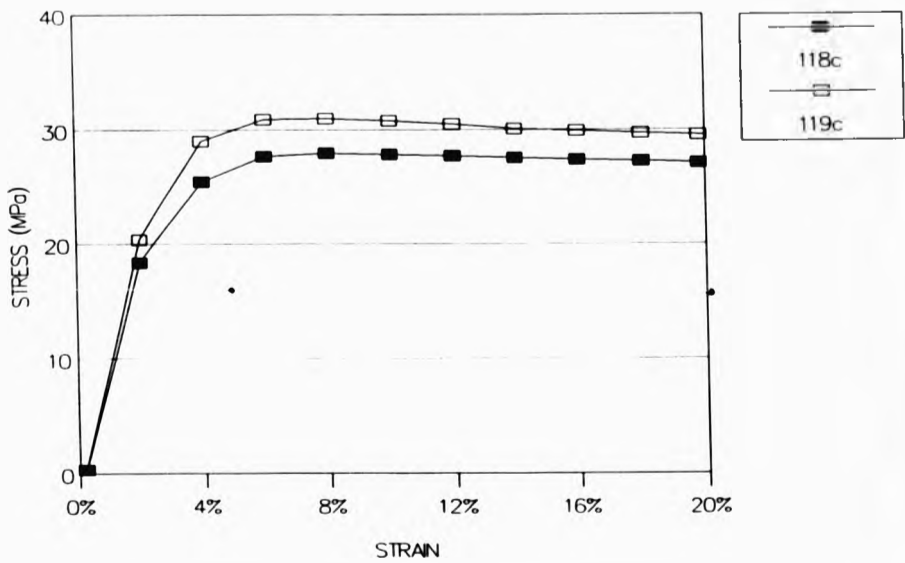


Fig. 4.6.2.6 - Stress vs. Strain; DDR = 2.0 (experiment 6)

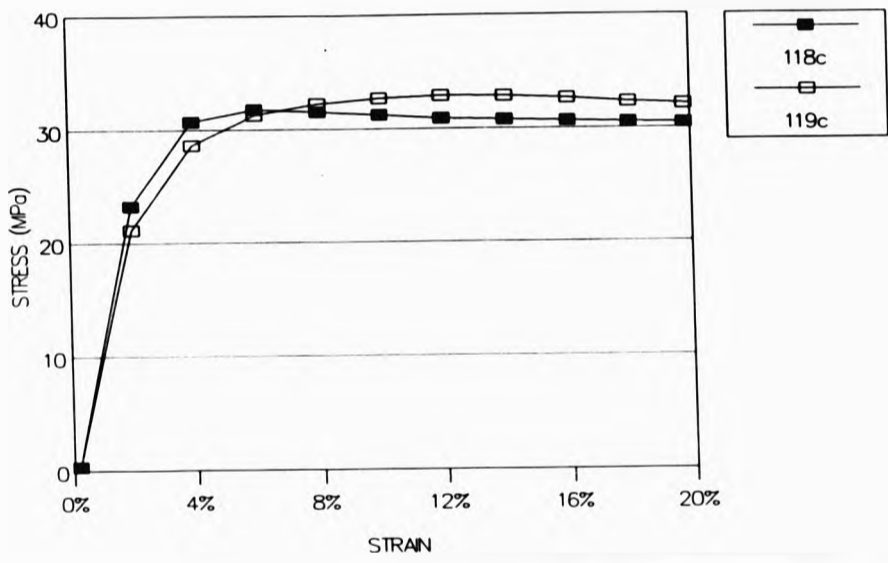


Fig. 4.6.2.7 - Stress vs. Strain; DDR = x2.25 (experiment 6)

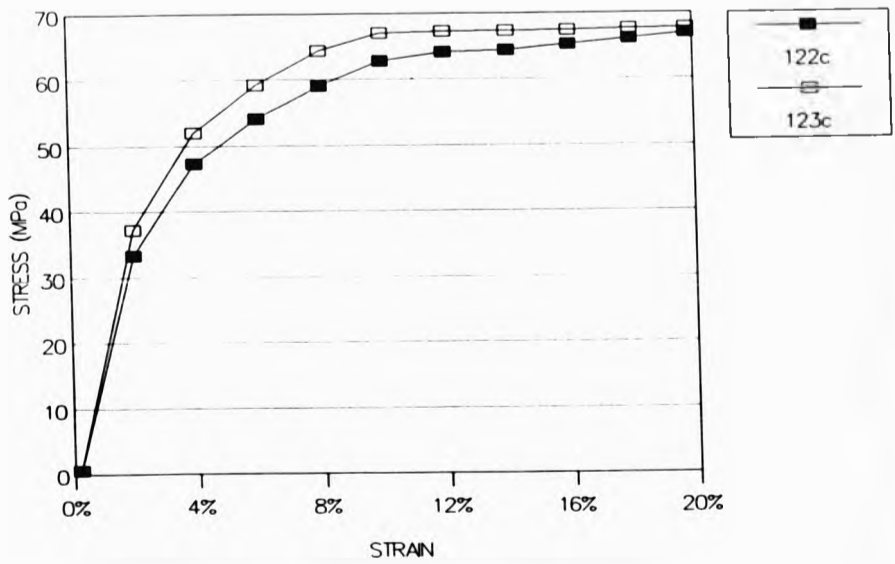


Fig. 4.6.2.8 - Stress vs. Strain; DDR = x4.58 (experiment 6)

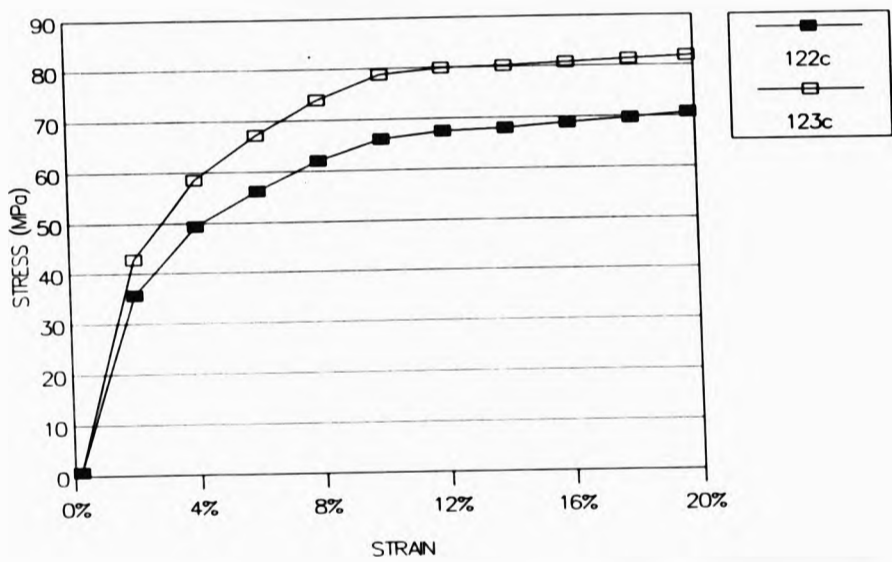


Fig. 4.6.2.9 - Stress vs. Strain; DDR = x5.00 (experiment 6)

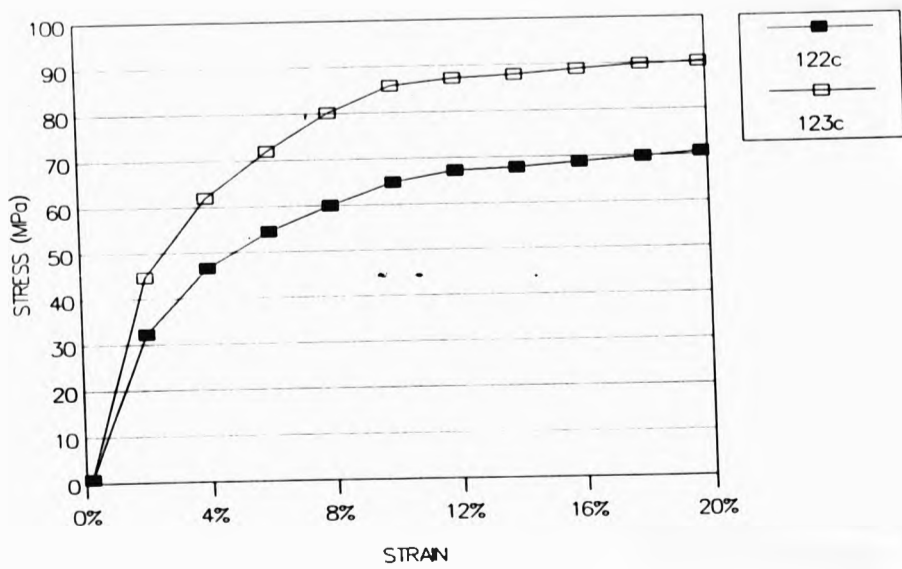


Fig. 4.6.2.10 - Stress vs. Strain; DDR = x5.83 (experiment 6)

TABLE 4.6.3 - STRESS AT 10% STRAIN (MPa)

DDR	BATH TEMPERATURE				
	117 c	118 c	119 c	122 c	123 c
0.75	25.26				
1.00	24.39				
1.25	26.54				
1.50		26.20			
1.75		27.95			
2.00		27.85	30.78		
2.25		31.24	32.69		
2.50			34.86		
2.75		30.37	35.58		
3.00			39.73		
3.50			45.04		
3.75					54.56
4.00			52.58		
4.50			56.88	62.76	67.02
5.00				66.09	78.87
5.87					77.17
6.25				65.50	
6.67				64.80	85.76
7.50					92.11
8.33					114.61
9.17					114.61

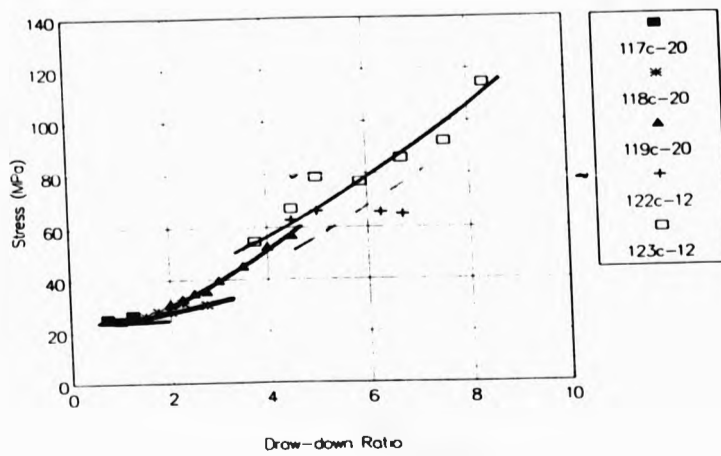


Fig. 4.6.3 - Stress at 10% Strain vs. DDR (experiment 6)

4.7 - SHRINKAGE RECOVERY OF EXTRUDATES

4.7.1 - EXTRUDATES FROM A CIRCULAR DIE

**TABLE 4.7.1.1 - FINAL LENGTH OF EXTRUDATES (cm)
(INITIAL LENGTH = 5cm)**

BT = 118c OR= 5rpm	Draw-Down Ratio				
	x2	x3	x4	x5	x6
Sample 1	0.89	0.68	0.63	0.54	0.50
Sample 2	0.90	0.68	0.64	0.52	0.48
Sample 3	0.90	0.71	0.60	0.52	0.49
Sample 4	0.90	0.70	0.61	0.52	0.48
Sample 5	0.97	0.68	0.61	0.53	0.50

BT = 118c OR=10rpm	Draw-Down Ratio				
	x2	x3	x4	x5	x6
Sample 1	0.78	0.55	0.42	0.40	0.33
Sample 2	0.81	0.56	0.41	0.39	0.34
Sample 3	0.80	0.54	0.43	0.39	0.33
Sample 4	0.78	0.57	0.44	0.40	0.34
Sample 5	0.79	0.55	0.44	0.41	0.32

BT = 118c OR=20rpm	Draw-Down Ratio				
	x2	x3	x4	x5	x6
Sample 1	0.64	0.57	0.48	0.32	0.27
Sample 2	0.67	0.56	0.48	0.33	0.28
Sample 3	0.66	0.56	0.47	0.33	0.27
Sample 4	0.64	0.57	0.47	0.32	0.28
Sample 5	0.64	0.57	0.48	0.33	0.29

BT = 118c OR=28rpm	Draw-Down Ratio			
	x2	x3	x4	x5
Sample 1	0.65	0.54	0.41	0.28
Sample 2	0.68	0.54	0.40	0.29
Sample 3	0.66	0.55	0.41	0.29
Sample 4	0.66	0.55	0.42	0.29
Sample 5	0.68	0.53	0.40	0.29

TABLE 4.7.1.2 - RECOVERY OF EXTRUDATES (LOG(L₀/L_f))

BT=118c DDR	OUTPUT RATE			
	5rpm	10rpm	20rpm	28rpm
2	0.739	0.800	0.886	0.876
3	0.860	0.956	0.946	0.965
4	0.908	1.068	1.021	1.088
5	0.978	1.099	1.186	1.240
6	1.009	1.178	1.255	

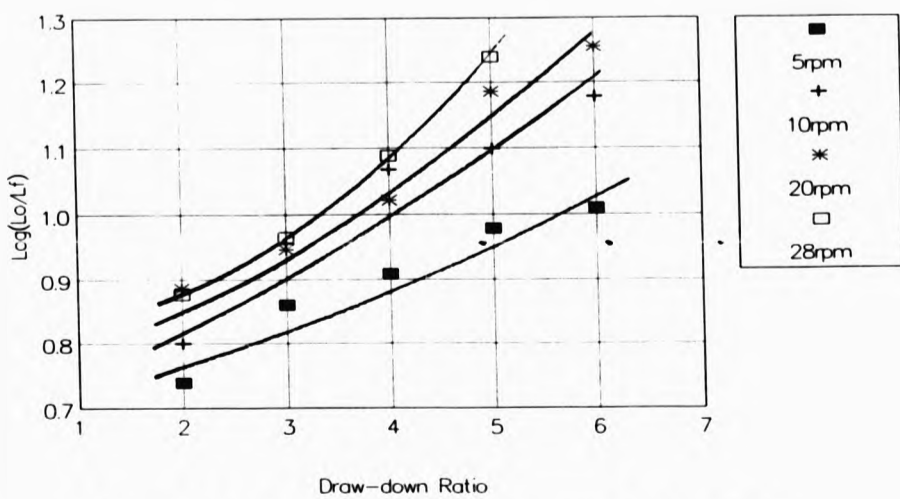


Fig. 4.7.1.2 - Shrinkage Recovery vs. DDR

4.7.2 - EXTRUDATES FROM A STRIP DIE

TABLE 4.7.2.1 - FINAL LENGTH OF EXTRUDATES (cm)
(INITIAL LENGTH = 5cm)

BT-118c OR-20rpm	Draw-Down Ratio			
	x2.0	x2.5	x3.0	x3.5
Sample 1	0.77	0.61	0.58	0.53
Sample 2	0.75	0.60	0.62	0.56
Sample 3	0.73	0.60	0.61	0.60
Sample 4	0.76	0.60	0.60	0.60
Sample 5	0.72	0.61	0.60	0.56

120c 20rpm	Draw-Down Ratio					
	x2.5	x3.0	x3.5	x4.0	x4.5	x5.0
Sample 1	0.54	0.49	0.44	0.42	0.35	0.30
Sample 2	0.54	0.46	0.46	0.43	0.36	0.32
Sample 3	0.57	0.51	0.45	0.43	0.38	0.33
Sample 4	0.55	0.49	0.45	0.44	0.37	0.38
Sample 5	0.52	0.48	0.45	0.43	0.36	0.37

122c 20rpm	Draw-Down Ratio				
	x3.5	x4.0	x4.5	x5.0	x5.5
Sample 1	0.32	0.27	0.27	0.21	0.20
Sample 2	0.29	0.27	0.27	0.22	0.21
Sample 3	0.29	0.27	0.27	0.30	0.21
Sample 4	0.31	0.27	0.26	0.27	0.21
Sample 5	0.30	0.28	0.28	0.31	0.22

122c 12rpm	Draw-Down Ratio				
	x4.0	x5.0	x6.0	x7.0	x8.0
Sample 1	0.30	0.25	0.20	0.19	0.17
Sample 2	0.30	0.24	0.20	0.19	0.16
Sample 3	0.31	0.25	0.20	0.18	0.18
Sample 4	0.31	0.25	0.21	0.20	0.18
Sample 5	0.31	0.25	0.21	0.20	

TABLE 4.7.2.2 - RECOVERY OF EXTRUDATES (LOG(L₀/L_f))

DDR	OR=20rpm			OR=12rpm
	BT=118c	BT=120c	BT=122c	BT=122c
2.0	0.826			
2.5	0.918	0.964		
3.0	0.919	1.013		
3.5	0.944	1.046	1.219	
4.0		1.066	1.264	1.175
4.5		1.138	1.268	
5.0		1.169	1.286	1.213
5.5		1.252	1.377	
6.0			1.357	1.305
7.0				1.389
8.0				1.416

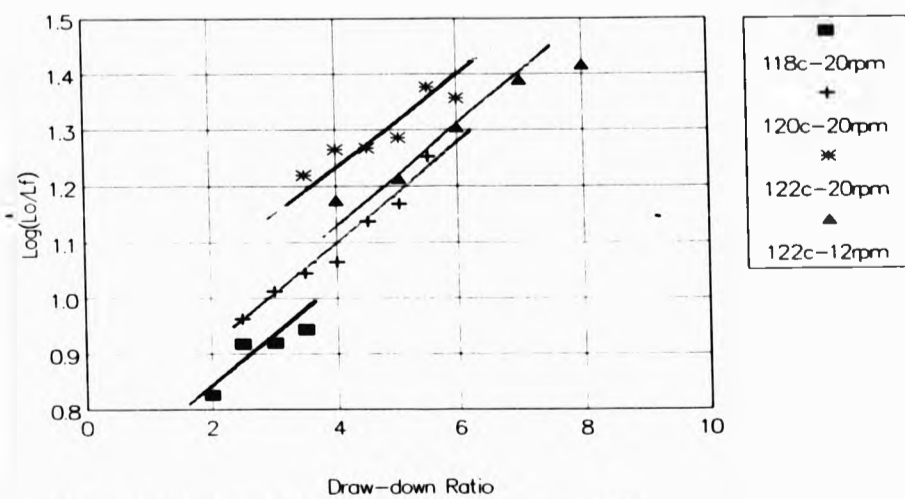


Fig. 4.7.2.2 - Shrinkage Recovery vs. DDR

4.7.3 - EXTRUDATES FROM A FILM DIE

TABLE 4.7.3.1 - FINAL LENGTH OF EXTRUDATES (cm)
(INITIAL LENGTH = 5cm)

BT-119c OR=20rpm	Draw-Down Ratio		
	2.25	2.50	3.00
Sample 1	0.31	0.24	0.35
Sample 2	0.33	0.21	0.35
Sample 3	0.32	0.24	0.36
Sample 4	0.29	0.28	0.35
Sample 5	0.32	0.28	0.35

BT-122c OP=12rpm	Draw-Down Ratio			
	4.58	5.00	5.83	6.25
Sample 1	0.34	0.24	0.23	0.21
Sample 2	0.35	0.22	0.21	0.24
Sample 3	0.32	0.19	0.22	0.24
Sample 4	0.35	0.19	0.23	0.22
Sample 5	0.34	0.22	0.20	0.23

BT-123c OP= 12rpm	Draw-Down Ratio				
	5.00	5.83	6.67	7.50	8.33
Sample 1	0.17	0.16	0.19	0.17	0.16
Sample 2	0.17	0.19	0.17	0.17	0.18
Sample 3	0.18	0.17	0.17	0.15	0.16
Sample 4	0.18	0.17	0.15	0.16	0.17
Sample 5		0.17	0.16	0.15	0.19

TABLE 4.7.3.2 - RECOVERY OF EXTRUDATES (LOG(l₀/l_f))

DDR	OR=12rpm		
	BT=119c	BT=122c	BT=123c
2.25	1.202		
2.50	1.304		
3.00	1.152		
4.58		1.168	
5.00		1.374	1.456
5.83		1.362	1.464
6.25		1.342	
6.67			1.475
7.50			1.496
8.33			1.464

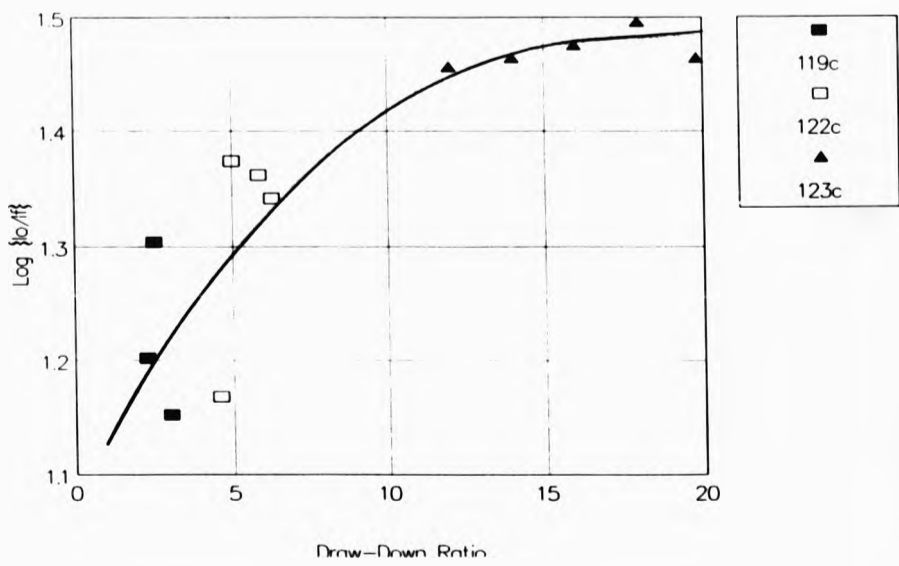


Fig. 4.7.3.2 - Shrinkage Recovery vs. DDR

4.8 ANNEALING OF EXTRUDATES

4.8.1 - ANNEALED IN LIQUID METAL ALLOY AT 117c

TABLE 4.8.1.1 - OUTPUT = 5rpm; HAUL-OFF SPEED = 10rpm
STRESS (MPa)

STRAIN	TIME OF ANNEALING				
	0s	60s	120s	300s	600s
0%	0.00	0.00	0.00	0.00	0.00
2%	13.26	13.12	11.86	11.26	16.49
4%	19.59	18.79	18.35	18.34	21.74
6%	22.24	21.28	21.44	21.61	24.37
8%	23.46	22.16	22.74	22.88	25.57
10%	23.87	21.63	23.07	23.60	25.80
12%	23.87	18.97	20.30	23.60	25.80
14%	23.46	18.79	19.33	23.42	25.57
16%	20.20	18.62	19.17	21.43	25.33
18%	19.99	18.44	19.00	20.70	25.09
20%	19.79	18.26	18.84	20.52	24.61

TABLE 4.8.1.2 - OUTPUT = 5rpm; HAUL-OFF SPEED = 25rpm
STRESS (MPa)

STRAIN	TIME OF ANNEALING				
	0s	60s	120s	300s	600s
0%	0.00	0.00	0.00	0.00	0.00
2%	23.07	13.47	15.79	13.79	18.34
4%	25.90	20.62	21.49	19.57	23.24
6%	29.19	23.99	24.12	22.78	25.27
8%	30.14	25.25	25.43	24.38	26.09
10%	30.61	26.10	26.31	25.02	26.50
12%	31.08	26.52	26.75	25.34	26.90
14%	31.08	26.94	26.75	25.66	26.90
16%	30.61	26.94	27.19	25.66	26.90
18%	30.61	26.94	27.19	25.66	26.90
20%	30.14	26.52	27.19	25.66	26.50

TABLE 4.8.1.3 - OUTPUT = 28rpm; HAUL-OFF SPEED = 140rpm
STRESS (MPa)

STRAIN	TIME OF ANNEALING							
	0s	5s	10s	30s	60s	120s	300s	600s
0%	0.00	0.00	0.00	0.00	0.00	0.00	0.00	0.00
2%	14.70	13.15	8.46	15.24	15.61	13.50	15.70	14.16
4%	21.91	20.38	16.27	21.62	22.55	20.98	23.08	21.66
6%	25.21	24.98	20.30	24.67	26.02	24.20	26.07	25.16
8%	26.56	26.95	22.12	26.12	27.76	25.82	27.64	26.82
10%	27.46	27.78	22.90	26.85	28.63	26.70	28.42	27.82
12%	27.91	28.43	23.55	27.28	29.15	27.14	29.05	28.49
14%	28.21	28.93	23.81	27.57	29.67	27.43	29.36	28.82
16%	28.51	29.25	24.07	27.86	30.01	27.72	29.68	29.16
18%	28.81	29.58	24.33	28.15	30.54	28.02	29.99	29.49
20%	28.96	29.91	24.73	28.30	30.88	28.31	30.31	29.82

TABLE 4.8.1.4 - OUTPUT = 28rpm; HAUL-OFF SPEED = 140rpm
STRESS (MPa)

STRAIN	TIME OF ANNEALING							
	0s	5s	10s	30s	60s	120s	300s	600s
0%	0.00	0.00	0.00	0.00	0.00	0.00	0.00	0.00
2%	24.64	25.83	29.23	23.92	25.43	27.07	21.77	21.11
4%	38.72	41.75	43.01	37.08	38.96	39.78	33.49	35.89
6%	48.22	52.95	53.04	45.85	47.16	47.98	41.53	45.60
8%	54.91	61.12	60.55	52.63	53.72	54.95	46.89	52.78
10%	60.54	67.58	68.07	58.21	59.46	60.28	51.57	57.84
12%	66.18	74.90	74.33	63.79	65.61	66.02	55.93	63.75
14%	71.46	82.22	81.43	67.78	71.36	72.59	60.95	69.66
16%	76.38	88.24	86.86	76.15	77.92	78.74	65.64	76.00
18%	78.85	90.82	89.37	81.73	83.66	83.66	69.66	81.06
20%	79.55	91.69	0.00	84.53	86.12	86.12	70.66	85.29

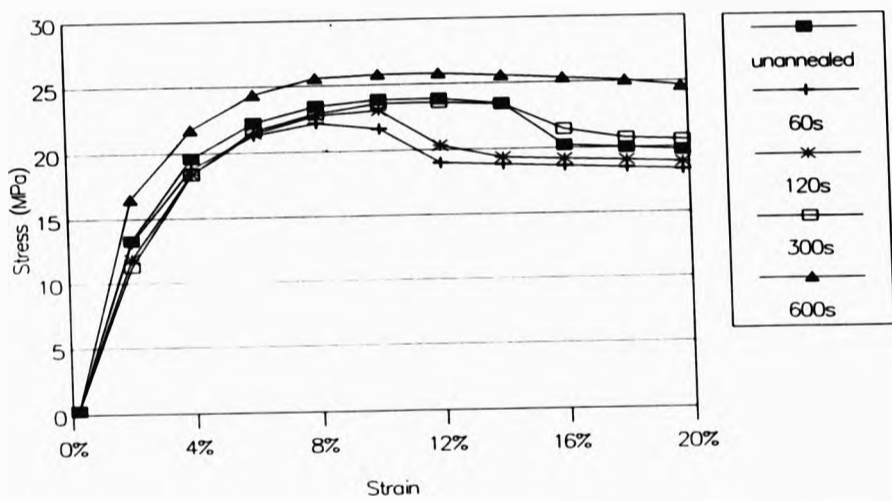
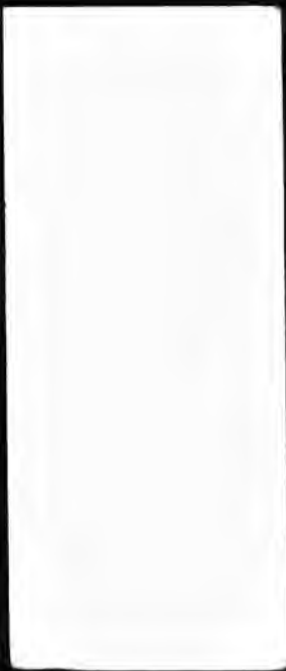


Fig. 4.8.1.1 - Stress vs. Strain; OR = 5 rpm, HOS = 10rpm

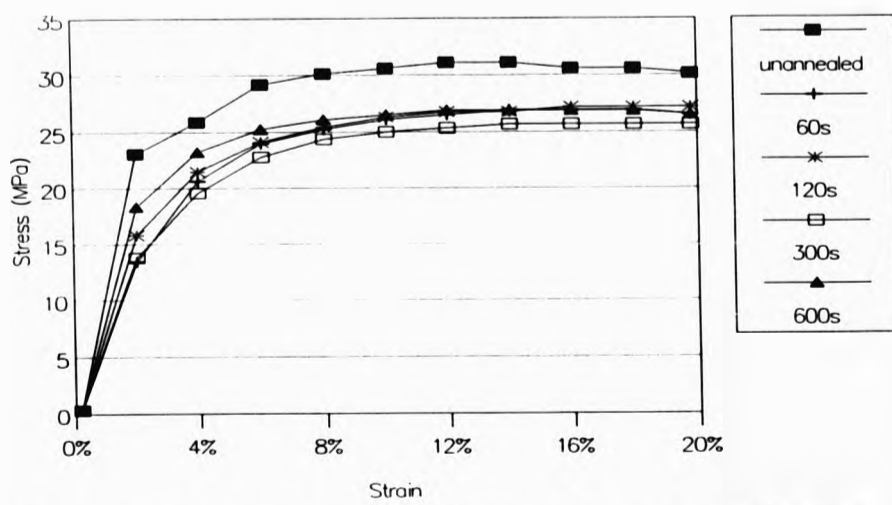


Fig. 4.8.1.2 - Stress vs. Strain; OR = 5 rpm, HOS = 25 rpm

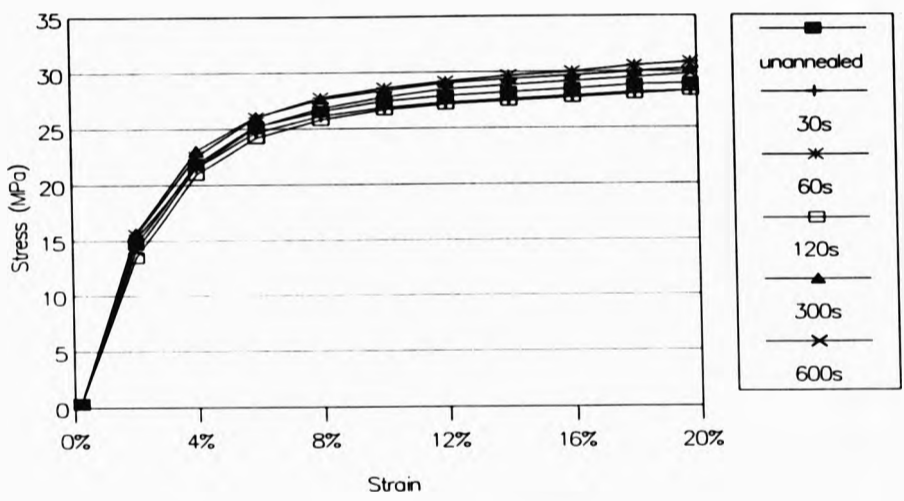
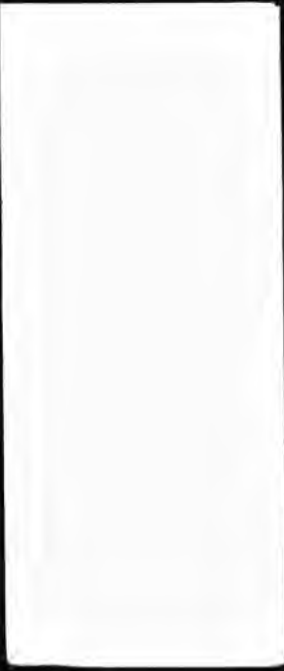


Fig. 4.8.1.3 - Stress vs. Strain; OR = 28 rpm, HOS = 56 rpm

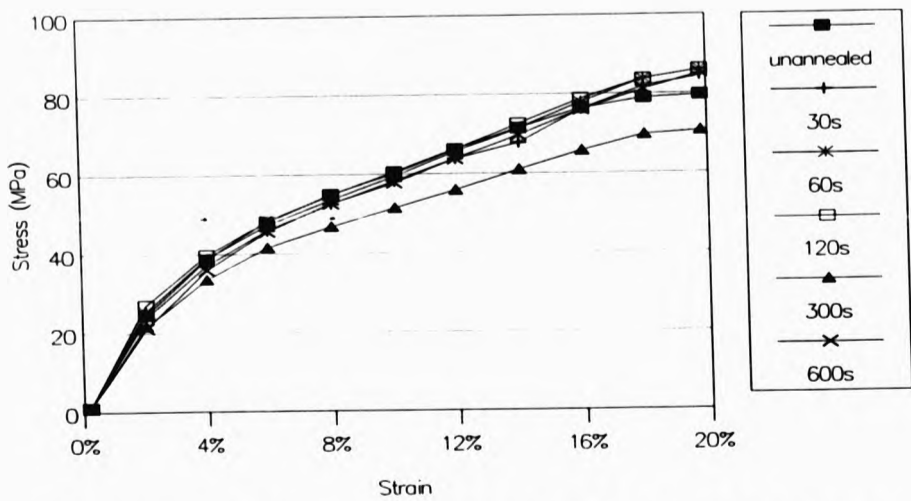


Fig. 4.8.1.4 - Stress vs. Strain; OR = 28 rpm, HOS = 140rpm

TABLE 4.8.1.5 - STRESS AT 10% STRAIN
STRESS (MPa)

TIME	OR = 5rpm		OR = 28rpm	
	DDR = 2	DDR = 5	DDR = 2	DDR = 5
0s	23.87	30.61	27.46	60.54
5s			27.78	67.58
10s			22.90	68.07
30s			26.85	58.21
60s	21.63	26.10	28.63	59.46
120s	23.07	26.31	26.70	60.28
300s	23.60	25.02	28.42	51.57
600s	25.80	26.50	27.82	57.84

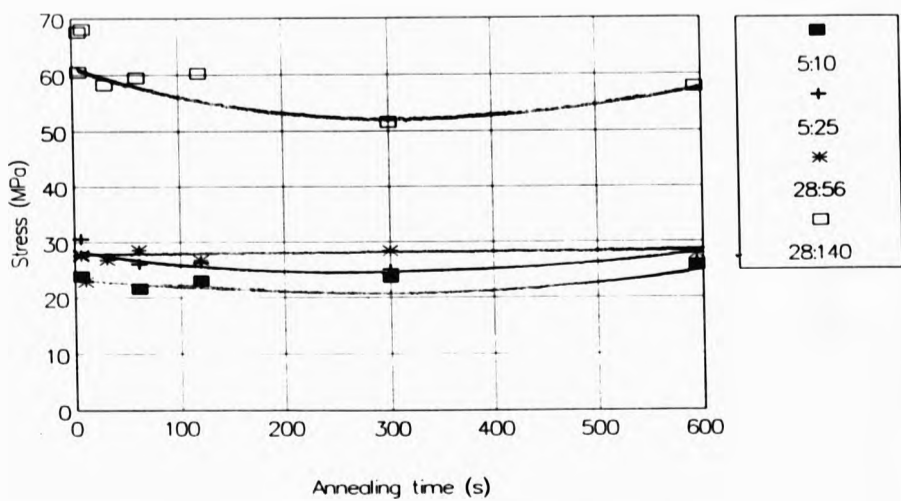


Fig. 4.8.1.5 - Stress at 10% Strain vs. t_a

**TABLE 4.8.1.6 - STRESS AT BREAK
STRESS (MPa)**

TIME	OR = 5rpm		OR = 28rpm	
	DDR = 2	DDR = 5	DDR = 2	DDR = 5
0s	43.45	61.68	31.81	80.26
5s			34.18	91.69
10s			27.72	89.37
30s			31.93	85.32
60s		52.19	34.70	86.94
120s	39.31	53.06	32.42	86.94
300s	41.94	48.76	34.07	73.01
600s	47.79	52.59	34.65	88.24

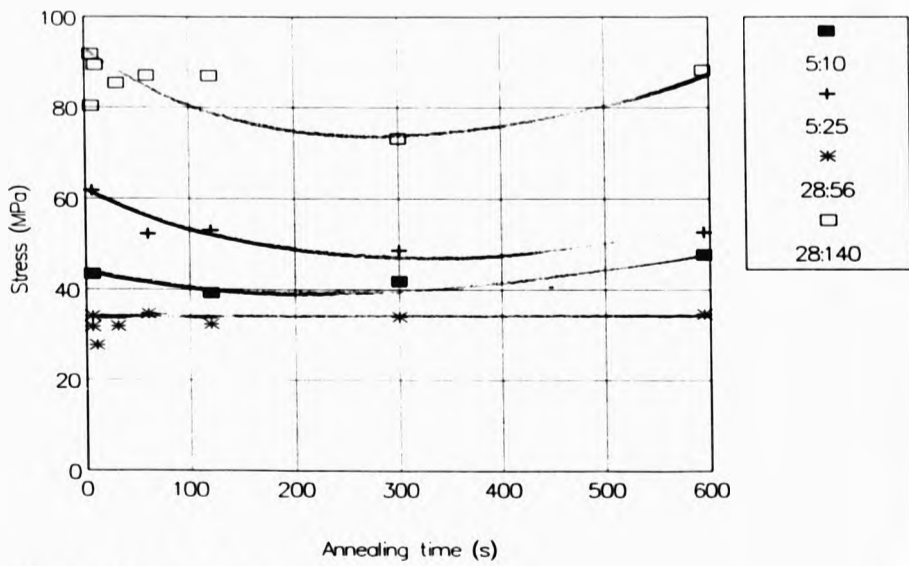


Fig. 4.8.1.6 - Stress at Break vs. t_a

TABLE 4.8.1.7 - ELONGATION AT BREAK

TIME	OR = 5rpm		OR = 28rpm	
	DDR = 2	DDR = 5	DDR = 2	DDR = 5
0s	1172%	776%	182%	25%
5s			161%	20%
10s			165%	19%
30s			177%	22%
60s	1180%	726%	127%	23%
120s	1180%	691%	209%	24%
300s	1175%	835%	186%	23%
600s	1092%	735%	174%	24%

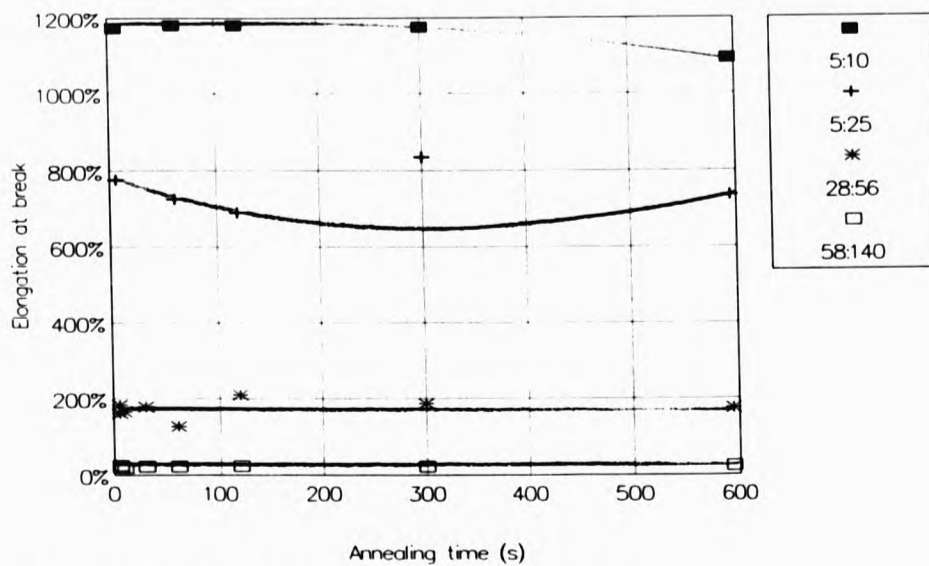


Fig. 4.8.1.7 - Elongation at Break vs. t_a

4.8.2 ANNEALED IN AIR AT 117c

TABLE 4.8.2.1 - OUTPUT = 5rpm; HAUL-OFF SPEED = 25rpm
STRESS (MPa)

STRAIN	ANNEALED AT 20c		ANNEALED AT 117c			
	1 DAY	50 DAYS	5 min	10 min	30 min	60 min
0%	0.00	0.00	0.00	0.00	0.00	0.00
2%	20.36	18.20	14.95	14.63	13.77	14.79
4%	23.08	24.59	19.49	20.52	19.46	20.50
6%	24.42	27.54	21.95	22.71	22.03	23.88
8%	25.11	29.02	23.09	24.02	23.31	25.57
10%	25.56	29.75	23.84	24.89	24.05	26.63
12%	25.73	30.00	24.22	25.33	24.41	27.47
14%	25.38	30.25	24.60	25.43	24.60	27.68
16%	25.29	30.00	24.79	25.76	24.97	28.11
18%	24.93	29.75	24.60	25.87	24.97	28.42
20%	24.84	29.51	24.60	25.87	24.97	28.42

TABLE 4.8.2.2 - OUTPUT = 28rpm; HAUL-OFF SPEED = 140rpm
STRESS (MPa)

STRAIN	ANNEALED AT 20c		ANNEALED AT 117c			
	1 DAY	50 DAYS	5 min	10 min	30 min	60 min
0%	0.00	0.00	0.00	0.00	0.00	0.00
2%	24.37	24.64	18.56	23.49	23.94	22.04
4%	38.64	38.72	32.67	34.87	33.65	31.58
6%	49.00	48.22	41.95	42.82	40.49	38.52
8%	57.44	54.91	49.74	49.14	45.53	43.90
10%	65.36	60.54	55.68	55.10	49.67	48.94
12%	72.49	66.18	61.25	60.34	54.89	53.27
14%	77.60	71.46	67.56	65.94	59.57	58.13
16%	79.78	76.38	73.13	70.46	63.71	61.78
18%	63.80	78.85	77.95	73.89		
20%	47.51	79.55	80.55			

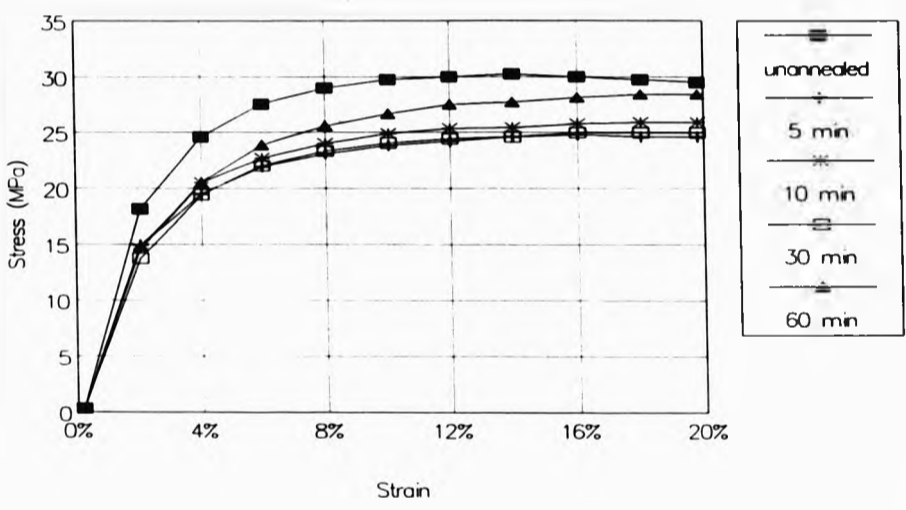
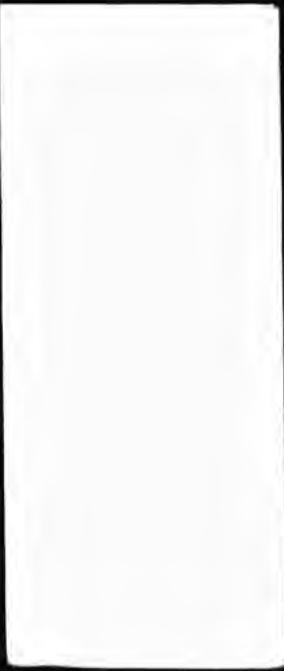


Fig. 4.8.2.1 - Stress vs. Strain; OR = 5 rpm, HOS = 25 rpm

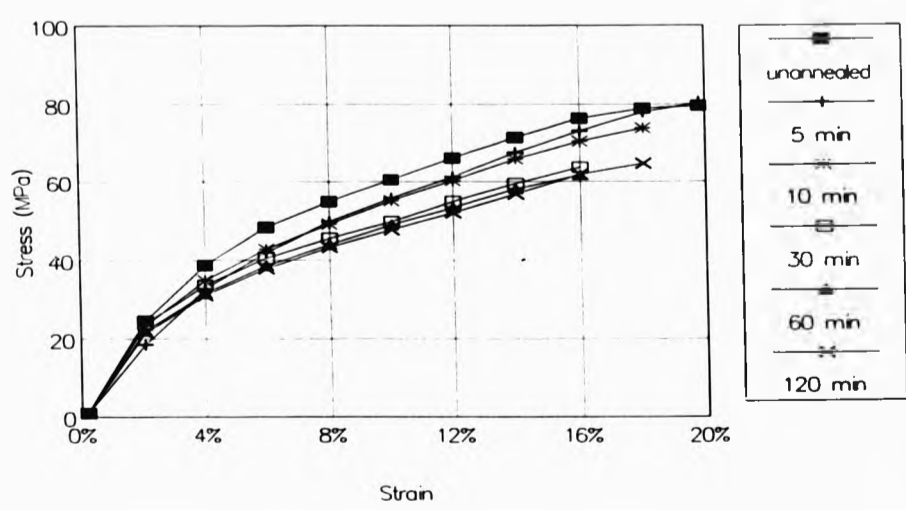


Fig. 4.8.2.2 - Stress vs. Strain; OR = 28 rpm, HOS = 140rpm

TABLE 4.8.2.3 - COMPARISON OF TENSILE CHARACTERISTICS

Annealing Time	STRESS @ 10%		S(Br)		E(Br)	
	5:25	28:140	5:25	28:140	5:25	28:140
(U) 1 D	25.56	65.36	57.23	80.60		
5 min	23.84	55.68	47.12	82.78	843%	21%
10 min	24.89	55.10	54.58	77.14	855%	24%
30 min	24.05	49.67	50.30	67.85	911%	18%
60 min	26.63	48.94	49.87	63.17	723%	17%
120 min		47.72		66.12		21%

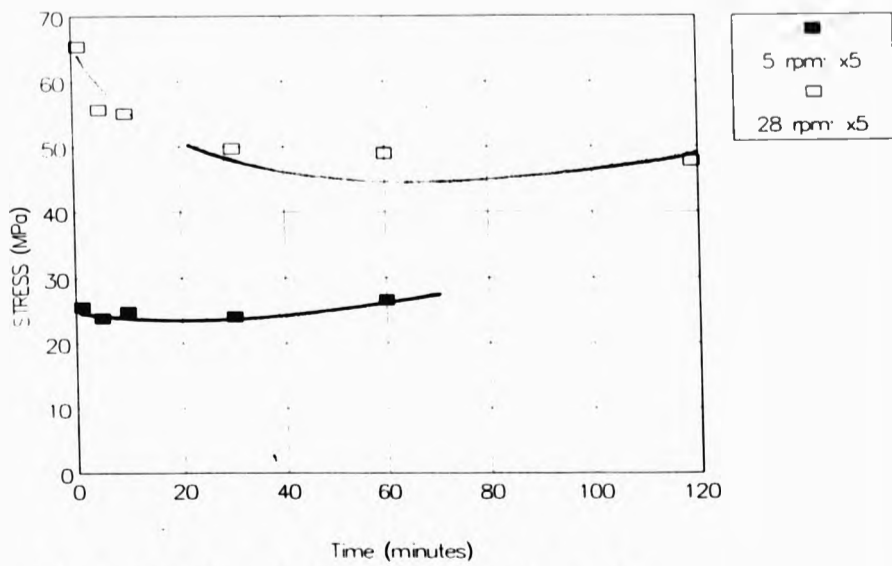


Fig. 4.8.2.3a - Stress at 10% Strain vs. t_a

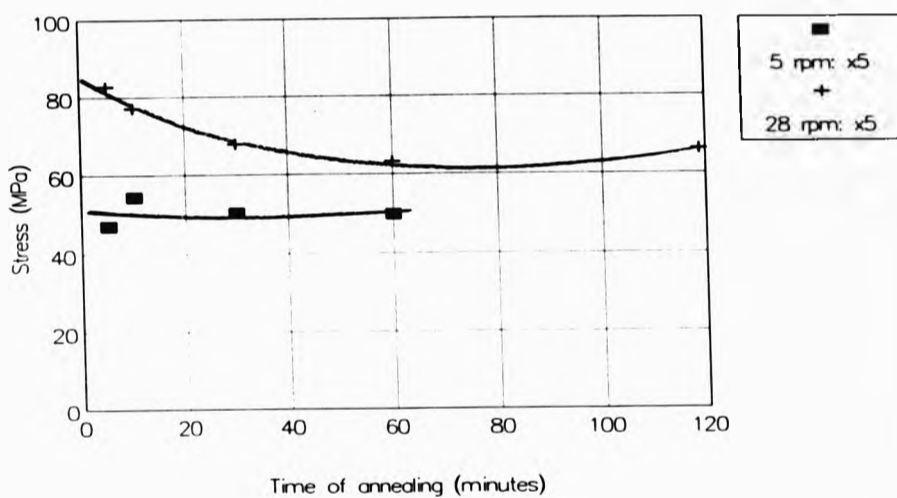


Fig. 4.8.2.3b - Stress at Break vs. t_a

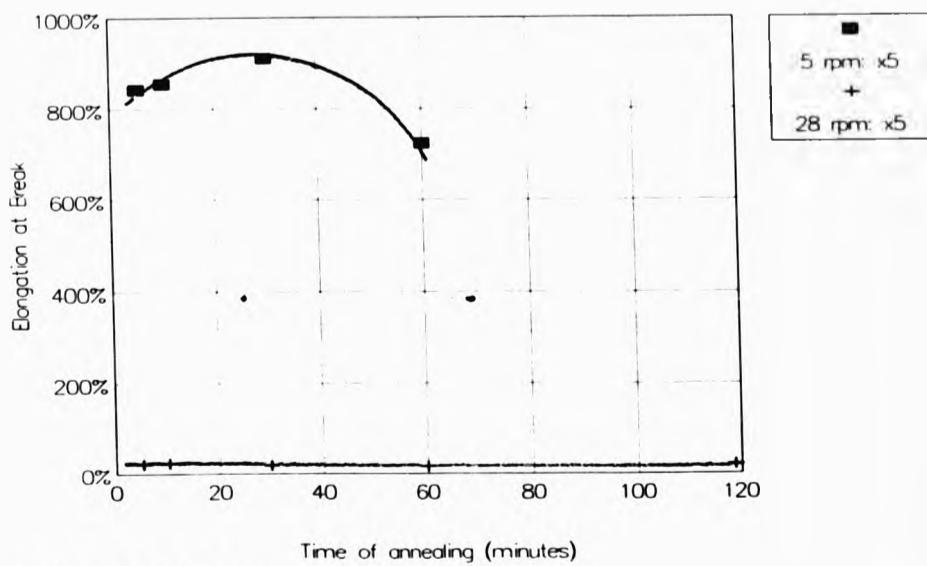


Fig 4.8.2.3c - Elongation at Break vs. t_a

4.8.3 - ANNEALING IN AIR AT ROOM TEMPERATURE

SEE TABLES 4.8.2.1 & 2 FOR STRESS vs. STRAIN FOR EXTRUDATES ANNEALED IN AIR AT ROOM TEMPERATURE

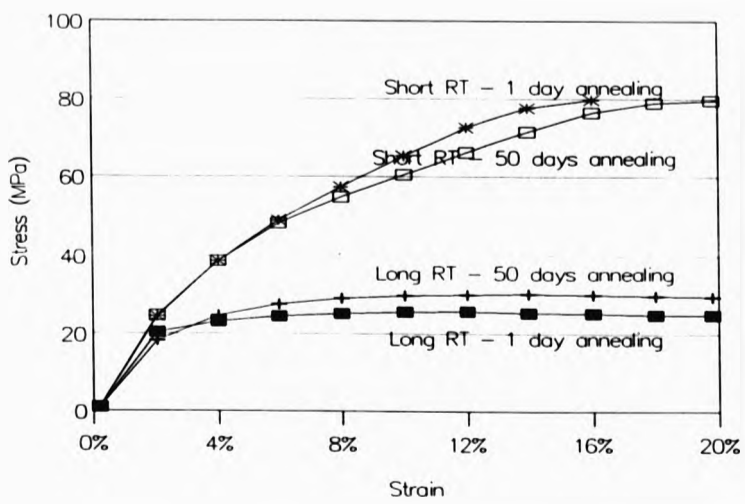


Fig. 4.8.3.1 - Stress vs. Strain; extrudates annealed in air at room temperature

4.9 - DENSITY OF EXTRUDATES

**4.9.1 - EXTRUDATES FROM A CIRCULAR DIE (1)
(FROM SECTION 4.2)**

TABLE 4.9.1.1 - CALIBRATION OF DENSITY COLUMN

Ball	Density (g/cc)	Position (cm)
Yellow	0.9547	9.1
Green	0.9516	27.3
R/G/B	0.9499	31.0
Blue	0.9452	45.5

**TABLE 4.9.1.2 - POSITION OF EXTRUDATES
IN THE DENSITY COLUMN (cm)**

HOS	BATH TEMPERATURE			
	111c	113c	115c	117c
40 rpm	43.0	39.2	40.5	35.9
60 rpm	42.0	39.1	38.2	35.8
80 rpm	41.9	37.2	35.5	35.7
100 rpm	39.4	37.7	35.3	35.4
120 rpm		36.1	34.4	35.0
140 rpm		36.3	34.0	32.5

TABLE 4.9.1.3 - DENSITY OF EXTRUDATES (g/cm³)

HOS	BATH TEMPERATURE			
	111c	113c	115c	117c
40 rpm	0.9465	0.9475	0.9472	0.9484
60 rpm	0.9468	0.9475	0.9478	0.9484
80 rpm	0.9468	0.9480	0.9485	0.9484
100 rpm	0.9475	0.9479	0.9485	0.9485
120 rpm		0.9483	0.9487	0.9486
140 rpm		0.9483	0.9489	0.9492

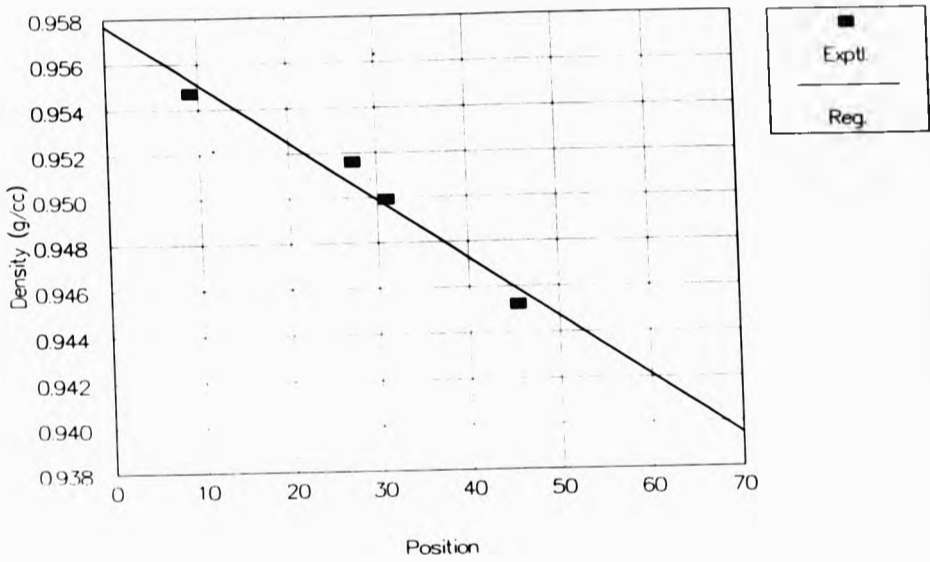


Fig. 4.9.1.1 - Calibration curve for density column

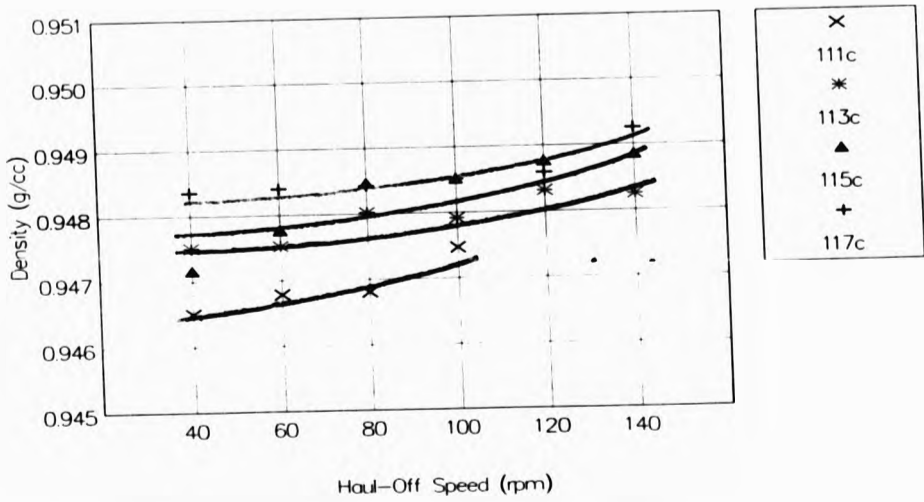


Fig. 4.9.1.3 - Density of extrudates

4.9.2 - EXTRUDATES FROM A CIRCULAR DIE (2)
(FROM SECTION 4.3)

TABLE 4.9.2.1 - CALIBRATION OF DENSITY COLUMN

Ball	DENSITY (g/cc)	POSITION (cm)
Green	0.9516	23.5
R/G/B	0.9499	50.9
Blue	0.9452	58.2

**TABLE 4.9.2.2 - POSITION OF EXTRUDATES
 IN THE DENSITY COLUMN (cm)**

DDR	OUTPUT RATE			
	5rpm	10rpm	20rpm	28rpm
x2		51.9		48.8
x3	52.6	51.3	51.6	38.2
x4	52.1	50.7	50.7	24.4
x5	51.3	50.5	46.8	13.6
x6	51.5	48.3	31.7	

TABLE 4.9.2.3 - DENSITY OF EXTRUDATES (g/cm³)

DDR	OUTPUT RATE			
	5rpm	10rpm	20rpm	28rpm
x2		0.9472		0.9479
x3	0.9471	0.9474	0.9473	0.9502
x4	0.9472	0.9475	0.9475	0.9532
x5	0.9474	0.9475	0.9483	0.9556
x6	0.9473	0.9480	0.9516	

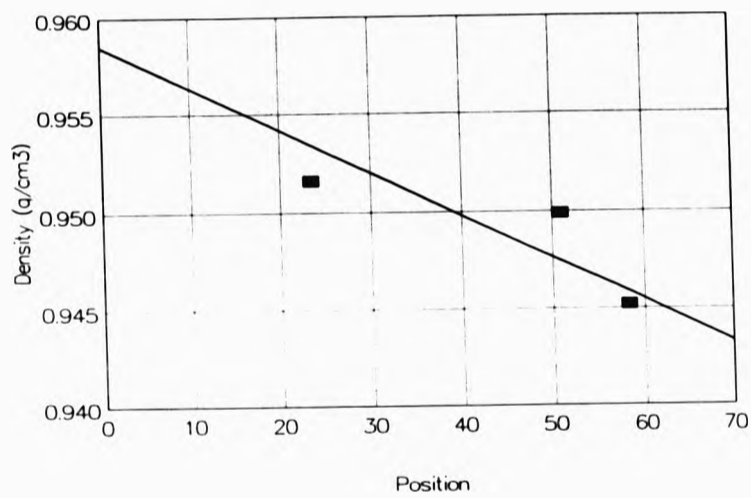
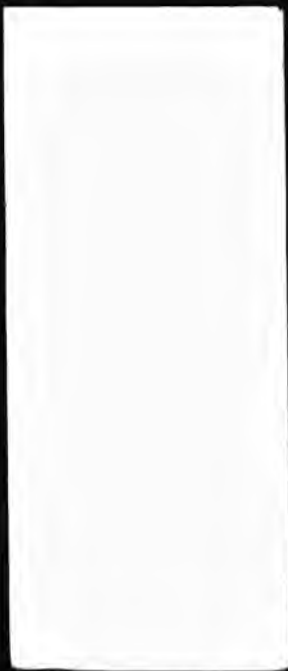


Fig. 4.9.2.1 - Calibration curve for density column

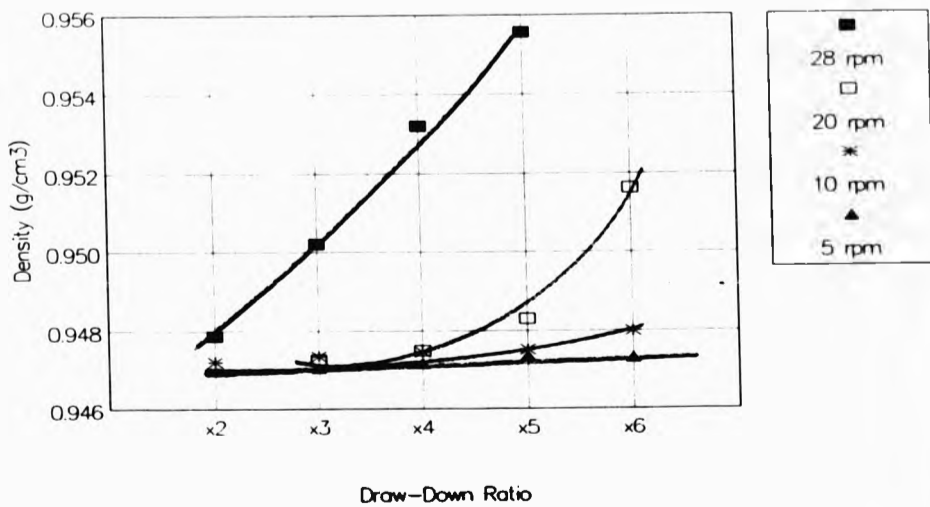


Fig. 4.9.2.3 - Density of extrudates

4.10 - CYCLIC STRAIN RECOVERY

All cyclic strain recovery values were calculated from the cyclic stress-strain curves using Equation (2) from section 3.2.3.

**4.10.1 - EXTRUDATES FROM A CIRCULAR DIE
(FROM SECTION 4.2)**

TABLE 4.10.1.1 - OUTPUT = 10 rpm - FIRST CYCLE RECOVERY

HOS	AIR QUENCHED	BATH TEMPERATURE	
		113c	115c
40rpm	33%	46%	46%
60rpm	36%	45%	47%
80rpm	38%	47%	51%
100rpm	40%	50%	53%
120rpm	39%	54%	---
140rpm	40%	57%	---

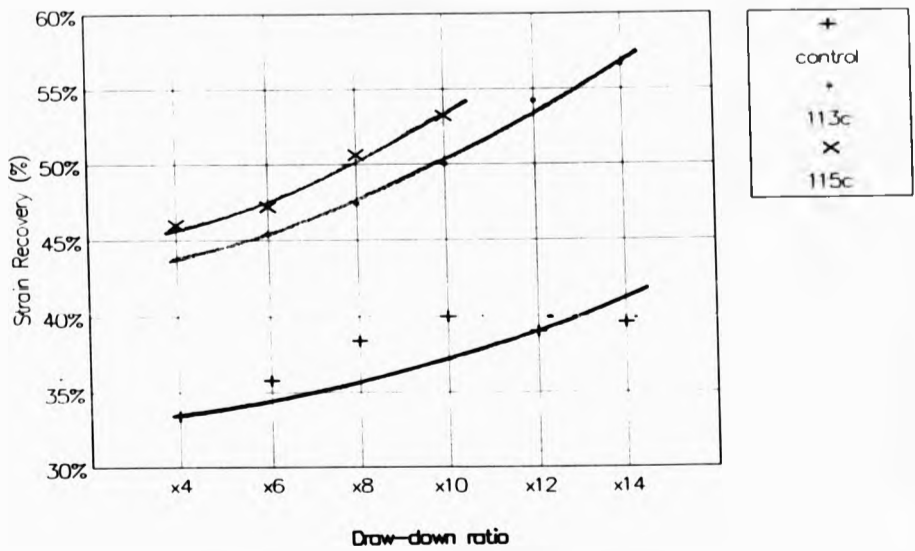


Fig. 4.10.1.1 - Cyclic Strain Recovery; OR = 10 rpm

4.10.2 - EXTRUDATES FROM A CIRCULAR DIE (FROM SECTION 4.3)

TABLE 4.10.2.1 - BATH TEMPERATURE = 118°C; OR = 5rpm
RECOVERY

CYCLE	DRAW-DOWN RATIO				
	2	3	4	5	6
1st	33%	33%	41%	43%	48%
2nd	28%	29%	34%	38%	41%
3rd	22%	28%	33%	33%	37%
4th	22%	27%	31%	32%	36%

TABLE 4.10.2.2 - BATH TEMPERATURE = 118°C; OR = 10rpm
RECOVERY

CYCLE	DRAW-DOWN RATIO				
	2	3	4	5	6
1st	46%	44%	48%	50%	52%
2nd	36%	38%	43%	44%	46%
3rd	34%	34%	39%	40%	44%
4th	32%	33%	38%	39%	40%

TABLE 4.10.2.3 - BATH TEMPERATURE = 118°C; OR = 20rpm
RECOVERY

CYCLE	DRAW-DOWN RATIO			
	2	3	4	5
1st	44%	44%	45%	50%
2nd	39%	36%	38%	43%
3rd	32%	33%	32%	42%
4th	30%	32%	31%	39%

TABLE 4.10.2.4 - BATH TEMPERATURE = 118°C; OR = 28rpm
RECOVERY

CYCLE	DRAW-DOWN RATIO		
	2	3	4
1st	43%	40%	44%
2nd	37%	36%	39%
3rd	34%	32%	36%
4th	33%	31%	35%

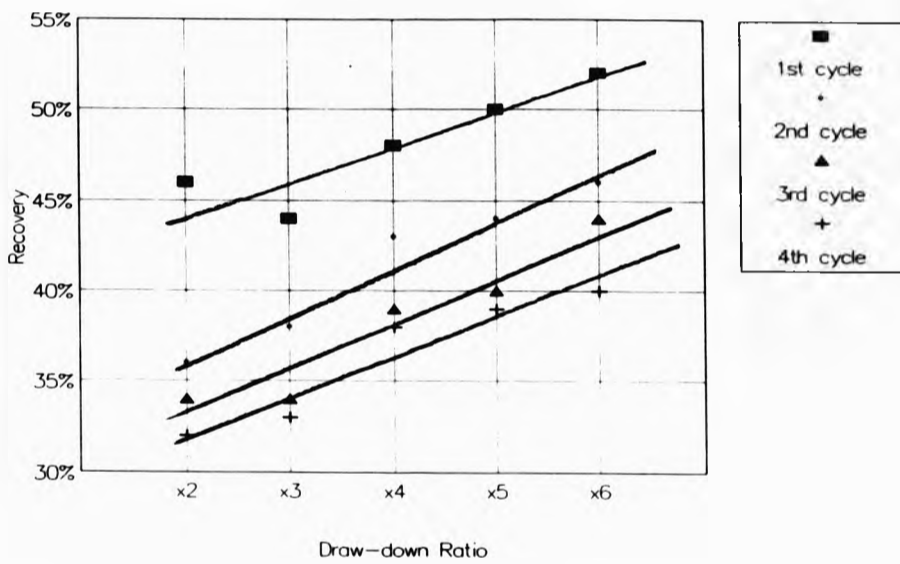


Fig. 4.10.2.1 - Cyclic Strain Recovery;
BT = 118°C, OR = 5rpm

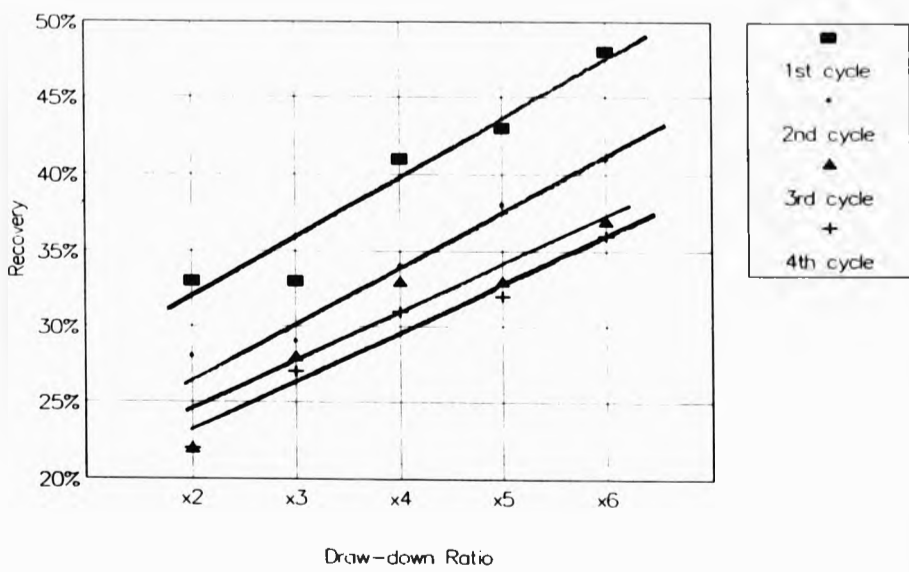


Fig. 4.10.2.2 - Cyclic Strain Recovery;
BT = 118°C, OR = 10rpm

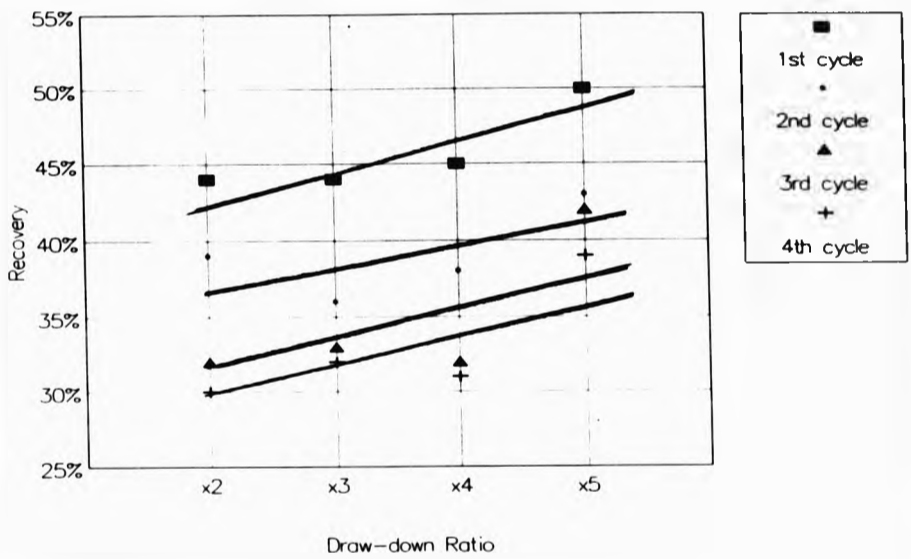


Fig. 4.10.2.3 - Cyclic Strain Recovery;
BT = 118°C, OR = 20rpm

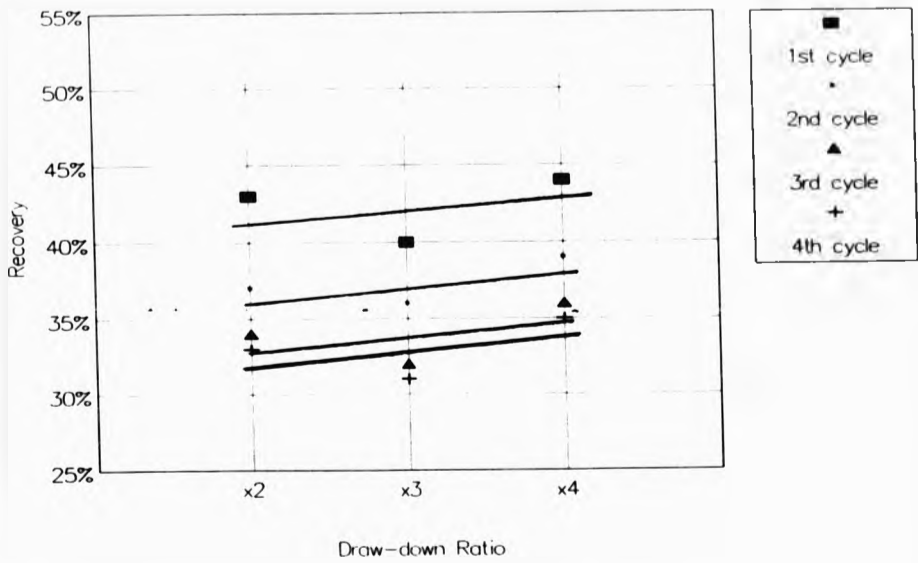


Fig. 4.10.2.4 - Cyclic Strain Recovery;
BT = 118°C, OR = 28rpm

TABLE 4.10.2.5 - 1st CYCLE COMPARISON

1st CYCLE	DRAW-DOWN RATIO				
	2	3	4	5	6
5rpm	33%	33%	41%	43%	48%
10rpm	46%	44%	48%	50%	52%
20rpm	44%	44%	45%	50%	
28rpm	43%	40%	44%		

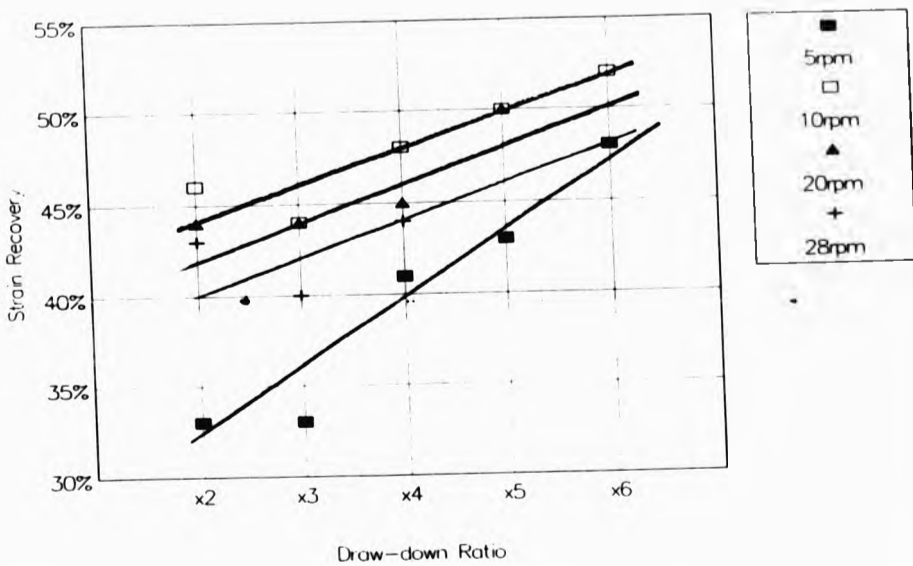


Fig. 4.10.2.5 - 1st Cycle Recovery vs. DDR

CHAPTER 5 - DISCUSSION

In this chapter, the results shown in chapter 4 will be discussed; trends will be shown in the data obtained from experiments and simple relationships will be established between the processing parameters and the tensile properties - strain recovery, orientation and density of the polymer samples. From these relationships, a mechanism will be proposed for the formation and deformation mechanisms of the extrudates. This chapter is broken into sections as follows:

5.1 The three most important processing parameters - or primary variables - will be defined in order that the results may be interpreted more clearly. Secondary variables, which result from a combination of primary variables, will also be defined.

5.2 The extrudates will be discussed in terms of their dimensions - the variance of the cross-sectional area and the a:b ratio with the primary and secondary variables.

5.3 The extrudates will be discussed in terms of the effect of the primary and secondary variables on the tensile properties, such as the stress at 10% strain ($S_{10\%}$), the yield stress (S_y), the break stress (S_{br}); and on the elongation at break (E_{br}) and the general shape of the stress-strain curve.

5.4 The extrudates will be discussed in terms of the effect of the primary and secondary variables on the molecular orientation, as shown by the shrinkage recovery.

5.5 The extrudates will be discussed in terms of the effect of the primary and secondary variables on the cyclic strain recovery.

5.6 The extrudates will be discussed in terms of the effect of the primary and secondary variables on the density.

5.7 The extrudates will be discussed in terms of the effect of subsequent annealing (in air and in liquid metal) on the tensile properties.

5.1 THE VARIABLES USED IN THE PREPARATION OF EXTRUDATES

This work involved the preparation of HDPE extrudates from each of three dies - circular, strip and flat film - for evaluation in terms of some or all of the above tests. The primary variables in the preparation of the samples were:

(i) The Bath Temperature (BT) - the temperature of the liquid metal alloy used in the quenching of the HDPE extrudates in all experiments except the control experiment (Section 4.1), in which the quenching medium was air at room temperature (see Section 5.6 for a discussion of the effect of different media on the quenching of HDPE extrudates).

(ii) The Output Rate of the extrudates (OR) - expressed in terms of the screw speed (rpm), as this was the true primary variable - the OR was approximately proportional to the screw speed at constant melt temperature:

$$OR (g) = k \times (\text{screw speed}) \quad (1)$$

where k was a constant, the value of which depended upon the grade of polymer and the type of die used.

(iii) The Haul-Off Speed (HOS) - the speed of rotation of the rubber rollers and was expressed in rpm. The actual speed of the extrudate (in m/s) was given by multiplying the HOS by a constant, the circumference of the roller (in metres) divided by 60 (seconds).

The ratio of the HOS divided by the OR gave a secondary variable, the draw-down ratio (DDR). This was more important than either of the primary variables, as it was responsible for the alignment of the polymer molecules, i.e. the orientation in the extrudate.

Three other primary variables were kept constant throughout the experiments:

- (iv) The height of liquid metal in the bath.
- (v) The position of the roller inside the bath.
- (vi) The position of the bath relative to the die.

The values of these parameters were found by trial and error during preliminary experiments, such that a continuous extrudate was produced which was molten on entering the bath and fully quenched on leaving it for a wide range of conditions. Two secondary variables were kept constant as a result:

a) The Air-Residence Distance (ARD) - this was the distance from the mouth of the die to the surface of the liquid metal alloy. This was dependent on (iv) and (vi) above. The greater the ARD, the greater the heat loss of the extrudate and the greater the temperature drop in the extrudate. Hence, if the ARD was too great, the extrudate would have been quenched before it entered the bath.


The ARD was minimised for each of the three dies used:

Circular die - 15 cm approx.;

Strip die - 10 cm approx.;

Slit die - 2 cm approx.

The reason for the large difference between ARDs for the three dies was that the apparatus was designed to allow an ARD of 0 cm for the slit die. It was decided not to use the minimum value as that would mean that the liquid metal alloy was in contact with the die, which would have affected the local temperature of the surface of the bath. As a result, a small but finite ARD was chosen (2cm).



The other two dies were significantly shorter vertically than the slit die, so that an ARD of 0 cm would require the bath to be almost completely full, which was not possible for reasons of safety. The minimum possible ARD was therefore dictated by the height of the liquid metal - which was kept constant for all experiments - and the vertical length of the die, as the bath was located at its highest possible position, flush with the neck of the extruder.

b) The Residence Distance (RD) - this was the distance that the extrudate travelled through the bath; it was double the distance between the surface of the liquid metal alloy and the furthest point on the internal roller when located into the bath. This was dependent on (iv) and (v) above. When the RD was divided by the average speed of the extrudate in the bath, the result was another secondary variable - the residence time (Rt) (appendix i) - which will be fully discussed later.

There was one other important variable, the quenching time (Qt) for the extrudates. Before quenching, the polymer extrudate was molten and, therefore, subject to a changes in cross-sectional area and geometry during the haul-off process. The Qt was dependent upon the following factors:

- a) The temperature at which the extrudates were quenched.
- b) The quenching medium, i.e. whether the extrudate was quenched in air or liquid metal.
- c) The cross-sectional area of the extrudate.
- d) The geometry of the extrudate.
- e) The grade of polymer used.


The numerous sample preparations and tests may be grouped into a series of experiments as follows. Such a grouping aids discussion of results.

Experiment 1 - the control experiment; the effect of orientation on air-quenched extrudates. The quenching medium was air at room temperature (about 20°C). The circular die was used; the OR was kept constant at 6 rpm and the HOS was varied from 40 rpm to 140 rpm in steps of 20 rpm. The results were given in section 4.1.

Experiment 2 - liquid metal quenched extrudates; the effect of the BT and the DDR at constant OR. The circular die was used; the OR was kept constant at 20 rpm and the same values of HOS were used as in experiment 1 at each of four values of the BT (111°C, 113°C, 115°C, 117°C). This allowed cross-analysis of the data, so that the individual effect of both DDR and BT could be deduced. The results were given in section 4.2.

Experiment 3 - liquid metal quenched extrudates; the effect of HOS and OR (and, therefore, DDR) at constant BT. The circular die was used; the BT was kept constant at 117°C and four values of OR (5, 10, 20, 28 rpm) were used and the ranges of HOS were varied so that the ranges of DDR (x2 - x6) were the same for each OR. This allowed comparison between the tensile properties of extrudates which had the same cross-sectional area, but which had different Rt in the bath. The results were given in section 4.3.

Experiment 4 - liquid metal quenched extrudates; the effect of HOS and OR at constant BT. The strip die was used; as in




experiment 3, four values of the OR were used (5, 10, 20, 40 rpm) and the ranges of HOS were chosen to give four values of the DDR (x2, x2.5, x3, x3.5). This allowed the same analysis as Experiment 3, but using a different die and a different grade of polymer, which showed whether the relationship between the primary variables and the properties of the extrudates was independent of die geometry or grade of polymer. The results were given in section 4.4.

Experiment 5 - liquid metal quenched extrudates; the effect of BT on the maximum possible DDR and the effect of high BT and high DDR on the properties of the extrudates. The strip die was used; all three primary variables were varied in order that a greater range of DDRs was possible. The range of BT used was 118-123°C and the OR was either 5, 12 or 20 rpm - the HOS was varied in order to achieve the highest DDR possible. The results were given in section 4.5.

Experiment 6 - liquid metal quenched extrudates; the aim of this experiment was the same as for experiment 5, except that the flat film die was used; The range of BT used was 117-123°C and the OR was either 12 or 20 rpm - the HOS was again varied in order to achieve the highest DDR possible. Similarly to experiments 3 and 4, experiments 5 and 6 allowed comparison between extrudates from different dies. The results were given in section 4.6.

It was ensured that the extrudates were all completely molten on entering the bath during all experiments by viewing the extrudate between the die and the bath. The melt remained clear on entry at all times, rather than




showing the white colour of semi-crystalline HDPE. Therefore it may be said that any difference between the morphology of the extrudates prepared in the course of this work and that of HDPE extrudates cooled in air was due to the effect of one or more of the processing parameters (i), (ii) and (iii) and no other factor.

It was noted that higher BT allowed higher levels of DDR to be used without the extrudate breaking - in the experiment using the flat film die, the maximum level of DDR possible at 123°C was several times greater than that at 117°C. At higher values of the DDR, the extrudate broke in the bath. On the other hand, however, the use of higher BTs raised the minimum DDR possible also. At DDRs below the minimum values, the extrudates showed a reluctance to pass through the bath in the usual manner. This could be seen clearly, as there was no tension in the extrudate between the die mouth and the surface of the liquid metal. It was possible to regain normal haul-off by increasing the DDR to a value above the minimum.

At temperatures above those used in each experiment, the same effect was seen - if the maximum DDR had been reached, the extrudate tended to sit on the surface of the liquid metal. This always led to the production of a very irregular extrudate - varying from 0.1 mm to several millimetres in diameter - after which the extrudate broke. Hence for each BT used there was a finite range of DDRs available when it was possible to prepare extrudates which were suitable for testing.

As a result, it was clear, as explained below, that the low maximum BT available to the extrudates from a circular die was due to the lower range of DDRs available. The ORs



for each of the experiments were of the same order of magnitude - 2.5-14 g/min for extrudates from the circular die, 2.5-20 g/min for the strip die and 6-10 g/min for the flat-film die. The speed at which the extrudate left the die orifice was inversely proportional to the area of the die orifice (at constant OR). The areas of the orifices of the strip die (39 mm²) and the flat-film die (50 mm²) were an order of magnitude greater than that of the circular die (2 mm²). Therefore, the range of speeds at which the extrudates left the circular die were an order of magnitude greater than for the other dies. As there was a maximum possible HOS, this meant that the maximum DDR possible was an order of magnitude lower for the extrudates from a circular die than for the other dies.

As a result, the degree of orientation and the possible range of BT was much lower for the extrudates from a circular die than for the other dies. In experiments 5 and 6, higher values of the DDR made it possible to process the extrudates at a higher BT.

5.2 DIMENSIONS OF EXTRUDATES

5.2.1 CROSS-SECTIONAL AREA OF EXTRUDATES

The cross-sectional areas of the flat-film and strip extrudates were calculated simply by multiplying the "a" and "b" dimensions - i.e. width times breadth for a rectangular cross-section. The cross-sectional areas of the extrudates from the circular die were calculated by means of a formula (appendix ii), which had been devised based on the assumption that all extrudates from the circular die had the same general shape, a circle that had had a section removed (see section 5.1.2). If that section was of zero

area, then the cross-section was a perfect circle. This assumption allowed a much better approximation to the area than merely averaging the "a" and "b" dimensions to get the mean diameter.

It was found that the areas of the extrudates from all three dies varied according to the relationship:

$$\text{Area} = \frac{k}{\text{DDR}} \quad (2)$$

where k varied for different grades of polymer and for different dies.


This relationship was predicted from consideration of the theory of conservation of mass, if it was assumed that the density of the polymer material remained constant throughout. In fact, the density of the extrudate was seen to vary, but the resultant change in cross-sectional area was less than the experimental error in measuring the samples, so equation 2 was true.

The ratio of the die area, A_0 , divided by the area of the extrudate gave a value, the actual draw-down (ADD), which allowed comparison between extrudates of different geometry:

$$\frac{A_0}{A} = \frac{\text{DDR}}{k_1} = \text{ADD} \quad (3)$$

where k_1 was a constant.

A plot of (A_0/A) versus DDR gave a straight line for each set of experiments (Appendix iii). The absolute value of k_1 for each extrudate was less important than the level of correlation shown for each set of data; if the draw-down of molten extrudate had taken place evenly during an experiment, then the correlation between (A_0/A) and DDR would have been very high, i.e. all the data points would




have fitted closely on to the straight line. If, however, the extrudate had drawn down unevenly, as it did occasionally, then the correlation would have been poor. If the draw-down had not been even throughout a sample, the morphology of that sample would have been variable also, so no useful information could have been gained from testing it. As a result of analysis of the areas of extrudates, therefore, the high quality of samples to be tested was ensured.

It was found that the circular extrudates had the most consistent draw-down; there was very little fluctuation in cross-sectional area, other than that due to the DDR. The extrudates from the other two dies both exhibited bowing, which will be discussed more fully in section 5.1.2. This in itself was not necessarily a sign of uneven draw-down, but it may have led to larger errors in the measurement of the "a" and "b" dimensions and, therefore, the area.

5.2.2 SHAPE OF EXTRUDATES

The shape of the extrudates was observed to change according to the magnitude of the primary variables. This change was most noticeable for the extrudates from a circular die, as the geometry of the extrudate cross-section changed from circular, via a squashed circle shape, to semi-circular, depending upon the processing conditions (see Appendix ii). For the other dies, the shape of the extrudates remained rectangular at all times, while the ratio of the lengths of the sides changed. When considering the reasons for this behaviour, it was possible to deduce what was happening inside the liquid metal bath, i.e. as the extrudate was being quenched.



If the extrudate was fully quenched when passing around the roller inside the bath, then the geometry of the cross-section of the extrudate would have been that of the die - the area of the extrudate would have been reduced by the effect of draw-down but the shape would have remained circular, as the solid extrudate would have resisted deformation. However, if the extrudate was partially or fully molten when passing around the roller, some flattening of the circular cross-section was observed. The degree of this flattening was dependent upon two factors:

a) the ratio of the half residence time ($1/2Rt$) (appendix i) to the quenching time (Qt) (appendix iv), which determined how fully quenched the extrudate was when passing around the roller.

b) the pressure on the partially-quenched extrudate as it passed around the roller. This pressure was due to the force created by draw-down. In order to induce orientation in the molten extrudate, the haul-off speed (in m/s) had to be greater than the output speed (in m/s). Consequently, the polymer melt was accelerated and a force resulted. Before the extrudate passed around the roller, all forces which acted upon it were in the direction of extrusion - i.e. the accelerating force and gravity were acting vertically downwards - so the only result was reduction in cross-sectional area. As the extrudate passed around the roller, a normal force was created. Again, this force acted vertically downwards, but this time the force acted against the upward motion of the extrudate. When this force was divided by the area of the extrudate in contact with the roller, it gave the pressure exerted upon the partially-

quenched extrudate which was responsible for it becoming deformed. The magnitude of this pressure was a complex function of the OR and the HOS.

For all extrudates, the simplest way to describe the shape in mathematical terms was by means of the ratio of the "a" dimension to the "b" dimension, the a:b ratio. By definition, the "a" dimension was greater than or equal to the "b" dimension. Hence the minimum value of the a:b ratio was unity (for a perfectly circular extrudate). This minimum value was much greater for extrudates from the other two dies, as the dies had a:b ratios greater than one - 4.33 for the strip die and 200 for the flat-film die. In order to compare the effect of the primary variables upon each of the dies, the $(a:b)/(a:b)_0$ ratio was used, which gave the initial value for each die as unity (Appendix v).

For all six experiments performed, the a:b ratio showed three fundamental relationships:

- i) the a:b ratio increased with increasing OR at constant DDR and BT. (The a:b ratio decreased with increasing OR at constant HOS; this was because the DDR was decreasing).
- ii) the a:b ratio increased with increasing DDR at constant OR and BT.
- iii) the a:b ratio increased with increasing BT at constant DDR and OR.

The simplest of the three relationships to describe was (i), as there were the fewest secondary variables to be taken into consideration. The cross-sectional area of the extrudate remained constant (within experimental error; see

section 5.1.1) as it was proportional to the DDR.

As the cross-sectional area was constant, so too was the time taken to quench the extrudate (Q_t) at constant BT. Any change in shape of the extrudate as it passed around the roller had negligible effect on the rate of cooling of the extrudate. If the Q_t was less than or equal to $1/2Rt$, then the a:b ratio of the extrudate was the same as that of the die as, by definition, the sample was quenched by the time that it reached the roller.

Some of the measured a:b values for extrudates from strip dies and, especially, flat-film dies were found to be less than those for their respective dies. This could be attributed to experimental error - the error was 5% in measuring the "b" dimension and a small error in the "b" dimension would have led to a large error in the a:b ratio.

If the Q_t was between $1/2Rt$ and Rt , then the extrudate was not fully quenched when passing around the roller, but was fully quenched on leaving the bath. Under these circumstances the a:b ratio was found to have increased. If $Q_t > Rt$, then the extrudate was not fully quenched when leaving the bath and was not suitable for testing.

As the OR increased, so too did the HOS, as the DDR was constant. As the OR increased, the speed of the extrudate increased and, as a result, the Rt decreased. Therefore, as the OR increased, the $Q_t:1/2Rt$ ratio increased (as the Q_t was constant). If the $Q_t:1/2Rt$ ratio was raised above unity, then the $(a:b)/(a:b)_0$ ratio was also raised above unity.

At the same time, however, the pressure on the extrudate (as it passed around the roller) increased with increasing

OR, as it was dependent on the difference between the HOS and the OR. The effect of this was to magnify the effect produced by the $Qt:1/2Rt$ ratio, i.e. it increased the value of the a:b ratio if $Qt > 1/2Rt$, but had no effect if $Qt < 1/2Rt$.

As a result, it was not possible to discern the sole effect of the $Qt:1/2Rt$ ratio, so it was not possible to explain what was happening inside the bath in terms of only one variable. Similarly, it was not possible to measure the Qt exactly for any extrudate, but it was possible to calculate an approximate value for certain extrudates. If an extrudate had an $(a:b)/(a:b)_0$ ratio of unity for given values of primary variables BT_1 , OR_1 and HOS_1 and an a:b ratio of slightly greater than unity for the values BT_1 , OR_1 and HOS_2 , it was approximated that the primary variables required to meet the condition $Qt = 1/2Rt$ were BT_1 , OR_1 and $(HOS_1 + HOS_2)/2$ (Appendix iv).

As an approximate value of the Qt was known and approximate values for the Rt had been calculated (Appendix i), it was simple to calculate approximate values for yet another secondary variable, the residual residence time (RRT). The RRT was defined as the amount of time the extrudate spent in the liquid metal bath after it had become fully quenched, i.e. $RRT = Rt - Qt$ (Appendix vi). The effect of the RRT will be discussed in section 5.7.

The effect of the DDR on the a:b ratio was similar to the effect of the OR described above with one extra variable: the cross-sectional area of the extrudate decreased as the DDR increased. As the area decreased, so too did the volume of polymer per unit length and, therefore, the quantity of heat which had to be removed for

the melt to become quenched. As a result, both the Q_t and the R_t decreased with increasing DDR, but not at the same rate. It seemed likely that the Q_t decreased more rapidly than the R_t , as the extrudates always appeared fully quenched on exiting the bath. The difference in the rates could not have been too great, as the a:b ratio would have decreased with increasing time to give an extrudate having an undeformed cross-section. Because there was an extra variable involved, it was more difficult to model the behaviour of the extrudate in the bath for constant DDR than for constant OR. The overall effect was that increasing the HOS at constant DDR increased the a:b ratio. The effect of increasing the BT at constant OR and HOS was to increase the a:b ratio. This was because the molten extrudate took longer to quench at higher temperatures. The rate of quenching of the polymer melt was proportional to the rate of removal of heat from it.

This depended on:

a) The temperature of the quenching medium - the higher the BT (in these experiments) the slower the rate of removal of heat. The rate of heat loss was proportional to the difference in temperature between the melting point of the polymer and the temperature of the medium, so a higher BT resulted in a smaller difference in temperature, which led to an increase in Q_t which, in turn, led to an increase in the a:b ratio.

b) The quenching medium - the greater the specific heat capacity (SHC) and thermal conductivity (TC) of the medium, the greater the rate of heat loss from the melt (at constant temperature difference between the melt and the

quenching medium). The values of both SHC and TC were much greater for liquid metal than for air, allowing much higher quenching temperatures whilst maintaining similar Qts.

When considering the correlation between the $(a:b)/(a:b)_0$ ratio and the DDR, it was found that some data did not sit close to the curve for the majority of the data. The areas for these extrudates were found to correlate well with the DDR, however, so it was assumed that draw-down had been even. It was concluded that the discrepancies seen in these points were due to small fluctuations in the BT during processing. These assumptions were also tested by checking other values - i.e. the tensile properties - for similar discrepancies, which were found in each case.

For example, this technique was used when considering the results from experiment 5, extrudates from the strip die at constant ranges of DDR. The graph of a:b ratio vs. DDR (fig. 4.4.1.3) showed that, at 40 rpm OR, the values for x2, x2.5 and x3 were far too high (almost 6). These discrepancies may have been due to a fluctuation in the BT or in the OR or the HOS, but the latter two would have resulted in a fluctuation in the cross-sectional areas, which was not observed (fig. 4.4.1.2). When the tensile properties of these extrudates were examined, it was found that the values for x2 and x2.5 were abnormally high. It was concluded from this analysis that these high values were a direct result of an increase in the BT of approximately 1°C.

Such analysis of the correlation between cross-sectional area and the DDR and between the a:b ratio and the DDR was

very important to the interpretation of the tensile data, in order that anomalies caused by temporary deviations from the recorded values of the primary variables could be explained, leaving a clearer relationship between the primary variables and the tensile properties of the extrudates.

5.3 EFFECT OF PRIMARY VARIABLES ON THE TENSILE PROPERTIES

When analysing the tensile properties of extrudates prepared in this work, it was not always possible to use the normal reference points for comparing conventional semi-crystalline polymers, such as:

a) the elastic modulus, given by the slope of the stress-strain curve at 0% strain. Unfortunately, there was too great an error in the measurement of the stress at 2% and 4% strain to measure the elastic modulus, due to the difficulty in placing the test specimen in the tensometer jaws such that there was neither tension nor slack. Hence, the extrudates could not be compared in terms of the elastic modulus. b) the yield stress - this was shown as a maximum in the stress-strain curve at approximately 10% strain. Many of the extrudates, however, did not exhibit a maximum in the stress-strain curve, so this was not a good means of comparison either.

Instead, it was necessary to find a different method which allowed comparison of the tensile properties of the extrudates. Two methods were used: the first was a purely quantitative method in that it was a direct comparison of physical data from the tensile testing experiments; the second method was partly qualitative - a comparison of the shape of the stress-strain curves for the extrudates.

5.3.1 QUANTITATIVE COMPARISON OF PHYSICAL DATA

5.3.1.1 STRESS AT 10% STRAIN

It was decided that a suitable means of comparison of samples would be the stress required to produce a 10% strain ($S_{10\%}$). This value was chosen because the yield stress for "normal" HDPE extrudates was at approximately 10% strain; all of the samples prepared in this work - with the exception of a few prepared at the highest levels of BT and DDR - were extensible to at least 10% strain. The $S_{10\%}$ also gave an indication of the modulus of the polymer samples; the $S_{10\%}$ multiplied by ten (i.e. divided by 10%) gave the secant modulus at 10% strain. This was much lower than the elastic modulus - the values for HDPE given in the literature were 900 MPa for the modulus and 230 MPa for the secant modulus at 10% strain - but the relationship between the two varied according to the shape of the stress-strain curve (see also section 5.2.2).

At constant quenching temperature - air temperature for the control experiment and BT for the rest - the $S_{10\%}$ was seen to increase with the DDR in the majority of cases. In the control experiment, where the extrudates were quenched in air, the range of DDRs was from x4 to x14. The $S_{10\%}$ for the lowest DDR was 23 MPa, the same as the value of the yield stress given for "normal" HDPE in the manufacturer's literature. The $S_{10\%}$ increased with increasing DDR such that the magnitude was increased by 14.8% at the highest DDR. This was only a very small increase in the $S_{10\%}$ for a large increase in the DDR.

In the experiment where circular extrudates were prepared at constant OR and the liquid metal alloy was the quenching medium (section 4.2), the $S_{10\%}$ was again seen to

increase with increasing DDR at constant quenching temperature (i.e. BT). In each case, the spread in the $S_{10\%}$ from x4 to x14 was greater than that for the air-quenched extrudates and the magnitude of the spread increased with increasing BT.

TABLE 5.1 - EFFECT OF BT ON THE $S_{10\%}$ SPREAD

BT °C	Increase in $S_{10\%}$
111	96.50%
113	112.83%
115	208.14%
117	273.14%


The highest value of the $S_{10\%}$, at x14 DDR and 117°C, was about four times greater than that for "normal" HDPE.

The aim of experiments 3 and 4, when the BT and the range of DDRs were both kept constant, was to vary only the residence time (Rt) in the bath for extrudates having the same cross-sectional area.

In these experiments, the $S_{10\%}$ was seen to increase with increasing OR in the majority of cases. This meant that the $S_{10\%}$ increased with decreasing Rt, as the greater the OR (at constant DDR), the faster the HOS and, therefore, the shorter the Rt. Obviously, there was a minimum Rt possible, equal to the Qt, below which the extrudate was not fully quenched on leaving the bath. Therefore it could be said that the decrease in the $S_{10\%}$ was proportional to the difference between the Rt and the Qt, the residual residence time (RRT) (appendix vii).

It was possible to calculate the Rt to a good degree of accuracy (appendix i) and to find a reasonable approximation to the Qt (appendix iv) and, therefore, to make a reasonable approximation to the RRT.

The $S_{10\%}$ decreased with increasing RRT (appendix vii) from the theoretical maximum - which depended upon the OR,



DDR and BT - at 0s to a value approximately 10% below that of the spherulitic morphology at the largest values of RRT (about 21 MPa for the extrudates from the circular die and about 25 MPa for the strip extrudates). At x5 DDR, the $S_{10\%}$ decreased from 65.4 MPa at high OR (i.e. low RRT) to 25.6 MPa at low OR.

Thus it was clear that the liquid metal medium had a destructive effect upon the morphology of the polymer samples prepared by this method if the extrudate continued to pass through the medium after the optimum morphology (as dictated by the BT and DDR) had formed.

The same relationship between the $S_{10\%}$ and the primary variables was seen - at higher values of DDR and BT - in the other experiments, although it was less easy to deduce this from the data in the case of the flat-film extrudates. A wider range of BT was used in this experiment compared to the others. As a result, the ranges of DDR which were used did not overlap to any significant extent, so it was not possible to cross reference the data as for the other experiments. Also, the extrudates were produced - through necessity, to achieve the required DDR - at varying values of the OR, which meant that the Rt, Qt and RRT could not be compared meaningfully. However there was no evidence to suggest that the flat-film extrudates behaved differently to the other extrudates.

5.3.1.2 STRESS AT BREAK

The stress at break (S_{br}) was chosen because it is a standard method of comparing polymer extrudates. The S_{br} was seen to increase with increasing DDR at constant OR and BT and with increasing OR at constant DDR and BT in a

similar manner to the $S_{10\%}$. The greatest range was seen for the strip extrudates (Table 4.5.4), where the S_{br} increased from about 30 MPa at low OR, low DDR, and low BT to about 180 MPa at high OR, DDR and BT. The S_{br} was seen to decrease from 80.6 MPa at x5 DDR at high OR (i.e. low RRT) to 57.2 MPa at X5 DDR at low OR, a decrease of 29%.

However, there was no obvious correlation between the S_{br} and the BT at constant DDR; the highest value of S_{br} was at the highest value of BT only because of the higher values of DDR allowed. This lack of dependence on BT was odd, as the deformation behaviour - as shown by the shape of the stress-strain curve - of the extrudate changed with BT at constant DDR. As a result, two extrudates which underwent completely different deformation mechanisms were found to have approximately the same S_{br} merely because they were quenched at the same draw-down ratio.

5.3.1.3 ELONGATION AT BREAK

The elongation at break (E_{br}) was also chosen because it is a conventional means of comparison of polymer extrudates. The E_{br} was seen to decrease with increasing DDR at constant OR and BT, with increasing OR at constant BT and DDR and with increasing BT at constant OR and DDR. At low values of BT and DDR, the E_{br} was greater than 1190% - this was the maximum elongation possible when the initial separation of the tensometer jaws was 5 cm - i.e. identical to that for "normal" HDPE. At the highest values of BT and DDR used in these experiments, the E_{br} was as low as 10%. This value was very low for a semi-crystalline polymer, more like that for an amorphous polymer, such as high impact polystyrene.

5.3.2 - GENERAL SHAPE OF STRESS-STRAIN CURVES

This method involved qualitative analysis of the shape of the stress-strain curves of the polymer extrudates whilst also taking into account the values of the $S_{10\%}$ and the E_{br} discussed in the previous section.

There were three distinct types of stress-strain curve exhibited by extrudates in the liquid metal alloy:

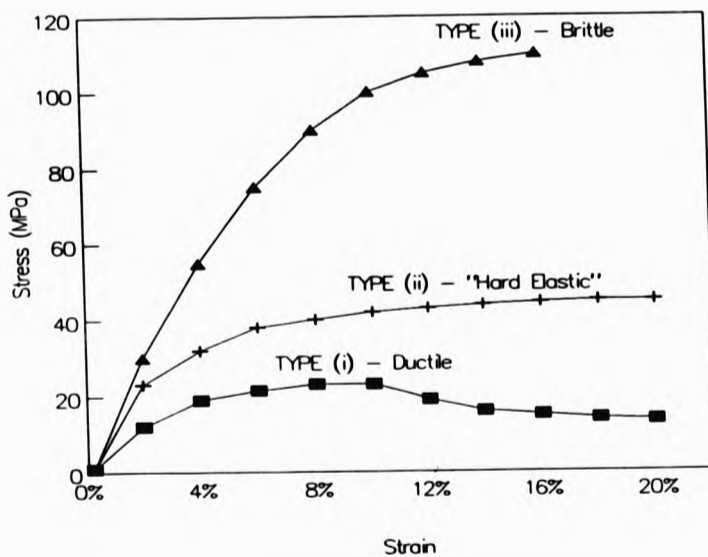


Fig. 5.3.2.1 - Three types of stress-strain curve

i) The stress-strain curve was essentially the same shape as that for air-quenched HDPE - there was a yield point at 8-10% strain followed by cold-drawing. The yield stress - or the $S_{10\%}$ was in the range 20-35 MPa and the E_{br} was in the range 300-1200%.

ii) The stress-strain curve showed the stress increasing with increasing strain until a plateau was reached - i.e.

the stress remained constant with increasing strain until the sample fractured. The $S_{10\%}$ was in the range 35-55 MPa and the E_{dr} was in the range 100-300%.

iii) The stress-strain curve showed the stress increasing with increasing strain until fracture - there was no yield point or plateau. The $S_{10\%}$ was in the range 55-144 MPa and the E_{dr} was in the range 10-100%.

Using the results from Experiment 2, the relationship between the type of stress-strain curve and the primary variables was:

TABLE 5.2 EFFECT OF PRIMARY VARIABLES ON SHAPE OF STRESS-STRAIN CURVES

	ZERO O	LOW O	HIGH O
AIR Q	TYPE (i)	TYPE (i)	TYPE (i)
LOW BT	TYPE (i)	TYPE (ii)	TYPE (ii)
HIGH BT	TYPE (ii)	TYPE (ii)	TYPE (iii)

However, it was clear that the change from type i to type ii was continuous - type i became type ii when the depth of the cold-drawing plateau was 0 MPa, i.e. the cold-drawing plateau and the yield point became the same. Similarly, the change from type ii to type iii was also observed to be continuous. This could be described in terms of the strain range for the cold-drawing plateau becoming zero percent.

Despite the continuity of the change from type i to type iii, it was also obvious that the deformation mechanism - the way in which the polymer sample responded to an applied tensile stress - exhibited by the most extreme type iii stress-strain curve was completely different from that of "normal" HDPE, i.e. type i.

The shape of the type iii of stress-strain curve closely resembled that for two-phase amorphous polymers, such as HIPS - single-phase amorphous polymers, such as polystyrene homopolymer, tended to fracture at lower strains - 0-5% - than those exhibited by the extrudates prepared in this work. It was also noted that there was a close resemblance between the type ii stress-strain curve and that for "Hard Elastic" polymers (section 1.5).

It was possible, therefore, that there were at least two distinct deformation mechanisms, as shown by types i and iii, and possibly three, depending whether type ii was a distinct deformation mechanism, or a composite of i and iii. This will be discussed fully in Chapter 6.

The effect of the RRT on the shape of the stress-strain curve was analogous to its effect on the $S_{10\%}$. Increasing RRT reversed the effect of increasing the DDR and BT - an extrudate which was type iii reverted to type ii and then type i if the RRT was sufficiently large (figs. 4.3.2.5 - 9). At the same time, the $S_{10\%}$ and the S_{br} decreased (see previous section) and the E_{br} increased - the sample prepared at x5 DDR changed from 19% at high OR (i.e. low RRT) to 786% at low OR.

5.4 - ORIENTATION OF EXTRUDATES

The degree of orientation of the polymer molecules in the extrudates was measured in terms of the shrinkage recovery (SR). This was the result of the entropy-driven change from chain-extended conformation to randomly coiled - i.e. isotropic - when the polymer sample was raised above its melting point and the polymer structure was destroyed. When the sample was allowed to cool again, the dimensions

remained approximately that of the shrunken melt (Section 4.7).

The greater the degree of orientation present in the original extrudate, the greater the change in dimensions that was observed during SR testing and, therefore, the greater the SR that was found. The volume of the sample remained approximately constant, although there was usually a very small change in the volume which was the result of a change in the density of the extrudate (section 4.9). The length of the sample, which was always measured in the direction of the draw-down, was the dimension which decreased during SR testing. The SR was measured as the logarithm of the ratio of the original length divided by the new length of the sample. This allowed comparison between extrudates prepared under different conditions, i.e. from different dies - it was also assumed that the two grades of HDPE used in these experiments were similar enough to allow comparison.

The samples tested in this manner were taken from the same batches as those used for tensile testing in sections 4.2-4.6, but not all types of extrudate were tested, as it was only intended to show trends in the relationship between the degree of orientation in the extrudates and the primary variables.

The degree of orientation in an extrudate was dictated by the DDR used - which induced the original orientation in the melt - and the level of entropy-driven relaxation of the molecules, which depended upon the BT, the Rt and the Qt; the longer the melt remained unquenched, the greater the stress relaxation, hence the lower the orientation in the quenched sample (at constant BT). The RRT had a similar

effect; the longer the quenched sample remained in the bath, the lower the degree of orientation.

In the experimental work, the SR was seen to increase with increasing DDR at constant BT and OR as expected. This was because:

- a) the increased DDR induced greater orientation through increased tension in the melt;
- b) the increased DDR reduced the cross-sectional area of the extrudates, thereby reducing the Q_t and, as a result, the relaxation of the molecules before quenching.

It was found that the degree of orientation decreased with increasing BT at constant DDR and OR (fig 4.7.2). This was expected, as the Q_t would have been increased by a higher BT, allowing a greater degree of relaxation of the oriented polymer chains.

At constant DDR and BT, the SR was seen to increase with increasing OR. This was because the R_t - and, therefore, the R_{Rt} - was reduced with increasing OR, so the degree of reversal of morphology - described in section 5.2 - was also decreased.

5.5 - ANNEALING OF EXTRUDATES

The annealing of samples - all of which were taken from experiment 3 - was carried out according to three different methods: a) In liquid metal alloy at 117°C. Four samples were treated in this manner: i) low OR, low DDR; ii) low OR, high DDR; iii) high OR, low DDR; iv) high OR, high DDR. The initial effect of annealing (i) and (ii) was to reduce the $S_{10\%}$ - after 120 seconds there was a significant decrease shown in both samples, followed by a subsequent

increase. After 600 seconds, sample i was slightly greater than at the start and sample ii was slightly smaller, although neither of the changes was necessarily significant, as only one sample of each type was tested (fig. 4.8.1.5). For samples iii and iv, the evidence was even less conclusive.

More interestingly, for sample i the shapes of the stress-strain curves changed - the yield stress, which was originally at about 10% strain, was seen to be at 8% strain after the sample was annealed for 60s and there was a definite yield point. However, after 600s the yield point was found at about 12% and the shape of the stress-strain curve was almost that of a type ii deformation (fig 4.8.1.1). This change in shape was not observed for the other samples, but these had type ii or type iii stress-strain curves initially, so there was no yield point by which to gauge the change in morphology.

The changes in the S_{br} and E_{br} reflected the changes described above - e.g. when the $S_{10\%}$ increased, the S_{br} increased and the E_{br} decreased.

b) In air at 117°C - the samples annealed in this experiment were: i) low OR, high DDR; ii) high OR, high DDR. For sample (i), the $S_{10\%}$ did not change appreciably with annealing time, although the S_{br} decreased after a short time (5 minutes) and then started to increase again. The value was slightly greater after two hours than at the start. Similarly, the E_{br} increased to a maximum at 30 minutes and then started to decrease again.

The effect of annealing sample (ii) was that the $S_{10\%}$ and S_{br} decreased with increasing annealing time to an

approximately constant value, whereas the E_{br} remained constant, within experimental error.

c) Annealed in air at room temperature - the same types of sample were used as in (b). The effect of this treatment - i.e. purely the change in morphology with time at constant (room) temperature - was that the $S_{10\%}$ for sample (i) increased slightly over the 50 day period, whereas the $S_{10\%}$ for sample (ii) decreased slightly.

The overall effect of annealing the extrudates prepared in this work was that, irrespective of the annealing medium or temperature, low order samples - i.e. those prepared at low DDR and at low BT - were improved by annealing after a certain time and high order samples had their tensile properties reduced. In all cases, however, there was an initial decrease in the tensile properties, corresponding to a change in morphology of the polymer.

5.6 - DENSITY OF EXTRUDATES

In this section, the densities of some of the extrudates from experiments 2 and 3 were measured using a density column (section 4.9).

For the samples from experiment 2, the density increased with increasing DDR (HOS) at constant OR and BT. It also increased with increasing BT at constant OR and DDR. The range of densities was from 0.9465 to 0.9492 g/cm³. Similarly, for the samples from experiment 3, the density increased with increasing DDR at constant BT and OR. It also increased with increasing OR at constant BT and DDR. The range was from 0.9471 to 0.9556 g/cm³.

Different density columns were used for the two tests

and the correlation between the position of the calibration balls and their densities was not very close (figs. 4.9.1.1 & 4.9.2.1). As a result, it was not meaningful to compare the results from the two experiments directly.

When the density was plotted against the orientation of the extrudates (appendix viii), it was found that the relationship was essentially the same as for density vs. DDR. Hence, at constant orientation, the density increased with increasing BT, which was consistent with the relationship between density and processing temperature described in Section 1.2).

5.7 - CYCLIC STRAIN RECOVERY

The cyclic strain recovery (CSR) experiment was designed to investigate whether any of the extrudates prepared in the course of this work exhibited similar behaviour to the "Hard Elastic" form of semi-crystalline polymers (section 1.5), which recovered up to 90% of a 50% strain on the first cycle.

The control experiment (Experiment 1), where the extrudates were quenched in air at room temperature, showed poor CSR, as was expected. The range of values was from 33% (at low DDR) to 40% (at high DDR).

When the extrudates were quenched in liquid metal, there was an improvement in the CSR in all cases, with one exception. Even when the extrudate was prepared at low DDR and BT, which gave tensile properties comparable to the control experiment, the range of CSRs was from 40% to 48% which was a definite improvement. Extrudates prepared at higher DDRs and BTs showed recovery as high as 57%. The exception to the above rule was for samples prepared at

high RRT - i.e. low OR and DDR - when the CSR was 32% on the first cycle (fig. 4.10.2.5).

The samples which exhibited CSRs greater than ~50% were those which underwent type ii tensile deformation (section 5.2.2), i.e. the shape of the stress-strain curve was very similar to that shown by "HE" polymers. The common factor was the plateau which, unlike the cold-drawing plateau in type i polymers, appeared to represent a reversible deformation which was responsible for the higher CSRs.

The extrudates which exhibited a type iii deformation did not have the best values of CSR - often the samples fractured at below 50% strain or on the second or third cycle. This showed that polymer chains were breaking rather than the structure deforming reversibly during CSR testing. Hence it could be said that the only extrudates which were comparable to the "HE" form were those that had a type ii stress-strain curve and even then the values of the CSR were quite low, which indicated that the deformation mechanism was less reversible than for the "HE" form.

5.8 EFFECT OF RESIDUAL RESIDENCE TIME ON TENSILE PROPERTIES

When, in experiments 3 and 4, extrudates were prepared at constant BT over the same ranges of DDR (i.e. x2 - x6) but at different ORs, it was observed that there were markedly different values of the tensile properties (e.g. $S_{10\%}$) for extrudates prepared at the same DDR and BT. It was originally supposed that these were the only parameters to have an effect on the morphology of an extrudate quenched in liquid metal - the DDR to determine the orientation and the BT to determine the lamellar thickness and degree of crystallinity - but it became clear that

there was another factor involved.

As the only difference in processing conditions between the extrudates was the OR, it was obvious that the variation in the tensile properties was related to the time that the extrudates were immersed in the bath (Rt).

However, it was also clear that the time in the bath required to fully quench an extrudate (Qt) depended upon the cross-sectional area and, to a lesser extent, the geometry of the extrudate. As has been discussed previously, it was possible to calculate approximate values for both Rt (appendix i) and Qt (appendix iv). The difference between the two was the residual residence time (RRT) (appendix vi). When the values of the $S_{10\%}$ were plotted against the RRT (appendix vii), it became clear that excess time in the liquid metal medium was the cause of the loss of tensile properties.

For example, an extrudate prepared at 118°C and x6 DDR exhibited a $S_{10\%}$ of 67.05 MPa when the RRT was 0.8s, 40.16 MPa when the RRT was 2s and 24.66 MPa when the RRT was 4.4s. The other samples showed the same type of correlation, the magnitude of the effect being proportional to the DDR.

The result of this time-dependent effect was that there was a maximum possible value of the tensile properties of an extrudate prepared at constant BT and DDR, which occurred when the Rt equalled the Qt, i.e. when the RRT was zero. If the Rt was too large (RRT +ve) or too small (RRT -ve), the properties decreased.

A negative value of the RRT meant that the extrudate was not fully quenched on leaving the bath, which explained why there was an observed reduction in properties.

A positive RRT meant that the extrudate was fully quenched in the bath; when the RRT was zero, the level of orientation and degree of crystallinity were at their maximum values, as were the tensile properties. After this point, both orientation (section 4.7.1) and degree of crystallinity - as proportional to the density of the sample (section 4.9.1) - decreased with time.

Because the change in $S_{10\%}$ was much greater for extrudates prepared at higher draw-down (appendix ix), it is proposed that the reduction in the orientation in the extrudates was due to stress-relaxation of the chain-extended polymer backbones at fairly high temperatures .

Furthermore, the reduction of the degree of crystallinity (appendix x) was caused by the instability of the lamellar structures at high temperatures. The effect of prolonged residence in the liquid metal medium was analogous to that shown by the quenched extrudates which were then immersed in liquid metal for a further period of time (section 4.8); the only extrudates which showed increased tensile properties at the end of the experiment were those with low orientation and relatively low crystallinity to start with. Even then, the time of annealing required to produce a significant increase was very much greater (600s) than the maximum RRT used; the initial change observed was a decrease in properties.

The extrudate prepared at DDR x2 having an RRT of approximately 8.6s had a lower $S_{10\%}$ than an air-quenched non-oriented sample. This was the result of having the large spherulite size due to the high temperature of crystallisation, but without the increased lamellar size or any residual orientation, as there was very little present

in the optimum morphology (i.e. $RRT = 0$) for these processing conditions.

Hence it is very important, when processing polymer extrudates by this method, to ensure that the RRT is as close to zero as possible, in order to maximise the effect of the BT and the HOS on the quenched morphology of the polymer.

CHAPTER 6 - MECHANISM OF FORMATION OF MORPHOLOGY /
DEFORMATION MECHANISM OF POLYMER SAMPLES

In the course of this study, it has not been possible to investigate the morphologies of the various types of extrudates directly, i.e. by means of electron microscopy or x-ray diffraction, but it is possible to theorise on a model which would explain the reported results and is consistent with other reported studies on morphology, such as those discussed in chapter 1.

It has been shown already that the morphology of a semi-crystalline polymer, such as HDPE, changes from spherulitic to distended spherulitic with increasing orientation of the melt (section 1.2.3). It has also been shown that it is possible to produce a different form of such a polymer under extreme conditions. This is known as a "shish-kebab" (SK) structure (section 1.2.3, Fig.7).³⁰⁻⁶⁴ Evidence of such a structure was originally shown in samples prepared from a rapidly stirred dilute solution of the polymer, not from an oriented melt.

However, it has now been shown that it is possible to produce a form of a semi-crystalline polymer which contains areas of SK morphology if a sufficiently high orienting force - i.e. draw-down - is applied to the melt and the resulting oriented melt is quenched sufficiently rapidly.⁵⁴ It is likely that these SK areas are not as highly developed as those prepared from dilute solution, as the polymer melt may be regarded as a solution of infinitely high concentration. By considering the effect of the viscosity of each medium on the quenching mechanism, it is possible to propose a number of fundamental differences between the two types of SK structure:

i) The length of the SK extended-chain backbones will be much longer when formed from dilute solution, as it is possible that entire polymer chains may exist in the chain-extended conformation, due to the very low number of entanglements between polymer chains in this low-viscosity environment. It is more likely, however, that individual polymer chains are incorporated into SK structures in both the chain-extended and the chain-folded conformations. Even if this is the case, the length of the melt-quenched SK structures should be significantly less than the solution-quenched because of the reduced freedom of movement of the polymer chains in the high-viscosity melt.

ii) The cross-sectional dimensions of the solution-quenched SK structures should be much smaller, as the number of chains involved in forming the extended-chain backbone would be fewer due to the lack of proximity of polymer molecules in the low-viscosity solution. Conversely, in the melt, more chains would be in suitably close proximity to form the extended-chain backbone due to the high viscosity of the melt.

iii) The solution-quenched SK structures are individual structures;³⁸⁻⁴⁵ no polymer chain is involved in more than one structure, again because of the large distances between the structures when forming in a low-viscosity medium. The SK structures formed in the oriented melt, however, are fully integrated into the surrounding polymer matrix, whether it is spherulitic or amorphous in nature. This is because virtually all of the polymer chains involved in the formation of the SK structures are prevented from becoming fully incorporated as a result of either:

a) being entangled with other polymer chains in the high-viscosity melt, thus becoming quenched as part of the amorphous phase;

b) being incorporated into a lamella in a spherulite.

Consequently, the two structures are quite different in appearance (Fig. 6.1), but the mechanisms of formation and deformation are essentially the same for both.

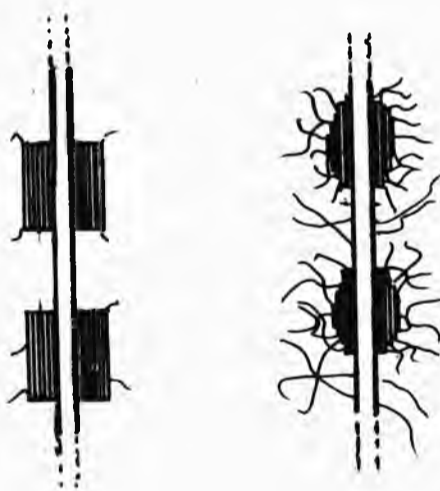


Fig. 6.1 - schematic diagrams of SK structures from:
(a) solution and (b) melt.

As the orientating force - or draw-down - increases, so the relative proportion of polymer involved in forming SK structures also increases. When the quenching medium is air (at room temperature), the evidence for SK structures - greatly increased modulus and a significant reduction in the depth of the cold-drawing plateau - is low, even at fairly high levels of draw-down, as the quenching rate is quite slow, despite there being a temperature difference of over 150°C between the melt temperature and the quenching temperature. This is because the specific heat capacity

(SHC) and the thermal conductivity (TC) of air are very low. The quenching time (Qt) for the air-quenched extrudates in experiment was observed to be in the range 2-5 seconds, which allowed sufficient relaxation to preclude the formation of a SK extended-chain backbone.

The SHC and TC of the liquid metal alloy used in experiments 2-6 are several orders of magnitude greater than those for air which means that, even at quenching temperatures approaching the melting point of the polymer, the Qt was much less than that for air. Hence, high bath temperatures (BT) could be used and sufficiently high levels of orientation retained for SK formation.

The use of liquid metal as quenching medium may possibly enhance the formation of extended-chain SK backbones due to the effect of its very high density ($\sim 8 \text{ g/cm}^3$) which exerts an inward pressure on the extrudate as it passes through the bath. In thermodynamic terms, the formation of a higher density material - increased lamellar size and longer extended-chain backbone - is favoured by the action of this pressure, as increased density means a smaller cross-sectional area. This effect is probably small, though, as the pressures involved are small compared to those used when annealing at high temperature and pressure to increase the density of a polymer (section 1.3.2).³

The simplest method of describing the effect of processing on the morphology of the samples prepared in this work is to consider samples prepared having three levels of orienting stress, or draw-down:

- 1) zero stress,
- 2) low - medium stress,
- 3) high stress;

and processed in three types of medium:

- a) air-quenched at room temperature,
- b) liquid metal-quenched at low BT,
- c) liquid metal-quenched at high BT.


The proposed nine resultant morphologies will show the changes effected by orientation of the melt and the quenching medium and temperature, both individually and together.

6.1 Zero Orientation

At zero orientation, the morphology of each of the samples (a, b, c) is spherulitic (Section 1.2.2.1). Differences between samples are limited to the number and size of the spherulites and the size of the lamellae and amorphous regions within the spherulites.

1a) An isotropic melt quenched in air at room temperature - the morphology of this sample is what may be considered the "normal" spherulitic morphology for this grade of polymer (Fig. 6.7a). The mechanism for the formation of the polymer structure is that described in section 1.2.2.2.

1b) When an isotropic melt is quenched in liquid metal at low BT (111°C), the size of the spherulites is dependent upon the rate of nucleation in the melt prior to crystallisation. This is dependent upon the rate of removal of heat from the melt which, in turn, depends on the SHC, the TC and the degree of supercooling, i.e. the temperature difference between the melt and the quenching medium (section 1.2.2.2). As described above, the speed of cooling for all the liquid metal quenched samples was much greater than for the air quenched. The rate of nucleation is much




lower than for (1a) because of the lower degree of supercooling, but the rate of crystallisation is much faster due to the higher processing temperature.¹²⁴ This gives (1b) a larger spherulite size than in (1a) but also a larger lamellar thickness and a higher degree of crystallinity (Fig. 6.7b). Sample (1b) has a slightly greater modulus and yield stress than (1a) because the increase in the tensile properties of the polymer due to the increased degree of crystallinity is greater than the decrease in the tensile properties due to the increased spherulite size.

1c) When an isotropic melt is quenched in liquid metal at high temperature (123°C), the resulting spherulitic morphology is different to (1b) in two ways: firstly, the spherulitic size is greater than that for (1b) - the rate of nucleation is lower than for (1b) again because the degree of supercooling is lower; secondly, the lamellar size is greater, due to the higher crystallisation temperature (Fig. 6.7c). Hence sample (1c) has a slightly higher modulus, etc. than (1b) for the same reasons that (1b) has a higher modulus than (1a).

Therefore it may be said that the order of spherulite size, the lamellar size and the degree of crystallinity is: $c > b > a$; the tensile properties are therefore in the same order. The deformation mechanism for all three types of extrudate was that of type (i) - ductile fracture.

6.2 Low - Medium Draw-Down

When orientation is introduced into the polymer melt, the mechanism of homogeneous nucleation is enhanced by the



restriction of the freedom of movement of the polymer chains, but the formation of spherulites may be restricted also.

If a low level of draw-down is applied to the melt, small regions of the melt become highly ordered, through local alignment of polymer chains, which have a reduced degree of freedom as a result of this orientation. Two things happen as a result of this:

i) If the highly-ordered region is small (the aspect ratio is of the order of 1 - 10) , it may act as a homogeneous nucleus for spherulite formation (Fig.6.2a).

ii) If the highly-ordered region is large (the aspect ratio is much greater than 10), a number of chain-extended backbones are formed through the crystallisation of the polymer chains in the extended state (Fig.6.2b).

These extended-chain backbones may act as sites for chain-folded nucleation (Fig.6.3).³⁻¹⁰ There are many sections of the polymer chains which are not under sufficient orienting stress to crystallise in the chain-extended formation but which are part of chains which comprise the extended-chain backbones; these sections are relatively free-moving and can use the smooth surface of the extended-chain backbones as nucleation sites for chain-folded crystallisation. The crystalline regions grow laterally, the characteristic lamellar length - which is dictated by the crystallisation temperature (see section 1.4.2) - is along the long axis of the extended-chain backbone.

It is likely that the formation of the extended-chain



backbone may take place at a slightly higher temperature than the formation of the spherulitic morphology, due to the reduced freedom of the polymer molecules preventing the dissolution of the ordered regions at temperatures where isotropic - i.e. unconstrained - nuclei would dissolve into the melt.¹²²

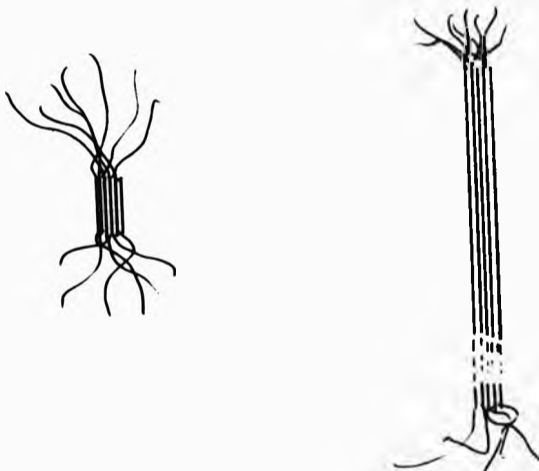


Fig. 6.2 - oriented sections of the polymer melt;
a) short, b) long.



Fig. 6.3 - the effect of high temperature quenching on oriented sections of the melt.

Therefore, in a melt subjected to a low to medium level of orientation, it is likely that both of the mechanisms

for nucleation described above take place, the SK structures forming first, at a slightly higher temperature, followed by the formation of spherulites in the remainder of the melt, which is almost completely isotropic due to entropy-driven stress relaxation of the polymer molecules that are not incorporated into the highly-ordered regions.

The formation of the spherulites is impeded by the presence of the SK structures, so the spherulites may not grow as perfect spheres - the only direction in which the growth is not impeded is along the axis of draw-down, so the spherulites become ellipsoid in shape. As the degree of orientation increases, then the proportion of polymer material comprising the SK structures increases and the remaining areas of spherulitic morphology become smaller and more deformed (Fig. 6.4).

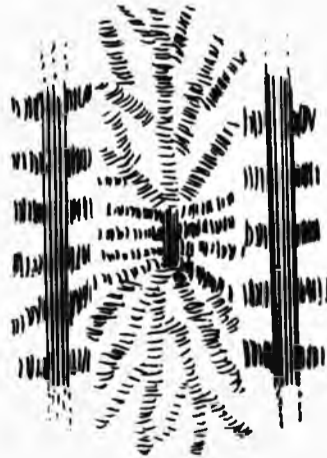



Fig. 6.4 - The effect of SK structures on spherulitic growth.

2a) When extrudates prepared at low to medium draw-down are quenched in air at room temperature, the orientation in the extrudate is low, as the high Q_t allows relaxation of the




extended polymer chains. In the resulting extrudate, the areas of SK morphology are small and widely separated - compared to those in the liquid metal quenched extrudates - and the areas of spherulitic morphology are only slightly deformed (Fig. 6.8a). The tensile properties of 2(a) extrudates are only slightly higher than the 1(a) extrudates, and the deformation mechanism is much the same also.

2b) When a melt prepared at low - to - medium draw-down is quenched in liquid metal at low temperature (111°C), the level of orientation is much higher than that for an air-quenched extrudate prepared at the same level of draw-down (2a), as the rate of quenching is much faster (the Q_t is lower). Therefore there is a much greater proportion of SK material in the quenched extrudate, which will further affect the formation of the spherulitic areas. The size of the lamellae - in both the spherulitic and the SK structures, as they are formed by the same mechanism but from different types of nucleus - will also be increased by the fact that the bath temperature is much higher than room temperature but, as discussed for samples 1(a) and 1(b), the increase is small, compared to the effect seen in 2(c) (Fig. 6.8b).

As the level of draw-down increases, the proportion of polymer material having the SK morphology increases too; as a result, the proportion of polymer material having spherulitic morphology decreases - in this range of draw-downs, it may be assumed that these are the only morphologies present in significant amounts.

When such an extrudate undergoes tensile deformation, the weaker morphology deforms preferentially. This means



that the SK structures remain undeformed while the spherulites deform in much the same way as when a normal spherulitic morphology deforms. However, the fact that the spherulites present in the extrudate are much smaller than for the normal spherulitic morphology and the presence of the SK structures - as molecular "shock absorbers" - help distribute the stress throughout the sample. As a result, no necking is observed; the overall effect of tensile deformation is a reduction in the cross-section along the whole length of the sample.

The spherulitic structures are not fully deformed, however, when the SK structures are first subjected to the deforming stress. This is because the SK structures are linked to the spherulitic structures by the sharing of polymer molecules, i.e. by tie molecules.


The stress-strain curve for polymer morphology type (2b) - and types (2c) and (3b) - is a composite of the normal deformation of the spherulitic structure and that of the SK structure; a simple composite model (Appendix XIa) would suffice if both mechanisms took effect at the same time - i.e. when the strain is first applied. In practice, however, the areas of spherulitic morphology deform preferentially but require a higher stress for the deformation than totally spherulitic samples; the SK structures behave like rigid rods,¹²³⁻¹²⁸ similar to that produced by incorporating fibrous or particulate fillers in a polymer matrix except that, in this case, the "filler" is chemically bonded to the polymer matrix, producing a much stronger reinforcing effect than usual. This may be modelled by a complex composite of the two deformation mechanisms (Appendix XIb), where the level of strain at

which the SK structures begin to take part in the deformation mechanism depends upon the proportion of SK morphology present. The overall effect is that the higher the proportion of SK structures, the higher the tensile properties of the extrudates.

The stress-strain curve for (2b) extrudates is still essentially that of yielding and cold-drawing, although the yield point is now almost a yield plateau and the drop in stress from this maximum level to the cold-drawing stress decreases with increasing draw-down. As the tensile properties of the extrudates increase with increasing proportion of SK structures, the elongation at break (E_{br}) of the extrudates decreases, as there is a lower proportion of the spherulitic morphology to deform.

2c) When a melt prepared at low - to - medium draw-down is quenched in liquid metal at high temperature (123°C), the levels of orientation obtained are slightly lower than for (2b) but still much higher than for (2a), for the same reasons as in (1). As before, the lamellar size - for both spherulitic and SK morphologies - is greater for (2c) than for (2b), due to the higher crystallisation temperature. The overall degree of crystallinity of the polymer sample has also been shown to increase; as the size of the SK extended-chain backbones increase - at increasing orientation - and the size of the chain-folded lamellar regions increase at high BT, then the SK structures become significant in determining the deformation mechanism of the extrudate (Fig. 6.8c).

At constant BT, the distance between the SK structures decreases with increasing orientation, because:



a) the relative proportion of polymer material incorporated into SK structures increases;

b) the cross-sectional area of the sample decreases, bringing the SK structures closer together.

At constant draw-down, the size of the chain-folded areas of the SK structures increases in all directions with increasing BT. The most important manifestation of this phenomenon is that the lateral width (not just the lamellar thickness) of the SK structures increases. At a critical level, the distance between the extended-chain backbones becomes less than the lateral width of the SK structures.

When this happens, deformation of the extrudate is affected - previously, the SK structures moved unhindered and undeformed as the spherulites deformed but now the bulky SK structures may prevent this happening. The stress required to deform an area of the extrudate where this takes place is much greater than that to deform a spherulite, as it is necessary either to fracture the SK structure or to provide a stress high enough to allow slippage of one of the SK structures. Both mechanisms take place during the overall deformation of the extrudate; the spherulitic deformation is the dominant mechanism at first and the SK deformation is dominant towards the end. In between, both deformations take place at the same time throughout the sample and the overall effect may again be considered as a complex composite of the individual effects.

For certain values of orientation and quenching temperature, the sum of the (positive) stress required for the deformation of the SK structures and the negative


stress required for the further deformation of spherulites in the region of 10-50% strain (analogous to the drop in the stress after the yield point has been reached in macroscopic terms) is constant over a period of increasing strain. This is the plateau characteristic of type (ii) deformation.

The relatively low proportion of spherulitic material - compared to (2b) and even (3b) - means that the yield stress/plateau stress is over a smaller strain range, as the deformation of the spherulites is complete at a lower strain; it also means that the E_{Dr} is lower. The fact that the majority of irreversible deformation takes place in the first 20-30% strain improves the cyclic strain recovery (CSR) characteristics. This is because the morphology of the sample at 50% deformation contains only rigid SK and aligned lamellar structures - from the deformation of the spherulites - which do not deform easily, and amorphous regions which do deform easily with a high level of entropy-driven recovery. Hence, the level of CSR for this type of sample is the highest of all the morphologies found in this work. If the proportion of amorphous material is too low, as in (3c), the sample fractures at a strain below 50%. However SR values are not as high as those for "HE" polymer samples (see (3c)).

6.3 High Draw-Down

When high orientation is introduced into the polymer melt through a high level of draw-down, the morphology of the quenched extrudate varies greatly with the means of quenching.

3a) When a polymer melt prepared using the maximum possible



draw-down ratio - for these experiments - is quenched in air, there is a higher proportion of SK structure in the quenched extrudate than for (2a) or (1a), despite considerable relaxation of the orientation during quenching. This level of orientation may be regarded as "medium" orientation - i.e. comparable to the level found in samples (2b) and (2c) - rather than high orientation as found in (3b) and (3c) (Fig. 6.9a). The deformation mechanism remains the same as that displayed by sample (2a) because the widths of the chain-extended sections of the SK structures are not sufficiently wide - due to the low quenching temperature - to produce the type of behaviour seen in sample (2c).

Indeed, it has been shown that highly-oriented melts of semi-crystalline polymers which have been quenched in air may only display behaviour like that seen in (2c) after annealing at high temperature, which increases the lamellar thickness and, consequently, the lateral width of the SK structures. The structure of this form of polymer is called "hard elastic" ("HE");³⁰⁻⁶⁴ its structure has been known for over thirty years and its deformation mechanism has been widely discussed (section 1.5.2) and its typical stress-strain curve is very similar to that of type ii extrudates discussed previously.

3b) When a polymer melt prepared at high draw-down is quenched in liquid metal at low BT, the level of orientation is greater than that for (2b) or (2c). The morphology of the sample is similar to that of sample (2c), a composite of SK structures and distended spherulites, except that the SK structures are more closely spaced - due to the higher draw-down - and the lamellar parts of the

structures are smaller, due to the lower temperature of crystallisation. As a result, the proportion of spherulitic polymer material is greater in sample (3b) than in (2c) (Fig. 6.9b). For this reason the (3b) samples have a slightly lower modulus and a slightly larger E_{br} than (2c) samples. As there is a larger proportion of spherulitic material, this also means that there is a greater level of non-reversible deformation - at 50% strain, deformation of the spherulitic structures is still taking place, so the degree of CSR is lower than for (2c); this is because the reversible deformation of the amorphous regions plays a smaller part in the overall deformation mechanism.

In order to achieve a higher level of CSR(50%) in this group of extrudates (and 2b, 2c), it would be necessary to strain the samples just enough to deform the spherulitic areas in each sample completely. At this stage in the deformation of the polymer sample, the morphology would comprise:


- i) undeformed SK structures;
- ii) lamellae, chain-extended crystalline regions
- iii) amorphous material

ii) and iii) above are the result of destruction of the spherulites during tensile deformation.

A polymer sample having this morphology would be expected to behave in an elastic manner for strains up to ~50%. The amorphous region would deform preferentially when a strain is applied and the entropy-driven recovery would be high when the strain is removed. If the applied strain is too high, some lamellar material would be destroyed, forming chain-extended crystalline material and amorphous

material in its place. Cleavage of polymer chains in the amorphous regions would also occur. Both of these effects would result in low values of CSR. The likelihood of a polymer sample exhibiting this high CSR behaviour may be assessed by measuring the value of the E_{br} , which reflects the relative proportions of spherulitic morphology ($E_{br} = 1200\%$) and SK morphology ($E_{br} = 10\%$) in the sample. If the E_{br} is greater than $\sim 200\%$, there is too much spherulitic material for a high CSR; if it is below $\sim 80\%$, there is too little spherulitic material to provide a sufficiently large amorphous phase to allow reversible deformation, so that a 50% strain would cause irreversible disruption of the structure, reducing the CSR. Hence the only samples to exhibit very high CSRs after being subjected to a cyclic strain of 50% were those having an E_{br} between 80% and 200%.


The main difference between "HE" morphology and the extrudates quenched in liquid metal from an oriented melt is the presence of the SK extended-chain backbones in the (2b), (2c) and especially the (3b) and (3c) structures, which are not present in the "HE" polymers. This is because the high temperature annealing employed in the preparation of "HE" polymers allows the extended-chain backbone to "dissolve" into the amorphous phase; the highly-oriented quenched extrudate is not held under tension (in most cases) whilst being heated, so much of the orientation is lost through stress relaxation. The polymer chains which formed the extended-chain backbone can no longer remain in close proximity at elevated temperatures when there is no orienting stress to reduce the freedom of movement of the chains. Consequently, the chains "dissolve" in the



amorphous phase - each individual chain relaxes and so becomes a part of the amorphous phase. This is reversible on application of a strain to the sample; the extended-chain backbone reforms as the polymer chains involved are not able to migrate through the polymer during annealing because they are fixed by the chain-folded parts of the SK structures which do not "dissolve" during annealing. On the other hand, quenching the melt under tension at high temperatures freezes the extended-chain backbone into place and is not reversible.

The high degree of strain recovery in "HE" polymers is due to the fact that the extended-chain backbone is regenerated under strain but then "dissolves" again when the strain is removed through an entropy-driven mechanism in the amorphous regions, allowing very high recovery of the original dimensions of the sample (section 1.5.2).

Depending upon the magnitude of the applied strain, a certain proportion of the amorphous material fractures as the extended-chain backbones form, creating voids in the extrudate; this process is also mostly reversible on removal of the strain. When the strain is cyclic, this process creates stable holes - or pores - this is a unique characteristic of "HE" polymers; the pores are stabilised by the presence of the tie molecules which form the extended-chain backbones, so it is critical that the strain is not so large as to destroy them during deformation. When type (ii) extrudates are subjected to a cyclic strain, however, the extended-chain backbones are already formed and are damaged as a consequence. The resulting pores are not stabilised in the same way as for "HE" polymers and are larger than for "HE" polymers and less stable and the



sample usually fractures on the third or fourth cycle.

3c) When a polymer melt prepared at high draw-down is quenched in liquid metal at high BT, there is a high degree of orientation and a high degree of crystallinity in the resultant extrudate. The morphology has the highest proportion of SK structures of the nine types of extrudate - the only other structure present is amorphous polymer material in the interstices between the SK structures (Fig. 6.9c). The increased size and proximity of the lamellar parts of the SKs mean that, once a small strain (5 - 20%, depending upon the values of BT and orientation used in the processing of the extrudate) has been applied, the overall effect is that of continuous bands of crystalline material, separated by narrow bands of amorphous material, in a very similar manner to "HE" polymers.

When a (3c) polymer extrudate is strained, however, the amorphous regions may not deform to such an extent as the "HE" extrudates, due to the presence of the already-formed extended-chain backbones. As a result, it is the extended-chain backbones which deform, after a small degree of slippage of the polymer chains; the voids formed as a result are larger and cannot be stabilised, as in (3b), and so the voids become cracks and the sample undergoes brittle fracture, or type iii deformation at a very low strain (Fig. 6.6).

Consequently, sample (3c) has the highest modulus and S_{br} , and the lowest E_{br} of all the nine groups discussed; the stress-strain curves show no sign of a yield point or even a plateau and displays an amorphous deformation mechanism.

These nine examples propose a mechanism by which the

morphology of HDPE changes with changing orientation and

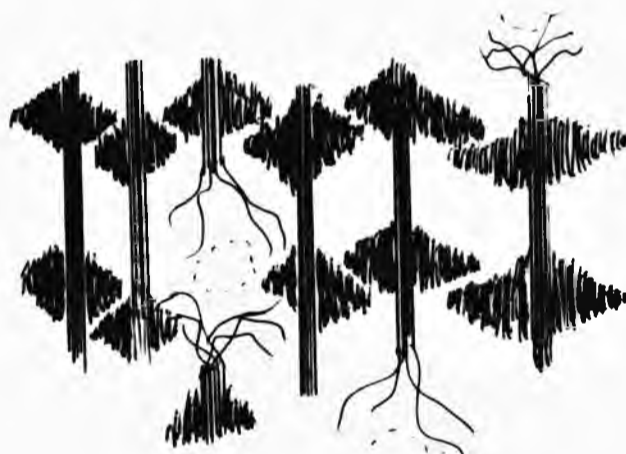


Fig. 6.6 - effect of tensile deformation on (3c) structure temperature of crystallisation. It should be stressed that these intermediate stages are only examples, and that the change between the two theoretical extremes ((1a) and (3c)) is continuous. It should, therefore, be possible to prepare an HDPE extrudate having a specific E_{br} , between 10% and 1200% strain, or a specific $S_{10\%}$, between 23 MPa and 140 MPa, or even a specific CSR, by interpolating between the processing parameters used to produce the samples exhibiting the values found in the nine examples above.

It should be remembered that the final morphology of the extrudates also depends upon the residual residence time, as excess time in the bath reversed the effect of the processing parameters - reducing the degree of orientation and also the degree of crystallinity as a function of time and bath temperature. The exact nature of this effect is complex, so it may only be said that the magnitude of the RRT must be taken into consideration when discussing the tensile properties and deformation mechanism of an extrudate prepared by this method.

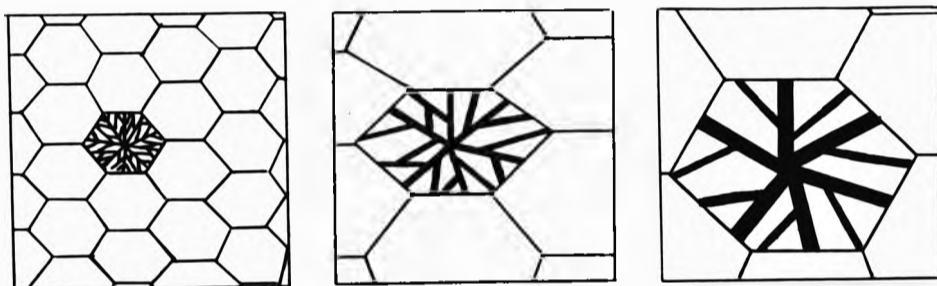


Fig. 6.7 - Zero orientation; quenched (a) in air, (b) liquid metal (111°C), (c) liquid metal (123°C) (showing schematic spherulite and twisted ribbon size).

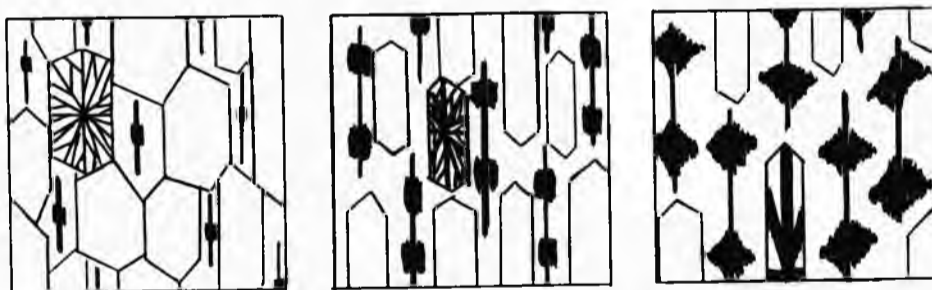


Fig. 6.8 - Low-to-medium orientation; quenched (a) in air, (b) liquid metal (111°C), (c) liquid metal (123°C) (showing schematic SK structures and spherulites).

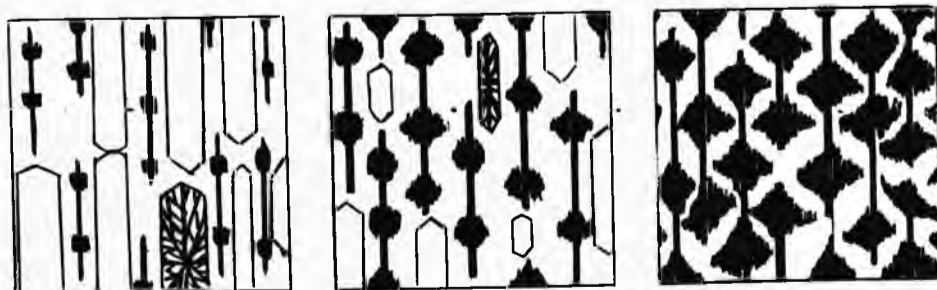


Fig. 6.9 - High orientation; quenched (a) in air, (b) liquid metal (111°C), (c) liquid metal (123°C) (SK and spherulite sizes not to scale, although trends in dimensional changes are inferred).

CHAPTER 7 - CONCLUSIONS

- i) It is possible to construct an apparatus by which a polymer melt may be extruded vertically downwards, pass through a liquid metal quenching medium, around a series of rollers and exit the medium vertically upwards, whilst under a constant draw-down as a continuous process.
- ii) It is possible to use a liquid metal alloy (M.Pt. 96°C) as the quenching medium in the temperature range $111^{\circ}\text{--}123^{\circ}\text{C}$ and obtain a continuous polymer extrudate from an oriented melt having good dimensional stability.
- iii) It is possible to vary the magnitude of the output rate of the extrudate, the haul-off speed and the bath temperature without affecting the continuity of the process.
- iv) The Young's modulus and other tensile properties of HDPE extrudates prepared in this manner are as least as high as and, in the majority of cases, much higher than those prepared by conventional processes. The magnitude of the increase in properties depends upon the magnitude of the processing parameters:
 - a) at constant bath temperature, the Young's modulus, yield stress, break stress, degree of crystallinity and orientation all increase with increasing draw-down ratio; the elongation at break decreases with increasing draw-down ratio.
 - b) at constant draw-down ratio, the Young's modulus, yield stress, break stress and degree of crystallinity all increase with increasing bath temperature; the

elongation at break decreases with increasing bath temperature.

v) the deformation mechanism, as shown by the shape of the stress-strain curve, changes as a function of the two main processing parameters, orientation and the quenching medium / temperature, and also the RRT, as described in section 5. Three distinct types of stress-strain curves have been observed, although the transformation between them is continuous. It is possible to explain the differences in the stress-strain curves for the extrudates in terms of their morphology:

Type i - at low levels of orientation and quenching temperature, the extrudates undergo plastic deformation, have a yield stress in the stress range 23-35 MPa and fracture at greater than 400-1200% strain. The morphology of this type of extrudate is predominantly spherulitic .

Type ii - at intermediate levels of orientation and quenching temperature, extrudates are obtained which exhibit a yield plateau, rather than a yield point. This plateau is at a higher stress range than for type (i). Samples fracture in the strain range 50-400%. The shape of the stress-strain curve is similar to that for Hard Elastic polymers, but the morphology is significantly different. This is shown by the difference in the values of the cyclic strain recovery - Hard Elastic polymers can recover up to 95% from a 50% strain, whereas type ii polymers can only achieve 50% at best. When subjected to a cyclic strain, Hard Elastic materials form stable pores, whereas type ii materials tend to rupture, sometimes breaking on the third

or fourth cycle. The morphology of this type of sample is a mixture of shish-kebab, spherulitic and amorphous morphologies.

Type iii - these polymer extrudates have a very high modulus, often a fivefold increase over that produced by quenching the same polymer melt in air. There is no yield point observed and the samples fracture at less than 50% strain. The morphology of this type of polymer is that of a high proportion of shish-kebab structures in an amorphous matrix.

APPENDIX (i) - CALCULATION OF APPROXIMATE RESIDENCE TIME

The Rt of an extrudate depends primarily upon the value of OR and HOS. In order that draw-down is achieved, HOS must be greater than OR; as a result, the melt is subjected to an acceleration equal to $(HOS - OR) / Qt$, where HOS and OR are measured in m/s and Qt is the time taken (in seconds) for the extrudate to quench. After the extrudate has quenched, its speed is that of the HOS.

The distance between the die and the bath is small, so the speed of the extrudate on entering the bath may be assumed to be OR. The extrudate passes through a distance of 0.48 m of liquid metal in the bath. In order to calculate the average speed, a guess must be made as to the point, P (as a proportion of the RD), in the bath at which the extrudate becomes fully quenched. This guess was made using the a:b ratio data as a rough guide, given that the a:b ratio is 1 for $0 < P < 0.5$.

The Rt may then be calculated from the formula:

$$Rt = \frac{P \times 0.48}{1/2 \times [OR + HOS]} + \frac{(1 - P) \times 0.48}{HOS}$$

The first term represents the time spent in the bath during quenching and the second term represents the time spent in the bath after quenching.

* TABLE 1 - APPROXIMATE RESIDENCE TIMES

DDR	OUTPUT RATE (rpm)			
	5 rpm	10 rpm	20 rpm	28 rpm
x2	12.27	6.32	3.25	2.38
x3	8.84	4.60	2.39	1.79
x4	7.04	3.68	1.92	1.46
x5	5.92	3.10	1.62	1.10
x6	5.16	2.71	1.42	

APPENDIX (ii) - CALCULATION OF CROSS-SECTIONAL AREA FOR CIRCULAR EXTRUDATES

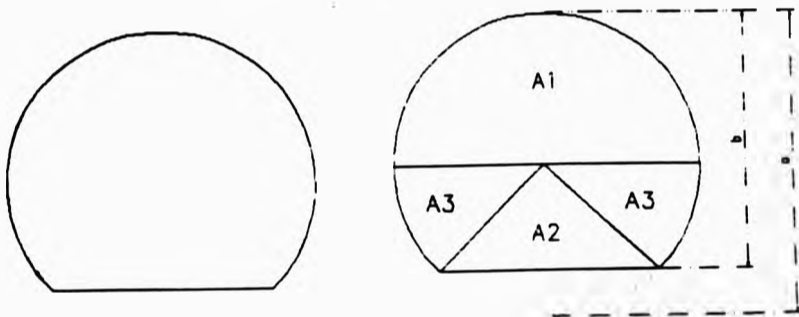


Fig. A1a

Fig. A1b

The extrudate shape (Fig. A1a) may be considered as a circle which has had a chord removed. This shape may now be represented as a composite of four sections, two of which are identical (Fig.A1b), whose areas may be defined in terms of the parameters a and b , the maximum and minimum thicknesses of the extrudate;

i) a semi-circle; its area, A_1 , is given by the formula:

$$A_1 = \text{Pi} \times a^2/8$$

which is simply half the area of a circle.

ii) a triangle; its area, A_2 (Fig.A1c), is given by the formula:

$$A_2 = (b - a/2)(ab - b^2)^{1/2}$$

which is the product of the height, $(b - a/2)$, and c (Fig. A1c), which is half the base length; c is found by applying Pythagoras' Theorem, given that the length of the other two sides of the triangle are known.

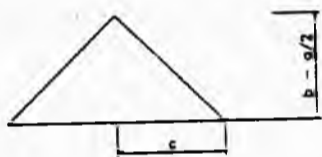


Fig. A1c

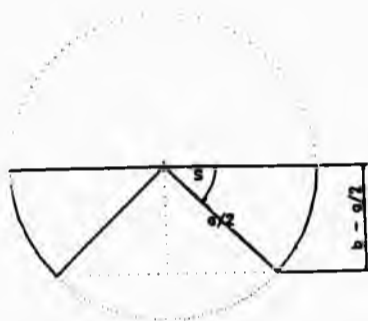


Fig. A1d

iii) two segments; each segment has an area given by the formula (Fig. A1d):

$$A_3 = a^2/8 \times \text{ArcSin}(2b/a - 1)$$

which is the area of a segment of a circle - given by the ratio of the subtended angle over 360° multiplied by the area of the circle; the sine of the subtended angle is given by the ratio of the opposite angle over the hypotenuse - $(b - a/2)$ divided by $a/2$.

Therefore, the total area, A , is given by:

$$A = A_1 + A_2 + (2 \times A_3)$$

$$A = \text{Pi} \times a^2/8 + (b - a/2)(ab - b^2)^{1/2} + 2[a^2/8 \times \text{ArcSin}(2b/a - 1)]$$

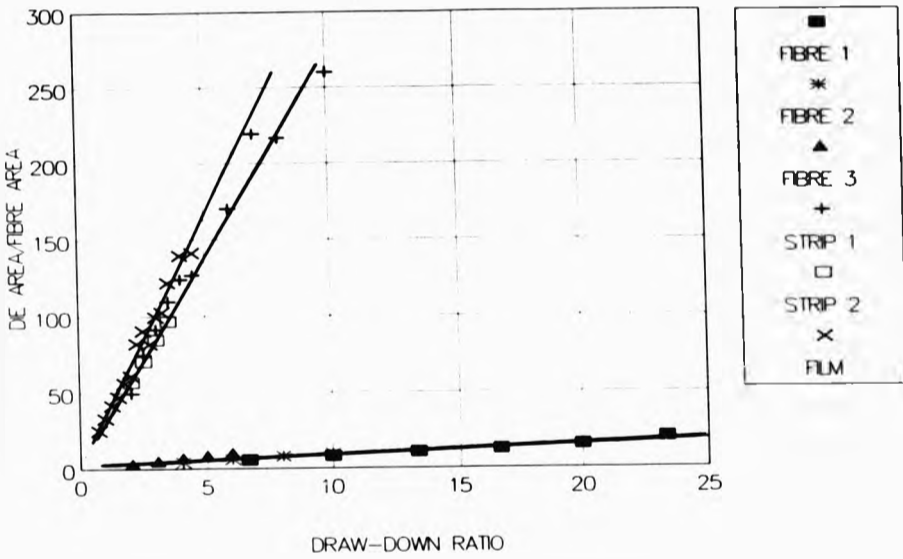
When the limiting values of b are inserted into this formula, the equation may be simplified: i) for a semicircular cross-section, $b = a/2$; the values of A_2 and A_3 become zero, i.e. the area of the cross-section is given by A_1 .

ii) for a circular cross-section, $a = b$; the value of A_2 becomes zero. The angles in each area A_3 are 90° , so the area of the cross-section is given by $A_1 + (2 \times A_3)$.



APPENDIX (iii) - ACTUAL DRAW-DOWN VS. DRAW-DOWN RATIO

The actual draw-down was calculated by dividing the area of the die by the area of the extrudate.



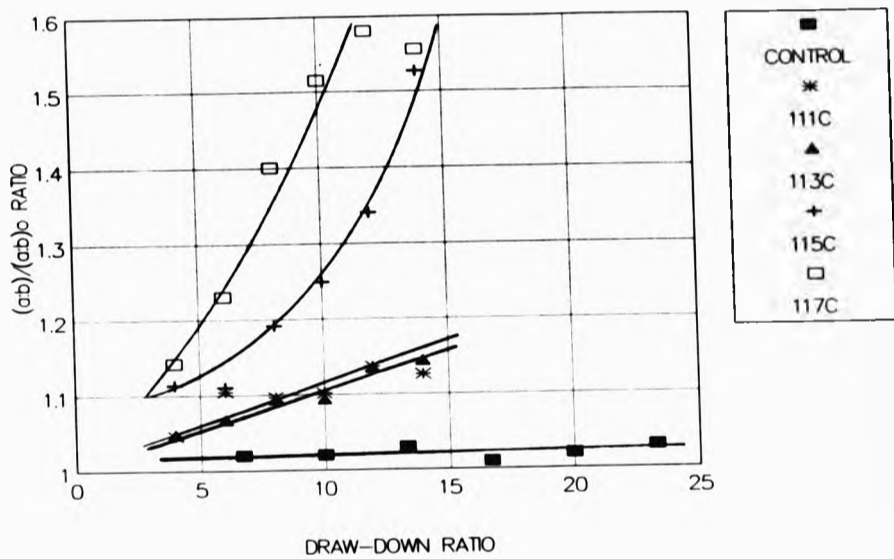
APPENDIX (iv) - CALCULATION OF APPROXIMATE QUENCH TIME

The approximate Qt for experiment 3 was calculated by the following method. The a:b ratios and Rts for the series of extrudates prepared at 5 rpm and 10 rpm OR were studied; it was noted that the extrudates prepared at 5 rpm, x5 DDR and 10 rpm, x2 DDR had approximately the same Rt and a:b ratio; the latter was unity, within experimental error. The next value in each series was considered; the value at 5 rpm, x6 was still circular but the value at 10 rpm, x3 had and a:b ratio of 1.05 - a slight deformation. The 1/2Rt for the latter extrudate was, at 2.3 s, almost a second less than the former. It was deduced from this that the Qt of the sample was prepared at DDR x2 was approximately 2 s. The Qt for the extrudates prepared at other values of DDR was calculated approximately by comparing the cross-sectional areas and circumferences of the samples (it was assumed that the relationship between heat loss and the surface area/volume ratio was linear).

TABLE (iv) - APPROXIMATE QUENCHING TIME

DDR	OUTPUT RATE (rpm)			
	5 rpm	10 rpm	20 rpm	28 rpm
x2	3.68	3.75	3.72	3.73
x3	2.07	2.00	2.03	1.95
x4	1.35	1.26	1.28	1.17
x5	0.90	0.92	0.90	0.87
x6	0.74	0.72	0.65	

APPENDIX (v) - (a:b)/(a:b)₀ RATIO vs. Draw-down Ratio



APPENDIX (vi) - CALCULATION OF RESIDUAL RESIDENCE TIME

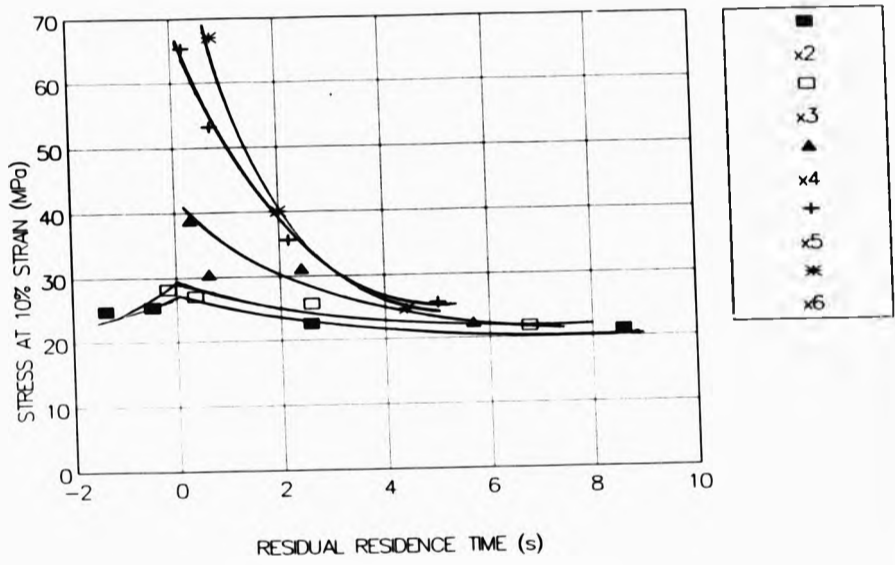
As the Q_t and the R_t was known for each sample in experiment 3, the residual residence time (RRt) could be calculated:

$$RRt = R_t - Q_t$$

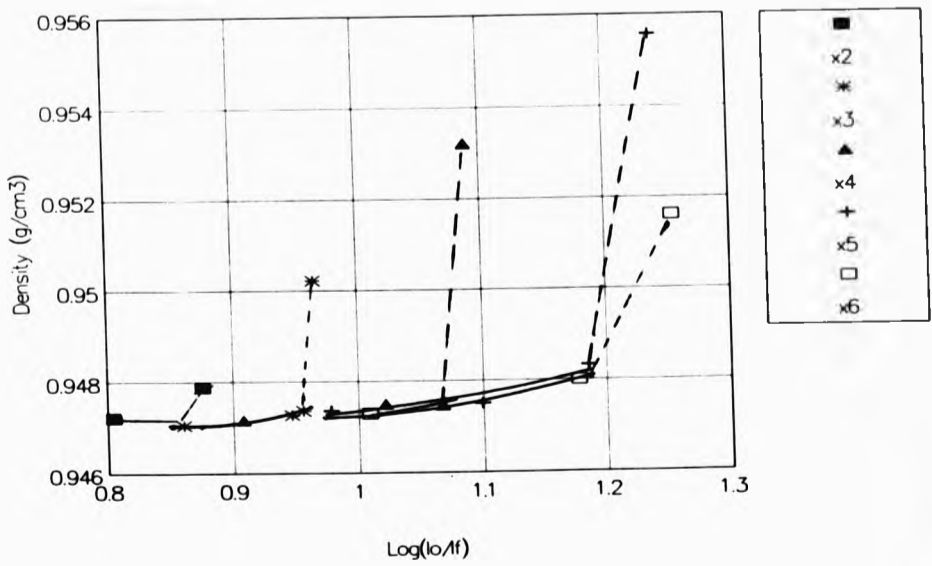
TABLE (vi) - APPROXIMATE RESIDUAL RESIDENCE TIME

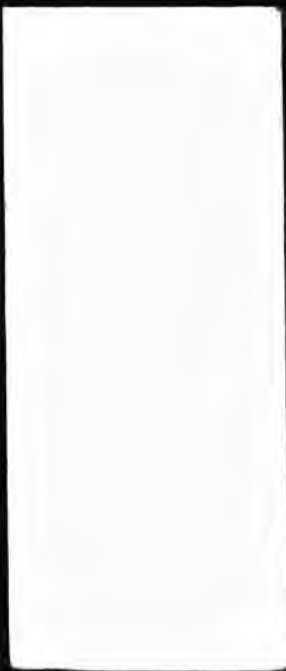
DDR	OUTPUT RATE (rpm)			
	5 rpm	10 rpm	20 rpm	28 rpm
x2	8.59	2.57	-0.47	-1.35
x3	6.77	2.60	0.36	-0.16
x4	5.69	2.42	0.64	0.29
x5	5.02	2.18	0.72	0.23
x6	4.42	1.99	0.77	

APPENDIX (vii) - EFFECT OF RESIDUAL RESIDENCE TIME ON STRESS AT 10% STRAIN

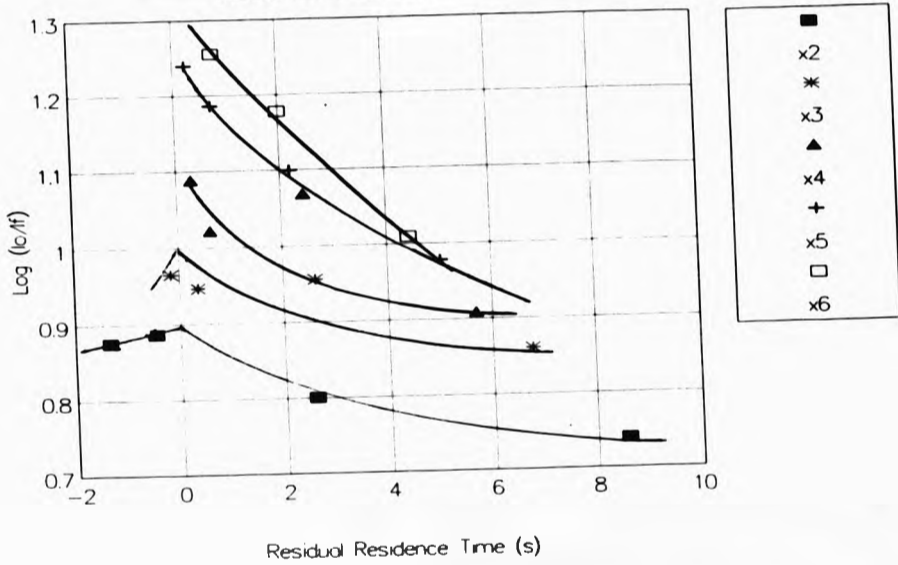


APPENDIX (viii) - DENSITY vs. ORIENTATION

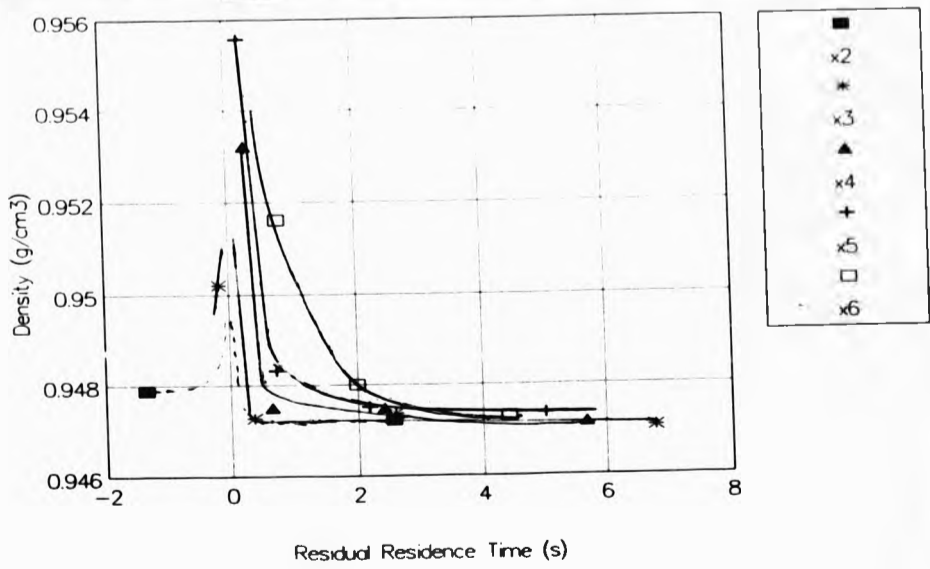




APPENDIX (ix) - ORIENTATION AS A FUNCTION OF RESIDUAL RESIDENCE TIME



APPENDIX (x) - DENSITY AS A FUNCTION OF RESIDUAL RESIDENCE TIME



APPENDIX XI - MODELS OF COMPOSITES OF SHISH-KEBAB AND SPHERULITIC MORPHOLOGY

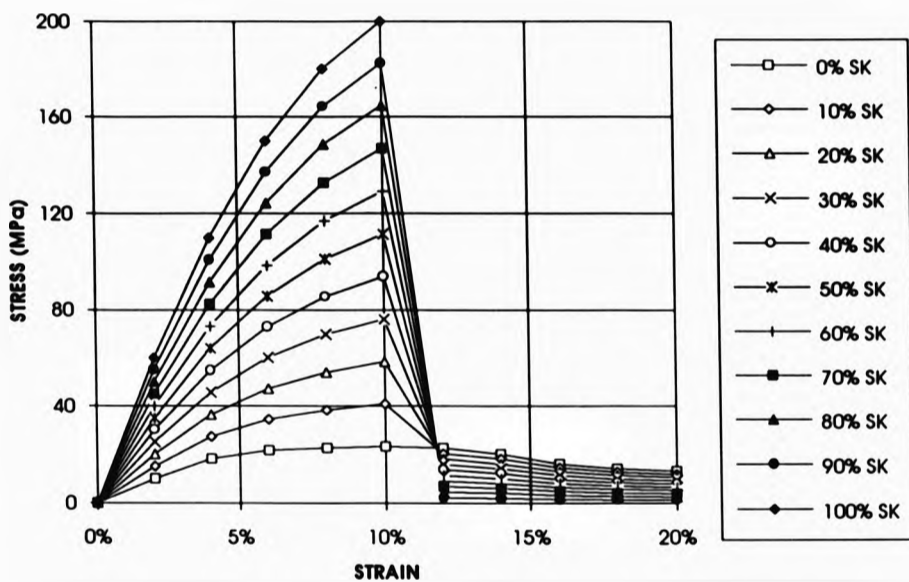


Fig. XIa - Simple composite - calculated as average of the stress-strain curves for the two morphologies. The curve for the SK deformation is an estimate.

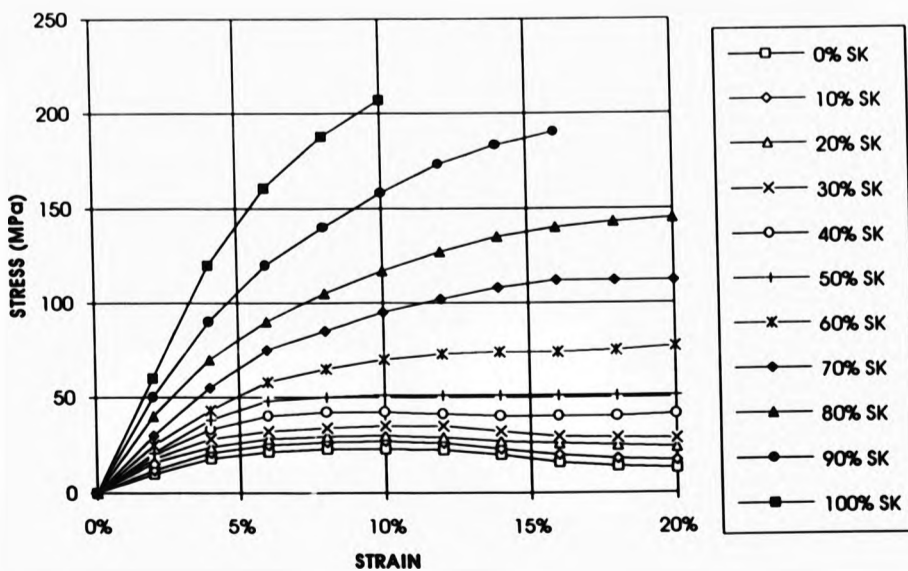


Fig. XIb - Complex composite - calculated as a weighted average of the two curves: the higher the SK content, the earlier in the deformation that its effect is seen.

REFERENCES

- 1) Dawson, I.M.; Proc. Roy. Soc. (London) Series A, 214, 72 (1952).
- 2) Geil, P.H.; Polymer single crystals, Wiley-Interscience, New York (1963).
- 3) Basset, D.C.; Principles of Polymer Morphology. Cambridge Press (1981). 4) Cowie, M.G.; Polymers: Chemistry and Physics of Modern Materials. Blackie (1991).
- 5) Nicholson, J.W.; The Chemistry of Polymers. RSC paperbacks (1991).
- 6) Sharples, A.; Introduction to Polymer Crystallisation, Edward Arnold (1966).
- 7) Deanin, R.D.; Polymer Structure, Properties and Applications (ch. 5). Cahners Books (1972).
- 8) Young, R.J.; Introduction to Polymers (ch. 4). Chapman and Hall (1981).
- 9) Wunderlich, B.; Macromolecular Physics, Volume 1 (ch.3). Academic Press (1973).
- 10) Structure of Crystalline Polymers, Edited Hall, I.H., Elsevier Applied Science, London, (1984).
- 11) Basset, D.C., Dammont, F.R. and Salovey, R.; (1964) Polymer, 5, 579.
- 12) Basset, D.C. and Carder, D.R.; (1973) Phil. Mag., 28, 513
- 13) Basset, D.C.; (1976) Polymer, 17, 460
- 14) Arlie, J.P., Specht, W. and Skoulios, A.; (1967) Makromol. Chemie 104, 212.
- 15) Kovacs, A.J., Gonthier, A. and Straupe, C.; (1975). J. Polym. Sci., Polymer Symposia, 50, 283.
- 16) Keller, A.; (1957) Phil. Mag., 2, 1171.
- 17) Lauritzen, J.I. and Hoffman, J.D.; (1960) J. Res. Bur. Std., 64A, 73.
- 18) Frank, F.C. and Tosi, M.P.; (1961) Proc. Roy. Soc. A, 263, 323.
- 19) Hoffman, J.D., Davis, G.T. and Lauritzen, J.I.; (1976) in Treatise on Solid State Chemistry, Vol 3 (ed Hannay, N.B.) Chapter 7, New York Plenum.
- 20) Woodward, A.E.; Atlas of Polymer Morphology, Hanser, Munich (1979).
- 21) Kardos, J.L., Li, H.-M. and Huckswold, K.; (1971) J. Polym. Sci. A-2, (9)2, 2061-80.

- 22) Statton, W.O. and Geil, P.H.; (1960) *J. Appl. Polymer Sci.*, **3**, 357.
- 23) Wunderlich, B.; (1973) *J. Polymer Sci.*, **C**, **43**, 29.
- 24) Flory, P.J.; (1953) *Principles of Polymer Chemistry* Cornell U. Press, Ithaca, New York.
- 25) Keith, H.D. and Padden, F.J.; (1963) *J. Appl. Phys.*, **34**, 2409.
- 26) Keith, H.D. and Padden, F.J.; (1964) *J. Appl. Phys.*, **35**, 1270.
- 27) Keith, H.D. and Padden, F.J.; (1963) *J. Appl. Phys.*, **35**, 1286.
- 28) Keith, H.D., Padden, F.J. and Vadimsky, R.G.; (1966) *J. Polymer Sci.*, **A-2**, **4**, 267.
- 29) Keith, H.D., Padden, F.J. and Vadimsky, R.G.; (1966) *J. Appl. Phys.*, **42**, 4585.
- 30) Keller, A.; Machin, M.J.; (1967) *J. Macromol. Sci. (Phys.)*, **B1(1)**, 41-91.
- 31) Mackley, M.R. and Keller, A.; (1975) *Phil. Trans.*, **278**, 29.
- 32) Pennings, A.J.; (1977) *J. Polym. Sci. (Symposia)*, **59**, 55.
- 33) Hoffman, J.D.; (1979) *Polymer*, **20**, 1071.
- 34) Gohil, R.M. and Peterman, J.; (1982) *Colloid Polym. Sci.*, **260**, 312.
- 35) Mandelkern, L.; (1964) *Crystallisation of polymers* (ch.9), New York, McGraw-Hill.
- 36) Lindenmeyer, P.H.; (1964) *SPE Trans.*, **4(3)**, 1.
- 37) Garber, C.A.; Clark, S.E.; *J. Macromol. Sci. - Phys.*, **B4(3)**, 499-518 (Sept, 1970).
- 38) Pornimit, B and Ehrenstein, G.W.; (1992) *Adv. Polym. Technol.* **11** No.2, 91.
- 39) Bauer, A., Hofmann, D. and Schulz, E.; (1992) *Acta Polymerica*, **43**, No.1, 27.
- 40) Ania, F., Balta Calleja, F.J. and Bayer, R.K.; (1991) *Polymer*, **32**, No.17, 3252.
- 41) Hofmann, D., Schulz, E. and Walenta, E.; (1990) *Acta Polymerica*, **41**, No.7, 371.
- 42) Ehrenstein, G.W.; (1990) *Angew. Makromol. Chem.*, **Vol. 175**, 187.

- 43) Reneker, D.H., Schneir, J., Howell, B. and Harary, H; (1990) *Polym. Comm.*, 31, No.5, 167.
- 44) Hoogsteen, W., Brinke, G.T and Pennings, A.J.; (1990) *J. Mat. Sci.*, 25, No.3, 1551.
- 45) Xu, Y., Zhou, E., Yu, F. and Qian, B.; (1989) *J. Polym. Sci.*, 7, No.1, 1.
- 46) Braby, J.M. and Thomas, E.L.; (1989) *J. Mat. Sci.*, 24, No.9, 3311.
- 47) Bashir, Z., Odell, J.A. and Keller, A.; (1984) *J. Mat. Sci.*, 19, 3713.
- 48) Bashir, Z., Odell, J.A. and Keller, A.; (1986) *J. Mat. Sci.*, 21, 3993.
- 49) Bigg, D.M.; (1987) *Conf. Proc., New Advances in Oriented Plastics*, pp 5-29.
- 50) Barham, P.J.; (1982) *Polymer*, 23, No.8, 1112.
- 51) Davis, H.A.; (1966) *J. Polym. Sci.*, A2(4), 1009.
- 52) Nagou, S. and Azuma, K.; (1979) *J. Macromol. Sci., Phys.*, B16, 435.
- 53) Pope, D. and Keller, A.; (1975) *J. Polym. Sci., Phys.*, 13, 533.
- 54) Smith, p. and Pennings, A.J.; (1975) *Brit. Polym. J.*, 7, No.5, 343.
- 55) Hofmann, D. and Schulze, E.; (1989) *Polymer*, 30, No.11, 1964.
- 56) Allen, P.S., Bevis, M.J., Ogbonna, C. and Thapar, H.; (1988) *Conf. Proc., Deformation, Yield and Fracture of Polymers*, p54.
- 57) van Aerle, N.A.J.M. and Lemstra, P.J.; (1988) *Makromol. Chem.*, 189, No.6, 1253.
- 58) Fujiyama, M., Wakino, T. and Kawasaki, Y.; (1988) *J. Appl. Polym. Sci.*, 35, No.1, 29.
- 59) Maertin, C., and Ehrenstein, G.W.; (1987) *Conf. Proc. Antec '87. Plastics - pioneering the 21st century*, 816.
- 60) Barham, P.J. and Keller, I.; (1985) *J. Mat. Sci.*, 20, 2281.
- 61) Kreuger, D. and Yeh, G.S.Y.; (1972) *J. Macromol. Sci.*, B6, No.3, 431.
- 62) Keller, A. and Willmouth, F.M.; (1972) *J. Macromol. Sci.*, B6, No.3, 493.
- 63) Moonen, J.A.H.M.; (1991) *Polymer*, 32, No.17, 3252.

- 64) Shouxi Chen, Yonge Jin and Renyuan Qian; (1987) Makromol. Chem., 188, No. 11, 2713.
- 65) Geil, P.H., Anderson, F.R., Wunderlich, B. and Arakawa, T.; J. Polym. Sci., A, 2, 3707 (1964).
- 66) Barnett, J.D., Block, S. and Piermarini, G.J.; (1973) Rev. Sci. Inst., 44, 1.
- 67) Blackadder, D.A. and Lewell, P.A.; (1970) Polymer, 11, 659.
- 68) Lam, R. and Geil, P.H.; (1981) J. Macromol. Sci., B20, No.1, 37.
- 69) Matsuoka, S.; (1962) J. Polym. Sci. 57, 569.
- 70) Reneker, D.H.; (1962) J. Mat. Sci., 59, 539.
- 71) Peterlin, A.; Morphology and fracture of drawn crystalline polymers in Solid state of polymers, ed. Geil, P.H., New York, Dekker (1974).
- 72) Glenz, W. and Peterlin, A.; Plastic deformation of polymers, ed. Peterlin, A. (1972).
- 73) Andrews, E.H.; (1968) Fracture in polymers. London, Oliver and Boyd.
- 74) Ward, I.M.; (1971) Mechanical properties of solid polymers. Chichester, Wiley-Interscience.
- 75) Sprague, B.; (1973) J. Macromol. Sci. - Phys., B8 (1-2), 157-187 .
- 76) Quynn, R.G.; Brody, H.; J. Macromol. Sci., B5(4), 721-738 (Dec., 1971).
- 77) Quynn, R.G. and Sprague; (1970) J. Polym. Sci., (A-2)8, 1971.
- 78) Keller, A.; (1955) J. Polym. Sci., 15, 31.
- 79) Keller, A.; (1956) J. Polym. Sci., 21, 363.
- 80) Noether, H.D.; Polym. Eng. and Sci., Mid-May (1979), Vol. 19, No. 6, 427-432.
- 81) Noether, H.D. and Whitney, W.; (1973) Kolloid-Z, 251, 991.
- 82) Park, I.K. and Noether, H.D.; (1975) Colloid Polym. Sci., 253, 824.
- 83) Cannon, S.L., McKenna, G.B. and Stratton, W.O.; Macromol. Rev., 11, 209 (1976).
- 84) Spruiell, J.E. and White, J.L.; (1975) Appl. Polym. Symp., 27, 121.
- 85) Quynn, R.G.; (1970) J. Macromol. Sci. B4, 953.

- 86) Yamakazi, T; (1975) Polymer, 16, 425.
- 87) Herrman, J.; US Patent 3,256,258.
- 88) Du Pont De Nemours & co.; UK Patent 935,809.
- 89) Tessier, J.D.L.; UK Patent 962,231.
- 90) Hercules Powder co.; UK Patent 1,052,550.
- 91) Knobloch, F.W. et al; US Patent 3,299,171.
- 92) Noether, H.D.; US Patent 3,513,110.
- 93) Celanese co.; UK Patent 1,180,066.
- 94) Celanese co.; UK Patent 1,198,695.
- 95) Isaacson, R.B. et al; US Patent 3,558,764.
- 96) Druin, M.L. et al; US Patent 3,679,538.
- 97) Celanese co.; UK Patent 1,287,504.
- 98) Encyclopedia of Polym. Sci. Eng., 1986, (5), 408-15.
- 99) Cayrol, B. and Peterman, J; (1975) Colloid Polymer Sci., 253, 840.
- 100) Miles, M., Peterman, J. and Gleiter, H.; (1979) J. Macromol. Sci. Phys. B16, 127.
- 101) Goritz, D. and Muller, F.H.; (1979) Colloid Polym. Sci., 253, 862.
- 102) Xu, G., Du, Q. and Wang, L.H.; (1987) Makromol. Chem. Rapid Communications, 8, No.11, 539.
- 103) Hashimoto, T, Nagatoshi, K., Todd, A. and Kawai, H.; (1976) Polymer, 17, No.12, 1063.
- 104) Ren, W.; (1992) Coll. Polym. Sci., 270, No.10, 990.
- 105) Ren, W.; (1992) Coll. Polym. Sci., 270, No.10, 943.
- 106) Ren, W.; (1992) Coll. Polym. Sci., 270, No.8, 747.
- 107) Kau, C., Huber, L., Hiltner, A. and Baer, E.; (1992) J. Appl. Polym. Sci., 44, No.12, 2081.
- 108) Zhu, Y., Okui, N., Tanaka, T., Umemoto, S. and Sakai, T.; (1991) Polymer, 32, No.14, 2588.
- 109) Yu, T., Du, Q. and Hu, J.; (1989) Conf. Proc., Integration of fundamental polymer science and technology, 328.
- 110) Dosiere, M; (1989) Makromol Chem, Macromol. Symp., Vol.23, 205.

- 111) Hosemann, R. and Schulze, I.; (1987) Coll. Polym. Sci., 265, No.8, 686.
- 112) Petermann, J. Karbach, A. and Feit, K.; (1987) Polym. Bull., 18, No.4, 355.
- 113) Miles, M., Petermann, J. and Gleiter, H.; (1976) J. Macromol. Sci. B, 12, No.4, 523.
- 114) Spruiell, J.E. and White, J.L.; (1975) Polym. Eng. Sci., 15, No.9, 660.
- 115) Siesler, H.W.; (1984) Adv. Polym. Sci., No.65, 1.
- 116) Loboda-Cackovic, J. and Hosemann, R.; (1979) J. Macromol. Sci., Phys., 16, 145.
- 117) Walton, K., Moet, A. and Baer, E.; (1984) in Contemporary Topics in Polymer Science, Vol.14, Plenum Publishing Corporation, p977.
- 118) Chou, C.J., Hiltner, A. and Baer, E.; (1986) Polymer, 27, 369.
- 119) Cannon, S.L., Stratton, W.O. and Hearle, J.W.S.; (1975) Polym. Eng. Sci., 15(19), 633.
- 120) Sawatari, C. and Matuo, S.; (1989) Macromolecules, 22(7), 2968.
- 121) Hendra, P. et al; Private Communication (1987).
- 122) Czornyj, G. and Wunderlich, B.; (1977) Makromol. Chem., 178, No.3, 843.
- 123) Peterlin, A.; (1987) Coll. Polym. Sci., 265, No.5, 357.
- 124) Ishikawa, H., Numa, H. and Nagura, M.; (1979) Polymer, 20, 516.
- 125) Petermann, J., Gohil, R.M., Massud, M. and Goeritz, D.; (1982) J. Mat. Sci., 17, No.1, 100.
- 126) van Hutten, P.F. and Pennings, A.J.; (1980) Makromol. Chem. Rapid Comm., 1, No.8, 477.
- 127) van Hutten, P.F. and Pennings, A.J.; (1980) J. Polym. Sci., Polym. Phys., 18, No.5, 927.
- 128) Grubb, D.T. and Keller, A.; (1978) Coll. Polym. Sci., 256, No.3, 218.

THE BRITISH LIBRARY
BRITISH THESIS SERVICE

TITLE AN INVESTIGATION INTO THE POLYETHYLENE
EXTRUDATES PRODUCED BY SIMULTANEOUS
ORIENTATION AND HIGH TEMPERATURE
QUENCHING.

AUTHOR Colin
BERRY

DEGREE Ph.D

**AWARDING
BODY** University of North London

DATE 1994

**THESIS
NUMBER** DX179741

THIS THESIS HAS BEEN MICROFILMED EXACTLY AS RECEIVED

The quality of this reproduction is dependent upon the quality of the original thesis submitted for microfilming. Every effort has been made to ensure the highest quality of reproduction. Some pages may have indistinct print, especially if the original papers were poorly produced or if awarding body sent an inferior copy. If pages are missing, please contact the awarding body which granted the degree.

Previously copyrighted materials (journals articles, published texts etc.) are not filmed.

This copy of the thesis has been supplied on condition that anyone who consults it is understood to recognise that its copyright rests with its author and that no information derived from it may be published without the author's prior written consent.

Reproduction of this thesis, other than as permitted under the United Kingdom Copyright Designs and Patents Act 1988, or under specific agreement with the copyright holder, is prohibited.

DX

179741